

Topics in Medicinal Chemistry 36

Stefan Laufer *Editor*

Proteinkinase Inhibitors

 Springer

Series Editors

Peter R. Bernstein, Philadelphia, Pennsylvania, USA

Amanda L. Garner, Ann Arbor, Michigan, USA

Gunda I. Georg, Minneapolis, Minnesota, USA

Stefan Laufer, Tübingen, Germany

John A. Lowe, Stonington, Connecticut, USA

Nicholas A. Meanwell, Princeton, New Jersey, USA

Anil Kumar Saxena, Lucknow, India

Claudiu T. Supuran, Sesto Fiorentino, Italy

Ao Zhang, Shanghai, China

Nuska Tschammer, Martinsried, Germany

Sally-Ann Poulsen, Nathan, Australia

Aims and Scope

Topics in Medicinal Chemistry (TMC) covers all relevant aspects of medicinal chemistry research, e.g. pathobiochemistry of diseases, identification and validation of (emerging) drug targets, structural biology, drugability of targets, drug design approaches, chemogenomics, synthetic chemistry including combinatorial methods, bioorganic chemistry, natural compounds, high-throughput screening, pharmacological in vitro and in vivo investigations, drug-receptor interactions on the molecular level, structure-activity relationships, drug absorption, distribution, metabolism, elimination, toxicology and pharmacogenomics. Drug research requires interdisciplinary team-work at the interface between chemistry, biology and medicine. To fulfil this need, TMC is intended for researchers and experts working in academia and in the pharmaceutical industry, and also for graduates that look for a carefully selected collection of high quality review articles on their respective field of expertise.

Medicinal chemistry is both science and art. The science of medicinal chemistry offers mankind one of its best hopes for improving the quality of life. The art of medicinal chemistry continues to challenge its practitioners with the need for both intuition and experience to discover new drugs. Hence sharing the experience of drug research is uniquely beneficial to the field of medicinal chemistry.

All chapters from Topics in Medicinal Chemistry are published OnlineFirst with an individual DOI. In references, Topics in Medicinal Chemistry is abbreviated as Top Med Chem and cited as a journal.

More information about this series at <http://www.springer.com/series/7355>

Stefan Laufer
Editor

Proteinkinase Inhibitors

With contributions by

E. J. Barreiro · D. Dauch · M. L. de Castro Barbosa ·
D. N. do Amaral · M. Forster · M. Gehringer · S. Knapp ·
P. Koch · A. Krämer · L. M. Lima · H. Minoux ·
A. Moschopoulou · A. Poso · S. Röhm · L. Schio ·
L. Zender · S. Zwirner

 Springer

Editor

Stefan Laufer
Eberhard Karls Universität
Pharmazeutisches Institut Eberhard Karls Universität,
Tuebingen Center for Academic Drug Discovery
(TueCAD2)
Tübingen, Germany

ISSN 1862-2461

Topics in Medicinal Chemistry

ISBN 978-3-030-68179-1

<https://doi.org/10.1007/978-3-030-68180-7>

ISSN 1862-247X (electronic)

ISBN 978-3-030-68180-7 (eBook)

© Springer Nature Switzerland AG 2021

This work is subject to copyright. All rights are reserved by the Publisher, whether the whole or part of the material is concerned, specifically the rights of translation, reprinting, reuse of illustrations, recitation, broadcasting, reproduction on microfilms or in any other physical way, and transmission or information storage and retrieval, electronic adaptation, computer software, or by similar or dissimilar methodology now known or hereafter developed.

The use of general descriptive names, registered names, trademarks, service marks, etc. in this publication does not imply, even in the absence of a specific statement, that such names are exempt from the relevant protective laws and regulations and therefore free for general use.

The publisher, the authors, and the editors are safe to assume that the advice and information in this book are believed to be true and accurate at the date of publication. Neither the publisher nor the authors or the editors give a warranty, expressed or implied, with respect to the material contained herein or for any errors or omissions that may have been made. The publisher remains neutral with regard to jurisdictional claims in published maps and institutional affiliations.

This Springer imprint is published by the registered company Springer Nature Switzerland AG.
The registered company address is: Gewerbestrasse 11, 6330 Cham, Switzerland

Preface

The history of protein kinase inhibitors (PKI) is remarkable in many ways. Scientifically, as some 30 years ago, selective inhibition of protein kinases by ATP-site-directed PKIs was considered as principally impossible, both due to the highly conserved nature of this site and the high intracellular concentration of ATP. Now we have several highly selective inhibitors for various kinases, and designing selectivity is a daily practice for medicinal chemists in this field. Commercially, PKIs are remarkable as well. 20 years after the launch of the first product, imatinib, we have more than 60 registered drugs on the market with more than US\$25 billion annual sales worldwide. The future is bright as well, since new indications beside cancer, e.g. inflammation, autoimmunity, and neurodegeneration have been explored, new inhibition mechanisms as allosteric inhibitors, covalent inhibitors, and substrate-specific inhibitors have showed up or are close to come – what’s next? The pipeline of clinical candidates is full, more than 500 new chemical entities are in clinical trials.

In such a dynamic field, a book is outdated even before it is published. Our goal was therefore less to show the latest state of the art, but rather to focus on principles of design and examples of successful implementation. A mix of authors from industry and academia, old experts, and young talents will give us a broader view from all sides.

We thank all who contributed to this book, the authors, the publisher, and MS. K. Schmidt for language polishing and proofreading.

Tübingen, Germany
December 2020

Stefan Laufer

Contents

Function, Structure and Topology of Protein Kinases	1
Sandra Röhm, Andreas Krämer, and Stefan Knapp	
Molecular Modeling of Protein Kinases: Current Status and Challenges	25
Antti Poso	
Covalent Kinase Inhibitors: An Overview	43
Matthias Gehring	
Achieving High Levels of Selectivity for Kinase Inhibitors	95
Laurent Schio and Herve Minoux	
Exploiting Kinase Inhibitors for Cancer Treatment: An Overview of Clinical Results and Outlook	125
Athina Moschopoulou, Stefan Zwirner, Lars Zender, and Daniel Dauch	
Case Study on Receptor Tyrosine Kinases EGFR, VEGFR, and PDGFR	155
Lídia Moreira Lima, Maria Letícia de Castro Barbosa, Daniel Nascimento do Amaral, and Eliezer J. Barreiro	
Inhibitors of c-Jun N-Terminal Kinase 3	203
Pierre Koch	
Covalent Janus Kinase 3 Inhibitors	225
Matthias Gehring and Michael Forster	

Function, Structure and Topology of Protein Kinases



Sandra Röhm, Andreas Krämer, and Stefan Knapp

Contents

1	Introduction	2
2	The Kinase Active State	3
3	Mechanism of Kinase Activation	6
3.1	Kinase Activation by Interacting Domains and Proteins	9
4	Canonical Type-I and Type-II Inhibitor Binding Mode	10
4.1	Noncanonical Binding Modes	12
4.2	Allosteric Kinase Inhibitors	13
5	Conclusions and Outlook	17
	References	18

Abstract Protein kinases represent one of the most successful target classes for the development of new medicines. Because of their key roles in cellular signalling, kinases are stringently regulated by a large diversity of mechanisms such as post-translational modifications, interacting domains and proteins and cellular localization. The high plasticity of protein kinases has been exploited for the development of new inhibitor types such as type-II and type-I $\frac{1}{2}$ inhibitors targeting inactive states of the kinase catalytic domain and allosteric inhibitors that target induced binding pockets either adjacent (type-III) or distantly located (type-IV) to the kinase ATP-binding site. Here we discuss structural elements of the kinase active site, key mechanisms of kinase regulation and how these mechanisms can be exploited for the development of selective kinase inhibitors.

Keywords Allosteric inhibitors, Kinase activation, Kinase regulation, Structure-based drug design

S. Röhm, A. Krämer, and S. Knapp (✉)
Johann Wolfgang Goethe-University, Institute for Pharmaceutical Chemistry, Frankfurt, Germany

Johann Wolfgang Goethe-University, Buchmann Institute for Life Sciences, Frankfurt, Germany

e-mail: knapp@pharmchem.uni-frankfurt.de

1 Introduction

The human kinome constitutes a large superfamily of essential enzymes with more than 500 family members [1]. Kinases can be grouped in two main classes based on their catalytic activity on serine/threonine and on tyrosine residues. Based on their primary sequence and conserved structural features, the human kinome has been classified into eight major kinase groups, namely, the AGC (protein kinase A, G and C), CaMK (calcium/calmodulin-dependent kinases), CMGC (cyclin-dependant kinases, MAP kinases, glycogen synthase kinases, casein kinases 2), TK (tyrosine kinases), STE (homologues of yeast sterile 7), CK1 (casein kinases), TKL (tyrosine kinase-like) and the RCG (receptor guanylate cyclases) kinase families [1]. In addition, a large number of kinases share only weak sequence homology with any of these major groups and have been classified as “other” and atypical kinases. While the group of other kinases are typical protein kinases, the group of atypical kinases lack canonical sequence motifs of the kinase catalytic domain. Some of the atypical kinases have therefore been reassigned as non-kinase proteins, whereas there are also several recent additions to this group such as the FAM20 kinases [2–4]. Interestingly, around 10% of all human kinases are considered catalytically inactive and have been classified as pseudokinases. Pseudokinases share a typical kinase domain fold, but they lack at least one conserved structural motif which is considered important for catalytic activity [5, 6]. Pseudokinases have essential signalling function despite their lack of catalytic activity by acting as scaffolding proteins and allosteric regulators of catalytically active kinases.

Many protein kinases are deregulated in human disease which made protein kinases major drug targets. However, only few have been targeted to date offering huge opportunities for future drug development efforts [7, 8]. The high sequence homology within the kinase ATP-binding site which is the target of most kinase inhibitors poses however challenges on the development of selective inhibitors. On the other hand, design efforts for selective inhibitors are now facilitated by the large number of crystal structures that are now available covering about 40% of the kinase family. The protein data bank (PDB; <http://www.rcsb.org/>) and the KLIFS database (<http://klifs.vu-compmedchem.nl/>) [9] currently list 4,521 crystal structures covering 293 kinases. Current strategies for the development of selective inhibitors comprise now several structure-based strategies such as covalent targeting of unique cysteine residues within the ATP-binding site [10, 11], allosteric inhibitors [12, 13] and conventional inhibitors with good shape complementarity [14]. Here we review structural features important for kinase catalytic function and regulation as well as strategies for structure-based kinase inhibitor design.

2 The Kinase Active State

The tertiary structure and overall folding of the kinase catalytic domain is highly conserved throughout the kinase family and harbours around 300 amino acids. The first crystal structure of PKA in complex with ATP and a pseudosubstrate in 1991 paved the way for a better understanding of the catalytic mechanism, cofactor binding and kinase regulation [15–17].

The canonical kinase catalytic domain fold consists of two domains, also called lobes, which are connected to each other via a flexible hinge region. Both lobes form a hydrophobic cleft which serves as binding site for ATP (Fig. 1a). The smaller N-terminal lobe (N-lobe) comprises five β -sheets (β 1– β 5) and one helix called α C, whereas the C-terminal lobe (C-lobe) is mainly alpha helical in structure (α D– α L).

Four main interactions were evident from the first PKA crystal structure [15–17]: (1) The adenosine ring of ATP is placed in the catalytic centre and forms hydrogen bonds with the hinge region amino acids. (2) A flexible loop region between the sheets β 1 and β 2 harbours a glycine-rich sequence motif GXGX φ G, where φ refers to a hydrophobic residue which coordinates the ATP phosphates coining the name phosphate-binding loop. (3) The β 3-sheet contains a conserved VIAK (Val-Ile-Ala-Lys) motif. The lysine adopts important structural features, by forming a salt bridge with ATP phosphate groups and to a conserved glutamate residue

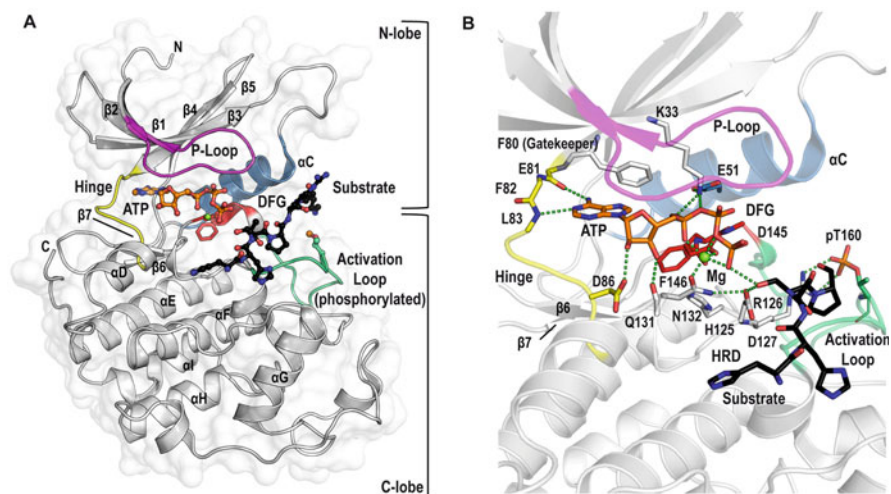


Fig. 1 Architecture of the kinase catalytic domain. (a) Conserved tertiary structure of a protein kinase exemplified by CDK2 (PDB: 1QMZ). Catalytic active state of CDK2 in complex with ATP and a peptide substrate. The P-loop is highlighted in pink, the α C-helix in blue, the hinge region in yellow, the activation loop in green, ATP in orange and the peptide substrate in black. The Mg^{2+} ion is shown as green sphere. The N- and C-termini are marked. (b) Details of the ATP-binding site. ATP and substrate are shown in stick representation. Colour schemes highlighting structural elements are the same as in panel (a). Key hydrogen bonds are shown as dotted lines

located in helix α C. Subsequent crystal structures showed that helix α C is flexible and can dislodge from the active site (α C out). The VIAK lysine/ α C glutamate salt bridge is therefore a hallmark of the active kinase conformation. (4) A tripeptide motif DFG (Asp-Phe-Gly) is located between strands β 8 and β 9 in the C-lobe and marks the beginning of the activation segment (A-loop). The conserved Asp interacts with Mg^{2+} itself coordinating to the ATP phosphates [18].

Protein kinases phosphorylate their substrates on Ser/Thr or Tyr residues after binding of substrate sequences to the substrate binding site in an extended conformation. The substrate interaction site can be described as a shallow surface groove that is formed by side chains located in the four main C-terminal lobe helices (α D– α H) as well as the A-loop APE (Ala-Pro-Glu) motif. Usually the A-loop is 20–30 residues long, and it is usually unstructured in kinases that are regulated by A-loop phosphorylation [19]. The unstructured inactive A-loop conformation partially impedes substrate interactions, but does not necessarily affect substrate binding [20]. Phosphorylation of the A-loop locked this flexible motif in a defined conformation resulting in kinase activation as described below.

A hallmark of the active kinase conformation is the accurate spatial arrangement of the conserved catalytic domain motifs for efficient catalysis. The active conformation is therefore structurally well-defined as exemplified for CDK2 in Fig. 1b. Active protein kinases harbour a highly conserved Y/HRD (Tyr/His-Arg-Asp) motif between strand β 6 and β 7. While some variations of the Y/HRD motif exist in active kinases, the aspartate of this motif is strictly required for catalytic activity of the phosphoryl transfer reaction. The Tyr/His in Y/HRD typically forms hydrogen bond interactions with the DFG backbone linking these two key elements. A salt bridge network between Y/H in Y/HRD to the phosphate moiety of the activation loop phosphorylation site (pThr160 in CDK2) stabilizes the activation segment and further links this segment to the catalytic loop. The “R” in the HRD motif is not strictly conserved. The presence of this residue has been thought to be indicative of the requirement of A-loop phosphorylation (so-called RD kinases) which seems not always be the case [21]. However, in RD kinases the polar interactions of the HRD arginine with the A-loop phosphorylation site largely contribute to the conformation and stability of the A-loop. Finally, the Asp (D127 in CDK2) of the HRD motif acts as a catalytic base deprotonating the hydroxyl group of the peptide substrate Ser/Thr or Tyr residue promoting the nucleophilic attack onto the γ -phosphate of ATP. The Asp is further stabilized by a conserved hydrogen bond with an Asn from the activation loop (N132 in CDK2) [22].

Overall the kinase active state is characterized by a structured A-loop with a “DFG-in” conformation and an α C-helix in closed proximity to ATP site. A characteristic canonical salt bridge between the VIAK motif lysine and the conserved α C glutamate residue stabilizes the active form. Normally the N- and C-lobes adopt a closed conformation with a structured P-loop, although some of these structural features may not be present in crystal structures of active kinases.

Because of the structural diversity that is also often observed in active kinases, Taylor et al. established a better definition of the active state by analysis of hydrophobic spines that bridge both kinase lobes and interconnect all elements important for activity. The spines are present in all active kinases, and this structural feature seems therefore better suited defining the active state. Consequently, in inactive kinases the spines are broken leaving one of more structural motif disconnected from the active state position [23–26] (Fig. 2).

The “catalytic spine” (C-spine) is complemented by the ATP cofactor with an aromatic interaction of the adenine ring system bridging both kinase lobes. In PKA (protein kinase A), the C-spine comprises two bulky hydrophobic residues (Met231 and Leu227) located in helix α F in the C-lobe linking this helix via Met128 to α D and the sheet β 7 (Leu172, Ile174). Leu173 in the β 7 sheet extends the C-spine to the ATP-binding side and is complemented in the ATP-bound state by the adenine ring which connects the C-spine to the N-lobe where the C-spine is complemented by Val57 and Ala70.

The “regulatory spine” (R-spine) starts with Tyr164 in the C-terminal kinase lobe of PKA interacting with the DFG phenylalanine (Phe185) which forms the bridge to

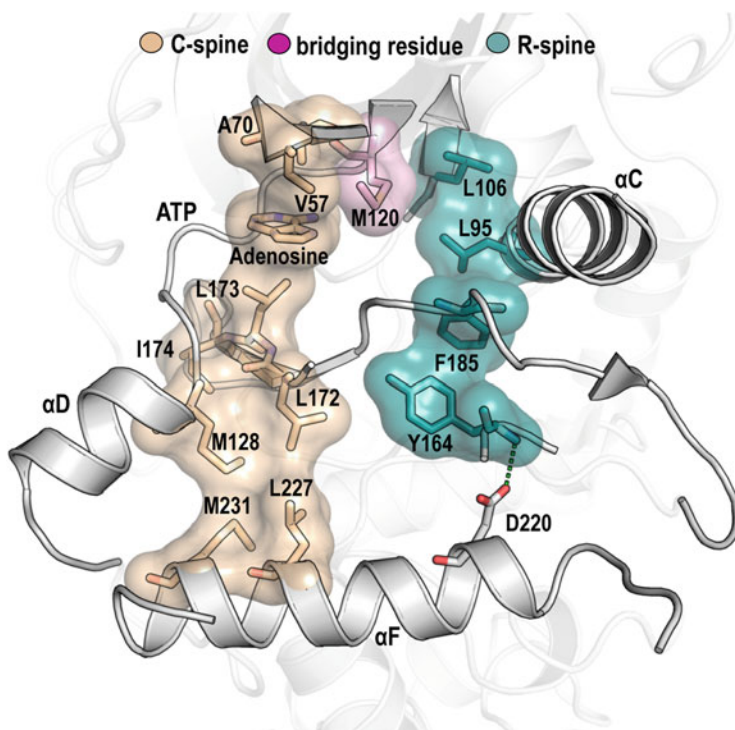


Fig. 2 Alignment of hydrophobic spines in the catalytic domain of active PKA (PDB:1ATP). C-spine is coloured in gold and R-spine in teal. The bridging residue between both spines in the N-terminal lobe, Met120, is highlighted in pink

the N-lobe. The R-spine is completed by the N-lobe residues L95 (alpha C) and Leu106 located in the β 4-strand. The formation of the R-spine is indicative of an active conformation of α C and the DFG-motif and is therefore a structural hallmark of the kinase active state.

In agreement with the important structural role of the C-spine, mutation of Leu173 to alanine in PKA and the analogous residue in CDK2 results in kinase inactivation [27], and R-spine mutations have been detected oncogenic mutants resulting in kinase activation in particular in the so-called C-spine gatekeeper position that controls access to an extended ATP pocket in kinases with small amino acids in this position [28–30].

3 Mechanism of Kinase Activation

Activation of protein kinase is tightly controlled by a multitude of regulatory mechanisms. A key regulatory structural element is the activation segment, which is typically 20–40 residues long and consists of the DFG magnesium ion-binding motif, a short β -strand (β 9), the actual activation loop and the P+1 loop. The activation segment shows considerable conformational diversity between two invariable anchor points at the N- and C-terminus of this segment: the DFG motif and the P+1 loop linking the activation segment to helix α EF [19].

For kinases requiring phosphorylation for activity, the unphosphorylated activation segment is usually unstructured or assumes an inactive conformation [31, 32]. Phosphorylation of the activation segment at a serine, threonine or tyrosine residue located typically about 11 residues N-terminal to the APE sequence motif stabilizes the A-loop. (Fig. 3). The role of further phosphorylation sites is however less clear. Phosphorylation at a secondary site is required for the activity of extracellular signal-regulated kinase 2 (ERK2) [33]. In contrast, introducing a second phosphorylation site in glycogen synthase kinase 3 (GSK3) increases the catalytic activity only moderately, and modulation of substrate selectivity has been suggested as a potential role of these phosphorylation events [34].

There are two mechanisms of activation segment phosphorylation – autoactivation and phosphorylation by a kinase acting upstream in a signal transduction pathway. Autoactivation is poorly understood as it requires that an inactive (unphosphorylated) kinase activates itself by *trans*-phosphorylation. Several models have been established including increasing local concentration by ligand-induced receptor dimerization [35, 36] or oligomerization in the cytoplasm as observed for CAMK2 [37–39]. Some intramolecular mechanisms have also been described. For instance, the -dual-specificity tyrosine phosphorylation-regulated kinase phosphorylates its own activation segment on a tyrosine residue. After this initial intramolecular phosphorylation event, this kinase *trans*-phosphorylates exclusively substrates on serine and threonine residues, whereas tyrosine autophosphorylation in GSK3 requires the presence of chaperonins [40, 41].

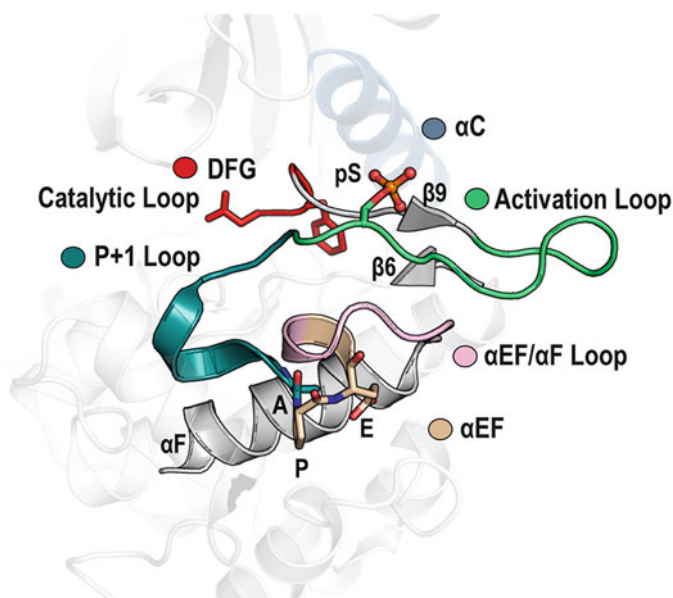


Fig. 3 Architecture of the kinase activation segment. Shown is the phosphorylated activation segment of PAK4 (PDB: 2CDZ). Highlighted are the activation segment structural elements including the DFG motif (red), the activation loop region (green) and the P+1 loop (dark green). The phosphorylation site is shown in ball and stick representation. The APE is indicated

An interesting model of autoactivation has been recently suggested. A number of kinases have been reported to form transient dimers in crystal structures. Intriguingly, these kinases all contain additional domains increasing local concentration and therefore the dimeric state of the inactive enzyme. In dimers of these kinases, the activation segment domain-exchanged, thereby forming an active kinase in a trans configuration, in which the phosphorylation sites are placed in the active site of the interacting protomer. It has been suggested that this conformation is important for autoactivation of kinases at non-consensus sites, offering an explanation of how kinases can active on sites [42–44] (Fig. 4a).

Dimerization of the catalytic domain plays also a role for a number of diverse kinases, but in contrast to the symmetric dimers reported for kinases autophosphorylating at non-consensus sites, these kinases form asymmetric dimers or heterodimers. The receptor tyrosine kinase EGF1R (epidermal growth factor-1 receptor), for instance, forms homo- or heterodimers with its closely related family members HER2, HER3 and HER4 including the inactive pseudokinase HER3 [45, 46]. This activation model represents a refined mechanism of the canonical ligand-induced receptor activation which has major implications for our understanding of the mode of action of selective therapeutic antibodies and kinase drugs [47–49]. Ligand binding to the extracellular domain of EGFR induces large structural rearrangements and dimerization which orients the catalytic domains

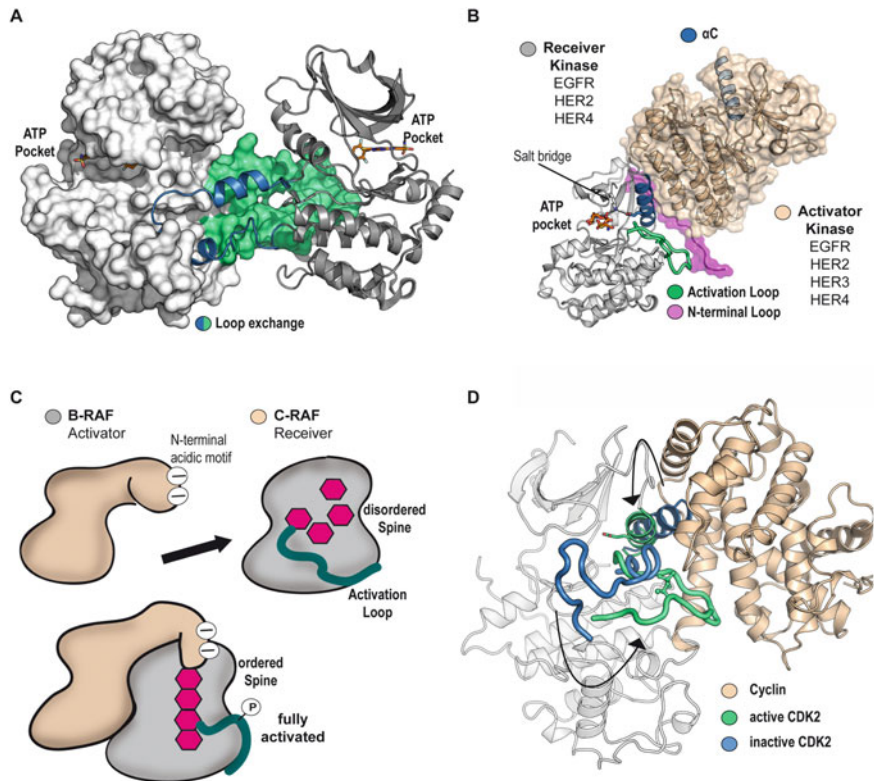


Fig. 4 Activation models of kinases. (a) Activation by activation loop exchange allowing phosphorylation on non-consensus sites. (b) Asymmetric activation of EGFR receptor kinases. (c) Activation of B/C-RAF by heterodimerization. (d) Activation of CDK2 by cyclin interaction. Shown is inactive CDK2 (PDB: 1HCK) superimposed onto active CDK2/cyclin A (PDB: 1JST)

on the cytoplasmic side in an asymmetric dimeric assembly in which the C-lobe of one protomer, called *the activator*, stabilizes the second catalytic domain, called *the receiver*, in an active state. This allosteric activation is achieved by a tight contact of the C-lobe of the activator catalytic domain with the N-lobe of the receiver kinase domain in a conformation that is reminiscent of the interaction of activating cyclins with cyclin-dependent kinases (Fig. 4d) [50–53]. This model explains how also catalytically inactive kinases such as HER3 participate in EGFR signalling by acting as activators in heterodimeric receptors [54]. Recent extension of this model also suggested multimeric assemblies [55] (Fig. 4b).

Dimerization is also a key regulatory event in the activation of mitogen-activated protein kinase (MAPK) signalling. The RAS-RAF-MEK-ERK cascade represents a key MAPK signalling pathway controlling cellular proliferation and survival [56] which is often deregulated in cancer [57, 58]. Similar to EGFR several isoforms exist on each level of this pathway. For instance, the serine/threonine-specific

protein kinase RAF (rapidly accelerated fibrosarcoma) comprises three isoforms, A-RAF, B-RAF and C-RAF, which despite their homology differ in the mechanism of their activation. The highly studied family member B-RAF dimerizes in a typical receiver/acceptor asymmetric dimer. Interestingly, kinase inhibitors that bind to the active state of B-RAF stabilize the activator kinase resulting in paradoxical activation of MAPK signalling [59, 60]. The activation of the pathway is also thought to be mediated by C-RAF though B-RAF/C-RAF heterodimerization [61–63]. Kinase inactive mutants of B-RAF, but not C-RAF, can therefore still activate the MAPK cascade by acting as allosteric B-RAF activators [64]. The structural reasons explaining the inability of C-RAF kinase dead mutants activating MAPK signalling have recently been elucidated [65]. Full activity of RAF requires phosphorylation at the activation segment [66, 67] at two sites as well as at the N-terminal acidic (NtA) motif [68, 69]. In B-RAF the NtA motif is acidic (sequence SSDD) and constitutively phosphorylated [69]. In contrast C-RAF and A-RAF lack the two acidic aspartate residues requiring phosphorylation by upstream kinases on their SSYY and SGYY NtA motifs [70]. Hu et al. revealed that NtA motif phosphorylation is only required for the “activator” but not the “receiver” kinase offering a rational why B-RAF can activate C-RAF but not vice versa [65]. Importantly, the oncogenic mutant B-RAF(V600E) does not require dimerization for activity explaining the efficacy of B-RAF inhibitors suppressing MAPK signalling in tumours harbouring this mutant but not in wild-type tissue where activation is observed. The paradoxical activation of MAPK signalling in wild-type tissue has been associated with the development of both benign and malignant cutaneous manifestations, ranging from seborrheic dermatitis-like rashes to eruptive keratoacanthomas and squamous cell carcinomas [71]. These examples demonstrate how the complex activation mechanisms of protein kinases may lead to unexpected adverse clinical manifestations. A schematic of the B-RAF/C-RAF activation model is shown in Fig. 4c.

3.1 Kinase Activation by Interacting Domains and Proteins

The dimerization models of kinase activation highlight the importance of protein interactions stabilizing the kinase active state and suggest that also other proteins and domains may act as kinase activators or inhibitors. Indeed, a large number of interactions regulating kinase activity have been described which include flanking domains, for instance, the SH2 which plays a role stabilizing the inactive [72, 73] as well as active state [74, 75], and these interactions might be exploited therapeutically [76].

One of the best studied examples of kinase regulation by an interacting protein is the cyclin-dependent kinases (CDKs) which are stringently regulated by their interaction partners the cyclins. CDKs are master regulators of the cell cycle, and dysfunction of CDK regulation is a major driver of tumourigenesis and attractive drug targets [77–79]. CDKs typically require activation segment as well as binding of a cyclin for full activity [80–82]. In addition, ATP and peptide binding contribute

to the active state [83]. The main role of the cyclin interaction is to push α C towards the active site, while phosphorylation stabilizes an active conformation of the activation segment by interaction with the HRD arginine residue as described above (Fig. 4d).

In analogy to the role of the pseudokinase HER3 in EGFR activation, other catalytically inactive (pseudo) kinases have been shown to activate catalytically competent kinases in trans. Examples include the activation of JAK family members by N-terminal pseudokinase domains [84] as well as the activation of LKB1 (liver kinase B1) by the pseudokinase “STE20-related adaptor protein” (STRAD α or STRAD β) [85]. STRAD forms a heterotrimeric complex with LKB1 and the scaffolding protein MO25 which dramatically enhances the activity of LKB1, a kinase that does not require activation segment phosphorylation [86]. Despite the lack of catalytic activity, STRAD is still capable of binding ATP with high affinity. The structure of the trimeric complex revealed that MO25 and ATP binding stabilizes an active-like state of STRAD in which MO25 stabilizes active conformation of α C in a similar way as reported for CDK2. This interaction was also observed in dimeric complexes of MO25 with active kinases [87]. The active-like conformation of STRAD is required for LKB1 activation which is achieved by tight contacts of STRAD with the LKB1 substrate binding site [88, 89].

4 Canonical Type-I and Type-II Inhibitor Binding Mode

The plasticity of the kinase catalytic domain that is essential for kinase regulation also offers an opportunity of targeting structurally diverse states. The most explored design strategies are inhibitors targeting the active state (type-I inhibitors), as well as inhibitors that target the so-called DFG-out conformation (type-II inhibitors), an inactive conformation of the DFG motif that leads to an additional large pocket. Since the active state is most stable, the largest fraction of known structural models available in the protein data bank represent the type-I binding mode. Type-I inhibitors are ATP mimetics, thus similar to the adenosine ring of ATP, they form 1-3 hydrogen bonds with the main chain backbone of the kinase hinge region. A large number of typically heterocyclic aromatic mono- to tricyclic ring systems have been explored as ATP mimetic type-I scaffolds. As the active state is highly conserved, selectivity of many type-I inhibitors is low. However, shape complementarity and sequence variations can be used for the development of inhibitors with high or restricted selectivity (Fig. 5a).

For instance, unique sequence features flanking the hinge, such as rare amino acids in hydrophobic regions and variable structural elements, have been shown to increase selectivity of type-I inhibitors. Noteworthy is the gatekeeper residue, which controls the access to the hydrophobic back cavity. Small gatekeeper residues such as threonine provide access to a larger back cavity and are present in only about 5% of all kinases. Type-I inhibitors targeting this hydrophobic site have therefore favourable selectivity profiles by excluding ATP sites with bulkier gatekeeper

residues. Mutating this residue to glycine, which is not present in any human kinases, has been exploited for the development of kinase-specific ATP analogues for functional studies [28].

Combination of two rare sequence variations led to exclusively selective inhibitors. For instance, the p38 inhibitor skepinone-L is a potent and selective type-I inhibitor exploiting the presence of a small gatekeeper residue and an unusual glycine residue located in the kinase hinge region [90–92].

Canonical type-II inhibitors are ATP competitive and target an inactive state of the kinase catalytic domain which is created by the “outward” flip of the DFG motif. This binding mode gained popularity in drug design after it has been found that the first approved kinase inhibitor Gleevec induces and stabilizes this conformation in its main targets ABL and KIT kinase [93, 94]. All type-II inhibitors protrude into the so-called deep pocket which is made accessible in this inactive state. Type-II inhibitors are therefore slightly elongated small molecules when compared to type-I inhibitors. However, the type-II binding mode needs to be confirmed experimentally as a large diversity of binding modes have been observed for putative type-II inhibitors including canonical type-I interactions. In the DFG-out state, the aspartate of the DFG rotates $\sim 180^\circ$ and moves $\sim 5 \text{ \AA}$ away from the ATP-binding site, inactivating the kinase. However, the canonical DFG-out state represents only one of many possible conformations of the DFG motif, and a large number of intermediate states have been described.

Initial expectations that type-II inhibitors would be more selective since they include the dynamic properties of the DFG-out movement were however not confirmed by more comprehensive studies, demonstrating that the DFG-out conformation can be induced by many kinases including also CDKs that are additionally constrained by interaction with cyclins [95–98]. A number of studies

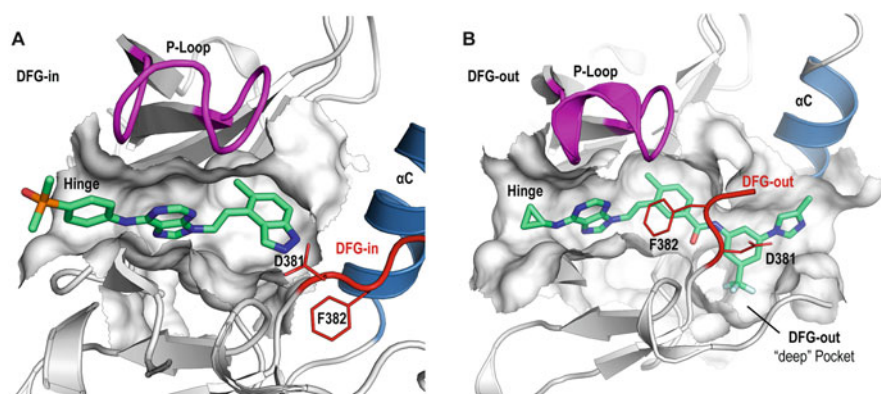


Fig. 5 Comparison of the ATP-binding site in the DFG-in and DFG-out conformation of mouse ABL kinase. Shown is the active state (a) (PDB: 3KF4) and the canonical DFG-out conformation in (b) (PDB: 3KFA). The ATP pocket is shown as a solid surface to demonstrate the structural differences within the pocket. The DFG motif (red) in panels. Inhibitors are shown as stick representation

demonstrated that type-II inhibitors have slow off-rates resulting in prolonged target residence times. However, comparing larger data sets, slow off-rates have also been reported for canonical type-I inhibitors suggesting that a diversity of structural mechanisms contribute to target residency [22, 99, 100].

The type-II pharmacophore shares a common heterocyclic hinge-binding head group which is connected with typically an amide, urea or another hydrophilic linker with a hydrophobic deep pocket binding moiety. Besides the important hinge-binding donor and acceptor interactions, contacts with the highly conserved aspartate backbone from the DFG motif and glutamate present in the α C-helix are common [13, 101].

4.1 *Noncanonical Binding Modes*

The dynamic nature of the kinase catalytic domain gives rise to many noncanonical binding modes that target additional pockets or that constitute intermediate states between classical type-I and type-II binding modes discussed above. One variant is the type-I $\frac{1}{2}$ binding mode, an ATP competitive binding mode recognizing an either active or an intermediate conformation of the DFG motif which is not fully in the canonical out conformation. Often also an α C-out conformation is observed in type-I $\frac{1}{2}$ structures resulting in distorted or interrupted R-spines [102]. An interesting type-I $\frac{1}{2}$ inhibitor is, for instance, a derivative of the p38 type-I inhibitor skepinone-L, which interacts with the hinge region inducing the Gly110 backbone flip while inserting into the R-Spine with a thiophene moiety (Fig. 6a) [103]. Similar to some type-II inhibitors, the induced structural changes result in prolonged target residency and slow off-rate kinetics.

Flexible structure elements such as the α C-helix, P-loop or the A-loop can adopt several types of inactive conformations in addition to the DFG-in and DFG-out state. Besides canonical type-I, type-II and type-I $\frac{1}{2}$ binding, different ways of trapping inactive, high-energy conformations of a given kinase, creating less solvent exposed and more buried cavities, can be found in diverse studies. Lapatinib targets a DFG-in conformation inducing large, inactivating conformational rearrangements unique to the kinase domain in epidermal growth factor receptor (EGF1R) explaining the exceptional selectivity of this drug [104]. The DFG-in inhibitor GSK2606414 targets a unique binding pocket created by an inactive activation segment conformation in the protein kinase R (PKR)-like endoplasmic reticulum kinase (PERK) again resulting in exclusive selectivity [105, 106].

P-loop folded conformations have been found for a set of kinases which harbour aromatic amino acids such as Tyr and Phe at the tip of this loop region [107]. In the active state, these aromatic residues orient their side chains away from the ATP site supporting interaction with the ATP cofactor. In contrast, crystal structures of inhibitor complexes showed that these aromatic side chains can interact with the inhibitor resulting in distortion of the P-loop conformation and capture the P-loop inside the ATP-binding active site. Inhibitors inducing these

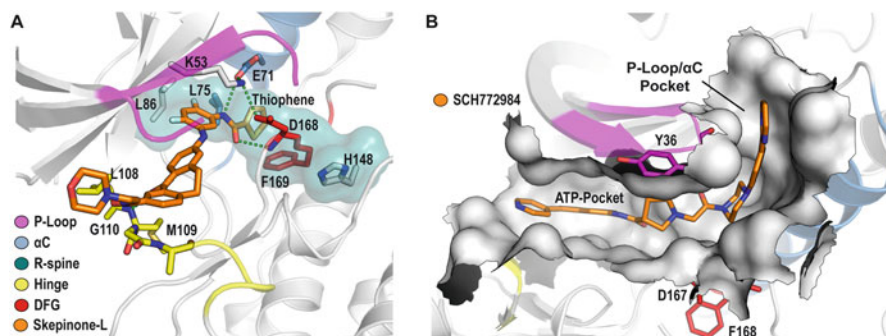


Fig. 6 Examples of noncanonical binding modes. **(a)** A derivative of the p38 inhibitor skepinone-L assuming a type-II/2½ inhibitor binding mode by inserting a thiophene moiety into the R-spine (PDB: 5TBE). **(b)** The ERK1/2 inhibitor SCH772984 targets a pocket induced by a folded P-loop and αC out (PDB: 4QTA)

folded P-loop conformations are usually characterized with significantly narrower selectivity profiles [107].

A folded P-loop allowed also access to a little conserved binding pocket located between the P-loop and αC-helix exemplified by the ERK1/2 inhibitor SCH772984. This unique binding pocket is additional enlarged by an out movement of αC (Fig. 6b). Also in this case, targeting of this unique pocket resulted in high inhibitor selectivity [108].

The MET inhibitor SGX523 binds to a DFG-in conformation with excellent shape complementarity with the ATP-binding site and targets an additional binding pocket created by an unusual conformation of the activation segment [109]. Aromatic stacking interactions of the ligand with the conserved Tyr¹²⁴⁸ residue relocated the A-loop with around a 14 Å conformational change inside the phosphate-binding region of ATP, thus inactivating the catalytic function of the kinase in a highly specific mode. Overall inhibitors with noncanonical binding modes have demonstrated to deliver highly potent and selective compounds, which mostly benefit over canonical type-I and type-II inhibitors. However, as most of the compounds were found serendipitous, it stays a challenging task to find lead structures for the design of noncanonical inhibitors addressing a kinase of interest [14].

4.2 Allosteric Kinase Inhibitors

Two types of allosteric inhibitors have been described: type-III and type-IV inhibitors. Type-III inhibitors interact with the allosteric back-pocket adjacent to the ATP-binding catalytic region, not participating in any hinge-binding interaction. They are considered as steady-state ATP uncompetitive or noncompetitive as

they can bind simultaneous with ATP to an active DFG-in conformation of a kinase disrupting catalytic function by distorting the kinase fold. Some type-III inhibitors also bind in an ATP competitive manner and stabilize the inactive DFG-out state as demonstrated by allosteric inhibitors targeting p38, FAK or IGF1R kinases [110–112]. The *N*-phenylsulfonamide LIMK2 inhibitor published by Goodwin et al. is the first example addressing tyrosin-like kinases (TKL) in an allosteric way. The high potency and the exceptional selectivity of the compound have been achieved by an DFG-out/ α C-out binding mode which has been confirmed by a *co*-crystal structure [113].

The most prominent examples of allosteric type-III inhibitors are clinically approved MEK1/2 inhibitors trametinib, cobimetinib, binimetinib [114–116] and many similar drug candidates that are currently in the clinical development pipeline. Trametinib shows exceptionally high efficiency, potency and selectivity, and it was the first allosteric kinase inhibitor approved by the FDA for the treatment of adult B-RafV600E and V600K-mutated metastatic melanoma [117]. The compound binds to the allosteric back-pocket adjacent to the ATP-binding site making hydrogen bounds to the conserved β 3-lysine and hydrophobic contacts to the β 5-strand, the activation loop and the α C-helix. Upon binding the α C-helix gets displaced leading to inhibition of the kinase activity. The activation loop further adopts a closed conformation prohibiting substrate binding [118, 119]. Stimulated by the success of the first-generation MEK inhibitors, many diverse allosteric MEK1/2 inhibitors occupying this pocket have been reported and are now tested clinically in diverse cancer indications such as non-small cell lung cancer (NSCLC), leukaemia and thyroid and colon cancer [120]. About 30 MEK kinase structures in complex with small-molecule allosteric inhibitors and ATP have been co-crystallized providing inside in important structural aspects of inhibitor binding. Figure 7a exemplifies the allosteric pocket of refametinib in complex with ATP [121].

A potent and isoform selective type-III inhibitor has been published recently by Bagal et al. targeting tropomyosin receptor kinases (TrkA) [122]. As confirmed by structural studies, the inhibitor interacts with an allosteric pocket adjacent to the ATP-binding site accessible in the DFG-out conformation of this kinase. Hydrophobic interactions and hydrogen bonds stabilize the inhibitor also taking advantage of the structurally diverse TrkA juxtamembrane domain. As the targeted pocket in the juxtamembrane domain is unique to TrkA, the compound gains selectivity over the closely related Trk family members TrkB and TrkC [123, 124]. The compound has demonstrated to be efficient in preclinical pain models [122].

Type-IV inhibitors bind reversibly to induced binding pocket that are in contrast to type-III inhibitors distantly located from the ATP-binding site. The ability of type-IV inhibitors inducing structural changes in the catalytic domain results often in inhibition, but not all induced or stable pockets targeted in kinases also abrogate catalytic activity [125]. For instance, a unique binding mode has been observed for GNF-2 with binds to the myristate pocket located at the C-terminal lobe of ABL (Fig. 7b) [126]. GNF-2 and its derivative have an interesting

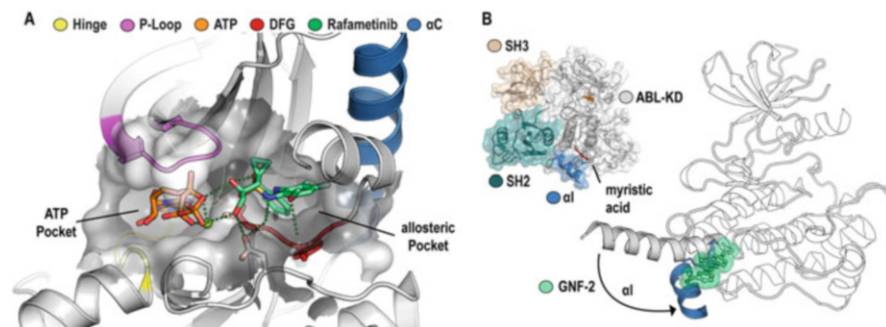


Fig. 7 Examples of binding modes of type-III and type-IV inhibitors. **(a)** Complex of refametinib (green) with MEK1. The inhibitor binds adjacent to the ATP site making hydrophilic interactions with ATP (orange) (PDB: 3E8N). **(b)** Induced changes by the type-IV inhibitor GNF-2. Structural changes of helix I are indicated (PDB: 3K5V and 3KF4). The insert shows the closed autoinhibited conformation of the ABL catalytic domain interacting with the flanking SH2 and SH3 domains. The location of the type-IV binding site is indicated (PDB: 1OPL)

mode of action: the inactive form of ABL is stabilized in an autoinhibited closed conformation, where a myristoylated N-terminal residue binds to the allosteric myristate cleft of the kinase domain (Fig. 7b) [127]. In the BCR-ABL fusion protein, which drives tumourigenesis in a subtype of chronic myelogenous leukaemia (CML) and acute lymphoblastic leukaemia (ALL), the autoinhibitory function of the kinase is lost due to the fusion with BCR, resulting in constitutive activation [128]. GNF-2 mimics the myristate residue disrupting the kinase catalytic function by inducing this inactive state [129]. Structural comparisons showed that the overall conformation is very similar to the native autoinhibition state of ABL, as the N-terminal α I-helix is rotated $\sim 90^\circ$ inwards upon binding of GNF-2 and assembles the SH2 and SH3 domain [126, 130, 131]. In the active state, this α I-helix normally adopts an extended conformation, which was exemplified by the use of allosteric agonists [132]. Interestingly, GNF-2 binding can take place simultaneously with inhibitors targeting the ATP-binding pocket, such as the ATP competitive inhibitors nilotinib, erlotinib or imatinib. Numerous reports in oncology have therefore highlighted the benefits of a combinatorial drug therapy using ATP competitive inhibitors together with type-IV inhibitors as this treatment strategy reduces the risk of drug-inactivating resistance mutations [126]. A promising novel allosteric type-IV BCR-ABL inhibitor asciminib (ABL001) has now entered clinical testing. The compound binds similar to GNF-2 to the myristate pocket of BCR-ABL, therefore interrupting the catalytic function of this constitutively active kinase [133, 134].

Besides the myristate pocket, also other allosteric pockets in the kinase domain have been targeted by allosteric inhibitors. Non-ATP competitive allosteric inhibitors of checkpoint kinase 1 (CHK1) such as the thioquinazolinones target an allosteric site adjacent to the α D-helix. As this pocket normally serves as a substrate recognition site of CHK1-activating kinases, the kinase cannot

longer be activated [135, 136]. The phosphoinositide-dependent protein kinase-1 (PDK1) inhibitors RS1 and RS2 target a hydrophobic motif called PDK1-interacting fragment (PIF) pocket, exclusively found at the N-terminal lobe of PDK1 [137]. Interaction of these inhibitors allosterically inactivates the catalytic function of PDK1.

AKT1 kinase is another interesting target for the design of allosteric inhibitors by offering an alternative mode of inhibition, as all previous described ATP-competitive inhibitors failed in clinical trials so far [132]. The complex domain architecture of AKT provides the possibility to target the kinase allosterically, as demonstrated by the highly selective AKT1 antagonist MK-2206 [138–140]. The compound binds via hydrogen bond and π - π stacking interactions at the interface between the AKT kinase domain and the pleckstrin homology (PH) domain locking the kinase in an inactive conformation preventing membrane association. In this closed so-called PH-in state, the ATP-binding pocket is no longer accessible. In addition, activation of AKT1 is prevented by abrogating recruitment to the plasma membrane. Other described allosteric AKT inhibitors address, for instance, the PH domain preventing structural rearrangements for activation [141–144].

The activation of cyclin-dependent kinases (CDKs) is reliant on their regulatory proteins of the cyclin family, and CDKs are key regulators of cell cycle control [145, 146]. CDKs have been extensively studied as drug targets, and their role in cancer and inflammatory diseases and three CDK4/6 inhibitors has been approved for treatment of cancer [147]. For CDK2 it has been shown that the kinase activity can be interrupted by targeting an allosteric pocket formed between the α C-helix and the β 3-, β 4- and β 5-strand of the N-lobe [148]. The simultaneous binding of two 8-anilino-1-naphthalene sulfonate (ANS) inhibitors changes the orientation of the β -strands, moving the α C-helix outwards and prohibit the binding of the cyclins [149, 150]. However, these inhibitors are at a very early stage of development and have still not been optimized for in vivo use.

As we outlined above, epidermal growth factor receptor (EGFR) kinases are activated by asymmetric dimerization where the C-terminal lobe of the activator kinase activates the receiver kinase domain. EGFR can form either homo- or heterodimeric structures that are reminiscent on the interactions observed in cyclin-dependent activation of CDKs [53, 151]. The recently published inhibitor EAI045 binds to an allosteric pocket formed by displacement of the α C-helix interfering with this activating interaction of the EGFR kinase domain. The excellent selectivity of this allosteric inhibitor allows mutant-selective targeting of EGFR, sparing EGFR wild-type. In combination with the therapeutic antibody cetuximab, EAI045 potently inhibits the mutants EGFR(L858R/T790M) and EGFR(L858R/T790M/C797S) efficiently overcoming resistance of these mutants to current ATP competitive inhibitors [152]. Further allosteric EGFR inhibitors are in development and open new opportunities for the treatment of diverse cancer types such as non-small cell lung cancer (NSCLC) [153, 154].

The first potent and selective I kappa-B kinase β (IKK β) allosteric inhibitor which prevents IKK β activation has been published by Liu et al. in 2018

[155]. The inhibitor 3,4-dichloro-2-ethoxy-*N*-(2,2,6,6-tetramethylpiperidin-4-yl) benzenesulfonamide targets the inactive form of IKK β by binding between the kinase domain and ubiquitin-like domain abrogating activation of IKK as suggested by molecular dynamic simulations. The compound potently inhibited I κ B β / α phosphorylation and NF- κ B activation in cells and opens the opportunity for the design of novel type-IV inhibitors for this key signalling kinase.

Even though the field of allosteric inhibitor development is in its infancy for most kinase targets, it has now been established that type-III and type-IV inhibitors offer several unique advantages when compared to conventional ATP competitive compounds. In particular, allosteric inhibitors are often exclusively selective for kinase isoforms or even mutants by exploring target specific mechanism of activation. They abrogate therefore not simply catalytic activity but also modulate scaffolding function of the kinase and its interaction with regulatory domains or proteins. Type-III and type-IV inhibitors open therefore opportunities for the development of inhibitors with new mode of action utilizing new and unexplored chemical scaffolds. However, despite these advantages, the design of novel lead structures remains a challenging task as no general strategies have been developed for their identification and optimization. Hence, allosteric inhibitors are often found serendipitously in high-throughput screens and by structural studies [13]. We predict, however, that type-III and type-IV inhibitors will play a major role in the future in kinase drug discovery.

5 Conclusions and Outlook

With 48 kinase targeting drugs that are currently approved, protein kinases have developed into one of the most promising areas of drug discovery. Recent approvals increasingly target kinases that play a role in a number of diverse diseases with small patient populations, such as rare oncogenic rearrangements and mutants which have been validated as dominant drivers of tumour development and growth. The current clinical inhibitors utilize predominantly conventional ATP mimetic scaffolds for the development of canonical type-I, type-I $\frac{1}{2}$ and type-II inhibitors. However, also new type of inhibitors such as covalent inhibitors [11] and allosteric inhibitors [13] have now entered clinical development pipelines and have been approved for clinical use.

Allosteric inhibitors are particularly attractive for the development of inhibitors with exclusive selectivity for closely related isoforms and in some cases even for oncogenic mutants. These recent developments may open other therapeutic areas for kinase inhibitor development that have not been successfully targeted by kinase inhibitors because of selectivity issues or the rigid hydrophobic nature of conventional ATP mimetic scaffolds that make it difficult to develop kinase inhibitors, for instance, for neurological applications or long-term systemic use. In addition, allosteric inhibitors also modulate scaffolding function of kinases and how they interact with regulatory proteins. These properties could be used

for the development of functional modulators of pseudokinases that have been linked to the development of many diseases but which have not been targeted so far. Efficient development of allosteric inhibitors would require an even better understanding of the molecular mechanisms of kinase regulation and the dynamic properties of these enzymes. The fraction of the kinome that has been successfully targeted is still quite small despite the large number of disease associations that have been identified for kinases that have not been extensively studied as targets for the development of drugs [8]. It is therefore likely that many new kinases will be explored for the development of new medicines in the future.

Compliance with Ethical Standards

Conflict of interest: The authors have no conflict of interest.

Funding: The authors are grateful for support by the SGC, a registered charity (number 1097737) that receives funds from AbbVie, Bayer Pharma AG, Boehringer Ingelheim, Canada Foundation for Innovation, Eshelman Institute for Innovation, Genome Canada, Innovative Medicines Initiative (EU/EFPIA), Janssen, Merck KGaA Darmstadt Germany, MSD, Novartis Pharma AG, Ontario Ministry of Economic Development and Innovation, Pfizer, São Paulo Research Foundation-FAPESP, Takeda, and Wellcome [106169/ZZ14/Z].

Ethical Approval: This manuscript is a review of previously published accounts, as such no animal or human studies were performed.

References

1. Manning G et al (2002) The protein kinase complement of the human genome. *Science* 298(5600):1912–1934
2. Ishikawa HO et al (2012) The Raine syndrome protein FAM20C is a Golgi kinase that phosphorylates bio-mineralization proteins. *PLoS One* 7(8):e42988
3. Cui J et al (2015) A secretory kinase complex regulates extracellular protein phosphorylation. *elife* 4:e06120
4. Zhang H et al (2018) Structure and evolution of the Fam20 kinases. *Nat Commun* 9(1):1218
5. Taylor SS et al (2013) Pseudokinases from a structural perspective. *Biochem Soc Trans* 41(4):981–986
6. Boudeau J et al (2006) Emerging roles of pseudokinases. *Trends Cell Biol* 16(9):443–452
7. Knapp S, Sundstrom M (2014) Recently targeted kinases and their inhibitors—the path to clinical trials. *Curr Opin Pharmacol* 17:58–63
8. Fedorov O, Muller S, Knapp S (2010) The (un)targeted cancer kinome. *Nat Chem Biol* 6(3):166–169
9. van Linden OP et al (2014) KLIFS: a knowledge-based structural database to navigate kinase-ligand interaction space. *J Med Chem* 57(2):249–277
10. Liu Q et al (2013) Developing irreversible inhibitors of the protein kinase cysteinome. *Chem Biol* 20(2):146–159
11. Chaikuad A et al (2018) The Cysteinome of protein kinases as a target in drug development. *Angew Chem Int Ed Engl* 57(16):4372–4385
12. Mobitz H, Jahnke W, Cowan-Jacob SW (2017) Expanding the opportunities for modulating kinase targets with allosteric approaches. *Curr Top Med Chem* 17(1):59–70
13. Cowan-Jacob SW, Jahnke W, Knapp S (2014) Novel approaches for targeting kinases: allosteric inhibition, allosteric activation and pseudokinases. *Future Med Chem* 6(5):541–561

14. Muller S et al (2015) The ins and outs of selective kinase inhibitor development. *Nat Chem Biol* 11(11):818–821
15. Zheng J et al (1993) 2.2 a refined crystal structure of the catalytic subunit of cAMP-dependent protein kinase complexed with MnATP and a peptide inhibitor. *Acta Crystallogr D Biol Crystallogr* 49(Pt 3):362–365
16. Knighton DR et al (1991) Crystal structure of the catalytic subunit of cyclic adenosine monophosphate-dependent protein kinase. *Science* 253(5018):407–414
17. Taylor SS et al (1992) Structural framework for the protein kinase family. *Annu Rev Cell Biol* 8:429–462
18. Fabbro D, Cowan-Jacob SW, Moebitz H (2015) Ten things you should know about protein kinases: IUPHAR review 14. *Br J Pharmacol* 172(11):2675–2700
19. Nolen B, Taylor S, Ghosh G (2004) Regulation of protein kinases; controlling activity through activation segment conformation. *Mol Cell* 15(5):661–675
20. Adams JA (2003) Activation loop phosphorylation and catalysis in protein kinases: is there functional evidence for the autoinhibitor model? *Biochemistry* 42(3):601–607
21. Johnson LN, Lewis RJ (2001) Structural basis for control by phosphorylation. *Chem Rev* 101(8):2209–2242
22. Roskoski Jr R (2015) A historical overview of protein kinases and their targeted small molecule inhibitors. *Pharmacol Res* 100:1–23
23. Kornev AP et al (2006) Surface comparison of active and inactive protein kinases identifies a conserved activation mechanism. *Proc Natl Acad Sci U S A* 103(47):17783–17788
24. Kornev AP, Taylor SS (2015) Dynamics-driven allostery in protein kinases. *Trends Biochem Sci* 40(11):628–647
25. Ten Eyck LF, Taylor SS, Kornev AP (2008) Conserved spatial patterns across the protein kinase family. *Biochim Biophys Acta* 1784(1):238–243
26. Taylor SS, Kornev AP (2011) Protein kinases: evolution of dynamic regulatory proteins. *Trends Biochem Sci* 36(2):65–77
27. Yang J et al (2009) Contribution of non-catalytic core residues to activity and regulation in protein kinase A. *J Biol Chem* 284(10):6241–6248
28. Bishop AC et al (2000) A chemical switch for inhibitor-sensitive alleles of any protein kinase. *Nature* 407(6802):395–401
29. Yun CH et al (2008) The T790M mutation in EGFR kinase causes drug resistance by increasing the affinity for ATP. *Proc Natl Acad Sci U S A* 105(6):2070–2075
30. Azam M et al (2008) Activation of tyrosine kinases by mutation of the gatekeeper threonine. *Nat Struct Mol Biol* 15(10):1109–1118
31. Sicheri F, Moarefi I, Kuriyan J (1997) Crystal structure of the Src family tyrosine kinase Hck. *Nature* 385(6617):602–609
32. Meng W et al (2002) Structure of mitogen-activated protein kinase-activated protein (MAPKAP) kinase 2 suggests a bifunctional switch that couples kinase activation with nuclear export. *J Biol Chem* 277(40):37401–37405
33. Prowse CN, Lew J (2001) Mechanism of activation of ERK2 by dual phosphorylation. *J Biol Chem* 276(1):99–103
34. Dajani R et al (2003) Structural basis for recruitment of glycogen synthase kinase 3beta to the axin-APC scaffold complex. *EMBO J* 22(3):494–501
35. Weiss A, Schlessinger J (1998) Switching signals on or off by receptor dimerization. *Cell* 94(3):277–280
36. Mellado M et al (2001) Chemokine signaling and functional responses: the role of receptor dimerization and TK pathway activation. *Annu Rev Immunol* 19:397–421
37. Rellos P et al (2010) Structure of the CaMKIIdelta/calmodulin complex reveals the molecular mechanism of CaMKII kinase activation. *PLoS Biol* 8(7):e1000426
38. Rosenberg OS et al (2006) Oligomerization states of the association domain and the holoenzyme of Ca²⁺/CaM kinase II. *FEBS J* 273(4):682–694
39. Rosenberg OS et al (2005) Structure of the autoinhibited kinase domain of CaMKII and SAXS analysis of the holoenzyme. *Cell* 123(5):849–860

40. Lochhead PA et al (2006) A chaperone-dependent GSK3beta transitional intermediate mediates activation-loop autophosphorylation. *Mol Cell* 24(4):627–633
41. Lochhead PA et al (2005) Activation-loop autophosphorylation is mediated by a novel transitional intermediate form of DYRKs. *Cell* 121(6):925–936
42. Oliver AW, Knapp S, Pearl LH (2007) Activation segment exchange: a common mechanism of kinase autophosphorylation? *Trends Biochem Sci* 32(8):351–356
43. Oliver AW et al (2006) Trans-activation of the DNA-damage signalling protein kinase Chk2 by T-loop exchange. *EMBO J* 25(13):3179–3190
44. Pike AC et al (2008) Activation segment dimerization: a mechanism for kinase autophosphorylation of non-consensus sites. *EMBO J* 27(4):704–714
45. Yarden Y, Sliwkowski MX (2001) Untangling the ErbB signalling network. *Nat Rev Mol Cell Biol* 2(2):127–137
46. Citri A, Skaria KB, Yarden Y (2003) The deaf and the dumb: the biology of ErbB-2 and ErbB-3. *Exp Cell Res* 284(1):54–65
47. Yarden Y, Schlessinger J (1987) Self-phosphorylation of epidermal growth factor receptor: evidence for a model of intermolecular allosteric activation. *Biochemistry* 26(5):1434–1442
48. Lemmon MA, Schlessinger J, Ferguson KM (2014) The EGFR family: not so prototypical receptor tyrosine kinases. *Cold Spring Harb Perspect Biol* 6(4):a020768
49. Schlessinger J (2002) Ligand-induced, receptor-mediated dimerization and activation of EGF receptor. *Cell* 110(6):669–672
50. Jura N et al (2009) Mechanism for activation of the EGF receptor catalytic domain by the juxtamembrane segment. *Cell* 137(7):1293–1307
51. Jura N et al (2009) Structural analysis of the catalytically inactive kinase domain of the human EGF receptor 3. *Proc Natl Acad Sci U S A* 106(51):21608–21613
52. Jura N et al (2011) Catalytic control in the EGF receptor and its connection to general kinase regulatory mechanisms. *Mol Cell* 42(1):9–22
53. Zhang X et al (2006) An allosteric mechanism for activation of the kinase domain of epidermal growth factor receptor. *Cell* 125(6):1137–1149
54. Endres NF et al (2013) Conformational coupling across the plasma membrane in activation of the EGF receptor. *Cell* 152(3):543–556
55. Huang Y et al (2016) Molecular basis for multimerization in the activation of the epidermal growth factor receptor. *elife* 5:e14107
56. Wellbrock C, Karasarides M, Marais R (2004) The RAF proteins take centre stage. *Nat Rev Mol Cell Biol* 5(11):875–885
57. Brose MS et al (2002) BRAF and RAS mutations in human lung cancer and melanoma. *Cancer Res* 62(23):6997–7000
58. Davies H et al (2002) Mutations of the BRAF gene in human cancer. *Nature* 417(6892):949–954
59. Farrar MA, Alberol-Ila J, Perlmutter RM (1996) Activation of the Raf-1 kinase cascade by coumermycin-induced dimerization. *Nature* 383(6596):178–181
60. Hatzivassiliou G et al (2010) RAF inhibitors prime wild-type RAF to activate the MAPK pathway and enhance growth. *Nature* 464(7287):431–435
61. Weber CK et al (2001) Active Ras induces heterodimerization of cRaf and BRaf. *Cancer Res* 61(9):3595–3598
62. Heidorn SJ et al (2010) Kinase-dead BRAF and oncogenic RAS cooperate to drive tumor progression through CRAF. *Cell* 140(2):209–221
63. Poulikakos PI et al (2010) RAF inhibitors transactivate RAF dimers and ERK signalling in cells with wild-type BRAF. *Nature* 464(7287):427–430
64. Garnett MJ et al (2005) Wild-type and mutant B-RAF activate C-RAF through distinct mechanisms involving heterodimerization. *Mol Cell* 20(6):963–969
65. Hu J et al (2013) Allosteric activation of functionally asymmetric RAF kinase dimers. *Cell* 154(5):1036–1046

66. Chong H, Lee J, Guan KL (2001) Positive and negative regulation of Raf kinase activity and function by phosphorylation. *EMBO J* 20(14):3716–3727
67. Zhang BH, Guan KL (2000) Activation of B-Raf kinase requires phosphorylation of the conserved residues Thr598 and Ser601. *EMBO J* 19(20):5429–5439
68. Diaz B et al (1997) Phosphorylation of Raf-1 serine 338-serine 339 is an essential regulatory event for Ras-dependent activation and biological signaling. *Mol Cell Biol* 17(8):4509–4516
69. Mason CS et al (1999) Serine and tyrosine phosphorylations cooperate in Raf-1, but not B-Raf activation. *EMBO J* 18(8):2137–2148
70. Morrison DK, Cutler RE (1997) The complexity of Raf-1 regulation. *Curr Opin Cell Biol* 9(2):174–179
71. Owen JL, Lopez IE, Desai SR (2015) Cutaneous manifestations of vemurafenib therapy for metastatic melanoma. *J Drugs Dermatol* 14(5):509–510
72. Young MA et al (2001) Dynamic coupling between the SH2 and SH3 domains of c-Src and Hck underlies their inactivation by C-terminal tyrosine phosphorylation. *Cell* 105(1):115–126
73. Hantschel O et al (2003) A myristoyl/phosphotyrosine switch regulates c-Abl. *Cell* 112(6):845–857
74. Filippakopoulos P et al (2008) Structural coupling of SH2-kinase domains links Fes and Abl substrate recognition and kinase activation. *Cell* 134(5):793–803
75. Lorenz S et al (2015) Crystal structure of an SH2-kinase construct of c-Abl and effect of the SH2 domain on kinase activity. *Biochem J* 468(2):283–291
76. Grebien F et al (2011) Targeting the SH2-kinase interface in Bcr-Abl inhibits leukemogenesis. *Cell* 147(2):306–319
77. Malumbres M, Barbacid M (2009) Cell cycle, CDKs and cancer: a changing paradigm. *Nat Rev Cancer* 9(3):153–166
78. Asghar U et al (2015) The history and future of targeting cyclin-dependent kinases in cancer therapy. *Nat Rev Drug Discov* 14(2):130–146
79. Whittaker SR et al (2017) Inhibitors of cyclin-dependent kinases as cancer therapeutics. *Pharmacol Ther* 173:83–105
80. De Bondt HL et al (1993) Crystal structure of cyclin-dependent kinase 2. *Nature* 363(6430):595–602
81. Russo AA, Jeffrey PD, Pavletich NP (1996) Structural basis of cyclin-dependent kinase activation by phosphorylation. *Nat Struct Biol* 3(8):696–700
82. Echaliier A, Endicott JA, Noble ME (2010) Recent developments in cyclin-dependent kinase biochemical and structural studies. *Biochim Biophys Acta* 1804(3):511–519
83. Brown NR et al (1999) The structural basis for specificity of substrate and recruitment peptides for cyclin-dependent kinases. *Nat Cell Biol* 1(7):438–443
84. Babon JJ et al (2014) The molecular regulation of Janus kinase (JAK) activation. *Biochem J* 462(1):1–13
85. Boudeau J et al (2004) Analysis of the LKB1-STRAD-MO25 complex. *J Cell Sci* 117(Pt 26):6365–6375
86. Baas AF et al (2003) Activation of the tumour suppressor kinase LKB1 by the STE20-like pseudokinase STRAD. *EMBO J* 22(12):3062–3072
87. Mehellou Y et al (2013) Structural insights into the activation of MST3 by MO25. *Biochem Biophys Res Commun* 431(3):604–609
88. Zeqiraj E et al (2009) Structure of the LKB1-STRAD-MO25 complex reveals an allosteric mechanism of kinase activation. *Science* 326(5960):1707–1711
89. Zeqiraj E et al (2009) ATP and MO25alpha regulate the conformational state of the STRADalpha pseudokinase and activation of the LKB1 tumour suppressor. *PLoS Biol* 7(6):e1000126
90. Koeberle SC et al (2011) Skepinone-L is a selective p38 mitogen-activated protein kinase inhibitor. *Nat Chem Biol* 8(2):141–143

91. Fischer S et al (2013) Dibenzosuberones as p38 mitogen-activated protein kinase inhibitors with low ATP competitiveness and outstanding whole blood activity. *J Med Chem* 56(1):241–253
92. Martz KE et al (2012) Targeting the hinge glycine flip and the activation loop: novel approach to potent p38alpha inhibitors. *J Med Chem* 55(17):7862–7874
93. Schindler T et al (2000) Structural mechanism for STI-571 inhibition of abelson tyrosine kinase. *Science* 289(5486):1938–1942
94. Mol CD et al (2004) Structural basis for the autoinhibition and STI-571 inhibition of c-Kit tyrosine kinase. *J Biol Chem* 279(30):31655–31663
95. Karaman MW et al (2008) A quantitative analysis of kinase inhibitor selectivity. *Nat Biotechnol* 26(1):127–132
96. Goldstein DM, Gray NS, Zarrinkar PP (2008) High-throughput kinase profiling as a platform for drug discovery. *Nat Rev Drug Discov* 7(5):391–397
97. Zhao Z et al (2014) Exploration of type II binding mode: a privileged approach for kinase inhibitor focused drug discovery? *ACS Chem Biol* 9(6):1230–1241
98. Alexander LT et al (2015) Type II inhibitors targeting CDK2. *ACS Chem Biol* 10(9):2116–2125
99. Georgi V et al (2018) Binding kinetics survey of the drugged Kinome. *J Am Chem Soc* 140(46):15774–15782
100. Heroven C et al (2018) Halogen-aromatic pi interactions modulate inhibitor residence times. *Angew Chem Int Ed Engl* 57(24):7220–7224
101. Liu Y, Gray NS (2006) Rational design of inhibitors that bind to inactive kinase conformations. *Nat Chem Biol* 2(7):358–364
102. Zuccotto F et al (2010) Through the “gatekeeper door”: exploiting the active kinase conformation. *J Med Chem* 53(7):2681–2694
103. Wentsch HK et al (2017) Optimized target residence time: type II/2 inhibitors for p38alpha MAP kinase with improved binding kinetics through direct interaction with the R-spine. *Angew Chem Int Ed Engl* 56(19):5363–5367
104. Wood ER et al (2004) A unique structure for epidermal growth factor receptor bound to GW572016 (Lapatinib): relationships among protein conformation, inhibitor off-rate, and receptor activity in tumor cells. *Cancer Res* 64(18):6652–6659
105. Axten JM et al (2012) Discovery of 7-methyl-5-(1-([3-(trifluoromethyl)phenyl]acetyl)-2,3-dihydro-1H-indol-5-yl)-7H-pyrrolo[2,3-d]pyrimidin-4-amine (GSK2606414), a potent and selective first-in-class inhibitor of protein kinase R (PKR)-like endoplasmic reticulum kinase (PERK). *J Med Chem* 55(16):7193–7207
106. Wang H et al (2010) Structural determinants of PERK inhibitor potency and selectivity. *Chem Biol Drug Des* 76(6):480–495
107. Guimaraes CR et al (2011) Understanding the impact of the P-loop conformation on kinase selectivity. *J Chem Inf Model* 51(6):1199–1204
108. Chaikuad A et al (2014) A unique inhibitor binding site in ERK1/2 is associated with slow binding kinetics. *Nat Chem Biol* 10(10):853–860
109. Buchanan SG et al (2009) SGX523 is an exquisitely selective, ATP-competitive inhibitor of the MET receptor tyrosine kinase with antitumor activity in vivo. *Mol Cancer Ther* 8(12):3181–3190
110. Over B et al (2013) Natural-product-derived fragments for fragment-based ligand discovery. *Nat Chem* 5(1):21–28
111. Tomita N et al (2013) Structure-based discovery of cellular-active allosteric inhibitors of FAK. *Bioorg Med Chem Lett* 23(6):1779–1785
112. Heinrich T et al (2010) Allosteric IGF-1R inhibitors. *ACS Med Chem Lett* 1(5):199–203
113. Goodwin NC et al (2015) Discovery of a type III inhibitor of LIM kinase 2 that binds in a DFG-out conformation. *ACS Med Chem Lett* 6(1):53–57

114. Odogwu L et al (2018) FDA approval summary: Dabrafenib and Trametinib for the treatment of metastatic non-small cell lung cancers Harboring BRAF V600E mutations. *Oncologist* 23(6):740–745
115. Garnock-Jones KP (2015) Cobimetinib: First Global Approval. *Drugs* 75(15):1823–1830
116. Martin-Liberal J (2018) Encorafenib plus binimetinib: an embarrassment of riches. *Lancet Oncol* 19(10):1263–1264
117. Wu P, Clausen MH, Nielsen TE (2015) Allosteric small-molecule kinase inhibitors. *Pharmacol Ther* 156:59–68
118. Hashemzadeh S, Ramezani F, Rafii-Tabar H (2018) Study of molecular mechanism of the interaction between MEK1/2 and Trametinib with docking and molecular dynamic simulation. *Interdiscip Sci* 11(1):115–124
119. Roskoski Jr R (2017) Allosteric MEK1/2 inhibitors including cobimetanib and trametinib in the treatment of cutaneous melanomas. *Pharmacol Res* 117:20–31
120. Shang J et al (2016) Allosteric modulators of MEK1: drug design and discovery. *Chem Biol Drug Des* 88(4):485–497
121. Iverson C et al (2009) RDEA119/BAY 869766: a potent, selective, allosteric inhibitor of MEK1/2 for the treatment of cancer. *Cancer Res* 69(17):6839–6847
122. Bagal SK et al (2018) Discovery of allosteric, potent, subtype selective, and peripherally restricted TrkA kinase inhibitors. *J Med Chem* 62(1):247–265
123. Furuya N et al (2017) The juxtamembrane region of TrkA kinase is critical for inhibitor selectivity. *Bioorg Med Chem Lett* 27(5):1233–1236
124. Freeman SN, Mainwaring WI, Furr BJ (1989) A possible explanation for the peripheral selectivity of a novel non-steroidal pure antiandrogen, Casodex (ICI 176,334). *Br J Cancer* 60(5):664–668
125. Lamba V, Ghosh I (2012) New directions in targeting protein kinases: focusing upon true allosteric and bivalent inhibitors. *Curr Pharm Des* 18(20):2936–2945
126. Zhang J et al (2010) Targeting Bcr-Abl by combining allosteric with ATP-binding-site inhibitors. *Nature* 463(7280):501–506
127. Nagar B et al (2003) Structural basis for the autoinhibition of c-Abl tyrosine kinase. *Cell* 112(6):859–871
128. Pendergast AM, Witte ON (1987) Role of the ABL oncogene tyrosine kinase activity in human leukaemia. *Baillieres Clin Haematol* 1(4):1001–1020
129. Adrian FJ et al (2006) Allosteric inhibitors of Bcr-abl-dependent cell proliferation. *Nat Chem Biol* 2(2):95–102
130. Schneider R et al (2012) Direct binding assay for the detection of type IV allosteric inhibitors of Abl. *J Am Chem Soc* 134(22):9138–9141
131. Nagar B et al (2006) Organization of the SH3-SH2 unit in active and inactive forms of the c-Abl tyrosine kinase. *Mol Cell* 21(6):787–798
132. Fang Z, Grutter C, Rauh D (2013) Strategies for the selective regulation of kinases with allosteric modulators: exploiting exclusive structural features. *ACS Chem Biol* 8(1):58–70
133. Eadie LN et al (2018) The new allosteric inhibitor asciminib is susceptible to resistance mediated by ABCB1 and ABCG2 overexpression in vitro. *Oncotarget* 9(17):13423–13437
134. Schoepfer J et al (2018) Discovery of Asciminib (ABL001), an allosteric inhibitor of the tyrosine kinase activity of BCR-ABL1. *J Med Chem* 61(18):8120–8135
135. Converso A et al (2009) Development of thioquinazolinones, allosteric Chk1 kinase inhibitors. *Bioorg Med Chem Lett* 19(4):1240–1244
136. Vanderpool D et al (2009) Characterization of the CHK1 allosteric inhibitor binding site. *Biochemistry* 48(41):9823–9830
137. Rettenmaier TJ et al (2014) A small-molecule mimic of a peptide docking motif inhibits the protein kinase PDK1. *Proc Natl Acad Sci U S A* 111(52):18590–18595
138. Hartnett JC et al (2008) Optimization of 2,3,5-trisubstituted pyridine derivatives as potent allosteric Akt1 and Akt2 inhibitors. *Bioorg Med Chem Lett* 18(6):2194–2197

139. Siu T et al (2008) The design and synthesis of potent and cell-active allosteric dual Akt 1 and 2 inhibitors devoid of hERG activity. *Bioorg Med Chem Lett* 18(14):4191–4194
140. Bjune K et al (2018) MK-2206, an allosteric inhibitor of AKT, stimulates LDLR expression and LDL uptake: a potential hypocholesterolemic agent. *Atherosclerosis* 276:28–38
141. Huang BX et al (2017) Identification of 4-phenylquinolin-2(1H)-one as a specific allosteric inhibitor of Akt. *Sci Rep* 7(1):11673
142. Ahad AM et al (2011) Development of sulfonamide AKT PH domain inhibitors. *Bioorg Med Chem* 19(6):2046–2054
143. Kim D et al (2010) A small molecule inhibits Akt through direct binding to Akt and preventing Akt membrane translocation. *J Biol Chem* 285(11):8383–8394
144. Ranieri C et al (2018) In vitro efficacy of ARQ 092, an allosteric AKT inhibitor, on primary fibroblast cells derived from patients with PIK3CA-related overgrowth spectrum (PROS). *Neurogenetics* 19(2):77–91
145. Jeffrey PD et al (1995) Mechanism of CDK activation revealed by the structure of a cyclinA-CDK2 complex. *Nature* 376(6538):313–320
146. Roskoski Jr R (2018) Cyclin-dependent protein serine/threonine kinase inhibitors as anticancer drugs. *Pharmacol Res* 139:471–488
147. Thill M, Schmidt M (2018) Management of adverse events during cyclin-dependent kinase 4/6 (CDK4/6) inhibitor-based treatment in breast cancer. *Ther Adv Med Oncol* 10:1758835918793326
148. Christodoulou MS et al (2017) Probing an allosteric pocket of CDK2 with small molecules. *ChemMedChem* 12(1):33–41
149. Mariaule G, Belmont P (2014) Cyclin-dependent kinase inhibitors as marketed anticancer drugs: where are we now? A short survey. *Molecules* 19(9):14366–14382
150. Betzi S et al (2011) Discovery of a potential allosteric ligand binding site in CDK2. *ACS Chem Biol* 6(5):492–501
151. Zhao P et al (2018) Crystal structure of EGFR T790M/C797S/V948R in complex with EAI045. *Biochem Biophys Res Commun* 502(3):332–337
152. Jia Y et al (2016) Overcoming EGFR(T790M) and EGFR(C797S) resistance with mutant-selective allosteric inhibitors. *Nature* 534(7605):129–132
153. Caporuscio F et al (2018) Identification of small-molecule EGFR allosteric inhibitors by high-throughput docking. *Future Med Chem* 10(13):1545–1553
154. Carlino L et al (2018) Structure-activity relationships of Hexahydrocyclopenta[c]quinoline derivatives as allosteric inhibitors of CDK2 and EGFR. *ChemMedChem* 13(24):2627–2634
155. Liu H et al (2018) A novel allosteric inhibitor that prevents IKKbeta activation. *MedChemComm* 9(2):239–243

Molecular Modeling of Protein Kinases: Current Status and Challenges



Antti Poso

Contents

1	Introduction	26
2	Virtual Screening and Docking	29
3	MD Simulations	31
4	Allosteric Control of Kinases	34
5	Discussion	36
	References	37

Abstract Molecular modeling and virtual screening are currently among the main tools in kinase inhibitor design. In addition, molecular dynamics is actively used to study structural features and function of kinases. During the last 20 years, computational power has dramatically increased, and at the same time, algorithms have become more user-friendly. This has resulted in a situation where these powerful methods are more easily available for even larger groups of scientists. To effectively use computational methods, one should understand in great detail how protein kinases are functioning and how current protein kinase inhibitors interact with the kinase domain. This short review presents some of the main topics of kinase modeling, concentrating especially on proper selection and preparation of protein structure and general usage of MD simulations.

Keywords Docking, Molecular dynamics, Structure-based drug design, Virtual screening

A. Poso (✉)

School of Pharmacy, University of Eastern Finland, Kuopio, Finland

Department of Internal Medicine VIII, University Hospital Tübingen, Tübingen, Germany

e-mail: antti.poso@uef.fi

1 Introduction

One of the first molecular modeling studies dealing with protein kinases was published by Fry, Kuby, and Mildvan [1] in the mid-1980s. The authors used NMR NOE's and molecular modeling to understand how MgATP interacts with rabbit muscle adenylate kinase. This study can be understood as a starting point for a great deal of and increasingly more active research on small molecule-kinase interactions. Surprisingly, we are still facing partially the same obstacles as Fry et al. some 35 years ago. In a highly simplified way, we are trying to understand structural properties of kinases and how kinase inhibitors are modifying these properties. The current main question is how kinase function and conformation effect upon the inhibitor binding are related to each other. Although the current paradigm in kinase drug design is to interfere the biological activity of kinase with small molecules, we do now understand that this inhibition cannot be modeled only by a simple docking experiment between a small drug-like molecule and the ATP-binding site of the target kinase. Instead, it is mandatory to study the whole kinase domain with solvent and, in many cases, with additional domains and interacting proteins.

This chapter will deal with the molecular modeling of kinases. Although some structural biology data is also presented, I would warmly recommend the reader to study the excellent text by Röhme, Krämer, and Knapp in this book (Chap. XX) to begin with. Modeling is, after all, based on our knowledge of structural biology, and very little can be achieved without high-quality protein structures. In addition, protein kinases share several unique structural features, like hydrophobic spines [2], which one should know prior to looking at the details of molecular modeling around kinases. This chapter is not to be taken as a guide on how to model kinases, neither is it a complete review of the topic. The emphasis is more on indicating those critical factors which one must consider when and if protein kinases are modeled. At the same time, this chapter concentrates mainly on structure-based drug design aspects, and detailed analysis of quantum mechanical studies or QSAR/machine learning, for example, is not included. One reason why QSAR and related methods are not analyzed is that high-quality QSAR studies of kinase inhibitors are rare and most of the time only explanatory in nature. One can even argue that since the invention of 3D-QSAR studies in the late 1980s [3], the development of QSAR methods in drug discovery has been quite negligible, and structure-based methods are now the mainstream in drug design.

So, what are the modeling issues we are currently struggling with, and what are the main approaches computational medicinal chemists and molecular modelers are utilizing? A simple answer to this question is “molecular motion” and “molecular dynamics.” In other words, the aim is to go beyond simple virtual screening and docking and look at how topics like solvent effects, local and global molecular motions, and protein-protein interactions are modeled.

And yet, there is still one preliminary question to be answered: what is molecular modeling? Maybe the best response is offered by Ander Leach: “Molecular

modelling encompasses all methods, theoretical and computational, used to model or mimic the behavior of molecules.” The art of modeling is to include all those factors which are needed to gain correct results and not those which are not affecting the outcome. In early 2000 many scientists used to think that all that was needed to model kinase inhibitor binding and biological activity was a proper knowledge of the kinase binding cavity structure and a good scoring function. Unfortunately, kinase life (like protein life in general) is more complicated, and several findings have forced us to rethink what is important. As an example, the first-generation Raf inhibitors turned out to be both kinase inhibitors and activators at the same time [4]. This paradoxical finding cannot be explained simply by binding interactions or structural data based on protein kinase X-ray structures but requires considering kinase dimerization and allosteric effects between kinase domains [5]. Another classical example, shown by Wood et al. [6], demonstrates how three kinase inhibitors, lapatinib (Tykerb, GlaxoSmithKline: GW572916), gefitinib (Iressa, AstraZeneca: ZD-1839), and erlotinib (Tarceva, OSI: OSI-774) all bind the EGFR kinase domain with almost equal IC_{50} values but yet a dramatically different effect on cell cultures. As it turned out, these compounds have big differences in target residence times. So, simple IC_{50} or binding affinity in the form of pK_i is not the dictating factor for biological activity, but, instead, dynamic properties are critical. A third example demonstrates how solvent effects do explain kinase inhibitors’ structure-activity relationships. Direct interactions between cyclin G-associated kinase (GAK) and a library of 4-anilinoquin(az)olines were not able to explain structure-activity relationships (SAR). Instead, desolvation energies, reflecting enthalpy and entropy of individual water molecules within the GAK binding site, were critical for building a systematic SAR model. This example clearly indicates that water should not be neglected during kinase modeling [7]. Although these examples may seem to be quite unique, there is one common factor combining all the cases. To gain useful modeling results, we must consider the protein including solvent and dynamic aspects of the whole molecular system.

So, should we model protein kinases alone or inhibitor-kinase systems in general? A simple, fundamental answer originates from thermodynamics. Equation (1) shows the very basic relationship between binding affinity and Gibbs energy of binding:

$$\Delta G = -RT \ln K_a = -RT \ln \left(\frac{1}{K_d} \right) = \mu_{PL} - \mu_L - \mu_P \quad (1)$$

Equation (1), Gibbs energy of binding (ΔG^0), R = Gas constant, T = temperature (K), K_a = drug-binding association constant, K_d = drug-binding dissociation constant, μ_{PL} = chemical potential of protein/ligand complex in solution, μ_L = chemical potential of Ligand in solution and μ_P = chemical potential of protein in solution

As binding energy (and affinity) is related to the chemical potential of the protein-ligand system in solution, one must consider all the factors which are involved in the chemical potential. Thus, one must study how the solvent interacts with the protein/ligand and the protein-ligand complex. In addition, one must consider all the configurations (protein-ligand poses with different conformations) of the protein-ligand complex which are relevant for binding. This is not done by two very popular methods, namely, docking and QSAR, since in docking every individual pose is scored independently, and QSAR does usually not consider anything else than ligand 2D or 3D structural descriptors. Both of these methods have been successfully used for quite a long time, QSAR since early 1960 [8] and docking from the early 1990s [9]. As one can easily understand, those methods were developed to be fast and easily available, thus not requiring substantial computational power. This was only possible by making those major simplifications which, at the time, were acceptable but should be reconsidered in the current world.

Thanks to the current massive GPU and classical supercomputer environments, it is now possible to study a full protein-solvent-ligand ensemble in a dynamical fashion. Without going into details, it can be stated that molecular dynamics (MD) approaches are the natural answer to the problem presented in Eq. (1). Unfortunately, usage of MD simulations means that the computational burden is much higher than with classical molecular docking or QSAR. This is not the only issue, since results from MD simulations are quite complicated. Both, docking and QSAR, are popular methods, partially, because they deliver simple numerical results (scoring or predictions), easy to understand, and be compared. Even the most “complicated” QSAR method, CoMFA [3], returns a clear (and often misleading) 3D image indicating those regions around the ligand structure which should be modified to gain better binding interactions. The results from MD simulations are in the form of molecular trajectories, describing atomistic movement and corresponding kinetic and potential energies. One must use a substantial amount of time and, paradoxically, computing power to analyze large MD trajectories before results can be used to guide medicinal chemistry work. At the same time, there is no easy and general procedure how to analyze MD trajectories quantitatively. Analytical procedure strongly depends on the research question. Thus it may be very time-consuming just to find what to search for from the trajectory data.

Besides understanding atomic motion, one must use an appropriate protein conformation for kinase modeling. Kinase inhibitors are classified as types I, 1½, and II–VI [10]. The consensus is that type I inhibitors target catalytically active, DFG-in conformation, and thus compete with ATP, while type II inhibitors target inactive DFG-out conformation which lacks the ATP. Type 1½ inhibitors have high affinity toward both DFG-in-like and DFG-out conformations, while types III and IV are used for allosteric inhibitors. The last two types, V (bivalent inhibitor) and VI (covalent) are not commonly used. Since this classification is based on the kinase conformation, as seen in the corresponding inhibitor-kinase complex, one can easily understand that protein kinase conformation does actually matter. Modeling must be based on the protein structure matching the requirements of an inhibitor. Thus, if one is modeling a classical type II inhibitor but the target protein conformation is a

catalytically active DFG-in (type I), all the structure-based modeling methods will ultimately yield false results. The true issue is the fact that the kinase inhibitor structure alone is not enough to predict if the inhibitor is type I, II, or something else. Also very minor changes to the inhibitor structure might change the conformation of the target kinase [11].

2 Virtual Screening and Docking

Docking is the most commonly used tool in virtual screening. In the case of kinase inhibitors, one can easily find tens if not hundreds of publications showing different types of docking approaches used. There is indeed a large number of different software packages and scoring functions to choose from (for a recent review about docking in general and especially about the pitfalls, see Pantsar and Poso [12]), but one cannot claim that any specific method would be clearly better than another. This does not mean that all the approaches are working or that it doesn't matter how virtual screening is carried out [13]. Maybe one of the most critical aspects in molecular modeling of kinases is the selection of protein kinase conformations to be used in virtual screening. Kinases are well-known enzymes, and thus conformational variation has been extensively studied [14]. The main way to classify kinase structures is to use DFG-in and DFG-out families, which refer to the DFG domain orientation [15]. Although DFG-in and DFG-out are also well explained elsewhere in this book, it is good to look at the definition on a general level.

The activation loop of the kinase protein controls the enzymatic activity by relocating itself onto the surface of the protein, resulting in kinase inactivation. Additional activity control is reached by the DFG motif conformational shifts, so that the phenylalanine of DFG occupies the ATP binding pocket, and catalytically active aspartate is pointing away from the active site. In a catalytically active state, the kinase is always in DFG-in conformation binding the magnesium ion that interacts directly with an oxygen atom of the β phosphate of ATP. In addition, the active state includes glutamate from the C-helix in a salt bridge with a lysine of the β 3 strand. This salt bridge stabilizes the hydrogen bonds between lysine and oxygen atoms of the α and β phosphates of ATP [15].

When we look at the most recent molecular modeling studies where docking has been used for kinase inhibitor design, we only consider those studies where docking has been validated either by biological (in vitro) assays or/and X-ray crystallography. It is mandatory that if modeling data are published, and especially if there are predictions concerning a specific compound, these predictions must be supported by empirical data. In such a case where modeling is used to make and publish detailed activity predictions, it will create a situation where the given compounds, even the hypothetical ones, cannot be protected by patents.

Docking is basically just a method to create and score a protein-ligand binding pose. Indeed, the simplest way to use docking is to estimate a single compound binding mode like in the work of Lee et al. [16], which utilized docking together with

several other molecule methods. Although it is not mandatory, validation of the docking pose would increase the value of the study [17]. One simple approach was used by Ortuso et al. who combined several docking results (Glide XP) from X-ray structures of the Sgk1 kinase [18]. This approach yielded an average docking score which was used to identify a sub-micromolar Sgk1 inhibitor. Many research groups have used more complicated approaches and combined docking with binding free energy calculations and/or QSAR [19] or used a sequential approach with pharmacophore pre-screening before docking with different methods [20]. It is seldom that docking is used alone, and typically, docking is combined with one or several other modeling and screening methods. The reason for this complexity is quite simple: scoring functions are far from optimal, and typical docking results include a high number of false-positive and false-negative “hits” [12]. Due to this, kinase-specific scoring functions or rescoring have also been used resulting in the identification of a sub-micromolar FGFR1 inhibitor [21].

As mentioned above, the DFG domain conformation indicates if the kinase is in an active or inactive state. This DFG-domain description raises some questions that should be considered when carrying out virtual screening. The most important one is quite simple: Should we target DFG-in or DFG-out or some other conformations? Naturally, the simplest approach is to use whatever empirical structure is available. This is a valid option if one is ready to accept any type of inhibitor as a result. In many cases, researchers are more interested to find either type II or type I½ inhibitor, especially, since it has been stated that better selectivity is reached if inactive kinase conformation is targeted [22]. As most of the empirical kinase structures are the DFG-in type [23], targeting inactive kinase conformation is not automatically an option. In theory, one can modify the kinase structure and use, for example, homology modeling or MD simulations to produce a DFG-out structure by using a catalytically active DFG-in conformation as a starting point. In practice, this approach is difficult to use and requires a substantial amount of pre-existing structural data [24]. Docking itself is a static approach, and structural errors outside of the protein binding site do not affect the outcome. Thus, one should be able to get viable results if the binding cavity itself has an appropriate conformation. This is probably also valid for induced-fit docking methods, if the used method is not based on MD simulations. However, one cannot use a classical MD-ensemble docking if the kinase structure has structural issues anywhere near the binding site, since those errors would easily be reflected to the binding site of the protein kinase.

One way to modify the kinase structure is to use an induced-fit protocol and modify the target kinase conformation so that structural features are as required. This approach was used to identify inhibitors against zeta-chain protein kinase 70 kDa (ZAP70) [25]. The gatekeeper residue methionine 414 was modified to resemble the structure of Janus kinase 2 (JAK2) by aligning ZAP70 to JAK2 binding sites. In addition, a potent JAK2 inhibitor was docked to the resulting structure, and the ZAP70/JAK2-inhibitor complex was relaxed by MD simulation procedure. The induced-fit ZAP70 structure was used for the docking campaign, and several low and sub-micromolar ZAP70 inhibitors were identified. This protocol proves that although the structure used for the docking campaign was not a classical homology

model structure but a modification of an X-ray, the docking protocol was still able to identify several validated hit compounds. It is a common situation with many high-affinity compounds that the protein-ligand complex is highly complementary. In such a case, docking is often unable to produce a proper binding pose for inhibitors which are structurally different from the inhibitor within the X-ray structure. As an example, one can look at the data from Pedreira et al., in which both normal docking and induced-fit docking approaches were unable to create proper binding modes for type 1.5 p38alpha MAP kinase inhibitors [26]. Only after manual modification of kinase conformation, a proper binding pose was constructed. This pose was validated by long MD simulations (3.6 μ s) with three replicas for all studied systems. Unlike in many other modeling studies in which MD simulations are used to support the docking results, this extremely long MD simulation is truly validating the proposed docking poses. One cannot claim the same for those cases where MD simulation is either only single run and/or clearly shorter than 500–1,000 ns, as that timescale is just enough to cover protein side chain movements or so-called tier 1 movements [27, 28].

One additional point to discuss is related to the idea of targeting inactive kinase conformation. The question is if all DFG-in structures are also catalytically active kinase structures or if there are DFG-in-like structures which are catalytically inactive. It seems that this is the case, as a quite recent paper by Modi and Dunbrack [23] nicely demonstrates that only a small part of DFG-in conformations is catalytically active. To be catalytically active, the protein kinase should have all the structural features required for phosphorylation activity, including a proper setup to accommodate the ATP molecule and the magnesium ion. Indeed, there are several X-ray structures with DFG-in-like features but without proper conformation to accommodate the ATP and the metal ion. What is not known at the moment is whether these inactive DFG-in-like structures are thermodynamically distinct ones in vivo and thus biologically valid or whether the inactive DFG-in structures are just artifacts of the crystallization conditions. Current data indicate that the first option is valid, as combination of X-ray structure analysis and long-scale MD simulations with CDK2 was able to identify not only classical active and inactive kinase conformations but also several metastable states [29].

3 MD Simulations

As one can see, MD simulations are becoming an increasingly popular research tool to study both conformational aspects of protein kinases and for understanding drug-protein interactions. There are several factors which are making MD a true option, but the most important ones are the dramatically increased performance due to GPU implementation of software, better force fields, and especially the Markov State Modeling approach [30]. Around 10 years ago, most of the published MD simulations included at maximum 1 μ s simulation time, but current studies can easily be based on data from an over 1 ms timeframe [31]. In our group, a routine simulation

speed in the case of protein kinase MD is around 500 ns/24 h/kinase, and several simulations (typically more than 10) are run simultaneously. This equals to around 5 microseconds produced MD data within 24 h. Together with ever-continuing work on new protein-specific and general force fields [32–36], this has allowed researchers to carry out long enough simulations with good accuracy for the kinase inhibitor complex. Naturally, currently available force fields are far from perfect, and there are several attempts to include polarizability and proton transfers within classical force fields [37, 38]. However, the current status of force field methods is good enough to allow high-quality simulations which are reproducing empirical data within a reasonable error margin.

Force field development is not the only reason why MD simulations are nowadays useful in drug design. Another breakthrough is a method called Markov State Models (MSMs). MSMs are kinetic models of the process under study, usually based on MD trajectory data. The aim of the MSM approach is to build a simplified model, easy to understand and simple enough that new insight can be gained. MSM is a coarse-grained representation of the more detailed molecular trajectories for quantitative comparisons [30]. The method builds a model with individual (metastable) states and detects how often conversion from one state to another is happening. MSMs often have thousands of states or even more. The critical factor is the transition from one state to another, and with faster transitions, shorter simulations are needed to construct an MSM. As Pande et al. explain in their excellent review, the specific challenges for building an MSM can be broken down into (1) how does one define states in a kinetically meaningful scheme and (2) how can one transition the matrix in an efficient manner. If done properly, the MSM will yield both a detailed enough model about the phenomenon under study and at the same time a confirmation that the given simulation time is long enough to construct such a model [30].

Kinase inhibitor design is a typical structure-based design process, utilizing structural biology and X-ray structures. However, several MD simulation studies have recently been able to reproduce most, if not all, relevant protein conformations within selected protein kinase families [31, 39, 40]. In addition, similar studies have detected previously unknown inactive kinase structures, which have either been later validated by structural biology approaches or confirmed by X-ray structure in related kinases. Sultan, Kiss, and Pande [41] used an accelerated molecular dynamics (AMD) to study seven Src kinase structures simultaneously. They also utilized an extension of the MSM method which allowed the authors to compare MD trajectories of seven Src kinases, namely, Fyn, Lyn, Lck, Hck, Fgr, Yes, and Bl kinase. The total length of AMD simulations exceeded several milliseconds. Results indicated that the kinase active state of the seven Src kinases is typically within 1–2 kcal/mol of the inactive conformation. In addition, kinase activation is slower than deactivation. The active-inactive transitions require several metastable intermediates, and potentially those conformations can be targeted by specific inhibitors.

Although docking is carried out in vacuum, water molecules can be considered during the docking procedure. Protein-ligand solvation and desolvation are the major sources of binding energy during protein-ligand binding [42]. Indirectly, water is

included in some of the scoring functions, like Glide XP [42, 43]. However, a more direct approach is to use information from the X-ray structures and especially MD simulations with explicit solvent molecules. One example of these approaches is the already mentioned work by Lee et al., which also considered water networks within the binding site [16]. Protein cavities are not always fully solvated, and dewetted regions can substantially affect the binding affinity of ligands and inhibitors. An example of this is demonstrated by Asquith et al. [7, 44] in two studies where water networks within GAK and EGFR kinases. In both of these studies, the WaterMap method was used to identify the effect of individual water molecules, and the pure docking score was not able to rationally explain the structure-activity relationships.

One must recognize that solvent effects are not independent of equally fundamental ligand ionization properties. An excellent example of how these are connected to each other is the study by Heider et al., which showed that pyridinylimidazole as GSK3 β inhibitors were strongly affected by both preferred tautomer and solvent-related binding effects [45]. Naturally, one cannot reach these conclusions without a proper quantum mechanical evaluation of ligand behavior in solvent phase. This procedure, unfortunately, requires substantial computational resources and is thus not an option for a traditional virtual screening. It should therefore be limited to those cases where more traditional approaches are not satisfactory.

Protein ionization is typically kept fixed during all the modeling studies. This assumption has recently been challenged, as it is well known that protein side chain ionization does affect ligand binding, and protein dynamics and ionization are affected by the protein 3D environment, solvent, and ions nearby. In addition, since several side chains have their pK_a values near the physiological pH, the initially assigned protonation state might not be the one which is relevant for the phenomenon under examination. To solve this issue, Brooks et al. developed a method which combines classical MD simulation with explicit solvent for accurate molecular interactions, generalized Born implicit-solvent model for estimating the free energy of protein solvation, and a pH-based replica exchange scheme to significantly enhance both protonation and conformational state sampling [46, 47]. The method, named as hybrid-solvent continuous constant pH molecular dynamics with pH replica exchange (CpHMD), was used by Shen et al. to study, for example, how the c-Src kinase DFG domain flip (DFG-in vs. DFG-out) is affected by the protonation of Asp [48]. The authors showed that protonated DFG-aspartate is compatible only with DFG-out conformation, while unprotonated aspartate is possible with both DFG forms. This clearly underlines that ionization of all relevant residues must be properly assigned before MD simulation or any structure-based drug design method is used. They also used CpHMD to identify catalytically active but nucleophilic (neutral) lysine residues which can be targeted by covalent inhibitors (the interested reader should look at the very comprehensive Chap. 30 by Gehringer). In addition, within the same study, the authors were able to identify charged cysteine residues within kinases which existed even at a physiological pH [49].

Thanks to the recent development of force field parametrization, MD simulations are currently quite reliable. It is still quite common that results from the force field methods are not fully in line with empirical data, and this is especially true if we consider X-ray crystallography. Long timescale simulation studies with p38a MAP kinase inhibitors were recently used to explain the discrepancy between X-ray and NMR data [50]. According to the classical activation mechanism, supported by X-ray structures [51], p38a MAP kinase activation with a double-phosphorylated structure should include a large reorientation of the activation loop A. However, NMR studies indicated that double phosphorylation does not induce any major conformational rearrangements [52]. Simulations with CHARMM force field were conducted with ten replicas, and simulation time was varied between 500 ns and 1 μ s, although in individual cases also longer simulation times were used. The results suggest that p38a predominantly samples conformations which are in contrast with the activation model obtained from X-ray crystallography. However, the authors analyzed crystal contacts and found several artifacts affecting the protein conformation, for example, an atypically long expression His-tag of a neighboring molecule bound to the hydrophobic docking groove of p38a MAP kinase. It is easy to agree with the statement of the Kuzmanic et al. [50] “These observations show how important it is to carefully analyze symmetry-related molecules and they call for caution in the interpretation of deposited X-ray structures, as they can be misleading.”

Basically, the abovementioned conclusion can be drawn also from the studies dealing with Aurora kinase A (AurA) [53, 54]. By combining experimental data and MD simulations, it has been demonstrated that AurA activation by phosphorylation occurs without a population shift from the DFG-out to the DFG-in state and that the activation loop of the activated kinase remains highly dynamic. This is, once more, against the traditional view of the X-ray. Instead, molecular dynamics simulations and electron paramagnetic resonance experiments show that phosphorylation triggers a switch within the DFG-in subpopulation from an autoinhibited DFG-in substate to an active DFG-in substate, leading to catalytic activation.

4 Allosteric Control of Kinases

Most of the kinase inhibitors target the ATP binding site of the corresponding kinase protein. While the ATP binding site is highly conserved among the kinome, the so-called exosites are much more unique, although to some extent also conserved. The first successful kinase inhibitor targeting exosites was imatinib [55]. From the modeling point of view, this paradigm shift was quite big as it demonstrated that target protein conformation is not static and that kinase conformation can be modified by targeting exosites. While, at the moment, most of the new kinase inhibitors are targeting the ATP-binding cleft between the N- and C-lobes of the kinase, interest toward allosteric inhibitors is growing due to some very evident benefits. The biggest advantage is the fact that the allosteric binding site has no

high-affinity endogenous ligand. The second major benefit is that one can, at least theoretically, control the target kinase function in a more precise fashion. However, a lot of research is needed to understand how the allosteric control mechanism works. Currently the best molecular modeling method to tackle this question is naturally molecular dynamics, as all other methods, like docking, QSAR, and pharmacophore, only give a static image of the drug-receptor complex.

Allosteric effects have been explained by different theoretical frameworks, most of which are not explained here. One of the most recent theoretical approaches is the so-called “violin” model, specifically proposed for protein kinases by Kornev and Taylor [56–59]. This model is developed directly to explain the type III and type IV kinase inhibitors’ mode of action. While more traditional theories of allosteric control rely on specific atomic interaction networks with a direct pathway from the allosteric site to the site of action, all of them have some caveats. The most notable is the high thermal motion of individual atoms within a protein. Unlike in the macroscopic world, thermal motion in the microcosmos is large enough to prevent simple one-pathway networks, and big parts of the information would be lost in the process. One can also easily understand the violin model based on the MD simulations. In the typical force field method, atoms and bonds are represented by ball and springs with corresponding spring constants and thus also with corresponding vibrations. These vibrations are, even at room temperature, strong enough to constantly break and re-make most of the interprotein interactions like H-bonds, ionic bonds, and hydrophobic (dispersion) interactions. As current force fields are accurate enough to reproduce a majority of the macroscopic parameters and spectra data, we can easily accept that these vibration and intramolecular motions are also represented accurately enough by modern all-atomic force fields.

Another important work dealing with allosterism, by McClendon et al. [58], is also based on MD simulations. The work includes microsecond scale MD simulations and the authors demonstrate that Protein Kinase A (PKA) has not just semi-rigid N- and C-lobes, but several semi-rigid communities interacting with each other and controlling in a rational way the function and activity of PKA. Correlated motions between these structurally contiguous communities are associated with a particular protein kinase function and/or a regulatory mechanism. A bit surprising is the finding that some well-known protein kinase motifs are split into different communities. The community maps are able to explain how different ligands induce long-distance allosteric coupling. These communities are also in agreement with the spine network [57].

Most of the kinase modeling studies are based on kinase domain structure alone, but there are also MD simulations which do include the regulatory units, like SH2 and SH3. A comprehensive study, combining MD simulations, free energy calculations, in vitro functional assays, and single point mutations, suggests that the SH2-kinase interactions are allosterically stabilizing the α C-helix of the c-Abl kinase domain [60]. One should recognize that while MD simulations were used with an unbiased classical all-atom AMBER-force field, the free-energy estimations were based on a hybrid coarse-grained model. A multidisciplinary approach combining simulations, functional assays, and mutagenesis has characterized the interdomain

coupling in the active SH3-SH2-Abl complex, suggesting that the SH2-KD interactions can allosterically stabilize the catalytically competent position of the α C-helix and thus exert control over the kinase activity [61]. The same system was also studied by using microsecond all-atom simulations and differential scanning calorimetry. The results from the dynamics of the SH3-SH2 tandem indicate a two-state switch, alternating between conformations observed in the autoinhibited and active complexes [62]. As a conclusion, computational studies of Abl and Src kinases regulation have indicated a complex interplay between the SH3 and SH2 domains, the SH2 linker, and the catalytic domain. These studies are in line with experimental results.

5 Discussion

Many important topics have not been discussed above, like phosphorylation effects and kinase dimerization. The main issue in modeling has hopefully been discussed sufficiently to draw some conclusions. The following conclusions are based on case studies in kinase modeling but, at the same time, are, after some modifications, generally applicable to all drug discovery type modeling efforts.

Successful modeling starts with the appropriate question or proper research hypothesis. This research question will lay the foundation for the selection of protein structures to be used. In the case of kinase modeling, one must know if potentially available protein structures (X-ray, Cryo-EM, or homology modeling) are in a biologically relevant state. The next critical point is the correct ligand/library preparation. Far too often, ligand tautomers/protomers are not based on detailed studies, but modelers trust too much in automatic procedures. The third critical point is too high confidence in docking and MD simulation results. Docking can, after all, create some kind of binding pose to almost all of the compounds in virtual screening libraries, although only a very small number of molecules are actually binding the target protein. The same is true for MD simulations. Many papers show single 100 ns simulations time stating that this is enough to identify binding/association/affinity. Since biological assays are usually done as triplicates, we should ask why this is not done with MD simulations [63, 64]. Instead of believing in one individual binding pose proposed by docking or short MD simulation, one should run several computational experiments with different setups, repeat MD simulations, and study how robust the proposed binding mode is to small changes in the system. At the same time, one should not think that empirical data are always superior over computational results. As discussed above, X-ray structures often do have issues affecting ligand structure, protein conformation, and structural determination, and sometimes the whole protein structure is wrong [65, 66]. This means that like in modeling and biological assays, one must look at all the structural biology data and combine information from different sources.

Most of us like good food and wine/beer/water. We also know that good food and drink cannot be created if we are using bad and rotten raw materials or dirty water.

The same is true for modeling and science in general. If the used method is not good, if protein structures are not adequate, or the ligands are not properly processed, one cannot obtain good data.

Compliance with Ethical Standards

Conflict of Interest: The author declares that he has no conflict of interest.

Funding: The author received no external funding during the preparation of this manuscript.

Ethical Approval: This article does not contain any studies with human participants or animals performed by the author.

Informed Consent: This article does not contain any studies which required DNA samples.

References

1. Fry DC, Kuby SA, Mildvan AS (1985) NMR studies of the MgATP binding site of adenylate kinase and of a 45-residue peptide fragment of the enzyme. *Biochemistry* 24:4680–4694. <https://doi.org/10.1021/bi00338a030>
2. Taylor SS, Kornev AP (2010) Protein kinases: evolution of dynamic regulatory proteins. *Trends Biochem Sci* 36:65–77. <https://doi.org/10.1016/j.tibs.2010.09.006>
3. Cramer RD, Patterson DE, Bunce JD (1988) Comparative molecular field analysis (CoMFA). 1. Effect of shape on binding of steroids to carrier proteins. *J Am Chem Soc* 110:5959–5967. <https://doi.org/10.1021/ja00226a005>
4. Poulidakos PI, Zhang C, Bollag G, Shokat KM, Rosen N (2010) RAF inhibitors transactivate RAF dimers and ERK signalling in cells with wild-type BRAF. *Nature* 464:427–430. <https://doi.org/10.1038/nature08902>
5. Durrant DE, Morrison DK (2017) Targeting the Raf kinases in human cancer: the Raf dimer dilemma. *Br J Cancer* 118:3–8. <https://doi.org/10.1038/bjc.2017.399>
6. Wood ER, Truesdale AT, McDonald OB, Yuan D, Hassell A, Dickerson SH, Ellis B, Pennisi C, Horne E, Lackey K, Alligood KJ, Rusnak DW, Gilmer TM, Shewchuk L (2004) A unique structure for epidermal growth factor receptor bound to GW572016 (Lapatinib). *Cancer Res* 64:6652–6659. <https://doi.org/10.1158/0008-5472.can-04-1168>
7. Asquith CRM, Tizzard GJ, Bennett JM, Wells CI, Elkins JM, Willson TM, Poso A, Laitinen T (2020) Targeting the water network in cyclin G associated kinase (GAK) with 4-anilino-quin (az)oline inhibitors. *ChemMedChem* 15(13):1200–1215. <https://doi.org/10.1002/cmcd.202000150>
8. Hansch C, Fujita T (1964) ρ - σ - π analysis. A method for the correlation of biological activity and chemical structure. *J Am Chem Soc* 86:1616–1626. <https://doi.org/10.1021/ja01062a035>
9. Meng EC, Shoichet BK, Kuntz ID (1992) Automated docking with grid-based energy evaluation. *J Comput Chem* 13:505–524. <https://doi.org/10.1002/jcc.540130412>
10. Roskoski R (2016) Classification of small molecule protein kinase inhibitors based upon the structures of their drug-enzyme complexes. *Pharmacol Res* 103:26–48. <https://doi.org/10.1016/j.phrs.2015.10.021>
11. Martz KE, Dorn A, Baur B, Schattel V, Goettert MI, Mayer-Wrangowski SC, Rauh D, Laufer SA (2012) Targeting the hinge glycine flip and the activation loop: novel approach to potent p38 α inhibitors. *J Med Chem* 55:7852. <https://doi.org/10.1021/jm300951u>
12. Pantsar T, Poso A (2018) Binding affinity via docking: fact and fiction. *Molecules* 23:1899. <https://doi.org/10.3390/molecules23081899>

13. Forli S (2015) Charting a path to success in virtual screening. *Molecules* 20:18732–18758. <https://doi.org/10.3390/molecules201018732>
14. Huse M, Kuriyan J (2002) The conformational plasticity of protein kinases. *Cell* 109:275–282. [https://doi.org/10.1016/s0092-8674\(02\)00741-9](https://doi.org/10.1016/s0092-8674(02)00741-9)
15. Jacobs MD, Caron PR, Hare BJ (2007) Classifying protein kinase structures guides use of ligand-selectivity profiles to predict inactive conformations: structure of lck/imatinib complex. *Proteins* 70:1451–1460. <https://doi.org/10.1002/prot.21633>
16. Lee M, Balupuri A, Jung Y, Choi S, Lee A, Cho Y, Kang N (2018) Design of a novel and selective IRAK4 inhibitor using topological water network analysis and molecular modeling approaches. *Molecules* 23:3136. <https://doi.org/10.3390/molecules23123136>
17. Walter NM, Wentsch HK, Bührmann M, Bauer SM, Döring E, Mayer-Wrangowski S, Sievers-Engler A, Willemsen-Seegers N, Zaman G, Buijsman R, Lämmerhofer M, Rauh D, Laufer SA (2017) Design, synthesis, and biological evaluation of novel type I(1)/2 p38 α MAP kinase inhibitors with excellent selectivity, high potency, and prolonged target residence time by interfering with the R-spine. *J Med Chem* 60:8027–8054. <https://doi.org/10.1021/acs.jmedchem.7b00745>
18. Ortuso F, Amato R, Artese A, D'antona L, Costa G, Talarico C, Gigliotti F, Bianco C, Trapasso F, Schenone S, Musumeci F, Botta L, Perrotti N, Alcaro S (2014) In silico identification and biological evaluation of novel selective serum/glucocorticoid-inducible kinase 1 inhibitors based on the pyrazolo-pyrimidine scaffold. *J Chem Inf Model* 54:1828–1832. <https://doi.org/10.1021/ci500235f>
19. Slynko I, Schmidt-kunz K, Rumpf T, Klaeger S, Heinzlmeir S, Najar A, Metzger E, Kuster B, Schüle R, Jung M, Sippl W (2016) Identification of highly potent protein kinase C-related kinase 1 inhibitors by virtual screening, binding free energy rescoring, and in vitro testing. *ChemMedChem* 11:2084–2094. <https://doi.org/10.1002/cmdc.201600284>
20. Singh N, Tiwari S, Srivastava KK, Siddiqi MI (2015) Identification of novel inhibitors of *Mycobacterium tuberculosis* PknG using pharmacophore based virtual screening, docking, molecular dynamics simulation, and their biological evaluation. *J Chem Inf Model* 55:1120–1129. <https://doi.org/10.1021/acs.jcim.5b00150>
21. Wang Y, Dai Y, Wu X, Li F, Liu B, Li C, Liu Q, Zhou Y, Wang B, Zhu M, Cui R, Tan X, Xiong Z, Liu J, Tan M, Xu Y, Geng M, Jiang H, Liu H, Ai J, Zheng M (2019) Discovery and development of a series of Pyrazolo[3,4-d]pyridazinone compounds as the novel covalent fibroblast growth factor receptor inhibitors by the rational drug design. *J Med Chem* 62:7473–7488. <https://doi.org/10.1021/acs.jmedchem.9b00510>
22. Xu M, Yu L, Wan B, Yu L, Huang Q (2011) Predicting inactive conformations of protein kinases using active structures: conformational selection of type-II inhibitors. *PLoS One* 6:e22644. <https://doi.org/10.1371/journal.pone.0022644>
23. Modi V, Dunbrack RL (2019) Defining a new nomenclature for the structures of active and inactive kinases. *Proc Natl Acad Sci U S A* 116:6818–6827. <https://doi.org/10.1073/pnas.1814279116>
24. Bethke E, Pinchuk B, Renn C, Witt L, Schlosser J, Peifer C (2016) From type I to type II: design, synthesis, and characterization of potent pyrazin-2-ones as DFG-out inhibitors of PDGFR β . *ChemMedChem* 11:2664–2674. <https://doi.org/10.1002/cmdc.201600494>
25. Zhao H, Caflisch A (2013) Discovery of ZAP70 inhibitors by high-throughput docking into a conformation of its kinase domain generated by molecular dynamics. *Bioorg Med Chem Lett* 23:5721–5726. <https://doi.org/10.1016/j.bmcl.2013.08.009>
26. Pedreira JGB, Nahidino P, Kudolo M, Pansar T, Berger B-T, Forster M, Knapp S, Laufer S, Barreiro EJ (2020) Bioisosteric replacement of arylamide-linked spine residues with N-Acylhydrazones and selenophenes as a design strategy to novel dibenzosuberone derivatives as type I 1/2 p38 α MAP kinase inhibitors. *J Med Chem* 63(13):7347–7354. <https://doi.org/10.1021/acs.jmedchem.0c00508>
27. Henzler-Wildman K, Kern D (2007) Dynamic personalities of proteins. *Nature* 450:964–972. <https://doi.org/10.1038/nature06522>

28. Frauenfelder H, Sligar S, Wolynes P (1991) The energy landscapes and motions of proteins. *Science* 254:1598–1603. <https://doi.org/10.1126/science.1749933>
29. Pisani P, Caporuscio F, Carlino L, Rastelli G (2016) Molecular dynamics simulations and classical multidimensional scaling unveil new metastable states in the conformational landscape of CDK2. *PLoS One* 11:e0154066. <https://doi.org/10.1371/journal.pone.0154066>
30. Pande VS, Beauchamp K, Bowman GR (2010) Everything you wanted to know about Markov State Models but were afraid to ask. *Methods* 52:99–105. <https://doi.org/10.1016/j.ymeth.2010.06.002>
31. Meng Y, Gao C, Clawson DK, Atwell S, Russell M, Vieth M, Roux B (2018) Predicting the conformational variability of Abl tyrosine kinase using molecular dynamics simulations and Markov state models. *J Chem Theory Comput* 14:2721–2732. <https://doi.org/10.1021/acs.jctc.7b01170>
32. Maier JA, Martinez C, Kasavajhala K, Wickstrom L, Hauser KE, Simmerling C (2015) ff14SB: improving the accuracy of protein side chain and backbone parameters from ff99SB. *J Chem Theory Comput* 11:3696–3713. <https://doi.org/10.1021/acs.jctc.5b00255>
33. Best RB, Zhu X, Shim J, Lopes PE, Mittal J, Feig M, MacKerell AD (2012) Optimization of the additive CHARMM all-atom protein force field targeting improved sampling of the backbone ϕ , ψ and side-chain χ_1 and χ_2 dihedral angles. *J Chem Theory Comput* 8:3257–3273. <https://doi.org/10.1021/ct300400x>
34. Vanommeslaeghe K, MacKerell AD (2014) CHARMM additive and polarizable force fields for biophysics and computer-aided drug design. *Biochim Biophys Acta* 1850:861–871. <https://doi.org/10.1016/j.bbagen.2014.08.004>
35. Harder E, Damm W, Maple J, Wu C, Reboul M, Xiang J, Wang L, Lupyan D, Dahlgren MK, Knight JL, Kaus JW, Cerutti DS, Krilov G, Jorgensen WL, Abel R, Friesner RA (2016) OPLS3: a force field providing broad coverage of drug-like small molecules and proteins. *J Chem Theory Comput* 12:281–296. <https://doi.org/10.1021/acs.jctc.5b00864>
36. Roos K, Wu C, Damm W, Reboul M, Stevenson JM, Lu C, Dahlgren MK, Mondal S, Chen W, Wang L, Abel R, Friesner RA, Harder ED (2019) OPLS3e: extending force field coverage for drug-like small molecules. *J Chem Theory Comput* 15(3):1863–1874. <https://doi.org/10.1021/acs.jctc.8b01026>
37. Asthana A, Wheeler DR (2013) A polarizable reactive force field for water to enable molecular dynamics simulations of proton transport. *J Chem Phys* 138:174502. <https://doi.org/10.1063/1.4798457>
38. Jing Z, Liu C, Cheng SY, Qi R, Walker BD, Piquemal J-P, Ren P (2019) Polarizable force fields for biomolecular simulations: recent advances and applications. *Annu Rev Biophys* 48:371–394. <https://doi.org/10.1146/annurev-biophys-070317-033349>
39. Paul F, Meng Y, Roux B (2020) Identification of druggable kinase target conformations using Markov model metastable states analysis of apo-Abl. *J Chem Theory Comput* 16:1896–1912. <https://doi.org/10.1021/acs.jctc.9b01158>
40. Sultan MM, Kiss G, Pande VS (2018) Towards simple kinetic models of functional dynamics for a kinase subfamily. *Nat Chem* 10:903–909. <https://doi.org/10.1038/s41557-018-0077-9>
41. Sultan MM, Denny RA, Unwalla R, Lovering F, Pande VS (2017) Millisecond dynamics of BTK reveal kinase-wide conformational plasticity within the apo kinase domain. *Sci Rep* 7:15604. <https://doi.org/10.1038/s41598-017-10697-0>
42. Friesner RA, Murphy RB, Repasky MP, Frye LL, Greenwood JR, Halgren TA, Sanschagrin PC, Mainz DT (2006) Extra precision glide: docking and scoring incorporating a model of hydrophobic enclosure for protein-ligand complexes. *J Med Chem* 49:6177–6196. <https://doi.org/10.1021/jm051256o>
43. Friesner RA, Banks JL, Murphy RB, Halgren TA, Klicic JJ, Mainz DT, Repasky MP, Knoll EH, Shelley M, Perry JK, Shaw DE, Francis P, Shenkin PS (2004) Glide: a new approach for rapid, accurate docking and scoring. 1. Method and assessment of docking accuracy. *J Med Chem* 47:1739–1749. <https://doi.org/10.1021/jm030643o>

44. Asquith CRM, Maffuid KA, Laitinen T, Torrice CD, Tizzard GJ, Crona DJ, Zuercher WJ (2019) Targeting an EGFR water network with 4-anilinoquin(az)oline inhibitors for chordoma. *ChemMedChem* 14:1693–1700. <https://doi.org/10.1002/cmdc.201900428>
45. Heider F, Pansar T, Kudolo M, Ansideri F, Simone AD, Pruccoli L, Schneider T, Goettert MI, Tarozzi A, Andrisano V, Laufer SA, Koch P (2019) Pyridinylimidazoles as GSK3 β inhibitors: the impact of tautomerism on compound activity via water networks. *ACS Med Chem Lett* 10:1407–1414. <https://doi.org/10.1021/acsmchemlett.9b00177>
46. Khandogin J, Brooks CL (2005) Constant pH molecular dynamics with proton tautomerism. *Biophys J* 89:141–157. <https://doi.org/10.1529/biophysj.105.061341>
47. Lee MS, Salsbury FR, Brooks CL (2004) Constant-pH molecular dynamics using continuous titration coordinates. *Proteins* 56:738–752. <https://doi.org/10.1002/prot.20128>
48. Tsai C-C, Yue Z, Shen J (2019) How electrostatic coupling enables conformational plasticity in a tyrosine kinase. *J Am Chem Soc* 141:15092–15101. <https://doi.org/10.1021/jacs.9b06064>
49. Liu R, Yue Z, Tsai C-C, Shen J (2019) Assessing lysine and cysteine reactivities for designing targeted covalent kinase inhibitors. *J Am Chem Soc* 141:6553–6560. <https://doi.org/10.1021/jacs.8b13248>
50. Kuzmanic A, Sutto L, Saladino G, Nebreda AR, Gervasio FL, Orozco M (2017) Changes in the free-energy landscape of p38 α MAP kinase through its canonical activation and binding events as studied by enhanced molecular dynamics simulations. *Elife* 6:e22175. <https://doi.org/10.7554/elife.22175>
51. Zhang Y-Y, Wu J-W, Wang Z-X (2011) Mitogen-activated protein kinase (MAPK) phosphatase 3-mediated cross-talk between MAPKs ERK2 and p38 α . *J Biol Chem* 286:16150–16162. <https://doi.org/10.1074/jbc.m110.203786>
52. Tokunaga Y, Takeuchi K, Takahashi H, Shimada I (2014) Allosteric enhancement of MAP kinase p38 α 's activity and substrate selectivity by docking interactions. *Nat Struct Mol Biol* 21:704–711. <https://doi.org/10.1038/nsmb.2861>
53. Lake EW, Muretta JM, Thompson AR, Rasmussen DM, Majumdar A, Faber EB, Ruff EF, Thomas DD, Levinson NM (2018) Quantitative conformational profiling of kinase inhibitors reveals origins of selectivity for Aurora kinase activation states. *Proc Natl Acad Sci U S A* 115: E11894–E11903. <https://doi.org/10.1073/pnas.1811158115>
54. Ruff EF, Muretta JM, Thompson AR, Lake EW, Cyphers S, Albanese SK, Hanson SM, Behr JM, Thomas DD, Chodera JD, Levinson NM (2018) A dynamic mechanism for allosteric activation of Aurora kinase A by activation loop phosphorylation. *Elife* 7:e32766. <https://doi.org/10.7554/elife.32766>
55. Schindler T, Borrmann W, Pellicena P, Miller WT, Clarkson B, Kuriyan J (2000) Structural mechanism for STI-571 inhibition of abelson tyrosine kinase. *Science* 289:1938–1942. <https://doi.org/10.1126/science.289.5486.1938>
56. Ahuja LG, Taylor SS, Kornev AP (2019) Tuning the “violin” of protein kinases: the role of dynamics-based allostery. *IUBMB Life* 71:685–696. <https://doi.org/10.1002/iub.2057>
57. Kornev AP, Taylor SS (2015) Dynamics-driven allostery in protein kinases. *Trends Biochem Sci* 40:628–647. <https://doi.org/10.1016/j.tibs.2015.09.002>
58. McClendon CL, Kornev AP, Gilson MK, Taylor SS (2014) Dynamic architecture of a protein kinase. *Proc Natl Acad Sci U S A* 111:E4623–E4631. <https://doi.org/10.1073/pnas.1418402111>
59. Kornev AP (2020) Allostery explained through synchronized oscillators and fractal networks. *Biophys J* 118:208a. <https://doi.org/10.1016/j.bpj.2019.11.1248>
60. Dölker N, Górná MW, Sutto L, Torralba AS, Superti-Furga G, Gervasio FL (2014) The SH2 domain regulates c-Abl kinase activation by a cyclin-like mechanism and remodulation of the hinge motion. *PLoS Comput Biol* 10:e1003863. <https://doi.org/10.1371/journal.pcbi.1003863>
61. Tse A, Verkhivker GM (2015) Molecular dynamics simulations and structural network analysis of c-Abl and c-Src kinase core proteins: capturing allosteric mechanisms and communication pathways from residue centrality. *J Chem Inf Model* 55:1645–1662. <https://doi.org/10.1021/acs.jcim.5b00240>

62. Fajer M, Meng Y, Roux B (2016) The activation of c-Src tyrosine kinase: conformational transition pathway and free energy landscape. *J Phys Chem B* 121:3352–3363. <https://doi.org/10.1021/acs.jpcc.6b08409>
63. Braun E, Gilmer J, Mayes H, Mobley D, Prasad S, Zuckerman D, Monroe J (2018) Best practices for foundations in molecular simulations [Article v1.0]. *Living J Comput Mol Sci* 1:5957. <https://doi.org/10.33011/livecoms.1.1.5957>
64. Grossfield A, Patrone P, Roe D, Schultz A, Siderius D, Zuckerman D (2018) Best practices for quantification of uncertainty and sampling quality in molecular simulations [Article v1.0]. *Living J Comput Mol Sci* 1:5067. <https://doi.org/10.33011/livecoms.1.1.5067>
65. Niedzialkowska E, Gasiorowska O, Handing KB, Majorek KA, Porebski PJ, Shabalin IG, Zasadzinska E, Cymborowski M, Minor W (2016) Protein purification and crystallization artifacts: the tale usually not told. *Protein Sci* 25:720–733. <https://doi.org/10.1002/pro.2861>
66. Cooper DR, Porebski PJ, Chruszcz M, Minor W (2011) X-ray crystallography: assessment and validation of protein–small molecule complexes for drug discovery. *Expert Opin Drug Discov* 6:771–782. <https://doi.org/10.1517/17460441.2011.585154>

Covalent Kinase Inhibitors: An Overview



Matthias Gehringer

Contents

1	Introduction	44
2	Covalent Protein Kinase Inhibitors	50
2.1	The Protein Kinases' Cysteine	50
2.2	Approved Covalent Protein Kinase Inhibitors	52
2.3	Natural Products as Covalent Protein Kinase Inhibitors	54
2.4	Development of Inhibitors Targeting Cysteines in the Front Region	57
2.5	Development of Inhibitors Targeting Cysteines around the P-Loop and in the Roof Region	67
2.6	Development of Inhibitors Targeting Cysteines in the Hinge Region	72
2.7	Development of Inhibitors Targeting Cysteines Around the DFG Motif and in the Activation Segment	74
2.8	Development of Inhibitors Targeting Remote Cysteines or Inactive Conformations ...	76
2.9	Development of Inhibitors Targeting Cysteines in Allosteric Pockets	78
2.10	Development of Inhibitors Targeting Lysine or Tyrosine	79
3	Summary and Outlook	82
	References	84

Abstract Covalent targeting has experienced a revival in the last decade, especially in the area of protein kinase inhibitor development. Generally, covalent inhibitors make use of an electrophilic moiety often termed “warhead” to react with a nucleophilic amino acid, most frequently a cysteine. High efficacy and excellent selectivity in the kinome have been achieved by addressing poorly conserved, non-catalytic cysteine residues with so-called targeted covalent inhibitors (TCIs). Despite the challenges associated with covalent modifiers, application of the TCI approach for the discovery of new treatments has been very successful with six covalent kinase inhibitors having gained approval in the last few years. A multitude of reactive chemical probes and tool compounds has further been developed. Beside cysteine, other nucleophilic amino acids including tyrosine and lysine have also been

M. Gehringer (✉)

Department of Pharmaceutical and Medicinal Chemistry, Institute of Pharmaceutical Sciences,
Eberhard Karls University of Tübingen, Tübingen, Germany
e-mail: matthias.gehringer@uni-tuebingen.de

addressed with suitable electrophiles and covalent-reversible chemistry has recently complemented our toolbox for designing covalent kinase inhibitors. Covalent ligands have also been used in the framework of chemical-genetics approaches or to tackle allosteric pockets, which are often difficult to address.

This chapter aims at providing a general introduction to covalent kinase inhibitors and an overview of the current state of research highlighting major targeting strategies, developments, and advances in this field. More detailed information on certain targets and approaches can be found in dedicated chapters of this book.

Keywords Chemical probes, Electrophilic warheads, Kinase inhibitors, Structure-based drug design, Targeted covalent inhibitors

1 Introduction

Covalent inhibitors have a long history in medicinal chemistry and various covalent modifiers, such as aspirin, β -lactam antibiotics or omeprazole, to name just a few, have been among the most frequently used drugs for decades [1]. However, many of the drug classes acting via a covalent mechanism have been discovered serendipitously. Due to concerns about their potential for haptization and idiosyncratic toxicity as well as side effects or toxicity arising from irreversible off-target labeling, reactive compounds have long been regarded with skepticism by pharmaceutical companies [2, 3]. Since the beginning of the twenty-first century, however, we have seen a resurgence of covalent targeting strategies in medicinal chemistry. Targeted covalent inhibitors (TCIs) which have been defined as “inhibitors bearing a bond-forming functional group of low reactivity that, following binding to the target protein, is positioned to react rapidly with a specific non-catalytic residue at the target site” [1] are now becoming more and more common especially in the field of protein kinase drug discovery [4–7].

The renewed interest in covalent inhibitors is based on the growing awareness that a well-designed TCI can offer a variety of benefits over classical, non-covalently binding molecules (an excellent review summarizing the opportunities and pitfalls associated with the development of covalent-modifier drugs has recently been provided by De Cesco et al. [8]). Currently, most TCIs address non-catalytic cysteine residues with an electrophilic headgroup termed “warhead” [9], which is highlighted in red throughout this chapter. Thereby, TCIs can make use of the combined specificity of two orthogonal selectivity filters: (1) reversible recognition and (2) the covalent bond-forming reaction. Consequently (and counterintuitively), covalent targeting can increase selectivity provided that the intrinsic reactivity of the warhead is low enough to hit only residues juxtaposed by the reversible binding event [3, 7]. This second selectivity filter is particularly useful when targeting the protein kinases’ ATP pocket, which features a high overall similarity throughout the

kinome but a relatively low degree of conservation in the so-called cysteinome (i.e., the entire set of cysteines present in the kinome) [7]. In addition, irreversible covalent binding eliminates the competition with natural ligands, substrates or co-factors (i.e., ATP in the case of kinases) thereby increasing overall efficacy [7]. Given the low millimolar ATP concentrations in cells, the lack of competitiveness after covalent bond formation is a key advantage. Due to their time-dependent binding behavior, efficient irreversible inhibitors can achieve full target occupancy even at very low concentrations, provided that the exposure time is long enough. Thus, lower doses may be sufficient to achieve equivalent therapeutic efficacy compared to reversibly binding drugs. At the same time, the target protein remains inhibited until its function is restored by de novo synthesis. If the re-synthesis rate is not too high, persistent target engagement leads to a decoupling of pharmacokinetics (PK) from pharmacodynamics (PD) which can translate into prolonged dosage intervals even for high-clearance compounds and a lower side effect burden due to a decreased overall exposure [2]. Since covalent bond formation can be used as a powerful promoter of potency and selectivity, it can also enable the reduction of molecule size and lipophilicity. Thereby, molecular obesity [10] may be prevented, and physicochemical properties be improved.

Covalent-reversible targeting strategies can be a viable alternative when off-target labeling, GSH-mediated clearance, or haptization is an issue, when sustained target engagement causes mechanism-based side effects, but also when high turnover targets need to be addressed. Ideally, the unmodified inhibitor dissociates after protein degradation to be “recycled” by engaging with a newly translated target protein. Moreover, this approach offers the potential to benefit from advantages of irreversible covalent inhibitors (e.g., prolonged target occupancy, increased potency, and selectivity) at a decreased risk of drug safety issues [11]. Remarkably, the target residence times of covalent-reversible inhibitors can be fine-tuned by both warhead chemistry and stabilization of the complex via non-covalent interactions, thus providing tailor-made solutions for the desired application. However, although these features hold the promise of enabling the design of better and safer kinase-targeted drugs, no covalent-reversible kinase inhibitors have been approved so far and critical evaluation of the benefit–risk balance in comparison to traditional non-reactive ligands will still be necessary.

As mentioned above, irreversible covalent inhibition is a non-equilibrium process. Due to its time-dependent nature, it can be accurately described neither by the equilibrium dissociation constant $K_i (= k_{\text{off}}/k_{\text{on}})$ nor by IC_{50} values [1]. TCI binding usually involves two steps (Fig. 1). In the first step, the inhibitor reversibly binds the target while covalent bond formation takes place in the second step. Importantly, only the first of these two steps is ATP-competitive. For irreversible covalent binders, the (reversible) binding affinity is described by the constant K_i being the inhibitor concentration required to achieve the half-maximal rate of covalent inactivation ($= k_{\text{inact}}/2$). It should be noted that K_i does not equal K_i although these values converge for $k_{\text{inact}} \ll k_{\text{off}}$. The first-order rate constant k_{inact} defines the maximal potential rate of covalent inactivation, i.e., the rate of covalent bond formation at full occupancy with the reversibly bound ligand. Accordingly, k_{inact} represents a measure for the efficiency of the covalent inactivation step. k_{inact}

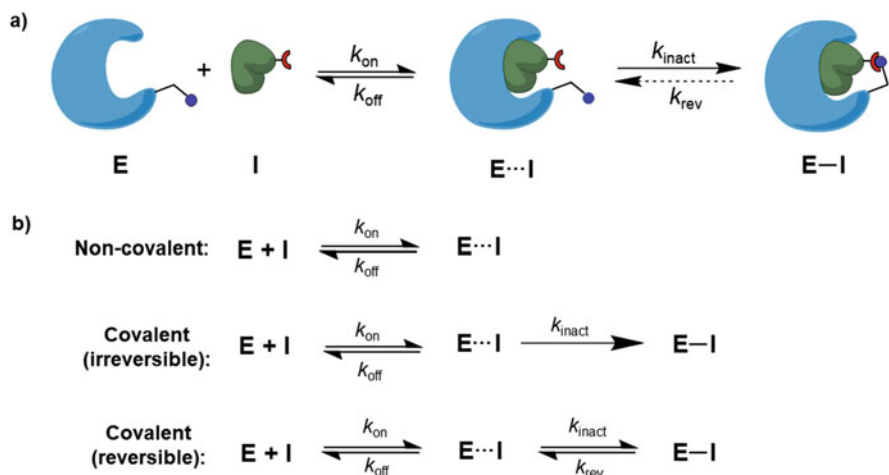


Fig. 1 (a) General mechanism of irreversible and reversible covalent target engagement by TCIs. An initial reversible binding event takes place and positions the reactive warhead (red) close to its target amino acid (dark blue). Covalent trapping represents the second step described by the rate constant k_{inact} . The rate of the reverse reaction (defined by k_{rev}) is negligible for (quasi)-irreversible inhibitors while being significant for covalent-reversible inhibitors. (b) General mechanism of one-step non-covalent (reversible), covalent-irreversible and covalent-reversible binding

depends on several factors including the intrinsic reactivity of the warhead and the target nucleophile, but also the accurate positioning of both reactive groups in terms of distance and angle to favor the reaction. The appropriate measure for the overall efficiency of the two-step binding event is the quotient $k_{\text{inact}}/K_{\text{I}}$ that is the second-order rate constant of covalent target inactivation [12]. The above descriptions refer to (quasi)-irreversible binders where the rate constant of covalent bond cleavage (denoted here as k_{rev}) approximates zero. However, k_{rev} can vary over a large range for covalent-reversible ligands, whose binding kinetics shall not be further discussed here. An in-depth description of the binding kinetics of both covalent-reversible and irreversible ligands is beyond the scope of this chapter and can be found elsewhere [8, 12, 13]. However, it should be noted that although $k_{\text{inact}}/K_{\text{I}}$ is the recommended potency measure for irreversible covalent inhibitors, the bulk of literature in the protein kinase field still relies on IC_{50} data which is much easier to obtain. Comparing covalent inhibitors on the basis of apparent IC_{50} values can be useful to deduce early SAR within a series provided that all compounds were tested in the same assay system under identical conditions. Nevertheless, it should be kept in mind that apparent IC_{50} values, which are determined at a single point in time, do neither provide a quantitative picture of a covalent inhibitor's overall efficiency nor allow for the deconvolution of contributions from reversible and covalent binding. Thus, caution should be exercised when comparing covalent inhibitors merely on the basis of IC_{50} data [13].

As mentioned before, the by-far most common residues to be addressed by TCIs are non-catalytic cysteines. The cysteine side chain ($\text{p}K_{\text{a}} \approx 8.5$) [14] can readily be deprotonated to form a strongly nucleophilic thiolate which has a much higher

reactivity than the neutral thiol form. Notably, cysteine has the strongest intrinsic nucleophilicity among the proteinogenic amino acids except the rare selenocysteine. While catalytic cysteines, that occur for example in cysteine proteases or phosphatases, are pK_a -depressed to favor the more nucleophilic deprotonated form, the neutral thiol is often dominant for non-catalytic cysteines at physiological pH making them more difficult to address.

Recent computational studies have suggested that most cysteine residues in kinases' active sites have even higher pK_a 's than the aforementioned reference value rendering those moieties comparably weak nucleophiles [14]. Nevertheless, even cysteines with a very high predicted pK_a of >20 (e.g., Cys814 in PDGFR α or Cys788 in c-KIT [14]) have been amenable to covalent targeting [15]. It should also be taken into account that the kinase conformation but also the presence of the ligand itself can influence a cysteine's pK_a and thereby its reactivity [16]. Moreover, not only the distance but also the orientation between the electrophilic warhead and the nucleophilic amino acid as well as the flexibility of the latter two are important determinants for the efficiency of covalent bond formation and may require further consideration in the design process [17, 18].

The prototypical warhead type for targeting non-catalytic cysteine residues are acrylamides and analogous attenuated Michael acceptors (vide infra). Usually, rational TCI design starts from an appropriate non-reactive ligand which is equipped with a warhead to target a proximal nucleophilic amino acid residue [19]. The design process is normally guided by structural information from X-ray crystallography allowing for the rational selection of suitable linkers and attachment points to install the reactive group. On the other hand, the off-target profiles of known covalent ligands can be used to identify starting points for re-design and optimization [6]. Alternative TCI discovery strategies that have recently been pursued include fragment-based approaches employing electrophiles of low structural complexity [20–22], which can then be optimized to become potent and specific TCIs. Moreover, DNA-encoded libraries featuring reactive compounds may be screened [23, 24]. A schematic overview of these strategies is depicted in Fig. 2.

In order to be useful for TCI design, warheads must fulfill several criteria. Ideally, reactivity is just sufficient to ensure rapid, proximity-driven covalent bond formation with the targeted residue while being too low for promiscuous bonding to other physiological nucleophiles. Since the requirements vary between different targets, the reactivity of the employed functional groups should be tunable over a wide range. An appropriate balance between target engagement and promiscuity needs to be found for each individual application. Moreover, warheads (and their metabolites) should be non-toxic and sufficiently stable against metabolic degradation. In some cases, however, rapid warhead depletion may be beneficial to make use of kinetic selectivity while minimizing off-target modification, especially if more reactive electrophiles are employed. As mentioned, α,β -unsaturated amides have been most frequently used as cysteine-targeted warheads since they feature a relatively low intrinsic reactivity, which can be adjusted by the addition of steric bulk or by tuning the electronic properties of the amide N -substituents [25]. Such moieties rapidly react with cysteine thiol(ate)s (Scheme 1a), and less frequently with other

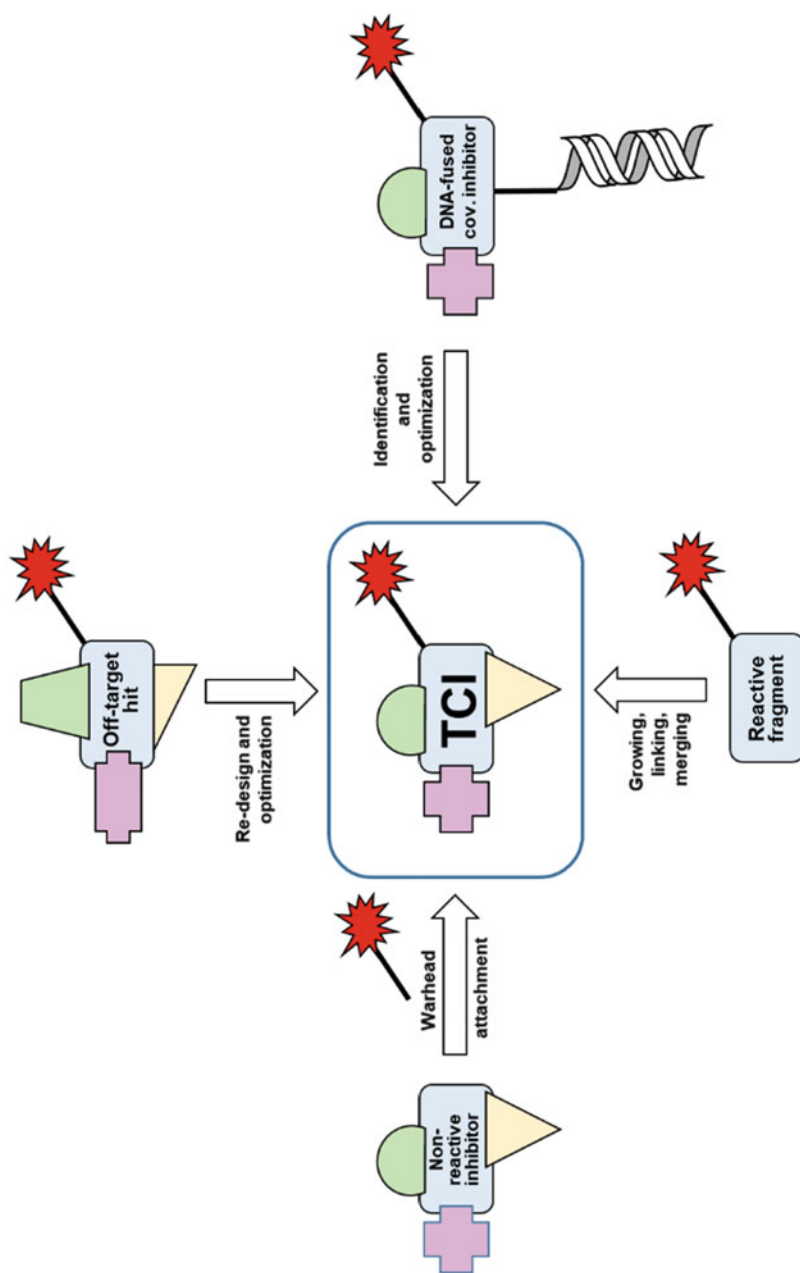
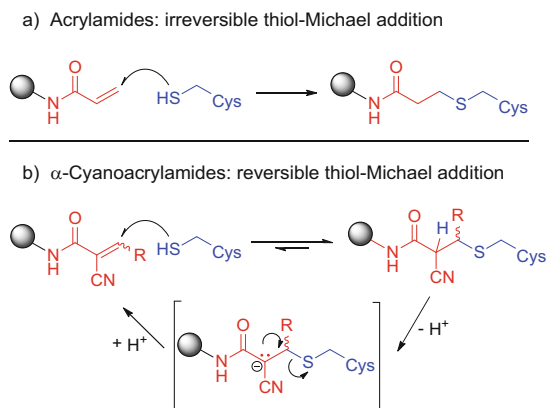


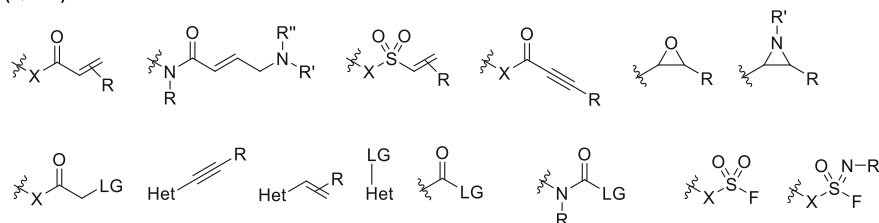
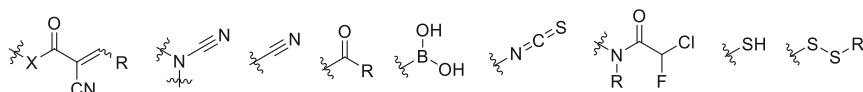
Fig. 2 Typical strategies for the discovery of TCIs



Scheme 1 Mechanisms of covalent cysteine modification by acrylamide-derived Michael acceptors. (a) (Quasi-)irreversible reaction of regular acrylamides with cysteine side chains via thiol-Michael addition. (b) Reversible reaction of α -cyanoacrylamides with cysteine side chains. The reverse β -elimination reaction is facilitated by the increased acidity of the α -proton arising from the additional electron-withdrawing α -substituent (exemplified by a nitrile group)

nucleophilic amino acids, e.g., lysine [9], if the latter are located nearby in the binding pocket and possess sufficient nucleophilicity and conformational flexibility to hit the electrophilic β -position via a favorable trajectory. Non-specific reaction with ubiquitous thiols, e.g., in glutathione (GSH) or cysteines from other proteins must be much slower to prevent premature inhibitor depletion and off-target-mediated side effects. Nucleophilic addition of the cysteines' thiol group leads to β -thioether adducts, which are generally stable with respect to the half-life of most target proteins.

An interesting recent development are TCIs with reversibly binding warheads [26]. For addressing cysteines transiently, α -cyanoacrylamides and analogous "hyper-activated" Michael acceptors have proven suitable. Although the dual activation by two electron-withdrawing group increases the intrinsic reactivity of such Michael acceptor systems, it also causes a thermodynamic destabilization of the addition product along with an increased α -CH-acidity promoting reversibility by favoring the elimination of the corresponding thiolate anion (Scheme 1b) [27, 28]. Hence, the half-life of the covalent adduct largely depends on stabilizing interactions with the protein's binding pocket and steric shielding of the α -proton. Ideally, off-targets, GSH, or the degraded target protein would not provide sufficient thermodynamic stabilization of the covalent complex, thus rapidly liberating the unmodified ligand while the ligand would bind the intact target in a quasi-irreversible fashion. Reactivity and dissociation rates of such dually activated Michael acceptors can readily be tuned by adjusting the activating group (e.g., acrylonitriles equipped with amides and similar $-M$ -substituents or with electron-deficient heterocycles) [28] and by modulating the steric bulk at the β -position [11]. Other covalent-reversible warhead types employed to address kinases include, for example, cysteine-targeted cyanamides [17] or aldehydes [29] and carboxylate-targeted boronic acids [30]. Moreover, chlorofluoroacetamides have very recently

(Quasi)-irreversible:**Reversible (or other cleavable):**

X = NH, NR', O, CH ₂ , Ar	Het = electron-deficient (hetero)aryl	R = H or various substituents	LG = leaving group
--------------------------------------	---------------------------------------	-------------------------------	--------------------

Fig. 3 Selected examples of reversibly and irreversibly binding warheads for TCIs

been shown to react with cysteines to form products that can be readily hydrolyzed to the corresponding (hydrated) glyoxamides [31].

The growing toolbox of novel or re-purposed warheads for targeting cysteines and other residues has recently been reviewed [9]. A representative selection of such headgroups is depicted in Fig. 3.

2 Covalent Protein Kinase Inhibitors

2.1 The Protein Kinases' Cysteinome

Protein kinases feature a deep and highly conserved ATP binding cleft. This pocket is perfectly ligandable and designing potent (typically low nanomolar), ATP-competitive kinase inhibitors is not considered a major challenge anymore. In contrast, achieving selectivity within the kinome, which includes more than 500 different protein kinases, can be very difficult due to the conserved nature of the ATP binding pocket [32]. Classical strategies for obtaining selective active site ligands, which are discussed by Knapp and co-workers in a dedicated chapter of this book, exploit subpockets that are not addressed by ATP (such as the hydrophobic clefts often referred to as hydrophobic regions I and II [33, 34]) since those regions are considerably less conserved. Moreover, inactive kinase conformations that are unique by themselves or that expose non-conserved regions can be addressed [35, 36]. Although poorly conserved allosteric pockets can also be targeted, this strategy is challenging due to the comparably shallow topology and the plasticity of these binding sites. Since most protein kinase inhibitors address the ATP pocket,

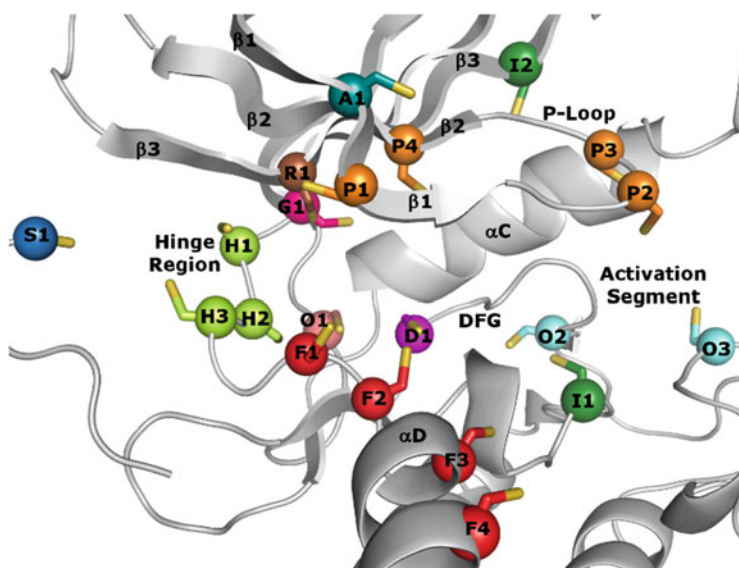


Fig. 4 Cysteine positions potentially amenable to covalent targeting according to Chaikuad et al. [7]. Cysteines were mutated in silico into the X-ray crystal structure of cAMP-dependent protein kinase catalytic subunit α in complex with ATP (PDB-code: 1ATP) and depicted as spheres with the side chains highlighted as sticks. Colors and identifiers were assigned according to the regions where the cysteines are located. *Orange* glycine-rich loop/P-loop, *pink* gatekeeper residue, *lime* hinge region, *red* front region, *magenta* pre-DFG motif, *salmon* backpocket, *brown* roof region, *cyan* activation segment, *blue* outside the ATP-pocket, *dark-green/deep-teal* positions exposed in inactive kinase conformations and additional positions (non-exhaustive). Positions are labeled according to the nomenclature used by Chaikuad et al [7]. Position **A1** has been complemented according to ref. [38]

therapeutic targeting is complicated by the high intracellular ATP concentrations (generally in the low millimolar range [37]) competing with the ligand. Covalent inhibitors hold the potential to address the aforementioned challenges as they combine the use of an additional selectivity filter with limited ATP-competitivity.

Protein kinases possess neither a catalytic cysteine residue nor any other highly activated nucleophile in the active site. Instead, they feature only non-catalytic cysteines that may have regulatory functions but are not directly involved in phosphate transfer. Collectively, these cysteine residues have been denominated the protein kinases' cysteinome [5, 6]. Cysteine residues are distributed at various locations inside and around the ATP pocket that could potentially be tackled by TCIs. According to a recent analysis by the groups of Koch, Laufer, and Knapp, there are at least 18 positions or subsites (a subsite includes several spatially similar positions) inside or proximal to the ATP pocket harboring cysteines with a high probability of being addressable by electrophilic inhibitors (see Fig. 4) [7]. Additional cysteine positions become accessible in inactive conformations (e.g., DFG-out or α C-out) [15]. Cysteines are very unevenly distributed among these locations (see

Table 1). For example, over 80 protein kinases feature a cysteine at the hinge region's H2 position (see Fig. 4 and Table 1) while only five kinases with a cysteine at the neighboring H1 position were identified [7]. Moreover, there is a bias in the availability of inhibitors targeting individual positions or subsites. While several locations have remained completely unaddressed so far, 8 out of 11 kinases with a cysteine at the F2 position ($\alpha\text{D} - 1$) were targeted with covalent inhibitors when this manuscript was written (February 2019). In the following sections, representative inhibitors engaging cysteine residues at the respective locations will be highlighted and the underlying design principles be discussed.

2.2 *Approved Covalent Protein Kinase Inhibitors*

So far, the bulk of efforts in covalent kinase inhibitor discovery has been directed toward kinases involved in cancer [39, 40]. The tremendous interest in covalent kinase targeting is highlighted by over 60 patents disclosed only between 2010 and 2013 [41]. Currently, six covalent kinase inhibitors are approved by the FDA (Fig. 5): afatinib (BIBW-2992, **1**), dacomitinib (PF-00299804, **2**), neratinib (HKI-272, **3**), osimertinib (AZD9291, **4**), ibrutinib (PCI-32765, **5**), and acalabrutinib (ACP-196, **6**). Among these, the first one to gain FDA approval (07/2013) was afatinib, a gefitinib (**7**)-derived second-generation EGFR/ErbB(HER) family kinase inhibitor (vide supra) developed by Boehringer Ingelheim, which is used in the therapy of metastatic non-small-cell lung cancer (NSCLC) driven by activating EGFR-mutations [42]. This compound hits a cysteine in the F2 position of the EGFR kinase domain (Cys797), which is also present in ErbB2 and ErbB4 but not in the pseudokinase ErbB3. Later in 2013, ibrutinib, an inhibitor addressing an equivalently positioned cysteine in Bruton's tyrosine kinase (BTK), was approved for the treatment of mantle cell lymphoma. The marketing authorization was later expanded to other conditions including chronic lymphocytic leukemia (2014) and chronic graft versus host disease (2017) [43] making ibrutinib one of the few small molecule kinase inhibitors therapeutically used for the modulation of immune response in a non-oncology setting. Osimertinib, a third-generation mutant-selective EGFR inhibitor, was approved in 2015 for metastatic NSCLC harboring the EGFR-T790M resistance mutation [44]. In July 2017, the FDA granted approval to neratinib, a quinoline-derived pan-ErbB-inhibitor for adjuvant treatment of early stage HER2-positive breast cancer. In October 2017, acalabrutinib, an ibrutinib-derived second-generation BTK inhibitor featuring a but-2-yne amide warhead, gained marketing authorization for the treatment of mantle cell lymphoma [45]. The sixth and most recently approved covalent kinase inhibitor is dacomitinib, a close structural analog of afatinib developed by Pfizer and employed in the treatment of metastatic NSCLC with activating EGFR mutations (L858R) or exon 19 deletions [46].

Table 1 Localization of cysteine residues according to the classification scheme by Chaikuad et al. [7]

Site	Position/ Subsite	Relative Position	Kinases
Glycine-rich loop (P-loop)	P1	tip-2/3 or (pen)ultimate of β 1	CK1 γ 1, CK1 γ 2, CK1 γ 3, ERK3, PEAK1(SgK269), PRAG1(SgK223), ZAK , ZAP70, <i>ROR1</i> , <i>SuRTK106</i>
	P2	tip-1	FGFR1 , FGFR2 , FGFR3 , FGFR4 , LIMK1, SRC , <i>FGR</i> , <i>SBK2</i> (Sgk069), <i>TNKI</i> , <i>YES</i>
	P3	tip of the loop	<i>CHK2</i> , <i>MKK7</i> , <i>SuRTK106</i> , <i>VACAMKL</i> (tip +1)
	P4	tip+3	MSK1 domain 2, NEK2 , PLK1, PLK2, PLK3, RSK1_domain2 , RSK2_domain2 , <i>MEKK1</i> , <i>MSK2</i> domain2, <i>RSK3</i> domain2, <i>RSK4</i> domain2
Roof region	R1	β 3+3/5	HER3 (ErbB3) [+3], WNK1 [+5], WNK3 [+5], <i>WNK2</i> [+5], <i>WNK4</i> [+5]
Gatekeeper	G1	GK residue	<i>MOK</i> , <i>SgK494</i>
	H1	GK+2	FGFR4 , MAPKAPK2, MAPKAPK3, TTK, <i>p70S6Kβ</i>
Hinge Region	H2	GK+3	AAK1, BIKE, BRAF, CDK5, CDK9, CDK11, CHK1, DLK(ZPK), FAK, FLT1, FLT3, Fms(CSFR), GAK, HGK(ZC1), HPK1(MAP4K1), IKK β , IKK α , IRE1(ERN1), KDR(VEGFR2), KHS2(MAP4K3), Kit, KSR2, LKB1, LOK, MELK, MST1, MST2, MYT1, NEK1, NEK2, PDGFR α , PEK, PKR, PKG1(PRKG1), PLK1, PLK2, PLK3, PLK4, RAF1, RNaseL, ROR2, SLK, TAO3, TBK1, TLK1, TNIK(ZC2), ULK1, ULK2, ULK3, Weel, Wee1b, <i>ARAF</i> , <i>CDK10</i> , <i>CDKL4</i> , <i>CLIK1</i> , <i>CLIK1L</i> , <i>FLT4</i> , <i>GCK</i> (MAP4K2), <i>GCN2</i> , <i>HRI</i> , <i>HUNK</i> , <i>IKKi</i> (IKK ϵ), <i>IRE2</i> , <i>KHS1</i> (MAP4K5), <i>KSR</i> , <i>Lmr1</i> , <i>Lmr2</i> , <i>Lmr3</i> , <i>LZK</i> , <i>MAP3K4</i> , <i>MINK</i> (ZC3), <i>MYO3A</i> , <i>MYO3B</i> , <i>NEK3</i> , <i>NEK4</i> , <i>NEK5</i> , <i>NEK9</i> , <i>NEK11</i> , <i>NRK</i> (ZC4), <i>Obscn</i> domain1&2, <i>PDGFRβ</i> , <i>PKG2</i> (PRKG2), <i>SPEG</i> domain1&2, <i>STK33</i> , <i>TAO1</i> , <i>TAO2</i> , <i>TLK2</i>
			H3
	F1	α D-2	EpHB3 [GK+6], LKB1 [GK+5], <i>PINK1</i> [GK+5]
Front Region	F2	α D-1	BMX , BTk , EGFR , HER2 (ErbB2), HER4 (ErbB4), ITK , JAK3 (catalytic domain), MKK7 , BLK , TEC , TXK ,
	F3	α D+2	JNK1 , JNK2 , JNK3
	F4	α D+6	PI3Kα (PIK3CA), AMPK α 1 AMPK α 2, STK5(STRADA)
	D1	DFG-1	AAK1 , BIKE , CDKL1 , CDKL2 , CDKL3 , CDKL5 , ERK1 , ERK2 , FLT1 , FLT3 , GAK , GSK3β , KDR (VEGFR2), KIT , MAP2K4 , MEK1 , MEK2 , MKK6 , MKK7 , MNK1 , MNK2 , NIK , PBK , PDGFRα , PRP4 , RSK1 domain2, RSK2 domain2, TAK1 , TGFBF2 , ZAK , <i>CDKL4</i> , <i>ERK7</i> , <i>FLT4</i> , <i>Fused</i> (STK36), <i>GSK3α</i> , <i>MAP2K5</i> , <i>MAPKAPK5</i> , <i>MKK3</i> , <i>NLK</i> , <i>Obscn</i> domain1, <i>PDGFRβ</i> , <i>PKD1</i> (PRKD1), <i>PKD2</i> (PRKD2), <i>PKD3</i> (PRKD3), <i>RSK3</i> domain2, <i>RSK4</i> domain2, <i>SPEG</i> domain1
Others	O1	backpocket behind or below GK	<i>EGFR</i> , <i>MELK</i> , PI3Kα (PIK3CA), PI3Kβ (PIK3CB), PI3Kδ (PIK3CD), PI3Kγ (PIK3CG), <i>TTBK1</i> , <i>PI3Kζ</i> α (PIK3C2A), <i>PI3Kζ</i> β (PIK3C2B)
	O2	DFG+1/2	AKT1 , AKT2 , DMPK , IRE1 , MELK , MRCCKβ , NDR1 , P70S6K , PAK1 , PAK3 , PAK4 , PAK5 (PAK7), PAK6 , PKCα , PKCβ , PKCη , PKCζ , PRK1 , PRK2 , ROCK1 , ROCK2 , SGK1 , AKT3 , <i>DMPK2</i> , <i>IRE2</i> , <i>LATS1</i> , <i>LATS2</i> , <i>MAP3K4</i> , <i>MOK</i> , <i>MOS</i> , <i>MRCCKα</i> , <i>NDP2</i> , <i>P70S6Kβ</i> , <i>PAK2</i> , <i>PINK1</i> , <i>PKCγ</i> , <i>PKCδ</i> , <i>PKCϵ</i> , <i>PKCζ</i> , <i>PKN3</i> , <i>SGK2</i> , <i>SGK3</i> , <i>Sgk496</i>
	O3	activation segment (often +2 after phosphorylation site)	AKT1 , AKT2 , MAP2K6 , MELK , MKK7 , MSK1 domain1, P70S6K , PKCα , PKCβ , PKCη , PKCζ , PRK1 , PRK2 , ROCK1 , ROCK2 , SGK1 , AKT3 , <i>MOS</i> , <i>P70S6Kβ</i> , <i>PKCγ</i> , <i>PKCδ</i> , <i>PKCϵ</i> , <i>PKCζ</i> , <i>PKN3</i> , <i>SGK2</i> , <i>SGK3</i>
Remote Cysteines ^a	S1	special position (outside ATP pocket) ^a	CDK7 , CDK12 (CRK7), CDK13 (CHED)
Inactive state or additional ^a	I1 & I2, A1	various positions ^a	KIT (I1, Cys788), PDGFRα (I1, Cys814), IKKα , IKKβ (I2, Cys46), FAK (A1, C427)

The positions or subsites (including several spatially similar locations) are assigned according to the identifiers provided in Fig. 4. The list is based on the analysis of Chaikuad et al. [7] and has been updated according to the literature available at the time of writing. The analysis did not include atypical kinases while lipid kinases from the phosphoinositide 3-kinase family (PI3Ks) were included. Assignments were made on the basis of respective X-ray crystal structures while cysteine locations in kinases without an available X-ray crystal structure (shown in italics) were assigned by sequence alignments. Kinases which have been targeted with covalent ligands are highlighted in magenta and only examples where covalent binding was experimentally proven by either X-ray or MS were included.

^aNon-exhaustive, only positions/kinases that were already covalently addressed have been considered

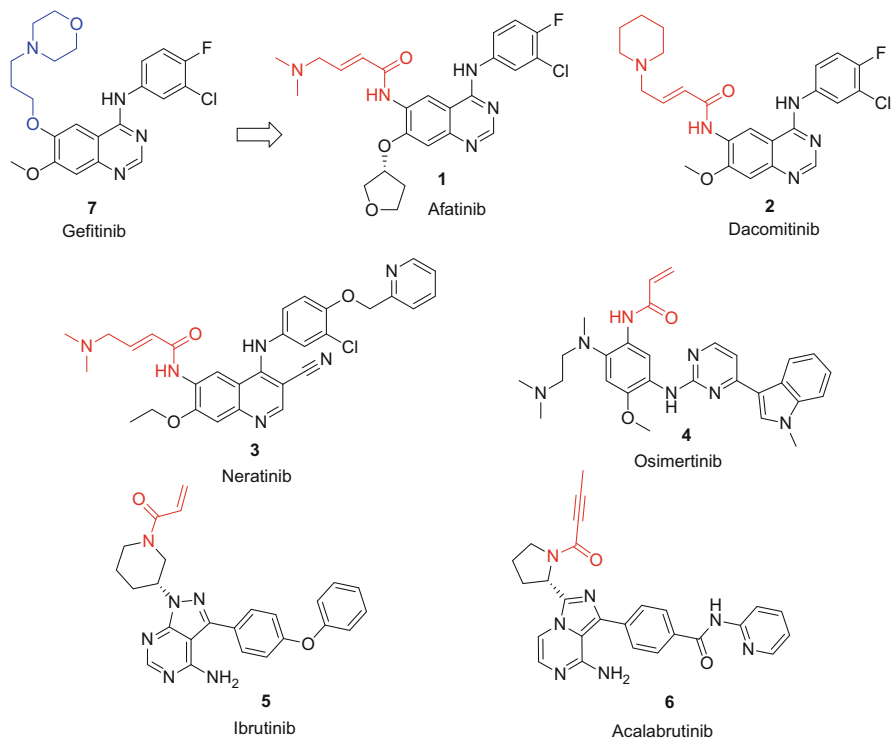


Fig. 5 Currently approved covalent kinase inhibitors. Gefitinib (7), a non-covalent EGFR inhibitor, is depicted as the structural template for the design of covalent (second generation) ErbB family kinase inhibitors

2.3 Natural Products as Covalent Protein Kinase Inhibitors

Natural products have been a rich source of covalent ligands [47] and such compounds have been known as covalent kinase inhibitors for more than two decades [48–50]. For example, hypothemycin (8, Fig. 6) and analogous resorcylic acid lactones (RALs) incorporating an endocyclic *cis*-enone motif engage cysteine residues preceding the conserved DFG motif (D1 position, e.g., Cys166 in ERK2 or Cys174 in TAK1). Equivalent cysteine residues are present in about 50 kinases from several distinct families [5–7] many of which are covalently inhibited by hypothemycin [51, 52]. Modification occurs via hypothemycin's reactive enone moiety while the epoxide, which is also present, behaves as a bystander electrophile in this context. LL-Z1640-2 (FR148083, 5*Z*-7-oxozeaenol, 9), a close analog of hypothemycin binds kinases such as ERK1/2 and TAK via the expected cysteine residues in the D1 position [53]. Despite the presence of a D1 cysteine, a distinct binding mode is observed for mitogen-activated protein kinase kinase MKK7 (MAP2K7). Here, a cysteine in the F2 position of the solvent-exposed front region

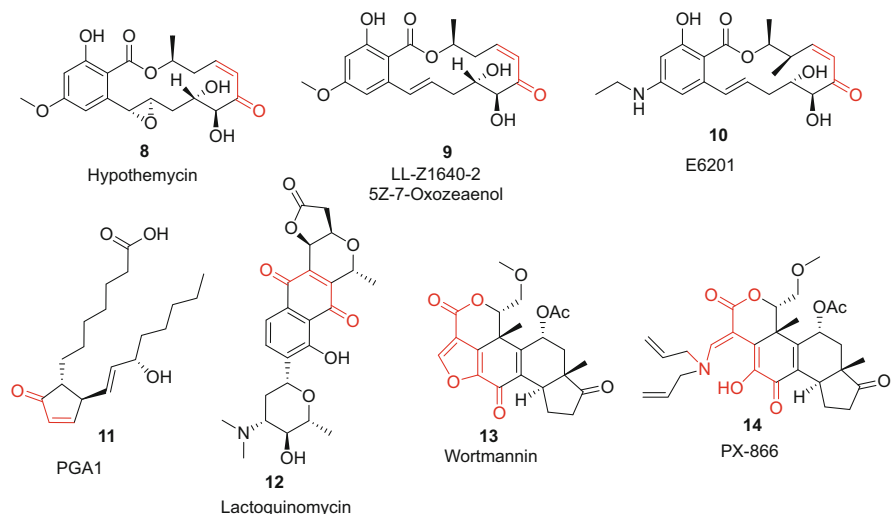


Fig. 6 Selected natural products or natural product derivatives covalently targeting kinases. The reactive moieties involved in covalent bond formation are highlighted in red

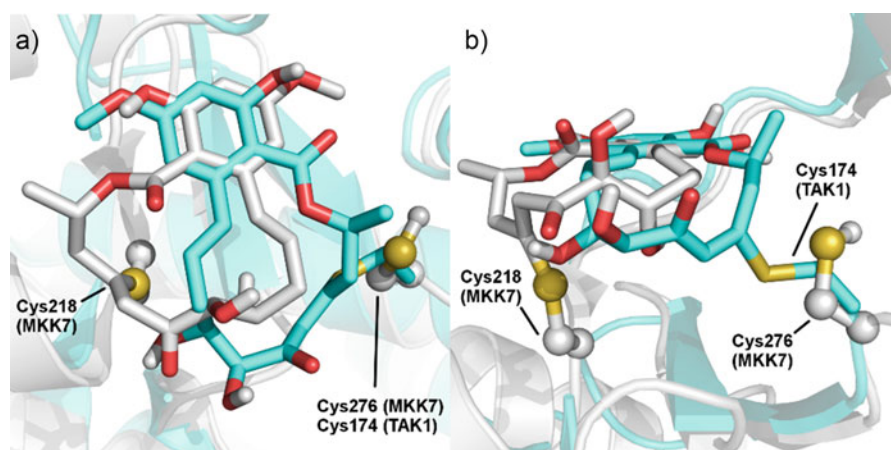


Fig. 7 Overlay of the X-ray crystal structures of **9** covalently bound to MKK7 (gray, both cysteine side chains depicted in the ball and stick representation; PDB: 3WZU) and TAK1 (cyan, cysteine side chain shown as sticks; PDB: 4GS6). While the cysteine moiety at the D1 position, which is common to both kinases is addressed in TAK1, an alternative binding mode engaging a distinct cysteine in the front region of the ATP cleft (F2 position) is observed in MKK7. (a) Top view. (b) Front view

is modified (see the overlay in Fig. 7a, b) [54]. LL-Z1640-2 was further developed to clinical candidate E6201 (**10**), a potent MEK/FLT3 inhibitor, by researchers from Eisai [55, 56]. The compound was efficacious in in vivo models and moved to phase II clinical studies for the treatment of psoriasis (NCT01268527, NCT00539929),

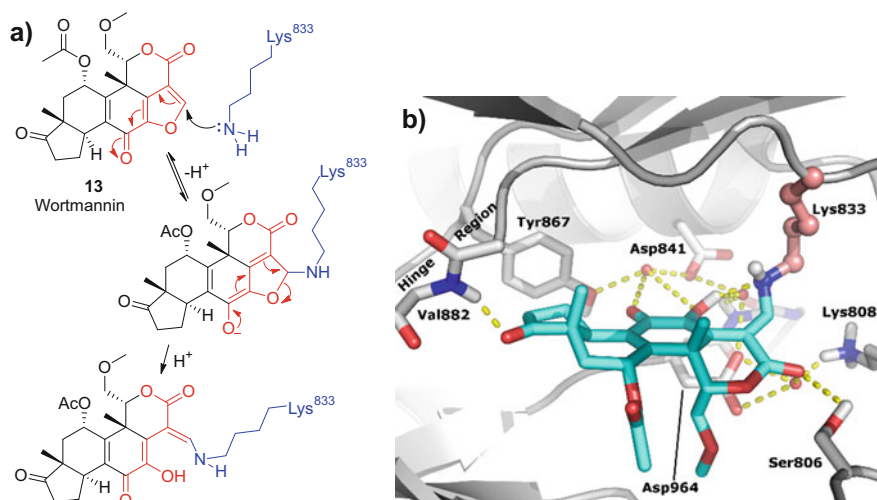


Fig. 8 Wortmannin (**13**), a lysine-targeted PI3 kinase inhibitor. (a) Mechanism suggested for the reaction with PI3K γ -Lys833. (b) Binding mode of **13** in the ATP-pocket of PI3K γ confirming the ring opening and the covalent binding to the Lys833 ϵ -amino group (PDB: 1E7U)

hematologic malignancies with FLT3 and/or Ras mutations (NCT02418000, terminated), and recently for melanoma CNS metastases (NCT03332589). Further natural products that are known to covalently engage protein kinases via cysteine adduction include, for example, cyclopentenone prostaglandins (e.g., PGA₁, **11**) targeting the activation loop cysteine (Cys178/179) in IKK α/β [57] or pyranonaphthoquinones (e.g., lactoquinomycin, **12**) targeting Cys296 and Cys310 (O2-position) in the activation loop of AKT1 [58].

Wortmannin (**13**), a natural product belonging to the viridin furanosteroids is a potent inhibitor of the lipid kinases from the phosphoinositide 3-kinases (PI3Ks) family. In contrast to the cysteine-targeted enones discussed above, this and analogous compounds covalently modify the conserved catalytic lysine (Lys833 in PI3K γ) [48]. Attack by the lysine's ϵ -amino group occurs at the unsubstituted carbon atom of the dually activated furan ring [59]. The furan undergoes a ring opening, presumably via an intermediate enolate, to form a conjugated enamine (see the mechanism and binding mode in Fig. 8a, b). Opening the ring with diallylamine furnished PX-866 (**14**), an analog with improved PK properties that moved to clinical trials. In contrast to the addition products of primary amines, which feature an inactive Z-configured enamine that is stabilized by an intramolecular hydrogen bond with the lactone's carbonyl oxygen atom, secondary amine-derived adducts retain inhibitory activity. The latter undergo exchange reactions with primary amines while the inverse reaction could not be observed [60]. Compound **14** alone or in combination was tested in phase II clinical trials for the treatment of different cancer types including prostate cancer (NCT01331083), glioblastoma (NCT01259869), and non-small cell lung cancer (NSCLC) (NCT01204099).

2.4 Development of Inhibitors Targeting Cysteines in the Front Region

2.4.1 Inhibitors Targeting the F2 Position

So far, the most extensive research efforts have been directed toward kinases featuring a cysteine residue at the F2 ($\alpha\text{D} - 1$) position. Being located in the solvent-exposed front region, F2 cysteines are common to 11 kinases, namely the ErbB family members EGFR, ErbB2, and ErbB4 (but not the pseudokinase ErbB3), the TEC family kinases (TEC, BTK, ITK, BMX, and TXK), the SRC kinase BLK, the Janus kinase JAK3, and the MAP kinase kinase MKK7. The most considerable drug discovery efforts have been aimed toward Cys797 of the EGFR receptor tyrosine kinase. As a member of the ErbB family, EGFR (also referred to as HER1 or ErbB1) transduces growth signals either as a homodimer or as a heterodimer with other ErbB family members. Aberrant EGFR activity is a common driver of non-small cell lung cancer (NSCLC) and patients with certain activating EGFR mutations (e.g., L858R or exon 19 deletions) showed impressive response rates to first-generation (reversible) EGFR inhibitors such as gefitinib (see Fig. 5) or erlotinib. Unfortunately, secondary resistance mutations, most notably the T790M mutation of the gatekeeper residue, appeared rapidly and rendered first-generation EGFR inhibitors virtually inactive in approximately half of the responder population. In this light, second- and third-generation EGFR inhibitors were developed to exploit the nucleophilic nature of Cys797.

Pioneering work was reported already in the late 1990s by Singh, Fry, and colleagues from Parke-Davis. They characterized 2'-thioadenosine (**15**, Fig. 9a) [61] and the 4-aminoquinazoline-derived acrylamide PD-168393 (**16**) [62] as covalent modifiers of EGFR-Cys797 and the analogous Cys805 in ErbB2 (and

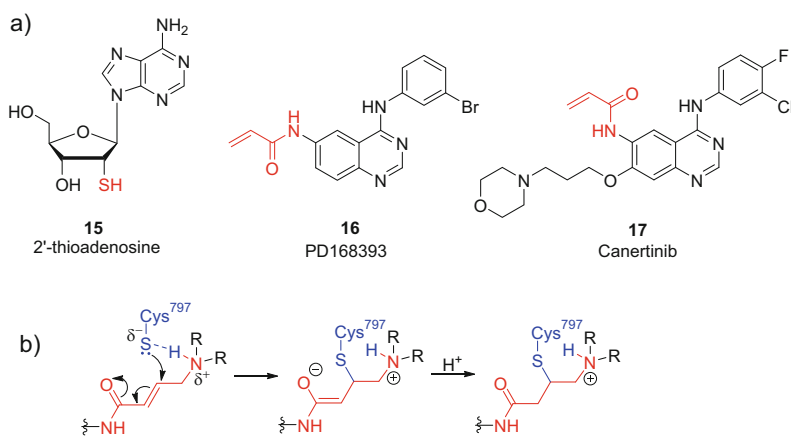


Fig. 9 (a) Early covalent ErbB family kinase inhibitors targeting the cysteine in the F2 position. (b) Mechanism of 4-(dialkylamino) crotonamide-assisted cysteine deprotonation/nucleophilic attack

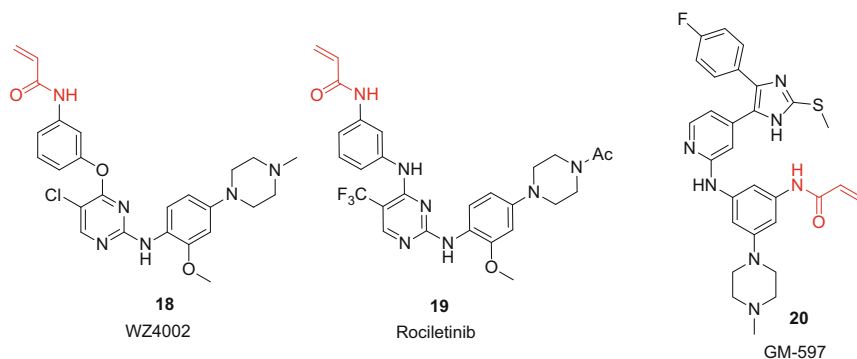


Fig. 10 Third-generation and more recent covalent EGFR/ErbB kinase inhibitors

presumably also Cys803 in ErbB4). Improved efficacy of **16** compared to the biochemically almost equipotent propionamide analog was observed in a xenograft model highlighting the potential pharmacological advantages of covalent inhibitors. Further development of analogous compounds led to canertinib (CI-1033, **17**), the first irreversible pan-ErbB inhibitor entering clinical trials [63]. The development of canertinib, however, was recently discontinued. Afatinib (**1**), the first approved covalent ErbB inhibitor features a very similar structure. Besides modifications at the quinazoline's C7 substituent, a key difference consists in the replacement of canertinib's acrylamide warhead by an analogous 4-(dialkylamino) crotonamide to assist the deprotonation of the cysteine's thiol group (see the mechanism in Fig. 9b). Although afatinib showed high efficacy in the treatment of NSCLC with activating EGFR mutations, the drug suffered from dose-limiting side effects hampering its use for overcoming the T790M resistance. Approval of the structural analog dacomitinib (**2**) was delayed until recently since early trials did not prove superiority compared to first generation EGFR inhibitors.

On the basis of the related quinoline scaffold, compounds featuring a carbonitrile group at the C3-position of the heterocyclic core were developed in order to increase ErbB2 inhibitory activity, the latter being frequently overexpressed in breast cancer [64]. These efforts culminated in the recent approval of neratinib (**3**).

Third-generation EGFR inhibitors were designed to target resistant/activating EGFR-mutants (e.g., EGFR L858R/T790M) while sparing the wild-type kinase to decrease dose-limiting side effects, which constitute a key liability of the second-generation drugs. The structure of such compounds does not rely on the prototypical 4-aminoquinazoline scaffold. WZ4002 (**18**, Fig. 10), the first third-generation irreversible ErbB kinase inhibitor, was reported in 2009 by researchers at the Dana-Farber Cancer Institute [65]. This 2-aminopyrimidine derivative features a moderate selectivity for EGFR with an activating L858R plus the aforementioned T790M resistance mutation. An X-ray crystal structure of the compound bound to the EGFR T790M mutant shows the formation of two hydrogen bonds between the aminopyrimidine and the hinge region and confirms labeling of Cys797 by the acrylamide warhead (PDB: 3IKA). Moreover, a hydrophobic contact between the

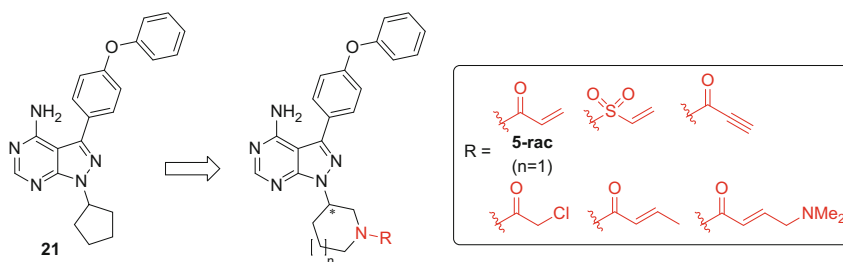


Fig. 11 Development of irreversible BTK inhibitors from reversible inhibitor **21**. The *R*-enantiomer of compound **5-rac** equals ibrutinib

pyrimidine's 5-chloro substituent and the sulfur atom of the gatekeeper methionine residue is observed. The latter interaction, which also can be interpreted within the conceptual framework of halogen bonding [66, 67], is thought to contribute to the observed selectivity for the T790M mutant. Rociletinib (CO1686, **19**), a structurally related inhibitor developed by Clovis Oncology and tested in clinical trials up to phase III (NCT02322281) was dropped in May 2016 for several reasons including lower response rates and a less favorable benefit–risk profile compared to osimertinib [68], which was simultaneously developed by AstraZeneca. Osimertinib successfully gained fast track approval in 2015/16 [69].

Besides escape pathways (e.g., HER2 and MET amplification or PI3K/AKT/mTOR activation), resistance to third-generation EGFR inhibitors is frequently driven by mutation of the reactive cysteine to serine. The common L858R/T790M/C797S triple mutant, for example, precludes covalent binding and is resistant against all EGFR inhibitor generations. A new EGFR inhibitor type (exemplified by GM-597, **20**) that covalently binds gefitinib-resistant double mutants while maintaining nanomolar reversible activity against EGFR L858R/T790M/C797S has recently been described by Günther et al. [70, 71].

The second class of clinically successful covalent kinase inhibitors addresses Bruton's tyrosine kinase (BTK), with two compounds being currently approved by the FDA (vide supra). BTK is a cytoplasmic tyrosine kinase belonging to the TEC family and plays a key role in B-cell receptor signaling. Due to its essential function in B-cell development, BTK has been selected as a target not only for the treatment of B-cell malignancies, but also for inflammatory and autoimmune disorders. Like the aforementioned ErbB family kinases, BTK features a cysteine residue in the F2 position (Cys481). In 2006, the first covalent BTK inhibitors were reported by researchers from Celera Genomics [72] and subsequently employed as tool compounds [73]. A structure-based design approach was used to transform the potent reversible BTK inhibitor **21** (Fig. 11) into reactive analogs addressing Cys481. Key compound **5-rac**, an inhibitor with subnanomolar potency featuring an acrylamide warhead attached to a piperidin-3-yl residue, was capable of covalently modifying BTK according to washout and MS-experiments. In this context, it is worth mentioning that aliphatic amine-derived acrylamides typically feature lower intrinsic

reactivities compared to analogous anilides [74] which might translate into decreased promiscuity. Compound **5-rac** was effective in an arthritis mouse model and the more potent *R*-enantiomer now known as ibrutinib (**5**, see Fig. 5) was further developed by Pharmacyclics and Johnson & Johnson. Interestingly, ibrutinib was later shown to potently inhibit most other kinases with an equivalently positioned cysteine [45].

Acalabrutinib (**6**, see Fig. 5), an approved second-generation covalent BTK inhibitor, features a related imidazo[1,5-*a*]pyrazine core [45]. In this case, a but-2-ynamide warhead linked via the nitrogen atom of an *S*-configured pyrrolidin-2-yl substituent was employed. While propiolamides are more reactive than analogous acrylamides, but-2-ynamides are slightly less reactive [74] making acalabrutinib more stable toward GSH when compared to ibrutinib ($t_{1/2} = 5.5$ h vs. 1.9 h). Acalabrutinib ($IC_{50}^{BTK} = 5.1$ nM, $k_{inact}/K_I = 3.1 \times 10^4$ M⁻¹ s⁻¹) was shown to be slightly less potent than ibrutinib ($IC_{50}^{BTK} = 1.5$ nM, $k_{inact}/K_I = 4.8 \times 10^5$ M⁻¹ s⁻¹) but relatively selective against most kinases harboring an F2 cysteine with only ErbB4 ($IC_{50} = 16$ nM), BMX ($IC_{50} = 46$ nM), and TEC ($IC_{50} = 126$ nM) being significantly hit (MKK7 was not tested). The compound features a clean kinome profile, oral availability, and durable target engagement in vivo (99% after 4 and 12 h, 100 mg p.o.) although being rapidly eliminated thus highlighting the disconnection between PD and PK, a key feature of many irreversible inhibitors. Acalabrutinib showed a tolerable adverse effect profile and gained accelerated approval by the FDA as second-line therapy for mantle cell lymphoma (MCL) [75]. Several phase III studies for the treatment of chronic lymphocytic leukemia (CLL) are ongoing. However, BTK C481S mutation renders both ibrutinib and acalabrutinib ineffective at the recommended dosage since the decreased potency in combination with the relatively fast clearance of these compounds precludes sustained reversible target engagement [76].

Besides the two aforementioned drugs, many other irreversible BTK inhibitors with distinct chemotypes and good or excellent selectivity profiles (e.g., CHMFL-BTK-11 [77], branebrutinib [78], spebrutinib [45], or poseltinib [79], **22–25**, Fig. 12a) have been investigated in preclinical and clinical studies. A covalent-reversible approach was chosen by researchers from the Taunton group and Principia Biopharma [11], who generated α -cyanoacrylamide derivatives of ibrutinib to engage BTK Cys481. Target residence times could be modulated as a function of the β -substituent. For example, compound **26a** (Fig. 12b) bearing a bulky *tert*-butyl group in the β -position retained >50% cellular target occupancy 20 h after washout. In contrast, occupancy of methyl-capped analog **26b** was negligible under the same conditions. The extended target residence time of compound **26a** may be rationalized by additional thermodynamic stabilization of the covalent complex via hydrophobic interactions with the bulky *tert*-butyl moiety, which simultaneously induces a conformation with decreased α -CH-acidity while also shielding the $C\alpha$ -proton from water thereby impeding its abstraction (see PDB: 4YHF). Further optimization with special emphasis on improving solubility and PK properties furnished a compound series exemplified by **27a** and **27b**. While **27a** ($IC_{50} = 0.7$ nM, $k_{inact}/K_I = 1.9 \times 10^3$ M⁻¹ s⁻¹) had a residence time of 34 h, key compound **27b** ($IC_{50} = 1.9$ nM, $k_{inact}/K_I = 4.3 \times 10^2$ M⁻¹ s⁻¹) behaved quasi-irreversible with a

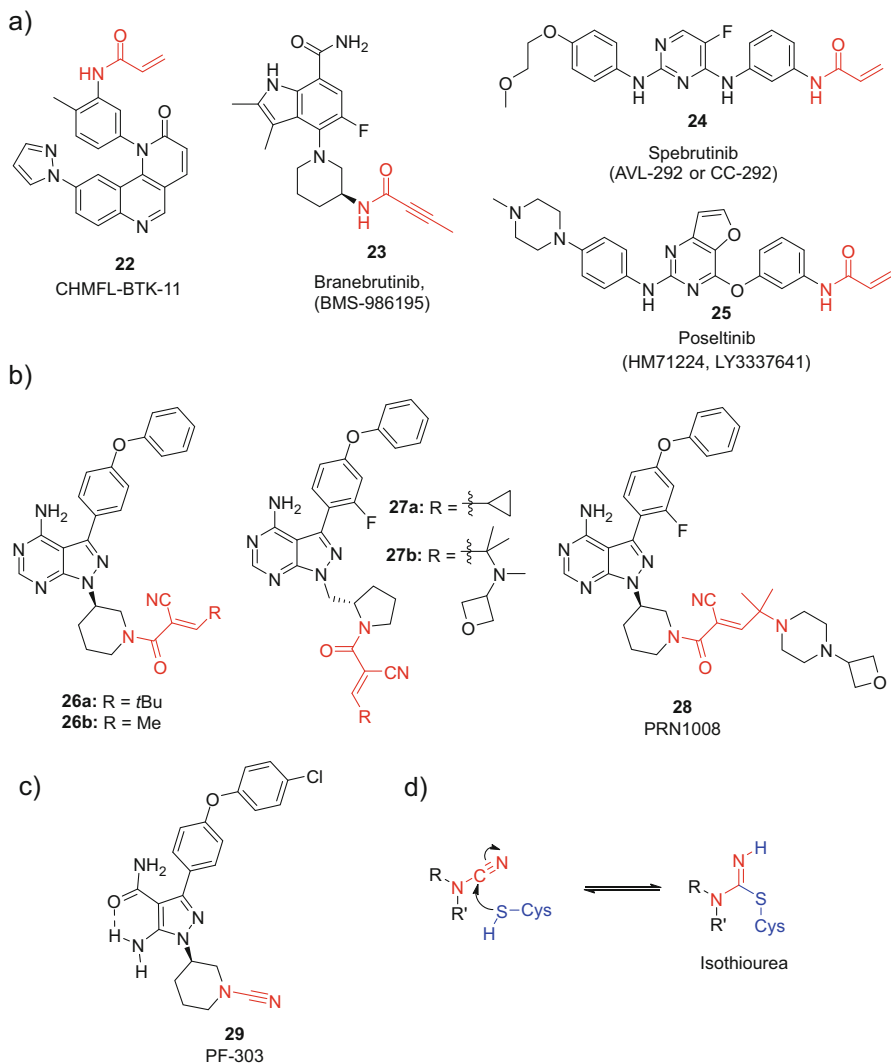


Fig. 12 (a) Selected examples of irreversible BTK inhibitors. (b) α -Cyanoacrylamide-based covalent-reversible BTK inhibitors. (c) Cyanamide-based covalent-reversible BTK inhibitor PF-303. (d) Mechanism of the reversible cysteine addition to cyanamides

residence time of approx. 1 week. In accordance with the applied design concept, binding was rapidly reversible after proteolysis. Compound **27b** showed sustained target occupancy after clearance in vivo (as determined with a fluorescent covalent probe) and had a relatively clean profile in a panel of 254 kinases. Nevertheless, five other kinases sharing the combination of an F2 cysteine and a threonine gatekeeper residue were strongly hit at 1 μ M including BMX, which was even inhibited >90% at 100 nM. The discussed compound series was further developed to drug candidate PRN1008 (**28**, IC_{50} = 1.3 nM) [80], an orally available, covalent-reversible BTK

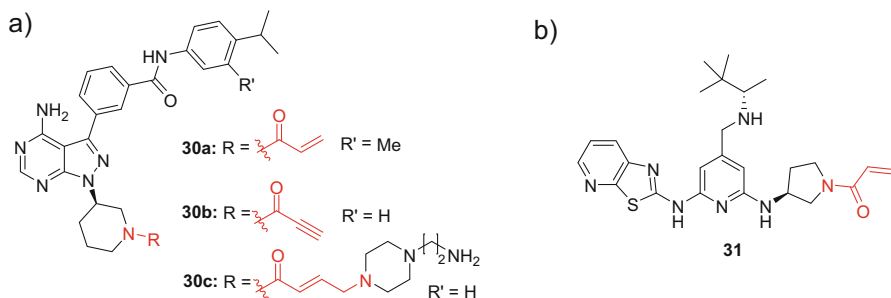


Fig. 13 Covalent ITK inhibitors from (a) Pfizer and (b) GSK

inhibitor with a slow dissociation rate that recently entered phase III clinical trials for the treatment of pemphigus (NCT03762265).

PF-303 (**29**, Fig. 12c), a covalent-reversible BTK inhibitor from Pfizer, addresses the same cysteine residue via a cyanamide group [81]. Cyanamides, a warheads class known from cysteine protease inhibitors [82, 83], react with cysteines at similar rates as acrylamides [74]. This Pinner-type addition results in the reversible formation of isothiourea products (Fig. 12d). PF-303, which can be regarded as an ibrutinib bioisostere, is a very potent BTK inhibitor ($IC_{50} = 0.64$ nM, $k_{inact}/K_I = 1.44 \times 10^5$ M⁻¹ s⁻¹) with a moderate dissociation rate ($t_{1/2} = 5$ h). While being highly selective against JAK3, ITK (both >10,000-fold), and several related kinases, PF303 inhibits TEC and BMX at similar potency as BTK. The compound efficiently blocked anti-IgM F(ab')₂-mediated proliferation of murine B-cells ($IC_{50} = 2$ nM) and showed *in vivo* activity in mice upon oral dosing.

Interleukin-2 inducible T-cell kinase (ITK) is closely related to BTK and features an equivalently positioned cysteine (Cys422) that was suggested to possess a lower nucleophilicity due to a pK_a increase promoted by the proximal Asp445 [84]. As a mediator of T-cell receptor signaling, ITK plays an important role in T-cell development, differentiation, and function. It is considered a promising target in the treatment of inflammatory and autoimmune disorders as well as T-cell malignancies. Based on the fact that ibrutinib and similar BTK inhibitors show significant off-target activity on ITK, researchers from Pfizer developed analogous compounds to address this kinase. A structure-based design approach furnished acrylamide **30a** (PF-06465469, Fig. 13a), a highly potent ITK inhibitor ($IC_{50} = 2$ nM at 1 mM ATP, $k_{inact}/K_I = 1.6 \times 10^4$ M⁻¹ s⁻¹) [84]. Several alternative warheads were tested, however, only the more reactive propiolamide **30b** showed similar potency. Compound **30a** was potent in a human whole blood assay and showed sustained activity in cells. Covalent engagement of Cys442 was confirmed for several analogs by X-ray crystallography (PDB: 4HCT, 4HCV, 4HCU). However, **30a** was also shown to be an equipotent inhibitor of BTK. Selectivity against BTK seems to be difficult to achieve not only because of the lower acidity of ITK's F2 cysteine but also due to its higher affinity toward ATP. Nevertheless, one compound with a moderate selectivity

for ITK could be obtained (**30c**) albeit at the expense of potency ($IC_{50}^{ITK} = 60$ nM vs. $IC_{50}^{BTK} = 1,050$ nM).

Another series of covalent ITK inhibitors exemplified by compound **31** (Fig. 13b) was reported by researchers at GSK [85]. This key compound possessed high potency ($IC_{50} = 5$ nM at 1 mM ATP), a more pronounced selectivity against BTK and a higher k_{inact}/K_I ratio (5.2×10^5 M⁻¹ s⁻¹) compared to the aforementioned inhibitors. Covalent binding was verified by jump-dilution, cellular washout, and X-ray crystallography using a close analog (PDB: 4KIO). Compound **31** demonstrated low reactivity toward GSH, favorable PK properties for inhaled dosing, and prevented anti-CD3-induced T-cell activation in rat lung tissue (p.i.). In human PBMCs, the compound further suppressed the production of T_H1, T_H2, and T_H17 cytokines.

Other kinases with a cysteine at the F2 position that have been addressed by rationally designed covalent inhibitors include JAK3, BMX, and MKK7. Efforts toward highly isoform-selective JAK3 inhibitors culminated in the development of the clinical candidate PF-06651600 (**32**, Fig. 14a) and have been summarized in a separate chapter of this book and a recent review [86]. Notably, efforts published very recently from researchers at Pfizer showed that JAK3 Cys909 is also amenable to covalent-reversible targeting with cyanamides (e.g., compound **33a**) [17]. The latter compound features excellent isoform selectivity (>245-fold vs. other JAKs at 1 mM ATP), high potency ($IC_{50} = 11$ nM at 1 mM ATP), and efficient inactivation kinetics ($k_{inact}/K_I = 1.9 \times 10^5$ M⁻¹ s⁻¹) while being reasonably stable against GSH. X-ray crystallography (e.g., with the analog **33b**) unambiguously confirmed isothiourea formation (Fig. 15a).

A distinct series of α -cyanoacrylamide-based covalent-reversible JAK3 inhibitors (exemplified by **34a** and **b**) with excellent isoform and kinome selectivity has been developed by Forster et al. [87, 88]. Remarkably, both the covalent and the non-covalent complexes coexist in the X-ray crystal structure of **34b** bound to JAK3 (Fig. 15b). The nitrile substituent of these compounds opens up a rare induced-fit pocket formed by Arg911, Arg953, and Asp912 which constitutes an additional selectivity filter contributing to the excellent selectivity of this compound class in the kinome.

Covalent inhibitors for other kinases with an F2 cysteine have also been reported. Inhibitors that target the kinase BMX include, for example, the dual BMX/BTK inhibitor BMX-IN-1 (**35**, Fig. 14b) [89], or the type II inhibitor CHMFL-BMX-078 (**36**) [90] featuring increased selectivity against BTK. As mentioned before, the MAP kinase kinase MKK7, one of the two activators of the c-Jun N-terminal kinases (JNKs) features several cysteines in the active site: one at the F2 position (Cys218), one at the D1 position (Cys276), one at the P3 position (Cys147), and one at the O3 subsite (Cys296). The F2 cysteine, which is also addressed by LL-Z1640-2 (**9**, see Figs. 6 and 7), has recently been targeted by indazole-derived inhibitors exemplified by **37** (MKK7-COV-2, Fig. 14c) discovered in a virtual screening campaign using DOCKoValent [91, 92]. Even more recently, ibrutinib-derived 1,2,3-triazoles (e.g., **38**) addressing MKK7-Cys218 have been reported by the Rauh group [93].

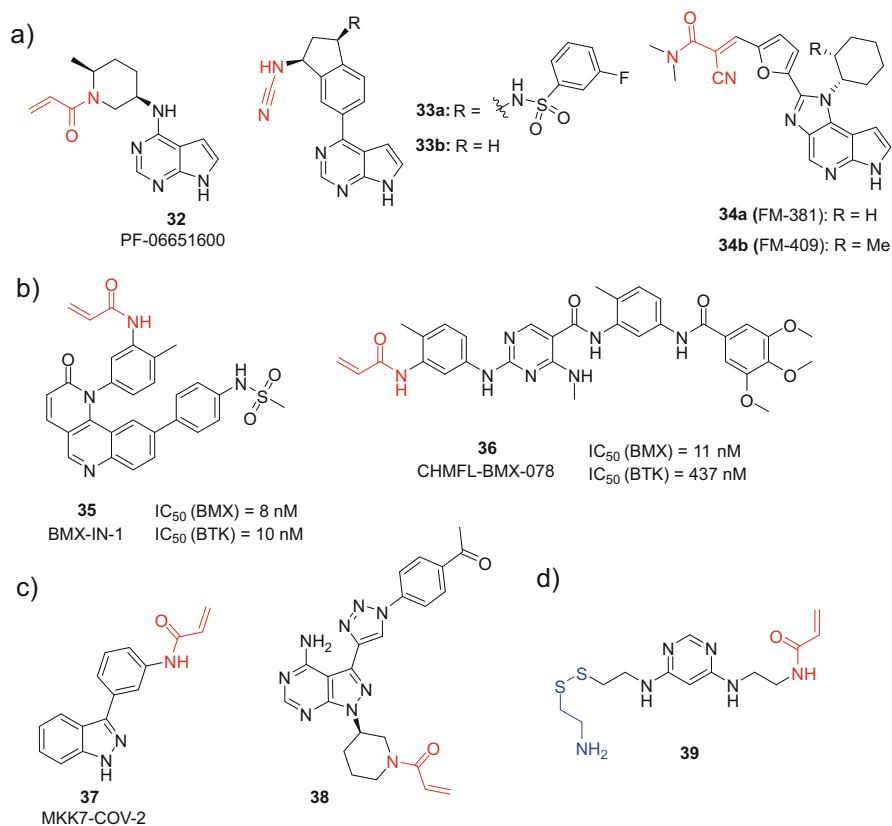


Fig. 14 (a) Examples of irreversible and covalent-reversible JAK3 inhibitors. (b) Irreversible covalent BMX inhibitors. (c) Irreversible covalent MKK7 inhibitors. (d) Disulfide-tagged covalent PDK1-E166C inhibitor **39**

An engineered cysteine at an equivalent position in PDK1 (E166C) has been addressed by Erlanson et al. using an acrylamide-based “extender” (**39**, Fig. 14d) equipped with a (di)sulfide-tag. A subsequent fragment-based disulfide tethering screen enabled the generation of potent reversible PDK1 inhibitors [94]. Moreover, the introduction of analogous engineered cysteines has been used in the context of chemical-genetics approaches to generate probes for kinases such as Aurora kinase [95] and c-SRC [96].

2.4.2 Inhibitors Targeting the F3 Position

The three c-Jun N-terminal kinases (JNK1–3) are the only kinases known to feature an accessible cysteine in the F3 position of the α D-helix (α D + 2), eight amino acids after the gatekeeper residue. This cysteine has been targeted by imatinib-derived

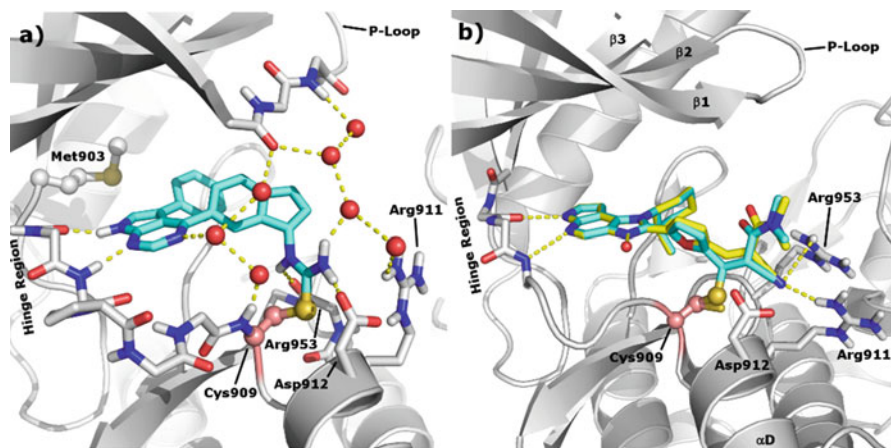


Fig. 15 (a) Binding mode of cyanamide-based covalent-reversible JAK3 inhibitor **33b** (PDB: 6DB4). The formed isothiourea is involved in several direct and water-mediated hydrogen bonds contributing to the stabilization of the covalent complex. In the hinge region and the P-loop region, side chains were omitted for clarity. (b) Binding modes of α -cyanoacrylamide-based covalent-reversible JAK3 inhibitor **34b** (PDB: 5LWN). The simultaneous presence of both, the covalently and the non-covalently bound compound (highlighted in cyan and yellow, respectively) is observed

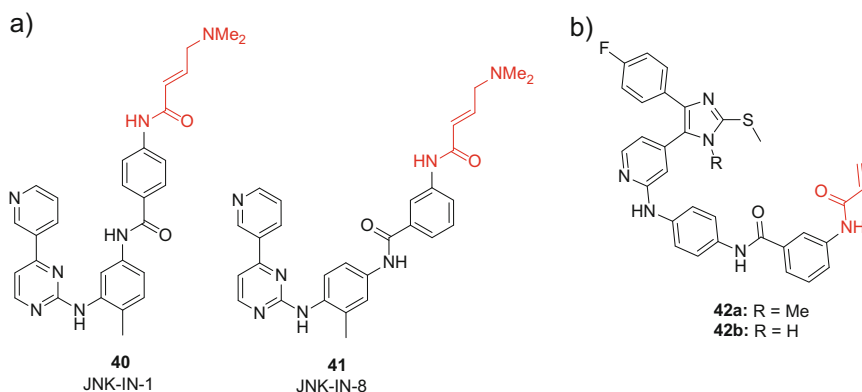


Fig. 16 (a) Imatinib-derived covalent JNK inhibitors. (b) Pyridinylimidazole-derived covalent JNK inhibitors

covalent inhibitors serendipitously discovered by Gray and co-workers [97]. These researchers initially aimed to address cysteines located in the catalytic loop of the PDGFR and c-KIT receptor tyrosine kinases being only accessible in the DFG-out conformation (subsite II, see Fig. 4 and Table 1). However, the designed compound JNK-IN-1 (**40**, Fig. 16a) showed strong off-target activity on JNKs [15]. Structure-guided optimization of this initial hit furnished the potent pan-JNK inhibitor JNK-IN-8 (**41**, IC_{50} = 4, 19, and 1 nM for JNK1–3, respectively), a compound

with an excellent selectivity in the kinome and reasonable cellular potency. Covalent modification of Cys154 (JNK3 numbering) was shown for some close analogs by MS and X-ray crystallography (see PDB: 3V6R and 3V6S).

Structurally distinct pyridinylimidazole-derived covalent JNK inhibitors (e.g., **42a** and **b**, Fig. 16a) were developed from reversible p38 α MAP kinase inhibitors in the groups of Koch and Laufer using a structure-based approach [98]. Both compounds potently block JNK3 enzymatic activity with IC₅₀ values bordering the picomolar range. The inhibitors covalently labeled JNK3 as confirmed by MS experiments while leaving the C154A mutant unmodified. However, while the tetra-substituted imidazole **42a** retained significant (reversible) inhibitory activity on p38 α (IC₅₀ = 36 nM), *N*-desmethyl analog **42b** displayed an approx. 1,000-fold selectivity window over the latter enzyme. Both compounds showed a relatively clean profile in a panel of 410 kinases. More detailed information on covalent and non-covalent JNK inhibitors can be found in a dedicated chapter of this book and in recent reviews [99, 100].

2.4.3 Inhibitors Targeting the F1 and the F4 Position

Further cysteines in the front region of protein kinases that have proven amenable to covalent targeting are located at the F1 ($\alpha D - 2$) and the F4 ($\alpha D + 6$) positions. According to the underlying analysis, an F1 cysteine occurs in the three kinases EphB3, LKB1, and PINK1 but it has only been addressed in the EphB3 receptor tyrosine kinase so far. In a series of 4-aminoquinazoline-derived inhibitors evaluated by Kung et al., different electrophiles were tested and chloroacetamide **43a** (Fig. 17a) potently blocked Eph3B kinase activity (IC₅₀ = 55 nM). Compound **43a** was devoid of significant inhibitory activity on the EphB3 C717S mutant and the related kinases EphA4 and EphB4 [101]. The analogous α -chloromethyl ketone **43b** showed an even higher apparent potency (IC₅₀ = 6 nM), presumably due to the increased intrinsic reactivity of this electrophile, and both compounds were active in cells. In contrast, analog **43c** lacking a leaving group showed only negligible inhibitory activity (IC₅₀ > 10 μ M). Covalent modification of Cys717 was confirmed by washout experiments, mass spectrometry, and X-ray crystallography (PDB: 5L6P

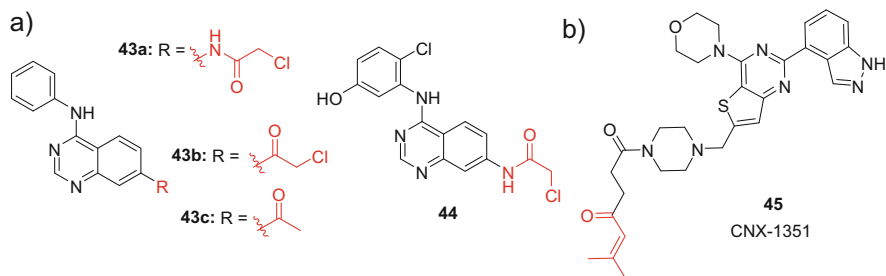


Fig. 17 (a) Covalent Eph3B kinase inhibitors. (b) Covalent PI3K α inhibitor **45**

and 5L6O). However, compound **43a** inhibited EGFR more potently than EphB3. The optimized analog **44** at 50 nM possessed a clean profile in a panel of 98 kinases while fully abrogating EphB3 activity. No substantial inhibition of LKB1 also possessing an F1 cysteine was observed. In this context, it is worth mentioning that although cysteines in LKB1 and PINK1 are positioned at F1 (i.e., two residues before the start of the α D helix), the hinge region of these kinases is shortened by one amino acid (GK + 5 position vs. GK + 6 in EphB3). Consequently, these cysteine residues adopt different orientations in the latter two kinases. A clickable analog of compound **44** suggested cellular target engagement and limited off-target modification at concentrations below 100 nM. Noteworthy, inhibitor **44** was used as a covalent probe for EphB1 in a chemical-genetics-based study where EphB1 was engineered to feature an equivalent cysteine (G703C mutant). An analogous approach was also applicable to the kinases FGFR4, ABL, and RAF [102].

Being among the few kinases known to harbor a cysteine residue in the F4 (α D + 6) position, the lipid kinase PI3K α was addressed with inhibitor CNX-1351 (**45**, Fig. 17b) [103]. This compound potentially hits PI3K α (6.8 nM) with good selectivity against some other PI3Ks. It caused prolonged inhibition of PI3K α signaling in cells and target engagement was demonstrated in vivo. Despite being equipped with an enone warhead, inhibitor **45** possessed only low reactivity toward GSH and several plasma proteins, showcasing that the β,β -dimethyl substitution efficiently attenuates the enone's intrinsic reactivity [25]. Covalent modification of Cys862 was demonstrated by MS and X-ray crystallography (PDB: 3ZIM). Due to the cysteine being located relatively far outside the ATP pocket, a long spacer was required. Remarkably, the morpholine oxygen atom acts as the non-canonical hinge-binding anchor of this compound.

2.5 Development of Inhibitors Targeting Cysteines around the P-Loop and in the Roof Region

2.5.1 Inhibitors Targeting the R1 Subsite

ErbB3 (HER3), a pseudokinase which forms catalytically active heterodimers with other ErbB kinases, is lacking the F2 cysteine residue common to the remaining ErbB family members. However, this protein has recently been addressed via Cys721, a cysteine located at the R1 subsite at the roof of the ATP binding cleft [104]. R1-cysteines are only known in four other kinases (WNK1–4) [7]. In the WNK family kinases, however, these moieties are located two positions further C-terminally (β 3 + 3 in ErbB3 vs. β 3 + 5 in WNKs) making the positioning of Cys271 unique. A non-reactive screening hit was developed to the initial lead compound TX1-85-1 (**46**, Fig. 18), a covalent ErbB3 ligand with nanomolar potency. Unfortunately, **46** was inefficient in suppressing the proliferation of ErbB3-addicted cell lines and ErbB3-dependent downstream signaling at concentrations that would fully label the target protein. However, transforming **46** into

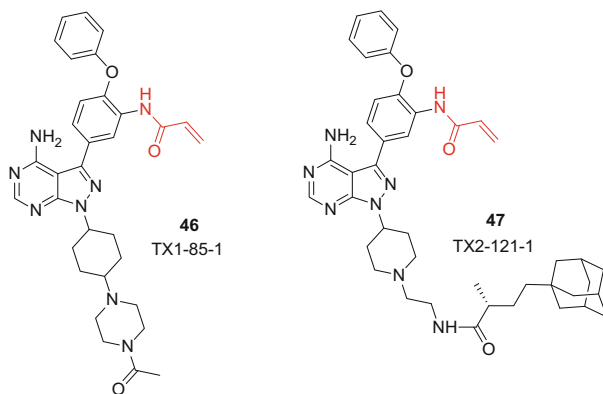


Fig. 18 Covalent ErbB3 ligand **46** and hydrophobically tagged degrader **47**

(partial) ErbB3-degrader TX2-121-1 (**47**) by employing a hydrophobic tagging approach resulted in a more pronounced reduction of ErbB3-dependent signal transduction and proliferation. These effects were not observed for the ErbB3 C721S mutant. Consistently, an analogous non-reactive degrader proved to be less efficient. In contrast to these data, covalent binding was recently found to impair PROTAC-promoted degradation of BTK [105].

2.5.2 Inhibitors Targeting the Positions or Subsites P1–P4 and A1

Another series of cysteines amenable to covalent targeting is located in the glycine-rich loop (P-loop) or the adjacent β -sheets (P1–P4). An additional cysteine (subsite A1; not included in earlier analyses [5–7, 15, 18]) can also be covalently trapped despite its orientation outward the ATP pocket as demonstrated by a recent study (vide infra) [38].

In their pioneering work, Taunton and co-workers developed fluoromethylketone-based inhibitor **48** (FMK, Fig. 19a) to address the C-terminal kinase domain (CTD) of p90 ribosomal protein S6 kinases (RSKs) via a cysteine located at position P4 [106]. The RSKs and the closely related mitogen- and stress-activated protein kinases (MSKs) possess two functional kinase domains i.e. the aforementioned CTD and an additional N-terminal kinase domain (NTD), with the P4 cysteine being only present in the CTD. Besides the four RSKs (RSK1–4), only 7 other kinases (PLK1–3, NEK2, MSK1/2, and MEKK1) are known to possess an analogous cysteine. In this approach, the relatively small threonine gatekeeper residue, which among these kinases is only shared by the CTDs of RSK1, 2, and 4 (RSK3 has a methionine gatekeeper), was used as an additional selectivity filter. Fluoromethylketone **48** is a potent RSK2-CTD inhibitor ($IC_{50} = 15$ nM) with high selectivity against the RSK2 C436V and the T493M gatekeeper mutant. In cells, the compound inactivated both RSK1 and RSK2 and cellular selectivity was demonstrated with a clickable probe in a subsequent study [107]. The same scaffold was also

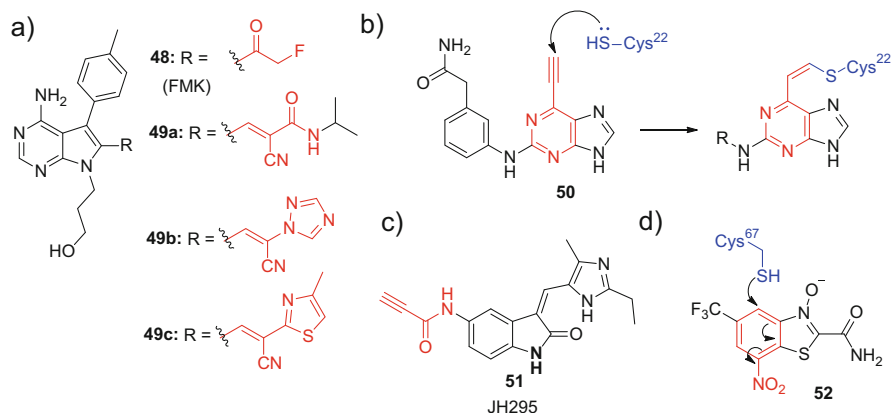


Fig. 19 (a) Irreversible and covalent-reversible RSK inhibitors. (b) Covalent NEK2 inhibitors featuring a 6-ethynyl purine warhead. (c) Irreversible NEK2 inhibitor **51**. (d) Electron-deficient heteroarenes suggested to target PLK1 via reversible Meisenheimer complex formation

used in Taunton's seminal work on dually activated Michael acceptors as tunable electrophiles for reversible cysteine targeting [27]. Replacement of the above α -fluoromethylketone by a β -linked α -cyanoacrylamide moiety furnished **49a**, a covalent-reversible inhibitor with a dissociation half-life of 245 min. As predicted, protein labeling was rapidly reversible upon unfolding. Besides the RSK2-CTD ($IC_{50} = 5$ nM), compound **49a** potently inhibited RSK1 and 4 (CTDs), while the RSK2 C436V mutation conferred resistance. In a large kinase panel, the compound showed high selectivity and sustained RSK1 and RSK2 occupancy was observed in cells. Covalent engagement of Cys436 was demonstrated for a close analog by X-ray crystallography (PDB: 4D9U) while no adducts could be detected in MS experiments. Modification of a second accessible cysteine (Cys560) located in the DFG-1 position was not observed. In a subsequent study, the above targeting concept was extended to (hetero)aryl-activated acrylonitriles exemplified by inhibitors **49b** and **49c** ($IC_{50}^{RSK2-CTD} = 47$ and 38 nM, respectively) [28]. The β -elimination rates of such compounds spanned three orders of magnitude. It is worth mentioning that Taunton and co-workers also identified α -cyanoacrylamide-based inhibitors for other kinases harboring the P4 cysteine such as MSK1-CTD, NEK2, or PLK1 [91, 108].

Interestingly, Cys22, the equivalent cysteine in NEK2, was recently shown to react with 6-ethynyl purines (e.g., compound **50**, Fig. 19b) to form vinyl thioether adducts [109, 110]. Furthermore, NEK2 has been covalently targeted by propiolamide JH295 (**51**, Fig. 19c) [111]. PLK1 has also been addressed non-canonically using electron-deficient heteroarenes exemplified by **52** (Fig. 19d) [112]. These compounds, which resulted from a virtual screening campaign aiming to identify non-covalent PLK1 inhibitors, presumably bind PLK1 Cys67 via the reversible formation of a stable Meisenheimer complex.

While cysteines located at the tip of the glycine-rich loop (P3 position) have not been deliberately addressed at the time of writing, a cysteine close to the end of the β 1-sheet (P1 subsite) has been shown to be trapped by ibrutinib in the MAP kinase

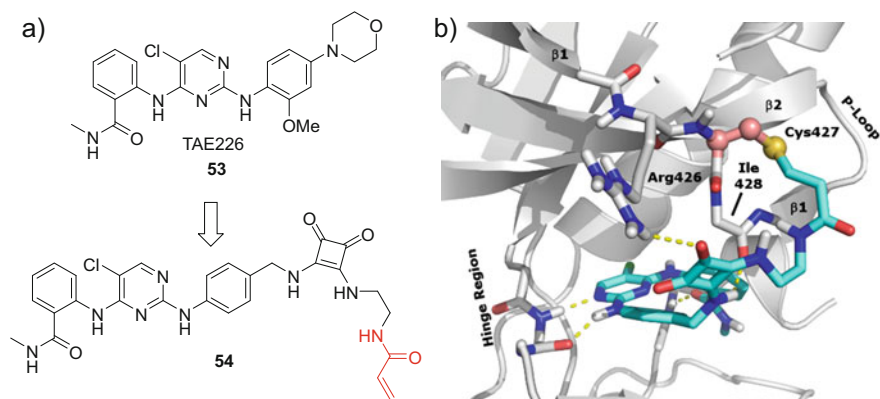


Fig. 20 Covalent FAK inhibitor **54**. (a) Design from unreactive reversible inhibitor TAE226. (b) Binding mode of compound **54** covalently linked to FAK (PDB: 6GCR). Hydrogen bonds between the backbone of Ile428 and the Arg426 side chain and the squaryldiamide linker favor an orientation facilitating covalent bond formation

kinase kinase ZAK [113]. As mentioned above, a very recent study proved the accessibility of a cysteine one position further N-terminally on the β 1-sheet (A1) present in few kinases including the non-receptor tyrosine kinase FAK (focal adhesion kinase). The A1 position has not been part of recent analyses presumably due to its unfavorable orientation pointing from the top of the β 1-sheet away from the ATP binding site. Design started from the structure of known reversible FAK inhibitor TAE226 (**53**, PDB: 2JKK) and led to subnanomolar inhibitor **54** (Fig. 20a) [38]. The key to achieve covalent engagement of the cysteine residue was the employment of a squaryldiamide linker forming hydrogen bonds with the side chain of Arg426 and the backbone of Ile428 directing the acrylamide warhead toward Cys427 (Fig. 20b).

Clinical candidates have arisen from targeting fibroblast growth factor receptor tyrosine kinases (FGFR1–4) all sharing a cysteine residue on the N-terminal side of the P-loop's tip (P2 position). An analogous cysteine has been identified in six other kinases (SCR, LIMK1, TNK1, FGR, YES, and SgK069/SBK2). FGFR tyrosine kinases represent promising targets for the treatment of different cancer types. The prototype covalent pan-FGFR inhibitor FIIN-1 (**56**, Fig. 21a) was designed in the Gray lab from the reversible inhibitor PD173074 (**55**) [114]. However, mutation of the gatekeeper valine moiety conferred resistance to this and other first-generation FGFR inhibitors. Efficacy could be restored by second-generation compounds exemplified by FIIN-2 (**57**) [115]. It is worth mentioning that the latter bind FGFR4 in a P-loop-induced DFG-out conformation. The same scaffold has been developed to phase I clinical candidate PRN1371 (**58a**; NCT02608125) by researchers from Principia Biopharma [116] and a similar approach furnished α -cyanoacrylamide **58b**, a related covalent-reversible FGFR inhibitor. Moreover, structurally distinct irreversible FGFR inhibitors such as TAS-120 (**59**, Fig. 21b)

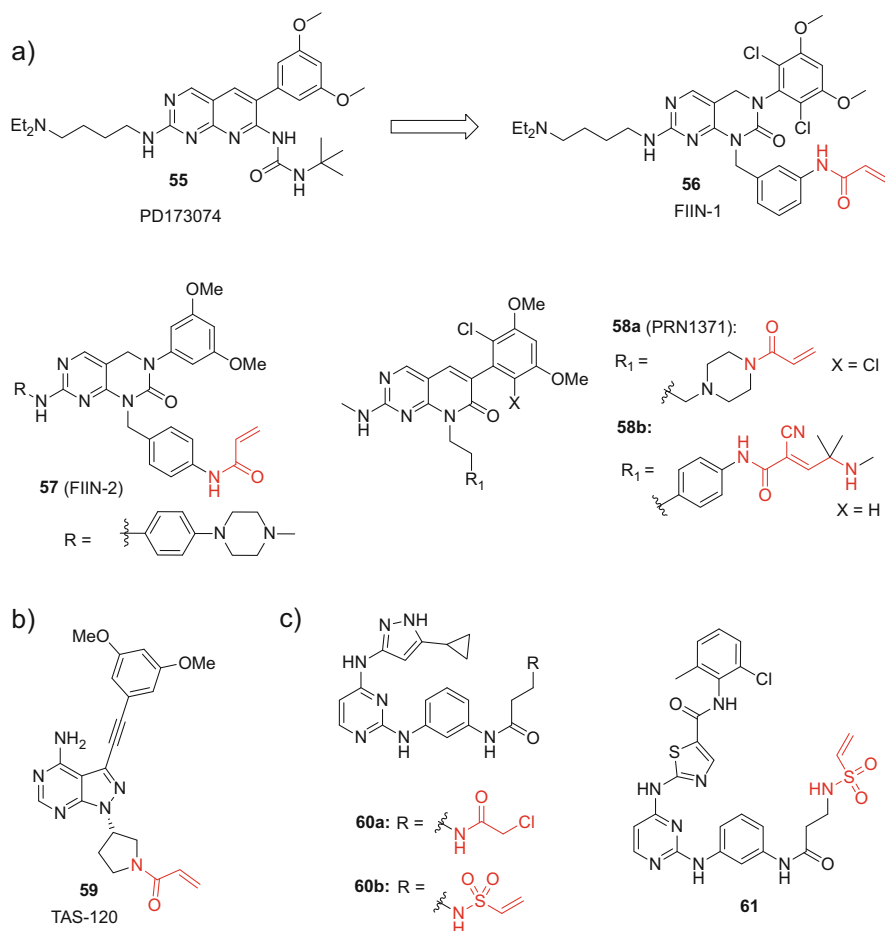


Fig. 21 (a) Irreversible and covalent-reversible FGFR kinase inhibitors derived from unreactive inhibitor PD173074. (b) 1*H*-pyrazolo[3,4-*d*]pyrimidine-derived covalent FGFR inhibitors exemplified by clinical candidate TAS-120. (c) Covalent c-SRC kinase inhibitors

[117], which is currently in phase I/II clinical studies (NCT02052778), have been reported.

Covalent inhibitors of the proto-oncogene c-SRC have been generated, for example, by Kwarczynski et al. via attaching electrophilic moieties to promiscuous kinase inhibitor scaffolds [118]. These compounds exemplified by **60a** and **60b** (Fig. 21c; IC₅₀ = 91 and 93 nM; $k_{\text{inact}}/K_{\text{I}} = 1.7 \times 10^3 \text{ M}^{-1}\text{s}^{-1}$ and $4.0 \times 10^3 \text{ M}^{-1}\text{s}^{-1}$) displayed good selectivity against the homologous kinases c-ABL and HCK both lacking the P2 cysteine (Cys277 in c-SRC). As expected, **60a/b** were found to strongly hit the c-ABL Q252C mutant where an equivalent cysteine had been introduced. Remarkably, compound **60b** inactivated c-ABL Q252C and also c-YES with a roughly two times higher k_{inact} compared to c-SRC

which was attributed to a kinked P-loop conformation in the former two kinases positioning the cysteine in closer proximity of the warhead. Similar inhibitors were designed from the scaffold of the c-SRC/BCR-ABL inhibitor dasatinib [118]. The exemplary vinyl sulfonamide **61** is a potent inhibitor of the dasatinib-resistant c-SRC T338M mutant ($IC_{50} = 44 \text{ nM}$; $k_{\text{inact}}/K_I = 4.0 \times 10^4 \text{ M}^{-1}\text{s}^{-1}$) with good cellular potency and increased selectivity compared to the relatively promiscuous template dasatinib.

2.6 Development of Inhibitors Targeting Cysteines in the Hinge Region

2.6.1 Inhibitors Targeting the H1 Position and the H3 Subsite

Among the four FGF receptor tyrosine kinases, FGFR4 stands out as the only family member harboring a cysteine at the H2 (GK + 2) position in the middle of the hinge region. Equivalent cysteines have only been identified in four other kinases, namely TTK, MAPKAPK2, MAPKAPK3, and p70S6K β . This cysteine (Cys552) was first covalently addressed by the inhibitor BLU9931 from Blueprint Medicines (**62a**, Fig. 22), another compound related to the FIIN series albeit with the warhead attached via the quinazoline C2-position [119]. Being a potent FGFR4 inhibitor ($IC_{50} = 3 \text{ nM}$; $k_{\text{inact}}/K_I = 0.6 \times 10^5 \text{ M}^{-1}\text{s}^{-1}$), BLU9931 showed high selectivity within the FGFR family, but also against several kinases with an equivalently positioned cysteine and the remaining kinome. It further demonstrated activity in cells and antitumor activity in hepatocellular carcinoma (HCC) xenograft models. Close analog BLU554 (**62b**) and the distantly related inhibitor H3B-6527 (**63**) from Eisai [120] entered phase I clinical trials (NCT02508467, NCT02834780) as potential oral treatments for patients with FGF19/FGFR4-driven HCC. These compounds feature an interesting binding mode with a U-shaped arrangement between the hinge-binding motif, the spacer moiety, and the warhead (Fig. 23a, b) directing the electrophile toward the cysteine sulfur atom. This conformation is stabilized by a bidentate hydrogen bond between the two *ortho*-amino groups of the

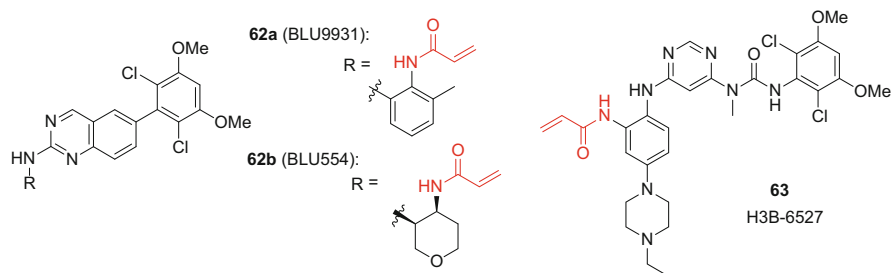


Fig. 22 Selected irreversible FGFR4 inhibitors

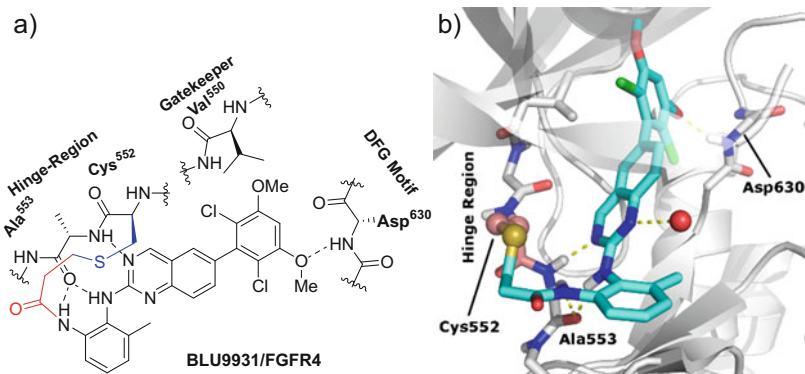


Fig. 23 (a) Schematic binding mode of prototypical covalent FGFR4 inhibitor BLU9931 (**62a**) deduced from the X-ray crystal structure of the covalent complex (PDB: 4XCU). (b) X-ray crystal structure of **62a** covalently bound to the FGFR4 ATP pocket. A U-shaped conformation is adopted to hit Cys552 located in the hinge region. A water-mediated H-bond of the inhibitor's amide oxygen atom and Arg483 was omitted for clarity

1,2-phenylenediamine spacer and the backbone carbonyl oxygen of Ala553. In the case of BLU9931, an additional *ortho*-methyl group forcing an “out-of-plane” conformation of the phenyl ring is required to obtain an optimal balance of FGFR4 potency and selectivity against FGFR1–3 [119]. A water-mediated hydrogen bond of the acrylamide oxygen atom with Arg483 may further assist in orienting the warhead to be attacked by Cys552.

Non-canonical approaches to address FGFR4-Cys552 have been reported by Fairhurst and colleagues from Novartis [121]. In an HTS campaign, they identified 6-chloro-3-nitropyridine **64** (Fig. 24a) as a potent inhibitor of FGFR4 ($IC_{50} = 32$ nM; $k_{inact}/K_I = 3.0 \times 10^4$ M⁻¹ s⁻¹) sparing FGFR1–3. The compound binds Cys552 via S_NAr-displacement of the chloride from the pyridine C6-atom as shown by X-ray crystallography (PDB: 5NUD). The same screening campaign identified 2-formylquinoline amide **65** (Fig. 24b) as an FGFR4 inhibitor ($IC_{50} = 65$ nM) engaging Cys552 by highly reversible hemithioacetal formation. The latter compound was further developed to clinical candidate FGF401 (**66**), an orally available inhibitor with a favorable preclinical profile currently undergoing phase I/II studies (NCT02325739) as a potential treatment of FGFR4/ β -klotho-positive HCC and solid tumors.

No reports describing the covalent targeting of other kinases with an H1 cysteine could be identified at the time of writing. Similarly, cysteines in the H2 position (GK + 3), which are present in a large set of kinases, have remained unaddressed so far. This is presumably owed to the H2 cysteines' limited flexibility and their location underneath the region that is usually occupied by the hinge-binding motif, which is difficult to reach with typical type I inhibitor scaffolds. However, a cysteine located at the H3 subsite (GK + 4/5) has recently been engaged in Fms-like tyrosine kinase 3 (FLT3) by 4-(dialkylamino)crotonamide-based inhibitor FF-10101 (**67**, Fig. 24c) [122]. Notably, this kinase representing a validated target in the treatment

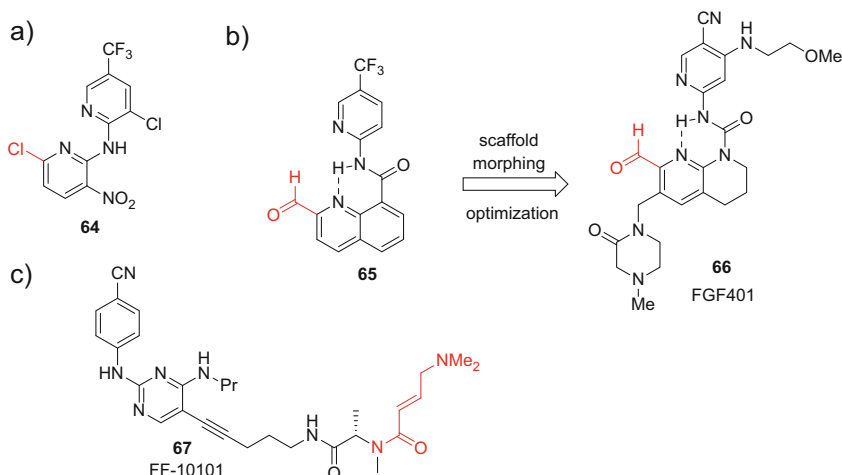


Fig. 24 (a) Irreversible FGFR4 inhibitor **64** engaging FGFR4-Cys552 via an S_NAr-electrophile. (b) Covalent-reversible FGFR4 inhibitors relying on an aldehyde warhead. (c) Covalent FLT3 inhibitor FF-10101

of acute myeloid leukemia features two other cysteines (D1 and H2 position) which could potentially be addressed. FF-10101 potently inhibits wild-type FLT3 (IC₅₀ = 0.2 nM) and shows a high activity against a variety of leukemia cell lines including those harboring quizartinib-resistance mutations. Along with several other kinases, the compound potently hit the two related kinases KIT and FMS (IC₅₀ = 0.9 nM and 2.0 nM, respectively) and, to a lesser extent, the non-receptor tyrosine kinase FGR (IC₅₀ = 12 nM), all sharing a H3-GK + 4 cysteine. Binding to Cys695 was demonstrated by X-ray crystallography (PDB: 5X02) and confirmed by a set of experiments using the FLT3 C695S mutant and an unreactive analog. FF-10101 showed promising effects in preclinical models and entered phase I/II clinical trials as a potential treatment for patients with relapsed or refractory hematological malignancies (NCT03194685 and NCT02193958).

2.7 Development of Inhibitors Targeting Cysteines Around the DFG Motif and in the Activation Segment

The activation segment is located between the conserved DFG and APE motifs and contains the activation loop and the P + 1 loop. It represents a very flexible region and is often poorly resolved in X-ray crystal structures. Thus, exhaustive analysis of cysteine positioning and accessibility is complicated and structure-based design approaches can be difficult to accomplish. A large set of kinases possesses cysteine moieties in direct neighborhood to the DFG motif, either at the O2 subsite (DFG + 1/2) or in the D1 position (DFG-1). Another set of cysteines can be found at the

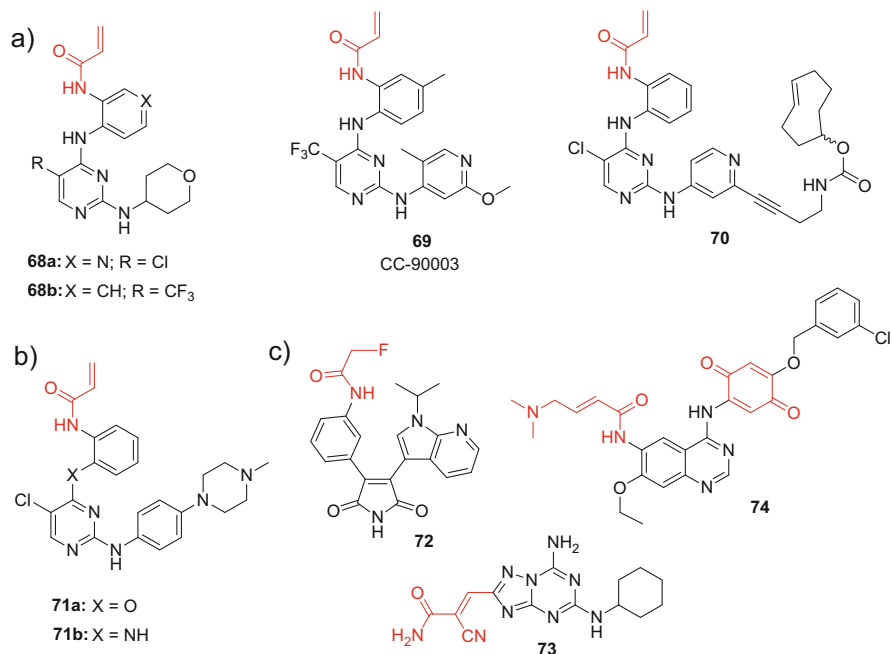


Fig. 25 (a) Irreversible ERK1/2 inhibitors including clickable TCO-probe **70**. (b and c) Covalent TAK1, dual EGFR/VEGFR2, and GSK-3 β /CK-1 δ inhibitors

activation segment's O3 subsite, frequently two residues after the phosphorylation site. Further accessible cysteines are located in the activation loop. Examples are Cys178 and 179 in IKK α and β , which have been identified as the target of natural products and endogenous ligands like PGA1 (vide supra) [5]. However, proper assignment of the activation loop cysteines is impeded by the highly plastic nature and the variable length of this region [5].

A cysteine located at O2 (Cys296, DFG + 2 position) in the protein kinases B (PKBs, also known as AKTs) is addressed by allosteric inhibitors (vide infra) and presumably also by pyranonaphthoquinones (vide supra) while many kinases with a D1 cysteine are targeted by the aforementioned resorcylic acid lactones like hypothemycin, LL-Z1640-2, and analogs thereof (see Fig. 6), albeit with limited specificity. D1 cysteine residues have also been tackled by rational design efforts. Although there are many kinases (\approx 10% of the kinome) featuring such a cysteine, these targets are distributed over almost all kinase families suggesting that distinct structural features may readily be exploited as additional selectivity filters. For example, Ward and co-workers from AstraZeneca reported on covalent ERK1/2 inhibitors derived from several reversible inhibitor classes using a structure-based approach [123]. The most promising series was based on a 2,4-diaminopyrimidine scaffold (exemplified by **68a** and **68b**, Fig. 25a). The study identified highly potent compounds covalently engaging Cys166 in ERK2 (see, for example, PDB: 4ZZO)

with good selectivity against several other kinases of this subset and in the kinome. CC-90003 (**69**) [124], a structurally related covalent ERK1/2 inhibitor from Celgene, was investigated in phase I clinical trials (NCT02313012) which were, however, terminated in 2016 due to lack of response, an inappropriate PK-profile, and neurotoxicity [125]. Analogous probe **70** (see also PDB: 5LCJ) enabled imaging of ERK1/2 in living cells by employing *trans*-cyclooctene (TCO)/tetrazine (Tz) click chemistry [126].

Covalent TAK1 targeting was accomplished by Gray and co-workers with closely related inhibitors such as **71a** ($IC_{50} = 5.1$ nM) and **71b** ($IC_{50} = 50$ nM; $k_{inact}/K_1 = 6.9 \times 10^3$ M⁻¹ s⁻¹) shown in Fig. 25b. Inhibitor **71b** hit multiple kinases in a panel among those being 10 kinases with a cysteine at the D1 position. However, both compounds possessed a moderate selectivity against MEK1 and ERK2 also sharing this cysteine. Interestingly, replacement of the acrylamide warhead by a shorter chloroacetamide moiety led to a strong increase in selectivity against the latter two kinases, which was accompanied by a rearrangement of the DFG motif in TAK as observed by X-ray crystallography (see, for example, the PDB structures 5JH6 vs. 5E7R).

Various warhead chemistries were evaluated by Yang et al. to covalently trap GSK-3 β [127]. Out of their series, one of the most promising inhibitors was fluoroacetamide **72** (Fig. 25c; $IC_{50} = 17$ nM). Labeling of Cys199 was suggested by experiments with a fluorescent competitor probe and by digestion/MS using an acrylamide-based analog. In contrast, two derivatives equipped with 2-chloropyridine moieties as S_NAr-type warheads proved to be reversible inhibitors albeit with similar biochemical potency. Another interesting study was conducted by Wissner et al. who installed two independent warheads on a quinazoline scaffold to generate dual irreversible inhibitors of EGFR and vascular endothelial growth factor receptor 2 (VEGFR2, also termed KDR) as exemplified by compound **73** [128]. While the 4-(dimethylamino)crotonamide residue was directed toward the aforementioned F2 cysteine in EGFR, the substituted benzoquinone moiety was meant to target Cys1045 located at the D1 position of VEGFR2, presumably via a radical-based reductive addition mechanism. Very recently, α -cyanoacrylamide **73** has been described as dual GSK-3 β /CK-1 δ inhibitor [129]. While being only moderately potent, the compound covalently modified GSK-3 β as shown by X-ray crystallography (PDB ID: 6H0U) while no covalent interaction can be assumed for CK-1 δ , which is devoid of cysteine moieties in the active site.

2.8 Development of Inhibitors Targeting Remote Cysteines or Inactive Conformations

Remote cysteines are located outside of the regular kinase domain. Such cysteines may also be amenable to covalent targeting with ATP pocket ligands, provided that the cysteine of interest is positioned in spatial proximity to ATP binding cleft. A first

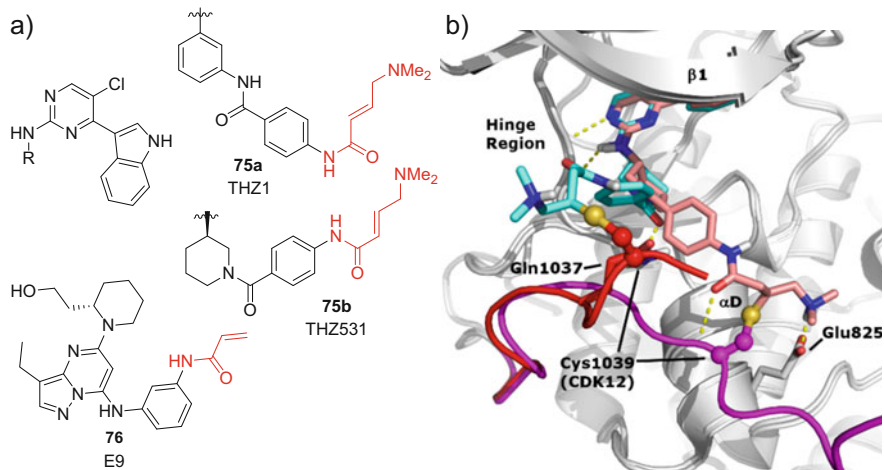


Fig. 26 (a) Covalent CDK inhibitors targeting remote cysteines. (b) Binding modes observed in the X-ray crystal structure of THZ531 covalently bound to CDK12 (PDB: 5ACB)

study employing this approach was reported in 2014 by researchers from the Dana-Farber Cancer Institute and MIT [130]. A screening campaign identified THZ1 (**75a**, Fig. 26a) as low nanomolar inhibitor of the cyclin-dependent kinase CDK7. Since saturation of the reactive α,β -unsaturated amide moiety led to a strong loss in anti-proliferative and biochemical activity, a covalent binding mode was assumed, which was confirmed with a biotinylated analog. Subsequent MS experiments confirmed Cys312, a residue located in a C-terminal extension traversing the ATP pocket, as the site of modification. As expected, mutation of the target cysteine to serine prevented labeling. Besides several kinases that were hit reversibly, higher inhibitor concentrations also affected CDK12 and CDK13 possessing cysteines that occupy spatially similar locations. Optimization toward these kinases furnished THZ531 (**75b**), a CDK12/13 inhibitor with IC_{50} values in the mid-nanomolar range and good selectivity against CDK7 and CDK9 [131]. The compound demonstrated high specificity in a cellular KiNativ screen which was corroborated in cell lysates by means of a biotin-labeled probe. In contrast, several off-targets were hit in a large kinase panel. Remarkably, potent binding to JNKs was observed. JNKs feature a cysteine in the F3 position on the first turn of the α D-helix which can probably be reached by the same warhead/spacer combination. As confirmed by X-ray crystallography and MS, covalent modification of CDK12 occurred at Cys1039 while the CDK12-C1039S mutant resisted covalent labeling in cells. Interestingly, two different binding modes were observed in which both, the loop bearing Cys1039 and the piperidine-linked amide moiety, adopted distinct conformations to enable covalent bond formation (Fig. 26b). Compound **75b** strongly inhibited the expression of DNA damage response (DDR) and super-enhancer genes in cells and induced apoptosis. Since resistance to the THZ-series of compounds was acquired by up-regulation of ABC-transporters, the structurally unrelated follow-up CDK12 inhibitor E9 (**76**) was developed to escape ABC-transporter-mediated efflux [132].

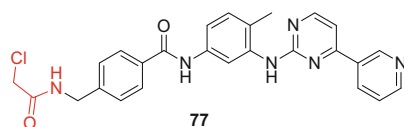


Fig. 27 Covalent PDGFR/KIT inhibitor **77**

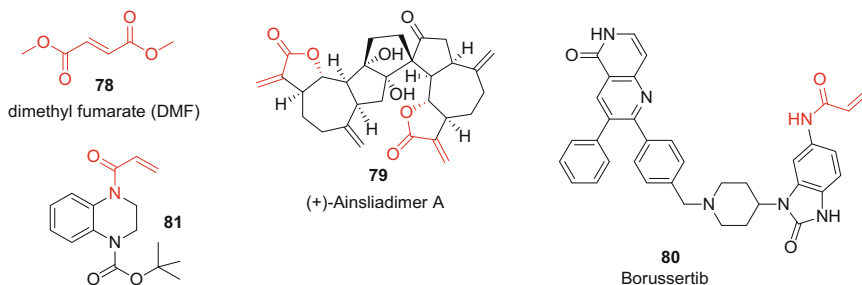


Fig. 28 Examples of covalent kinase inhibitors targeting allosteric pockets

Plasticity is a key regulatory feature of the kinases' catalytic domain. However, only few cysteines accessible in inactive conformations have been targeted to date. In their seminal work analyzing cysteines available in DFG-out and α C-helix-out conformations, Leproult et al. also designed imatinib-derived electrophilic inhibitors to target the kinases KIT and PDGFR α (platelet-derived growth factor receptor α) via cysteine moieties in the catalytic loop (Cys788 and Cys814, respectively) [15]. Despite its relatively weak apparent potency, key compound **77** (Fig. 27) labeled the predicted cysteines as shown by MS and hit only seven other targets (PDGFR β , JNK 1–3, DDR1, BRAFV600E, and CSF1R) in a panel of 440 kinases. Notably, the panel contained 17 out of 20 kinases sharing an equivalently positioned cysteine of which (besides KIT and PDGFR α) only PDGFR β and CSF1R were potently bound.

2.9 Development of Inhibitors Targeting Cysteines in Allosteric Pockets

Besides ligands addressing the ATP pocket, covalent kinase inhibitors engaging allosteric sites have also been identified. As an example, covalent allosteric inhibition of RSKs and MSKs has been suggested to contribute to the biological activity of dimethyl fumarate (**78**, Fig. 28), a reactive low molecular weight drug used in the treatment of psoriasis and multiple sclerosis [133]. The complex natural product (+)-ainsliadimer A (**79**) featuring two Michael acceptor moieties has also been shown to act as a covalent kinase inhibitor targeting IKK α and IKK β via a (putative) allosteric

pocket involving Cys46 [134]. Recently discovered acrylamide-based covalent allosteric inhibitors include the AKT inhibitor borussertib (**80**) [135] and the fragment **81** addressing CDK2 [136]. Moreover, chemical-genetics approaches have been used to enable covalent targeting of non-canonical binding sites via the introduction of cysteines. For example, Bührmann et al. recently identified probes covalently binding to a lipid pocket of p38 α MAP kinase cysteine mutants (S251C and S252C) without labeling the wild-type enzyme [137]. It should, however, be noted that ligands addressing allosteric- and other non-canonical binding sites are often identified serendipitously since such pockets tend to be highly plastic and are frequently not observed in the apo-structures.

2.10 Development of Inhibitors Targeting Lysine or Tyrosine

As mentioned before (see Sect. 2.3), natural products covalently engaging kinases via lysine residues are well-known. In addition, lysine and tyrosine moieties have been addressed with synthetic small molecules. For example, activated esters have been employed to target the catalytic lysine in PI3K δ by researchers at GSK [138]. Since the sulfonamide substituent of the reversible PI3K δ inhibitor GSK2292767 (**82**, Fig. 29a) interacts with the ϵ -amino group of PI3K δ -Lys779, replacement of this moiety by activated phenolic esters was considered as a strategy to address the amino nucleophile. Biochemical potencies of the generated compounds roughly correlated with the leaving group properties of the corresponding phenolates reaching down to the subnanomolar range for the most activated derivative (**83a**, IC₅₀ = 0.6 nM; $k_{\text{inact}}/K_I = 1.9 \times 10^5 \text{ M}^{-1} \text{ s}^{-1}$). Interestingly, analysis of binding kinetics revealed that k_{inact} was relatively constant in the series while differences in the overall potency seemed to be mainly driven by K_I . This finding was attributed to a more complex reaction mechanism as compared to the canonical

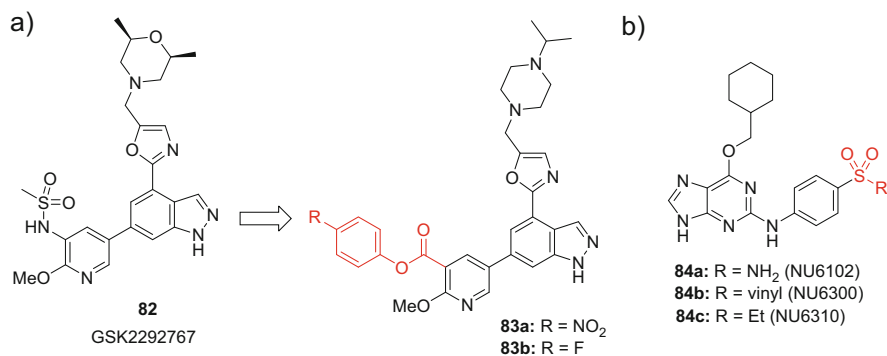


Fig. 29 Examples of lysine-targeted covalent kinase inhibitors. (a) Design of activated esters addressing the catalytic lysine in PI3K δ . (b) Vinyl sulfones targeting the solvent-exposed Lys89 in CDK2

two-step model (see Fig. 1). Notably, the analogous non-activated methyl ester bound only reversibly to the enzyme. Key compound **83b** showed high activity in the enzymatic assay ($IC_{50} = 8 \text{ nM}$; $k_{\text{inact}}/K_I = 2.1 \times 10^4 \text{ M}^{-1} \text{ s}^{-1}$) and in human whole blood ($IC_{50} = 13 \text{ nM}$) while being selective against other PI3K isoforms (ca. three orders of magnitude against PI3K $\alpha/\beta/\gamma$) and in a larger kinase panel. A clean chemoproteomic profile was shown for an analogous azide-labeled probe. Exclusive labeling of Lys779 was further demonstrated by MS analysis and X-ray crystallography (see Fig. 31a). The inhibitor also showed a selectivity window in which PI3K δ was covalently inhibited while PI3K α and β engagement was reversible.

Michael-acceptor chemistry was used by Anscombe et al. to obtain an irreversible CDK2 inhibitor [139]. Starting from non-covalently binding sulfonamide NU6102 (**84a**, Fig. 29b), replacement of this functional group by an electrophilic vinyl sulfone furnished covalent analog NU6300 (**84b**). In this context, it is worth mentioning that previous model experiments by Dahal et al. demonstrated vinyl sulfones and vinyl sulfonamides to have a certain preference to react with lysine over cysteine [9, 140]. Covalent binding of compound **84b** to Lys89 located in the front region of the ATP pocket was suggested by MS experiments and confirmed by X-ray crystallography (PDB: 5CYI). The inhibitor, however, featured only moderate reversible binding affinity ($K_I = 1.31 \mu\text{M}$) and showed relatively slow inactivation kinetics, presumably due to the solvent-exposed nature of the target lysine favoring the protonated state.

Sulfonyl fluorides have frequently been used to address the lysines [9]. For example, ATP-derived probe 5'-O-4-((fluorosulfonyl)benzoyl)adenosine (*p*-

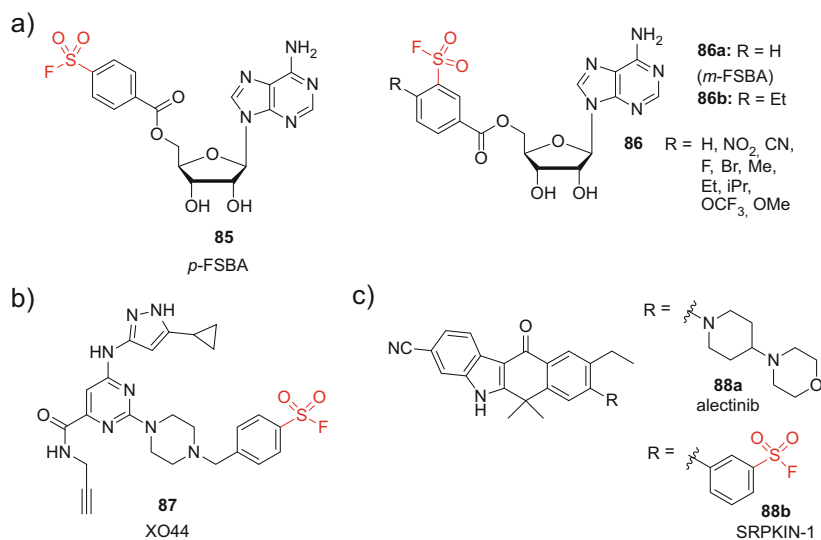


Fig. 30 Lysine and tyrosine-targeted sulfonyl fluorides. (a) *p*-*m*-FSBA and analogs. (b) Broad-spectrum kinase probe XO44. (c) Tyrosine-targeted SRPK1/2 inhibitor SRPKIN-1

FSBA, **85**, Fig. 30a) acts as a non-selective covalent kinase inhibitor typically modifying the catalytic lysine. While investigating the reactivity of sulfur (VI) fluorides, Mukherjee and colleagues from AstraZeneca tested *meta*-substituted FSBA analogs (*m*-FSBAs, general structure **86**) with a variety of additional substituents in the 4-position of the phenyl ring ($-R$, *ortho* to the sulfonyl fluoride warhead) as inhibitors of the kinases FGFR1 and SYK. Covalent binding of the two analogs **86a** and **86b** to Lys514 in FGFR1 was shown by X-ray crystallography (PDB: 5O49A and 5O4A) and only a single product was observed in MS. The rate of covalent complex formation correlated reasonably with the σ_p^- parameter of the substituent $-R$ and also with the reactivity data previously determined using model amino acids. In contrast, negligible covalent modification was observed for two analogous aryl fluorosulfates derived from *m*- and *p*-FSBA, respectively, which is in line with the very low intrinsic reactivity described for this electrophile.

An interesting application for sulfonyl fluoride-based probes was recently reported by Zhao et al. [141]. Pyrimidinyl 3-aminopyrazole XO44 (**87**, Fig. 30b) was designed as a clickable broad-spectrum kinase ligand enabling chemoproteomic selectivity profiling. As predicted, the compound specifically labeled the catalytic lysine (Lys295; see Fig. 31b) in the model kinase *c*-SRC. A similar binding mode was observed in the EGFR kinase domain (PDB: 5U8L). At a concentration of 1 μM , XO44 inhibited 219 of 375 protein kinases in a panel ($\geq 50\%$) and captured 133 kinases in Jurkat T-cells. Although many non-kinase off-targets were also modified, kinases accounted for most of the signal intensity in MS experiments. Using the poorly selective reversible kinase inhibitor dasatinib as a competitor, compound **87** was validated as a probe enabling cellular selectivity profiling.

A very recent example of a tyrosine-targeted covalent kinase inhibitor was provided by Hatcher et al. [142]. After discovering that the approved reversible anaplastic lymphoma kinase (ALK) inhibitor alectinib (**88a**, Fig. 30c) strongly

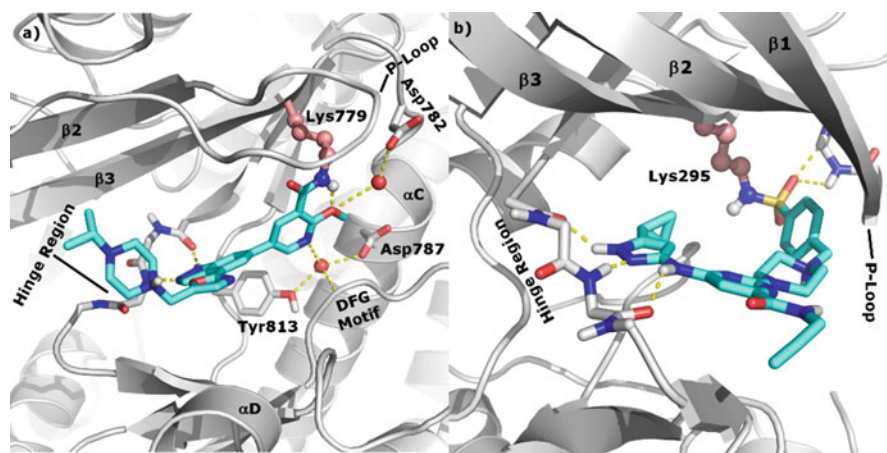


Fig. 31 (a) Inhibitor **83b** covalently bound to Lys779 of PI3K δ (PDB: 6EYZ). (b) Probe XO44 covalently bound to chicken *c*-SRC-Lys295 (PDB: 5K9I)

inhibits the SR-protein kinase SRPK1 ($IC_{50} = 11$ nM), an *m*-phenylsulfonyl fluoride moiety was introduced to address Tyr227, a unique tyrosine adjacent to the solvent-exposed front region of the SRPK1 active site. The obtained inhibitor SRPKIN-1 (**88b**) showed similar SRPK1 activity ($IC_{50} = 36$ nM) while retaining only moderate potency on ALK ($IC_{50} = 195$ nM). No kinetic analysis was provided to deduce the contribution of covalent bond formation to the observed activity. However, washout experiments supported a covalent binding mode and MS experiments confirmed the predicted labeling of Tyr227. Cellular profiling revealed good selectivity for SRPK1 and SRPK2 and the inhibitor suppressed neovascularization in a choroidal neovascularization (CNV) model.

3 Summary and Outlook

The field of covalent protein kinase inhibitor research has matured over the last years. Covalent targeting strategies have enabled the design of chemical probes with excellent selectivity in the kinome and the benefits of TCIs have successfully been implemented in drug discovery. Covalent approaches have been used, for example, to boost potency and break resistance (e.g., with covalent EGFR inhibitors), to achieve durable target occupancy (e.g., with covalent BTK inhibitors), or to promote excellent selectivity over closely related enzymes (e.g., with covalent JAK3 or FGFR4 inhibitors). The recent FDA approval of six irreversible kinase inhibitors impressively highlights the utility of covalent design strategies for the discovery of new medicines. Although covalent kinase inhibitors have almost exclusively been approved for cancer treatment so far, substantial efforts are currently being made to develop such drugs for non-oncology indications, especially for the treatment of inflammatory and autoimmune disorders.

In the current practice, covalent kinase targeting largely relies on limited warhead chemistry. Generally, attenuated Michael acceptors such as α,β -unsaturated amides are used to address non-catalytic cysteines in a (quasi)-irreversible fashion. However, more diverse warhead types are increasingly receiving attention [9]. Most notably, covalent-reversible targeting approaches relying, for example, on dually activated Michael acceptors, but also on other electrophiles such as cyanamides or aldehydes, are gaining importance as highlighted by the inhibitors PRN1008 and FGF401 (see Figs. 12b and 24b) which are currently under clinical investigation. Furthermore, attempts to address other nucleophilic amino acids inside or proximal to the ATP binding pocket (e.g., Lys and Tyr) or cysteine moieties at allosteric sites have recently been successful and such approaches are expected to gain traction in the near future. Although the structure-guided modification of known reversible inhibitors, which is facilitated by the steeply increasing amount of publicly available X-ray crystal structures, is still by far the most common strategy for the discovery of kinase TCIs, alternative concepts such as the screening of reactive fragments or DNA-encoded libraries show great promise. Methods for estimating the extent of specific and non-specific labeling by irreversible covalent inhibitors in living

systems have also advanced. Especially MS-based chemoproteomic approaches are now enabling a more complete understanding of the cellular labeling profiles of covalent inhibitors while biotinylated or fluorescent covalent probes have also been used as valuable tools to monitor target occupancy in cells or *in vivo*.

Nevertheless, we still face many challenges in the realm of covalent kinase inhibitor discovery, especially, when aiming for clinical applications. A general limitation of the TCI approach, especially in oncology, consists in its vulnerability to resistance development by mutation of the nucleophilic amino acid (e.g., cysteine to serine). This is an intrinsic liability since TCIs target non-conserved residues, which are typically not crucial for protein integrity and function. On the other hand, when aiming for other therapeutic areas beyond oncology where resistance mutations are less likely, an even more stringent benefit/risk assessment is required. The latter, however, is currently complicated by a lack of reliable models to predict toxicity and immune-mediated adverse events including idiosyncratic drug reactions, which may only become apparent in late stage clinical trials or even after long-term therapeutic application. Beside the frequently discussed issue of permanent off-target modification, we also lack a comprehensive understanding of how reversible interactions with unintended targets contribute to the biological profiles of reactive inhibitors, a fact that is rarely alluded to in the current literature. Similarly, covalent modification of non-protein off-targets (e.g., DNA or RNA) by kinase TCIs remains widely unexplored.

As mentioned in the introduction, a detailed analysis of target-binding kinetics is still not performed by default. Thus, the contribution of the covalent binding event to the observed overall biological effects often remains incompletely understood [13]. Further exploration of warhead chemistry to enable the generation of inhibitors with tailored reactivities specifically matching the requirements of the target of interest represents another future challenge [9]. There is also an increasing awareness of cysteine oxidation as a posttranslational modification, which may regulate kinase function and impair covalent binding [13]. The influence of the “cysteine redoxome” and its dynamics on the efficacy covalent inhibitors clearly merits further investigations which may have an important impact on our perspective on covalent cysteine targeting. Finally, and despite the success of covalent approaches in the development of chemical probes and drugs, the coverage of the kinases’ cysteinome by suitable inhibitors is still low and several of the presented cysteine locations (see Fig. 4 and Table 1) have not yet been targeted at all. While a thorough examination of the protein kinases’ lysinome and tyrosinome remains to be performed, it also unclear, how many ligandable cysteine locations, especially in inactive states or induced/allosteric pockets have not been captured in the published analyses. The latter may open up new avenues for covalent ligand design.

Despite the many challenges associated with covalent inhibitor development, a bright future can be expected for protein kinase TCIs. Since many kinases are still understudied and lack suitable chemical probes required for investigation of their function, there is a large and untapped potential for covalent kinase inhibitor discovery, which will inspire continuing research efforts. Moreover, a multitude of covalent protein kinase inhibitors are currently in clinical development for

application in cancer therapy and beyond. Therefore, we can expect many more success stories from this field lying ahead of us.

Acknowledgments The author thanks Kristine Schmidt for language proofreading and editing. Dr. Michael Forster, Dr. Marcel Günther, and Dr. Apirat Chaikuad are gratefully acknowledged for fruitful discussion and suggestions. Dr. Apirat Chaikuad and Prof. Dr. Stefan Knapp are further acknowledged for providing the data of their analysis of the protein kinases' cysteinome. The author appreciates financial support by the Postdoctoral Fellowship Program of the Baden-Württemberg Stiftung, the Institutional Strategy of the University of Tübingen (ZUK 63, German Research Foundation), the RiSC Program of the State Ministry of Baden-Württemberg for Sciences, Research and Arts, and the Max Buchner Research Foundation.

Compliance and Ethical Standards

Conflict of Interest The author declares that he has no conflict of interest.

Funding While preparing the manuscript, the author received funding from the Postdoctoral Fellowship Program of the Baden-Württemberg Stiftung, the Institutional Strategy of the University of Tübingen (ZUK 63, German Research Foundation), the RiSC Program of the State Ministry of Baden-Württemberg for Sciences, Research and Arts, and the Max Buchner Research Foundation.

Ethical Approval This article does not contain any studies with human participants or animals performed by the author.

References

1. Singh J, Petter RC, Baillie TA, Whitty A (2011) The resurgence of covalent drugs. *Nat Rev Drug Discov* 10:307–317. <https://doi.org/10.1038/nrd3410>
2. Bauer RA (2015) Covalent inhibitors in drug discovery: from accidental discoveries to avoided liabilities and designed therapies. *Drug Discov Today* 20:1061–1073. <https://doi.org/10.1016/j.drudis.2015.05.005>
3. Baillie TA (2016) Targeted covalent inhibitors for drug design. *Angew Chem Int Ed* 55:13408–13421. <https://doi.org/10.1002/anie.201601091>
4. Singh J, Petter RC, Kluge AF (2010) Targeted covalent drugs of the kinase family. *Curr Opin Chem Biol* 14:475–480. <https://doi.org/10.1016/j.cbpa.2010.06.168>
5. Barf T, Kaptein A (2012) Irreversible protein kinase inhibitors: balancing the benefits and risks. *J Med Chem* 55:6243–6262. <https://doi.org/10.1021/jm3003203>
6. Liu Q, Sabnis Y, Zhao Z, Zhang T, Buhrlage SJ, Jones LH, Gray NS (2013) Developing irreversible inhibitors of the protein kinase Cysteinome. *Chem Biol* 20:146–159. <https://doi.org/10.1016/j.chembiol.2012.12.006>
7. Chaikuad A, Koch P, Laufer SA, Knapp S (2018) The Cysteinome of protein kinases as a target in drug development. *Angew Chem Int Ed* 57:4372–4385. <https://doi.org/10.1002/anie.201707875>
8. de Cesco S, Kurian J, Dufresne C, Mittermaier AK, Moitessier N (2017) Covalent inhibitors design and discovery. *Eur J Med Chem* 138:96–114. <https://doi.org/10.1016/j.ejmech.2017.06.019>
9. Gehringer M, Laufer SA (2019) Emerging and re-emerging warheads for targeted covalent inhibitors: applications in medicinal chemistry and chemical biology. *J Med Chem* 62:5673–5724. <https://doi.org/10.1021/acs.jmedchem.8b01153>

10. Hann MM (2011) Molecular obesity, potency and other addictions in drug discovery. *Med Chem Commun* 2:349–355. <https://doi.org/10.1039/C1MD00017A>
11. Bradshaw JM, McFarland JM, Paavilainen VO, Bisconte A, Tam D, Phan VT, Romanov S, Finkle D, Shu J, Patel V, Ton T, Li X, Loughhead DG, Nunn PA, Karr DE, Gerritsen ME, Funk JO, Owens TD, Verner E, Brameld KA, Hill RJ, Goldstein DM, Taunton J (2015) Prolonged and tunable residence time using reversible covalent kinase inhibitors. *Nat Chem Biol* 11:525–531. <https://doi.org/10.1038/nchembio.1817>
12. Strelow JM (2017) A perspective on the kinetics of covalent and irreversible inhibition. *SLAS Discov* 22:3–20. <https://doi.org/10.1177/1087057116671509>
13. Schwartz PA, Kuzmic P, Solowiej J, Bergqvist S, Bolanos B, Almaden C, Nagata A, Ryan K, Feng J, Dalvie D, Kath JC, Xu M, Wani R, Murray BW (2014) Covalent EGFR inhibitor analysis reveals importance of reversible interactions to potency and mechanisms of drug resistance. *Proc Natl Acad Sci* 111:173–178. <https://doi.org/10.1073/pnas.1313733111>
14. Awoonor-Williams E, Rowley CN (2018) How reactive are druggable cysteines in protein kinases? *J Chem Inf Model* 58:1935–1946. <https://doi.org/10.1021/acs.jcim.8b00454>
15. Leproult E, Barluenga S, Moras D, Wurtz J-M, Winssinger N (2011) Cysteine mapping in conformationally distinct kinase nucleotide binding sites: application to the design of selective covalent inhibitors. *J Med Chem* 54:1347–1355. <https://doi.org/10.1021/jm101396q>
16. Onufriev AV, Alexov E (2013) Protonation and pK changes in protein–ligand binding. *Q Rev Biophys* 46:181–209. <https://doi.org/10.1017/S0033583513000024>
17. Casimiro-García A, Trujillo JL, Vajdos F, Juba B, Banker ME, Aulabaugh A, Balbo P, Bauman J, Chrencik J, Coe JW, Czerwinski R, Dowty M, Knafels JD, Kwon S, Leung L, Liang S, Robinson RP, Telliez J-B, Unwalla R, Yang X, Thorarensen A (2018) Identification of Cyanamide-based Janus kinase 3 (JAK3) covalent inhibitors. *J Med Chem*. <https://doi.org/10.1021/acs.jmedchem.8b01308>
18. Zhao Z, Liu Q, Bliven S, Xie L, Bourne PE (2017) Determining Cysteines available for covalent inhibition across the human Kinome. *J Med Chem* 60:2879–2889. <https://doi.org/10.1021/acs.jmedchem.6b01815>
19. Lonsdale R, Ward RA (2018) Structure-based design of targeted covalent inhibitors. *Chem Soc Rev* 47:3816–3830. <https://doi.org/10.1039/C7CS00220C>
20. Backus KM, Correia BE, Lum KM, Forli S, Horning BD, González-Páez GE, Chatterjee S, Lanning BR, Teijaro JR, Olson AJ, Wolan DW, Cravatt BF (2016) Proteome-wide covalent ligand discovery in native biological systems. *Nature* 534:570–574. <https://doi.org/10.1038/nature18002>
21. Kathman SG, Xu Z, Statsyuk AV (2014) A fragment-based method to discover irreversible covalent inhibitors of cysteine proteases. *J Med Chem* 57:4969–4974. <https://doi.org/10.1021/jm500345q>
22. Jöst C, Nitsche C, Scholz T, Roux L, Klein CD (2014) Promiscuity and selectivity in covalent enzyme inhibition: a systematic study of electrophilic fragments. *J Med Chem* 57:7590–7599. <https://doi.org/10.1021/jm5006918>
23. Zimmermann G, Rieder U, Bajic D, Vanetti S, Chaikuad A, Knapp S, Scheuermann J, Mattarella M, Neri D (2017) A specific and covalent JNK-1 ligand selected from an encoded self-assembling chemical library. *Chem Eur J* 23:8152–8155. <https://doi.org/10.1002/chem.201701644>
24. Chan AI, McGregor LM, Jain T, Liu DR (2017) Discovery of a covalent kinase inhibitor from a DNA-encoded small-molecule library × protein library selection. *J Am Chem Soc* 139:10192–10195. <https://doi.org/10.1021/jacs.7b04880>
25. Jackson PA, Widen JC, Harki DA, Brummond KM (2017) Covalent modifiers: a chemical perspective on the reactivity of α,β -unsaturated carbonyls with thiols via hetero-Michael addition reactions. *J Med Chem* 60:839–885. <https://doi.org/10.1021/acs.jmedchem.6b00788>
26. Bandyopadhyay A, Gao J (2016) Targeting biomolecules with reversible covalent chemistry. *Curr Opin Chem Biol* 34:110–116. <https://doi.org/10.1016/j.cbpa.2016.08.011>

27. Serafimova IM, Pufall MA, Krishnan S, Duda K, Cohen MS, Maglathlin RL, McFarland JM, Miller RM, Frödin M, Taunton J (2012) Reversible targeting of noncatalytic cysteines with chemically tuned electrophiles. *Nat Chem Biol* 8:471–476. <https://doi.org/10.1038/nchembio.925>
28. Krishnan S, Miller RM, Tian B, Mullins RD, Jacobson MP, Taunton J (2014) Design of reversible, cysteine-targeted Michael acceptors guided by kinetic and computational analysis. *J Am Chem Soc* 136:12624–12630. <https://doi.org/10.1021/ja505194w>
29. Knoepfel T, Furet P, Mah R, Buschmann N, Leblanc C, Ripoché S, Graus-Porta D, Wartmann M, Galuba I, Fairhurst RA (2018) 2-formylpyridyl ureas as highly selective reversible-covalent inhibitors of fibroblast growth factor receptor 4. *ACS Med Chem Lett* 9:215–220. <https://doi.org/10.1021/acsmchemlett.7b00485>
30. Müller J, Kirschner RA, Geyer A, Klebe G (2019) Conceptual design of self-assembling bisubstrate-like inhibitors of protein kinase A resulting in a Boronic acid glutamate linkage. *ACS Omega* 4:775–784. <https://doi.org/10.1021/acsomega.8b02364>
31. Shindo N, Fuchida H, Sato M, Watari K, Shibata T, Kuwata K, Miura C, Okamoto K, Hatsuyama Y, Tokunaga K, Sakamoto S, Morimoto S, Abe Y, Shiroishi M, Caaveiro JMM, Ueda T, Tamura T, Matsunaga N, Nakao T, Koyanagi S, Ohdo S, Yamaguchi Y, Hamachi I, Ono M, Ojida A (2019) Selective and reversible modification of kinase cysteines with chlorofluoroacetamides. *Nat Chem Biol* 15:250. <https://doi.org/10.1038/s41589-018-0204-3>
32. Zhang J, Yang PL, Gray NS (2009) Targeting cancer with small molecule kinase inhibitors. *Nat Rev Cancer* 9:28–39. <https://doi.org/10.1038/nrc2559>
33. Traxler P (1998) Tyrosine kinase inhibitors in cancer treatment (part II). *Expert Opin Ther Pat* 8:1599–1625. <https://doi.org/10.1517/13543776.8.12.1599>
34. Traxler P, Furet P (1999) Strategies toward the design of novel and selective protein tyrosine kinase inhibitors. *Pharmacol Ther* 82:195–206. [https://doi.org/10.1016/S0163-7258\(98\)00044-8](https://doi.org/10.1016/S0163-7258(98)00044-8)
35. Backes A, Zech B, Felber B, Klebl B, Müller G (2008) Small-molecule inhibitors binding to protein kinase. Part II: the novel pharmacophore approach of type II and type III inhibition. *Exp Opin Drug Discovery* 3:1427–1449. <https://doi.org/10.1517/17460440802580106>
36. Liao JJ-L (2007) Molecular recognition of protein kinase binding pockets for design of potent and selective kinase inhibitors. *J Med Chem* 50:409–424. <https://doi.org/10.1021/jm0608107>
37. Yoshida T, Kakizuka A, Imamura H (2016) BTeam, a novel BRET-based biosensor for the accurate quantification of ATP concentration within living cells. *Sci Rep* 6:39618. <https://doi.org/10.1038/srep39618>
38. Yen-Pon E, Li B, Acebrón-García-de-Eulate M, Tomkiewicz-Raulet C, Dawson J, Lietha D, Frame MC, Coumoul X, Garbay C, Etheve-Quellejeu M, Chen H (2018) Structure-based design, synthesis, and characterization of the first irreversible inhibitor of focal adhesion kinase. *ACS Chem Biol* 13:2067–2073. <https://doi.org/10.1021/acscchembio.8b00250>
39. Ferguson FM, Gray NS (2018) Kinase inhibitors: the road ahead. *Nat Rev Drug Discov* 17:353–377. <https://doi.org/10.1038/nrd.2018.21>
40. Zhao Z, Bourme PE (2018) Progress with covalent small-molecule kinase inhibitors. *Drug Discov Today* 23:727–735. <https://doi.org/10.1016/j.drudis.2018.01.035>
41. Gilbert AM (2014) Recent advances in irreversible kinase inhibitors. *Pharm Patent Anal* 3:375–386. <https://doi.org/10.4155/ppa.14.24>
42. Sanderson K (2013) Irreversible kinase inhibitors gain traction. *Nat Rev Drug Discov* 12:649–651. <https://doi.org/10.1038/nrd4103>
43. Miklos D, Cutler CS, Arora M, Waller EK, Jagasia M, Pusic I, Flowers ME, Logan AC, Nakamura R, Blazar BR, Li Y, Chang S, Lal I, Dubovsky J, James DF, Styles L, Jaglowski S (2017) Ibrutinib for chronic graft-versus-host disease after failure of prior therapy. *Blood* 130:2243–2250. <https://doi.org/10.1182/blood-2017-07-793786>
44. Soria J-C, Ohe Y, Vansteenkiste J, Reungwetwattana T, Chewaskulyong B, Lee KH, Dechaphunkul A, Imamura F, Nogami N, Kurata T, Okamoto I, Zhou C, Cho BC, Cheng Y, Cho EK, Voon PJ, Planchard D, Su W-C, Gray JE, Lee S-M, Hodge R,

- Marotti M, Rukazekov Y, Ramalingam SS (2017) Osimertinib in untreated EGFR-mutated advanced non-small-cell lung cancer. *N Engl J Med* 378:113–125. <https://doi.org/10.1056/NEJMoa1713137>
45. Barf T, Covey T, Izumi R, van de Kar B, Gulrajani M, van Lith B, van Hoek M, de Zwart E, Mittag D, Demont D, Verkaik S, Krantz F, Pearson PG, Ulrich R, Kaptein A (2017) Acalabrutinib (ACP-196): a covalent Bruton tyrosine kinase inhibitor with a differentiated selectivity and in vivo potency profile. *J Pharmacol Exp Ther* 363:240–252. <https://doi.org/10.1124/jpet.117.242909>
46. Shirley M (2018) Dacomitinib: first global approval. *Drugs*. <https://doi.org/10.1007/s40265-018-1028-x>
47. Lagoutte R, Winssinger N (2017) Following the lead from nature with covalent inhibitors. *CHIMIA Int J Chem* 71:703–711. <https://doi.org/10.2533/chimia.2017.703>
48. Wymann MP, Bulgarelli-Leva G, Zvelebil MJ, Pirola L, Vanhaesebroeck B, Waterfield MD, Panayotou G (1996) Wortmannin inactivates phosphoinositide 3-kinase by covalent modification of Lys-802, a residue involved in the phosphate transfer reaction. *Mol Cell Biol* 16:1722–1733. <https://doi.org/10.1128/MCB.16.4.1722>
49. Zhao A, Lee SH, Moiena M, Jenkins RG, Patrick DR, Huber HE, Goetz MA, Hensens OD, Zink DL, Vilella D, Dombrowski AW, Lingham RB, Huang L (1999) Resorcylic acid lactones: naturally occurring potent and selective inhibitors of MEK. *J Antibiot* 52:1086–1094. <https://doi.org/10.7164/antibiotics.52.1086>
50. Williams DH, Wilkinson SE, Purton T, Lamont A, Flotow H, Murray EJ (1998) Ro 09-2210 exhibits potent anti-proliferative effects on activated T cells by selectively blocking MKK activity. *Biochemistry* 37:9579–9585. <https://doi.org/10.1021/bi972914c>
51. Rastelli G, Rosenfeld R, Reid R, Santi DV (2008) Molecular modeling and crystal structure of ERK2–hypothemycin complexes. *J Struct Biol* 164:18–23. <https://doi.org/10.1016/j.jsb.2008.05.002>
52. Schirmer A, Kennedy J, Murli S, Reid R, Santi DV (2006) Targeted covalent inactivation of protein kinases by resorcylic acid lactone polyketides. *PNAS* 103:4234–4239. <https://doi.org/10.1073/pnas.0600445103>
53. Wu J, Powell F, Larsen NA, Lai Z, Byth KF, Read J, Gu R-F, Roth M, Toader D, Saeh JC, Chen H (2013) Mechanism and in vitro pharmacology of TAK1 inhibition by (5Z)-7-Oxozeaenol. *ACS Chem Biol* 8:643–650. <https://doi.org/10.1021/cb3005897>
54. Sogabe Y, Matsumoto T, Hashimoto T, Kirii Y, Sawa M, Kinoshita T (2015) 5Z-7-Oxozeaenol covalently binds to MAP2K7 at Cys218 in an unprecedented manner. *Bioorg Med Chem Lett* 25:593–596. <https://doi.org/10.1016/j.bmcl.2014.12.011>
55. Shen Y, Boivin R, Yoneda N, Du H, Schiller S, Matsushima T, Goto M, Shirota H, Gusovsky F, Lemelin C, Jiang Y, Zhang Z, Pelletier R, Ikemori-Kawada M, Kawakami Y, Inoue A, Schnaderbeck M, Wang Y (2010) Discovery of anti-inflammatory clinical candidate E6201, inspired from resorcylic lactone LL-Z1640-2, III. *Bioorg Med Chem Lett* 20:3155–3157. <https://doi.org/10.1016/j.bmcl.2010.03.087>
56. Borthakur G, Gao C, Chen Y, Lan YS, Ruvolo VR, Nomoto K, Zhao N, Konopleva M, Andreeff M (2013) Study of activity of E6201, a dual FLT3 and MEK inhibitor, in acute Myelogenous leukemia with FLT3 or RAS mutation. *Blood* 122:2683–2683
57. Rossi A, Kapahi P, Natoli G, Takahashi T, Chen Y, Karin M, Santoro MG (2000) Anti-inflammatory cyclopentenone prostaglandins are direct inhibitors of I κ B kinase. *Nature* 403:103–118. <https://doi.org/10.1038/47520>
58. Toral-Barza L, Zhang W-G, Huang X, McDonald LA, Salaski EJ, Barbieri LR, Ding W-D, Krishnamurthy G, Hu YB, Lucas J, Bernan VS, Cai P, Levin JI, Mansour TS, Gibbons JJ, Abraham RT, Yu K (2007) Discovery of lactoquinomycin and related pyranonaphthoquinones as potent and allosteric inhibitors of AKT/PKB: mechanistic involvement of AKT catalytic activation loop cysteines. *Mol Cancer Ther* 6:3028–3038. <https://doi.org/10.1158/1535-7163.MCT-07-0211>

59. Walker EH, Pacold ME, Perisic O, Stephens L, Hawkins PT, Wymann MP, Williams RL (2000) Structural determinants of phosphoinositide 3-kinase inhibition by wortmannin, LY294002, quercetin, myricetin, and staurosporine. *Mol Cell* 6:909–919. [https://doi.org/10.1016/S1097-2765\(05\)00089-4](https://doi.org/10.1016/S1097-2765(05)00089-4)
60. Norman BH, Shih C, Toth JE, Ray JE, Dodge JA, Johnson DW, Rutherford PG, Schultz RM, Worzalla JF, Vlahos CJ (1996) Studies on the mechanism of phosphatidylinositol 3-kinase inhibition by wortmannin and related analogs. *J Med Chem* 39:1106–1111. <https://doi.org/10.1021/jm950619p>
61. Singh J, Dobrusin EM, Fry DW, Haske T, Whitty A, McNamara DJ (1997) Structure-based design of a potent, selective, and irreversible inhibitor of the catalytic domain of the erbB receptor subfamily of protein tyrosine kinases. *J Med Chem* 40:1130–1135. <https://doi.org/10.1021/jm960380s>
62. Fry DW, Bridges AJ, Denny WA, Doherty A, Greis KD, Hicks JL, Hook KE, Keller PR, Leopold WR, Loo JA, McNamara DJ, Nelson JM, Sherwood V, Smaill JB, Trumpp-Kallmeyer S, Dobrusin EM (1998) Specific, irreversible inactivation of the epidermal growth factor receptor and erbB2, by a new class of tyrosine kinase inhibitor. *PNAS* 95:12022–12027. <https://doi.org/10.1073/pnas.95.20.12022>
63. Smaill JB, Gonzales AJ, Spicer JA, Lee H, Reed JE, Sexton K, Althaus IW, Zhu T, Black SL, Blaser A, Denny WA, Ellis PA, Fakhoury S, Harvey PJ, Hook K, McCarthy FOJ, Palmer BD, Rivault F, Schlosser K, Ellis T, Thompson AM, Trachet E, Winters RT, Tecle H, Bridges A (2016) Tyrosine kinase inhibitors. 20. Optimization of substituted Quinazoline and Pyrido [3,4-d]pyrimidine derivatives as orally active, irreversible inhibitors of the epidermal growth factor receptor family. *J Med Chem* 59:8103–8124. <https://doi.org/10.1021/acs.jmedchem.6b00883>
64. Tsou H-R, Overbeek-Klumpers EG, Hallett WA, Reich MF, Floyd MB, Johnson BD, Michalak RS, Nilakantan R, Discafani C, Golas J, Rabindran SK, Shen R, Shi X, Wang Y-F, Upeslaci J, Wissner A (2005) Optimization of 6,7-Disubstituted-4-(arylamino)quinoline-3-carbonitriles as orally active, irreversible inhibitors of human epidermal growth factor Receptor-2 kinase activity. *J Med Chem* 48:1107–1131. <https://doi.org/10.1021/jm040159c>
65. Zhou W, Ercan D, Chen L, Yun C-H, Li D, Capelletti M, Cortot AB, Chirieac L, Jacob RE, Padera R, Engen JR, Wong K-K, Eck MJ, Gray NS, Jänne PA (2009) Novel mutant-selective EGFR kinase inhibitors against EGFR T790M. *Nature* 462:1070–1074. <https://doi.org/10.1038/nature08622>
66. Wilcken R, Zimmermann MO, Lange A, Joerger AC, Boeckler FM (2013) Principles and applications of halogen bonding in medicinal chemistry and chemical biology. *J Med Chem* 56:1363–1388. <https://doi.org/10.1021/jm3012068>
67. Boeckler FM, Zimmermann M. Personal communication
68. Van Der Steen N, Caparello C, Rolfo C, Pauwels P, Peters GJ, Giovannetti E (2016) New developments in the management of non-small-cell lung cancer, focus on rociletinib: what went wrong? *Onco Targets Ther* 9:6065–6074. <https://doi.org/10.2147/OTT.S97644>
69. Yver A (2016) Osimertinib (AZD9291) – a science-driven, collaborative approach to rapid drug design and development. *Ann Oncol* 27:1165–1170. <https://doi.org/10.1093/annonc/mdw129>
70. Günther M, Juchum M, Kelter G, Fiebig H, Laufer S (2016) Lung cancer: EGFR inhibitors with low nanomolar activity against a therapy-resistant L858R/T790M/C797S mutant. *Angew Chem Int Ed* 55:10890–10894. <https://doi.org/10.1002/anie.201603736>
71. Günther M, Lategahn J, Juchum M, Döring E, Keul M, Engel J, Tumbrink HL, Rauh D, Laufer S (2017) Trisubstituted Pyridinylimidazoles as potent inhibitors of the clinically resistant L858R/T790M/C797S EGFR mutant: targeting of both hydrophobic regions and the phosphate binding site. *J Med Chem* 60:5613–5637. <https://doi.org/10.1021/acs.jmedchem.7b00316>
72. Pan Z, Scheerens H, Li S-J, Schultz BE, Sprengeler PA, Burrill LC, Mendonca RV, Sweeney MD, Scott KCK, Grothaus PG, Jeffery DA, Spoerke JM, Honigberg LA, Young PR,

- Dalrymple SA, Palmer JT (2006) Discovery of selective irreversible inhibitors for Bruton's tyrosine kinase. *ChemMedChem* 2:58–61. <https://doi.org/10.1002/cmdc.200600221>
73. Honigberg LA, Smith AM, Sirisawad M, Verner E, Loury D, Chang B, Li S, Pan Z, Thamm DH, Miller RA, Buggy JJ (2010) The Bruton tyrosine kinase inhibitor PCI-32765 blocks B-cell activation and is efficacious in models of autoimmune disease and B-cell malignancy. *PNAS* 107:13075–13080. <https://doi.org/10.1073/pnas.1004594107>
74. Flanagan ME, Abramite JA, Anderson DP, Aulabaugh A, Dahal UP, Gilbert AM, Li C, Montgomery J, Oppenheimer SR, Ryder T, Schuff BP, Uccello DP, Walker GS, Wu Y, Brown MF, Chen JM, Hayward MM, Noe MC, Obach RS, Philippe L, Shanmugasundaram V, Shapiro MJ, Starr J, Stroh J, Che Y (2014) Chemical and computational methods for the characterization of covalent reactive groups for the prospective design of irreversible inhibitors. *J Med Chem* 57:10072–10079. <https://doi.org/10.1021/jm501412a>
75. Markham A, Dhillon S (2018) Acalabrutinib: first global approval. *Drugs* 78:139–145. <https://doi.org/10.1007/s40265-017-0852-8>
76. Buhimschi AD, Armstrong HA, Toure M, Jaime-Figueroa S, Chen TL, Lehman AM, Woyach JA, Johnson AJ, Byrd JC, Crews CM (2018) Targeting the C481S ibrutinib-resistance mutation in Bruton's tyrosine kinase using PROTAC-mediated degradation. *Biochemistry* 57:3564–3575. <https://doi.org/10.1021/acs.biochem.8b00391>
77. Wu H, Huang Q, Qi Z, Chen Y, Wang A, Chen C, Liang Q, Wang J, Chen W, Dong J, Yu K, Hu C, Wang W, Liu X, Deng Y, Wang L, Wang B, Li X, Gray NS, Liu J, Wei W, Liu Q (2017) Irreversible inhibition of BTK kinase by a novel highly selective inhibitor CHMFL-BTK-11 suppresses inflammatory response in rheumatoid arthritis model. *Sci Rep* 7:466. <https://doi.org/10.1038/s41598-017-00482-4>
78. Watterson SH, Liu Q, Beaudoin Bertrand M, Batt DG, Li L, Pattoli MA, Skala S, Cheng L, Obermeier MT, Moore R, Yang Z, Vickery R, Elzinga PA, Discenza L, D'Arienzo C, Gillooly KM, Taylor TL, Pulicicchio C, Zhang Y, Heimrich E, McIntyre KW, Ruan Q, Westhouse RA, Catlett IM, Zheng N, Chaudhry C, Dai J, Galella MA, Tebben AJ, Pokross M, Li J, Zhao R, Smith D, Rampulla R, Allentoff A, Wallace MA, Mathur A, Salter-Cid L, Macor JE, Carter PH, Fura A, Burke JR, Tino JA (2019) Discovery of branebrutinib (BMS-986195): a strategy for identifying a highly potent and selective covalent inhibitor providing rapid in vivo inactivation of Bruton's tyrosine kinase (BTK). *J Med Chem* 62:3228–3250. <https://doi.org/10.1021/acs.jmedchem.9b00167>
79. Park JK, Byun J-Y, Park JA, Kim Y-Y, Lee YJ, Oh JI, Jang SY, Kim YH, Song YW, Son J, Suh KH, Lee Y-M, Lee EB (2016) HM71224, a novel Bruton's tyrosine kinase inhibitor, suppresses B cell and monocyte activation and ameliorates arthritis in a mouse model: a potential drug for rheumatoid arthritis. *Arthritis Res Ther* 18:91. <https://doi.org/10.1186/s13075-016-0988-z>
80. Smith PF, Krishnarajah J, Nunn PA, Hill RJ, Karr D, Tam D, Masjedizadeh M, Funk JO, Gourlay SG (2017) A phase I trial of PRN1008, a novel reversible covalent inhibitor of Bruton's tyrosine kinase, in healthy volunteers. *Br J Clin Pharmacol* 83:2367–2376. <https://doi.org/10.1111/bcp.13351>
81. Benson MJ, Rodriguez V, von Schack D, Keegan S, Cook TA, Edmonds J, Benoit S, Seth N, Du S, Messing D, Nickerson-Nutter CL, Dunussi-Joannopoulos K, Rankin AL, Ruzek M, Schnute ME, Douhan J (2014) Modeling the clinical phenotype of BTK inhibition in the mature murine immune system. *J Immunol* 193:185. <https://doi.org/10.4049/jimmunol.1302570>
82. Falgoutyret J-P, Oballa RM, Okamoto O, Wesolowski G, Aubin Y, Rydzewski RM, Prasit P, Riendeau D, Rodan SB, Percival MD (2001) Novel, nonpeptidic cyanamides as potent and reversible inhibitors of human Cathepsins K and L. *J Med Chem* 44:94–104. <https://doi.org/10.1021/jm0003440>
83. Lainé D, Palovich M, McClelland B, Petitjean E, Delhom I, Xie H, Deng J, Lin G, Davis R, Jolit A, Nevins N, Zhao B, Villa J, Schneck J, McDevitt P, Midgett R, Kmett C, Umbrecht S,

- Peck B, Davis AB, Bettoun D (2011) Discovery of novel Cyanamide-based inhibitors of Cathepsin C. *ACS Med Chem Lett* 2:142–147. <https://doi.org/10.1021/ml100212k>
84. Zapf CW, Gerstenberger BS, Xing L, Limburg DC, Anderson DR, Caspers N, Han S, Aulabaugh A, Kurumbail R, Shakya S, Li X, Spaulding V, Czerwinski RM, Seth N, Medley QG (2012) Covalent inhibitors of interleukin-2 inducible T cell kinase (Itk) with nanomolar potency in a whole-blood assay. *J Med Chem* 55:10047–10063. <https://doi.org/10.1021/jm301190s>
85. Harling JD, Deakin AM, Campos S, Grimley R, Chaudry L, Nye C, Polyakova O, Bessant CM, Barton N, Somers D, Barrett J, Graves RH, Hanns L, Kerr WJ, Solari R (2013) Discovery of novel irreversible inhibitors of interleukin (IL)-2-inducible tyrosine kinase (Itk) by targeting cysteine 442 in the ATP pocket. *J Biol Chem* 288:28195–28206. <https://doi.org/10.1074/jbc.M113.474114>
86. Forster M, Gehringer M, Laufer SA (2017) Recent advances in JAK3 inhibition: isoform selectivity by covalent cysteine targeting. *Bioorg Med Chem Lett* 27:4229–4237. <https://doi.org/10.1016/j.bmcl.2017.07.079>
87. Forster M, Chaikuad A, Bauer SM, Holstein J, Robers MB, Corona CR, Gehringer M, Pfaffenrot E, Ghoreschi K, Knapp S, Laufer SA (2016) Selective JAK3 inhibitors with a covalent reversible binding mode targeting a new induced fit binding pocket. *Cell Chem Biol* 23:1335–1340. <https://doi.org/10.1016/j.chembiol.2016.10.008>
88. Forster M, Chaikuad A, Dimitrov T, Döring E, Holstein J, Berger B-T, Gehringer M, Ghoreschi K, Müller S, Knapp S, Laufer SA (2018) Development, optimization, and structure–activity relationships of covalent-reversible JAK3 inhibitors based on a tricyclic Imidazo[5,4-d]pyrrolo[2,3-b]pyridine scaffold. *J Med Chem* 61:5350–5366. <https://doi.org/10.1021/acs.jmedchem.8b00571>
89. Liu F, Zhang X, Weisberg E, Chen S, Hur W, Wu H, Zhao Z, Wang W, Mao M, Cai C, Simon NI, Sanda T, Wang J, Look AT, Griffin JD, Balk SP, Liu Q, Gray NS (2013) Discovery of a selective irreversible BMX inhibitor for prostate cancer. *ACS Chem Biol* 8:1423–1428. <https://doi.org/10.1021/cb4000629>
90. Liang X, Lv F, Wang B, Yu K, Wu H, Qi Z, Jiang Z, Chen C, Wang A, Miao W, Wang W, Hu Z, Liu J, Liu X, Zhao Z, Wang L, Zhang S, Ye Z, Wang C, Ren T, Wang Y, Liu Q, Liu J (2017) Discovery of 2-((3-Acrylamido-4-methylphenyl)amino)-N-(2-methyl-5-(3,4,5-trimethoxybenzamido)phenyl)-4-(methylamino)pyrimidine-5-carboxamide (CHMFL-BMX-078) as a highly potent and selective type II irreversible bone marrow kinase in the X Chromosome (BMX) kinase inhibitor. *J Med Chem* 60:1793–1816. <https://doi.org/10.1021/acs.jmedchem.6b01413>
91. London N, Miller RM, Krishnan S, Uchida K, Irwin JJ, Eidam O, Gibold L, Cimermančič P, Bonnet R, Shoichet BK, Taunton J (2014) Covalent docking of large libraries for the discovery of chemical probes. *Nat Chem Biol* 10:1066–1072. <https://doi.org/10.1038/nchembio.1666>
92. Shraga A, Olshvang E, Davidzohn N, Khoshkenar P, Germain N, Shurrush K, Carvalho S, Avram L, Albeck S, Unger T, Lefker B, Subramanyam C, Hudkins RL, Mitchell A, Shulman Z, Kinoshita T, London N (2018) Covalent docking identifies a potent and selective MKK7 inhibitor. *Cell Chem Biol*. <https://doi.org/10.1016/j.chembiol.2018.10.011>
93. Wolle P, Hardick J, Cronin SJF, Engel J, Baumann M, Lategahn J, Penninger JM, Rauh D (2019) Targeting the MKK7–JNK (mitogen-activated protein kinase kinase 7–c-Jun N-terminal kinase) pathway with covalent inhibitors. *J Med Chem* 62:2843–2848. <https://doi.org/10.1021/acs.jmedchem.9b00102>
94. Erlanson DA, Arndt JW, Cancilla MT, Cao K, Elling RA, English N, Friedman J, Hansen SK, Hession C, Joseph I, Kumaravel G, Lee W-C, Lind KE, McDowell RS, Miatkowski K, Nguyen C, Nguyen TB, Park S, Pathan N, Penny DM, Romanowski MJ, Scott D, Silvan L, Simmons RL, Tangonan BT, Yang W, Sun L (2011) Discovery of a potent and highly selective PDK1 inhibitor via fragment-based drug discovery. *Bioorg Med Chem Lett* 21:3078–3083. <https://doi.org/10.1016/j.bmcl.2011.03.032>

95. Koch A, Rode HB, Richters A, Rauh D, Hauf S (2012) A chemical genetic approach for covalent inhibition of analogue-sensitive Aurora kinase. *ACS Chem Biol* 7:723–731. <https://doi.org/10.1021/cb200465c>
96. Blair JA, Rauh D, Kung C, Yun C-H, Fan Q-W, Rode H, Zhang C, Eck MJ, Weiss WA, Shokat KM (2007) Structure-guided development of affinity probes for tyrosine kinases using chemical genetics. *Nat Chem Biol* 3:229–238. <https://doi.org/10.1038/nchembio866>
97. Zhang T, Inesta-Vaquera F, Niepel M, Zhang J, Ficarro SB, Machleidt T, Xie T, Marto JA, Kim N, Sim T, Laughlin JD, Park H, LoGrasso PV, Patricelli M, Nomanbhoy TK, Sorger PK, Alessi DR, Gray NS (2012) Discovery of potent and selective covalent inhibitors of JNK. *Chem Biol* 19:140–154. <https://doi.org/10.1016/j.chembiol.2011.11.010>
98. Muth F, El-Gokha A, Ansideri F, Eitel M, Döring E, Sievers-Engler A, Lange A, Boeckler FM, Lämmerhofer M, Koch P, Laufer SA (2017) Tri- and tetrasubstituted pyridinylimidazoles as covalent inhibitors of c-Jun N-terminal kinase 3. *J Med Chem* 60:594–607. <https://doi.org/10.1021/acs.jmedchem.6b01180>
99. Koch P, Gehringer M, Laufer SA (2015) Inhibitors of c-Jun N-terminal kinases: an update. *J Med Chem* 58:72–95. <https://doi.org/10.1021/jm501212r>
100. Gehringer M, Muth F, Koch P, Laufer SA (2015) c-Jun N-terminal kinase inhibitors: a patent review (2010–2014). *Expert Opin Ther Patents* 25:849–872. <https://doi.org/10.1517/13543776.2015.1039984>
101. Kung A, Chen Y-C, Schimpl M, Ni F, Zhu J, Turner M, Molina H, Overman R, Zhang C (2016) Development of specific, irreversible inhibitors for a receptor tyrosine kinase EphB3. *J Am Chem Soc* 138:10554–10560. <https://doi.org/10.1021/jacs.6b05483>
102. Kung A, Schimpl M, Ekanayake A, Chen Y-C, Overman R, Zhang C (2017) A chemical-genetic approach to generate selective covalent inhibitors of protein kinases. *ACS Chem Biol* 12:1499–1503. <https://doi.org/10.1021/acscchembio.6b01083>
103. Nacht M, Qiao L, Sheets MP, St. Martin T, Labenski M, Mazdiyasi H, Karp R, Zhu Z, Chaturvedi P, Bhavsar D, Niu D, Westlin W, Petter RC, Medikonda AP, Singh J (2013) Discovery of a potent and isoform-selective targeted covalent inhibitor of the lipid kinase PI3K α . *J Med Chem* 56:712–721. <https://doi.org/10.1021/jm3008745>
104. Xie T, Lim SM, Westover KD, Dodge ME, Ercan D, Ficarro SB, Udayakumar D, Gurbani D, Tae HS, Riddle SM, Sim T, Marto JA, Jänne PA, Crews CM, Gray NS (2014) Pharmacological targeting of the pseudokinase Her3. *Nat Chem Biol* 10:1006–1012. <https://doi.org/10.1038/nchembio.1658>
105. Tinworth CP, Lithgow H, Dittus L, Bassi ZI, Hughes SE, Muelbaier M, Dai H, Smith IED, Kerr WJ, Burley GA, Bantscheff M, Harling JD (2019) PROTAC-mediated degradation of Bruton's tyrosine kinase is inhibited by covalent binding. *ACS Chem Biol* 14:342–347. <https://doi.org/10.1021/acscchembio.8b01094>
106. Cohen MS, Zhang C, Shokat KM, Taunton J (2005) Structural bioinformatics-based design of selective, irreversible kinase inhibitors. *Science* 308:1318–1321. <https://doi.org/10.1126/science1108367>
107. Cohen MS, Hadjivassiliou H, Taunton J (2007) A clickable inhibitor reveals context-dependent autoactivation of p90 RSK. *Nat Chem Biol* 3:156–160. <https://doi.org/10.1038/nchembio859>
108. Miller RM, Paavilainen VO, Krishnan S, Serafimova IM, Taunton J (2013) Electrophilic fragment-based design of reversible covalent kinase inhibitors. *J Am Chem Soc* 135:5298–5301. <https://doi.org/10.1021/ja401221b>
109. Lebraud H, Coxon CR, Archard SV, Bawn MC, Carbain B, Matheson JC, Turner MD, Cano C, Griffin JR, Hardcastle RI, Baisch U, Harrington WR, Golding TB (2014) Model system for irreversible inhibition of Nek2: thiol addition to ethynylpurines and related substituted heterocycles. *Org Biomol Chem* 12:141–148. <https://doi.org/10.1039/C3OB41806E>
110. Mitcheson DF, Bottrill AR, Carr K, Coxon CR, Cano C, Golding BT, Griffin RJ, Fry AM, Doerig C, Bayliss R, Tobin AB (2016) A new tool for the chemical genetic investigation of the

- Plasmodium falciparum Pfnek-2 NIMA-related kinase. *Malar J* 15:535. <https://doi.org/10.1186/s12936-016-1580-3>
111. Henise JC, Taunton J (2011) Irreversible Nek2 kinase inhibitors with cellular activity. *J Med Chem* 54:4133–4146. <https://doi.org/10.1021/jm200222m>
 112. Pearson RJ, Blake DG, Mezna M, Fischer PM, Westwood NJ, McInnes C (2018) The Meisenheimer complex as a paradigm in drug discovery: reversible covalent inhibition through C67 of the ATP binding site of PLK1. *Cell Chem Biol* 25:1107–1116.e4. <https://doi.org/10.1016/j.chembiol.2018.06.001>
 113. Dittus L, Werner T, Muelbaier M, Bantscheff M (2017) Differential kinobeads profiling for target identification of irreversible kinase inhibitors. *ACS Chem Biol* 12:2515–2521. <https://doi.org/10.1021/acscchembio.7b00617>
 114. Zhou W, Hur W, McDermott U, Dutt A, Xian W, Ficarro SB, Zhang J, Sharma SV, Brugge J, Meyerson M, Settleman J, Gray NS (2010) A structure-guided approach to creating covalent FGFR inhibitors. *Chem Biol* 17:285–295. <https://doi.org/10.1016/j.chembiol.2010.02.007>
 115. Tan L, Wang J, Tanizaki J, Huang Z, Aref AR, Rusan M, Zhu S-J, Zhang Y, Ercan D, Liao RG, Capelletti M, Zhou W, Hur W, Kim N, Sim T, Gaudet S, Barbie DA, Yeh J-RJ, Yun C-H, Hammerman PS, Mohammadi M, Jänne PA, Gray NS (2014) Development of covalent inhibitors that can overcome resistance to first-generation FGFR kinase inhibitors. *PNAS* 111:E4869–E4877. <https://doi.org/10.1073/pnas.1403438111>
 116. Brameld KA, Owens TD, Verner E, Venetsanos E, Bradshaw JM, Phan VT, Tam D, Leung K, Shu J, LaStant J, Loughhead DG, Ton T, Karr DE, Gerritsen ME, Goldstein DM, Funk JO (2017) Discovery of the irreversible covalent FGFR inhibitor 8-(3-(4-acryloylpiperazin-1-yl)propyl)-6-(2,6-dichloro-3,5-dimethoxyphenyl)-2-(methylamino)pyrido[2,3-d]pyrimidin-7(8H)-one (PRN1371) for the treatment of solid tumors. *J Med Chem* 60:6516–6527. <https://doi.org/10.1021/acs.jmedchem.7b00360>
 117. Kalyukina M, Yosaatmadja Y, Middleditch MJ, Patterson AV, Smaill JB, Squire CJ (2019) TAS-120 cancer target binding: defining reactivity and revealing the first fibroblast growth factor receptor 1 (FGFR1) irreversible structure. *ChemMedChem* 14:494–500. <https://doi.org/10.1002/cmdc.201800719>
 118. Kwarcinski FE, Fox CC, Steffey ME, Soellner MB (2012) Irreversible inhibitors of c-Src kinase that target a nonconserved cysteine. *ACS Chem Biol* 7:1910–1917. <https://doi.org/10.1021/cb300337u>
 119. Hagel M, Miduturu C, Sheets M, Rubin N, Weng W, Stransky N, Bifulco N, Kim JL, Hodous B, Brooijmans N, Shutes A, Winter C, Lengauer C, Kohl NE, Guzi T (2015) First selective small molecule inhibitor of FGFR4 for the treatment of hepatocellular carcinomas with an activated FGFR4 signaling pathway. *Cancer Discov* 5:424–437. <https://doi.org/10.1158/2159-8290.CD-14-1029>
 120. Joshi JJ, Coffey H, Corcoran E, Tsai J, Huang C-L, Ichikawa K, Prajapati S, Hao M-H, Bailey S, Wu J, Rimkunas V, Karr C, Subramanian V, Kumar P, MacKenzie C, Hurley R, Satoh T, Yu K, Park E, Rioux N, Kim A, Lai WG, Yu L, Zhu P, Buonamici S, Larsen N, Fekkes P, Wang J, Warmuth M, Reynolds DJ, Smith PG, Selvaraj A (2017) H3B-6527 is a potent and selective inhibitor of FGFR4 in FGF19-driven hepatocellular carcinoma. *Cancer Res* 77:6999–7013. <https://doi.org/10.1158/0008-5472.CAN-17-1865>
 121. Fairhurst AR, Knoepfel T, Leblanc C, Buschmann N, Gaul C, Blank J, Galuba I, Trappe J, Zou C, Voshol J, Genick C, Brunet-Lefevre P, Bitsch F, Graus-Porta D, Furet P (2017) Approaches to selective fibroblast growth factor receptor 4 inhibition through targeting the ATP-pocket middle-hinge region. *MedChemComm* 8:1604–1613. <https://doi.org/10.1039/C7MD00213K>
 122. Yamaura T, Nakatani T, Uda K, Ogura H, Shin W, Kurokawa N, Saito K, Fujikawa N, Date T, Takasaki M, Terada D, Hirai A, Akashi A, Chen F, Adachi Y, Ishikawa Y, Hayakawa F, Hagiwara S, Naoe T, Kiyoi H (2018) A novel irreversible FLT3 inhibitor, FF-10101, shows excellent efficacy against AML cells with FLT3 mutations. *Blood* 131:426–438. <https://doi.org/10.1182/blood-2017-05-786657>

123. Ward RA, Colclough N, Challinor M, Debreczeni JE, Eckersley K, Fairley G, Feron L, Flemington V, Graham MA, Greenwood R, Hopcroft P, Howard TD, James M, Jones CD, Jones CR, Renshaw J, Roberts K, Snow L, Tonge M, Yeung K (2015) Structure-guided design of highly selective and potent covalent inhibitors of ERK1/2. *J Med Chem* 58:4790–4801. <https://doi.org/10.1021/acs.jmedchem.5b00466>
124. Aronchik I, Dai Y, Labenski M, Barnes C, Jones T, Qiao L, Beebe L, Malek M, Elis W, Shi T, Mavrommatis K, Bray GL, Filvaroff EH (2018) Efficacy of a covalent ERK1/2 inhibitor, CC-90003, in KRAS mutant cancer models reveals novel mechanisms of response and resistance. *Mol Cancer Res Mol* 17:642–654. <https://doi.org/10.1158/1541-7786.MCR-17-0554>
125. Mita MM, LoRusso P, McArthur GA, Kim ES, Bray GL, Hock NH, Laille EJ, Aronchik I, Filvaroff E, Wu X, Bendell JC (2017) A phase Ia study of CC-90003, a selective extracellular signal-regulated kinase (ERK) inhibitor, in patients with relapsed or refractory BRAF or RAS-mutant tumors. *JCO* 35:2577–2577. https://doi.org/10.1200/JCO.2017.35.15_suppl.2577
126. Siphthorp J, Lebraud H, Gilley R, Kidger AM, Okkenhaug H, Saba-El-Leil M, Meloche S, Caunt CJ, Cook SJ, Heightman TD (2017) Visualization of endogenous ERK1/2 in cells with a bioorthogonal covalent probe. *Bioconjug Chem* 28:1677–1683. <https://doi.org/10.1021/acs.bioconjchem.7b00152>
127. Yang Z, Liu H, Pan B, He F, Pan Z (2018) Design and synthesis of (aza)indolyl maleimide-based covalent inhibitors of glycogen synthase kinase 3 β . *Org Biomol Chem*. <https://doi.org/10.1039/C8OB00642C>
128. Wissner A, Fraser HL, Ingalls CL, Dushin RG, Floyd MB, Cheung K, Nittoli T, Ravi MR, Tan X, Loganzo F (2007) Dual irreversible kinase inhibitors: Quinazoline-based inhibitors incorporating two independent reactive centers with each targeting different cysteine residues in the kinase domains of EGFR and VEGFR-2. *Bioorg Med Chem* 15:3635–3648. <https://doi.org/10.1016/j.bmc.2007.03.055>
129. Redenti S, Marcovich I, De Vita T, Pérez C, De Zorzi R, Demitri N, Perez DI, Bottegoni G, Bisignano P, Bissaro M, Moro S, Martinez A, Storici P, Spalluto G, Cavalli A, Federico S (2019) A Triazolotriazine-based dual GSK-3 β /CK-1 δ ligand as a potential Neuroprotective agent presenting two different mechanisms of enzymatic inhibition. *ChemMedChem* 14:310–314. <https://doi.org/10.1002/cmdc.201800778>
130. Kwiatkowski N, Zhang T, Rahl PB, Abraham BJ, Reddy J, Ficarro SB, Dastur A, Amzallag A, Ramaswamy S, Tesar B, Jenkins CE, Hannett NM, McMillin D, Sanda T, Sim T, Kim ND, Look T, Mitsiades CS, Weng AP, Brown JR, Benes CH, Marto JA, Young RA, Gray NS (2014) Targeting transcription regulation in cancer with a covalent CDK7 inhibitor. *Nature* 511:616. <https://doi.org/10.1038/nature13393>
131. Zhang T, Kwiatkowski N, Olson CM, Dixon-Clarke SE, Abraham BJ, Greifenberg AK, Ficarro SB, Elkins JM, Liang Y, Hannett NM, Manz T, Hao M, Bartkowiak B, Greenleaf AL, Marto JA, Geyer M, Bullock AN, Young RA, Gray NS (2016) Covalent targeting of remote cysteine residues to develop CDK12 and CDK13 inhibitors. *Nat Chem Biol* 12:876–884. <https://doi.org/10.1038/nchembio.2166>
132. Gao Y, Zhang T, Terai H, Ficarro SB, Kwiatkowski N, Hao M-F, Sharma B, Christensen CL, Chipumuro E, Wong K, Marto JA, Hammerman PS, Gray NS, George RE (2018) Overcoming resistance to the THZ series of covalent transcriptional CDK inhibitors. *Cell Chem Biol* 25:135–142.e5. <https://doi.org/10.1016/j.chembiol.2017.11.007>
133. Andersen JL, Gesser B, Funder ED, Nielsen CJF, Gotfred-Rasmussen H, Rasmussen MK, Toth R, Gothelf KV, Arthur JSC, Iversen L, Nissen P (2018) Dimethyl fumarate is an allosteric covalent inhibitor of the p90 ribosomal S6 kinases. *Nat Commun* 9:4344. <https://doi.org/10.1038/s41467-018-06787-w>
134. Dong T, Li C, Wang X, Dian L, Zhang X, Li L, Chen S, Cao R, Li L, Huang N, He S, Lei X (2015) Ainsliadimer A selectively inhibits IKK α/β by covalently binding a conserved cysteine. *Nat Commun* 6:ncomms7522. <https://doi.org/10.1038/ncomms7522>

135. Uhlenbrock N, Smith S, Weisner J, Landel I, Lindemann M, Le TA, Hardick J, Gontla R, Scheinpflug R, Czodrowski P, Janning P, Depta L, Quambusch L, Müller MP, Engels B, Rauh D (2019) Structural and chemical insights into the covalent-allosteric inhibition of the protein kinase Akt. *Chem Sci* 10:3573–3585. <https://doi.org/10.1039/C8SC05212C>
136. Craven GB, Affron DP, Allen CE, Matthies S, Greener JG, Morgan RML, Tate EW, Armstrong A, Mann DJ High-throughput kinetic analysis for target-directed covalent ligand discovery. *Angew Chem Int Ed* 57:5257–5261. <https://doi.org/10.1002/anie.201711825>
137. Bührmann M, Hardick J, Weisner J, Quambusch L, Rauh D (2017) Covalent lipid pocket ligands targeting p38 α MAPK mutants. *Angew Chem Int Ed* 56:13232–13236. <https://doi.org/10.1002/anie.201706345>
138. Dalton SE, Dittus L, Thomas DA, Convery MA, Nunes J, Bush JT, Evans JP, Werner T, Bantscheff M, Murphy JA, Campos S (2018) Selectively targeting the Kinome-conserved lysine of PI3K δ as a general approach to covalent kinase inhibition. *J Am Chem Soc* 140:932–939. <https://doi.org/10.1021/jacs.7b08979>
139. Anscombe E, Meschini E, Mora-Vidal R, Martin MP, Staunton D, Geitmann M, Danielson UH, Stanley WA, Wang LZ, Reuillon T, Golding BT, Cano C, Newell DR, Noble MEM, Wedge SR, Endicott JA, Griffin RJ (2015) Identification and characterization of an irreversible inhibitor of CDK2. *Cell Chem Biol* 22:1159–1164. <https://doi.org/10.1016/j.chembiol.2015.07.018>
140. Dahal UP, Gilbert AM, Obach RS, Flanagan ME, Chen JM, Garcia-Irizarry C, Starr JT, Schuff B, Uccello DP, Young JA (2016) Intrinsic reactivity profile of electrophilic moieties to guide covalent drug design: N- α -acetyl-L-lysine as an amine nucleophile. *Med Chem Commun* 7:864–872. <https://doi.org/10.1039/C6MD00017G>
141. Zhao Q, Ouyang X, Wan X, Gajiwala KS, Kath JC, Jones LH, Burlingame AL, Taunton J (2017) Broad-Spectrum kinase profiling in live cells with lysine-targeted Sulfonyl fluoride probes. *J Am Chem Soc* 139:680–685. <https://doi.org/10.1021/jacs.6b08536>
142. Hatcher JM, Wu G, Zeng C, Zhu J, Meng F, Patel S, Wang W, Ficarro SB, Leggett AL, Powell CE, Marto JA, Zhang K, Ngo JCK, Fu X-D, Zhang T, Gray NS (2018) SRPKIN-1: a covalent SRPK1/2 inhibitor that potently converts VEGF from pro-angiogenic to anti-angiogenic isoform. *Cell Chem Biol* 25:460–470.e6. <https://doi.org/10.1016/j.chembiol.2018.01.013>

Achieving High Levels of Selectivity for Kinase Inhibitors



Laurent Schio and Herve Minoux

Contents

1	Introduction	96
2	Discovery of an Exquisite Selective Aurora Inhibitor as Neo-Cytotoxic Agent	99
3	Development of a Selective MET Kinase Inhibitor Active Against Oncogenic Mutants	103
4	Design of Specific VPS34 Inhibitors for Autophagy Blockade in Tumors	109
5	PI3K β Inhibitor: Leveraging Water Molecules in the Active Site for Selectivity Enhancement	111
6	Conclusions	119
	References	120

Abstract Kinase inhibitors have emerged over the last two decades as one of the most prolific therapeutic classes of agents to reach clinical trials and to obtain marketing approval, mainly for oncology. We describe here the methodologies that we performed for hit and lead finding in the context of four internal projects to identify selective inhibitors for development or preclinical pharmacological evaluation.

Keywords Kinase inhibitors, Ligands, Oncology, Protein conformations, Selectivity, Targeted therapy

L. Schio (✉) and H. Minoux
Integrated Drug Discovery, Sanofi, Vitry-sur-Seine, France
e-mail: Laurent.Schio@sanofi.com

1 Introduction

It is estimated that 5% of the human genome is dedicated to protein phosphorylation. 518 different human kinases have been identified and clustered in sub-groups depending on substrate specificity and sequence similarity, but overall these enzymes catalyze the same biochemical reaction, the transfer of a phosphate group to a serine, threonine, or tyrosine residue [1]. From a pharmaceutical standpoint, there is huge evidence that kinase activities are deregulated in a broad range of diseases (cancer, inflammation, Parkinson, etc.) (<https://www.cellsignal.com/content/resources-reference-tables/kinase-disease-associations/science-tables-kinase-disease>) which has triggered over the last decades a massive interest in identifying and developing selective kinase inhibitors.

Cancer treatment is definitively the most important therapeutic domain where kinases inhibitors have found their application, and today approximately 50 small molecular weight kinase drugs have received marketing approval by the FDA, in addition to a dozen of monoclonal antibodies directed mainly against the human epidermal growth factor receptor kinase family (EGFR, HER2) [2, 3].

The first generation of marketed drugs (Gleevec, Sutent, Sprycel, etc.) [4] exhibited multi-kinase inhibition profiles, supporting the paradigm that better efficacy would be achieved by multi-cellular pathway blockade and giving the opportunity to register the same drug in different indications (e.g., Gleevec launched in 2001 for the treatment of patients with Philadelphia chromosome-positive chronic myeloid leukemia (CML) and in 2002 for the treatment of patients with Kit-positive unresectable and/or metastatic malignant gastrointestinal stromal tumor (GIST)) [5].

The development of the targeted therapy paradigm in oncology [6, 7] as well as the clinical demand for much better tolerated treatments has conducted research programs in pharmaceutical companies towards the discovery of selective to exquisite kinase inhibitors [8–10].

Successful development of drugs targeting specific deregulated cellular signaling pathways via selective inhibition of one targeted kinase (e.g., MEK) [11] or of oncogenic mutants (e.g., EGFR DM, V600E BRAF) [12] has been achieved recently [13, 14].

However, in the 1990s, when the first 3D crystal structure of a kinase (PKA) [15] was reported, a largely believed myth emerged that it would be impossible to develop selective and potent protein or lipid kinase inhibitors by targeting the ATP binding site due to a priori lack of specificity and high level of sequence similarity across the kinome. In mid-2019, more than 6,000 human protein kinases and more than 160 human lipid kinase 3D structures were deposited in the PDB (<https://www.rcsb.org/>). Thorough analyses of apo-structures vs ATP analog or ligand bound co-structures have revealed general modes of kinase activation [16, 17], including those behind oncogenic mutations [18–20], as well as subtle specific interactions in the active site and several preferred conformations (DFG-in, DFG-out, and α helix-out) [21, 22].

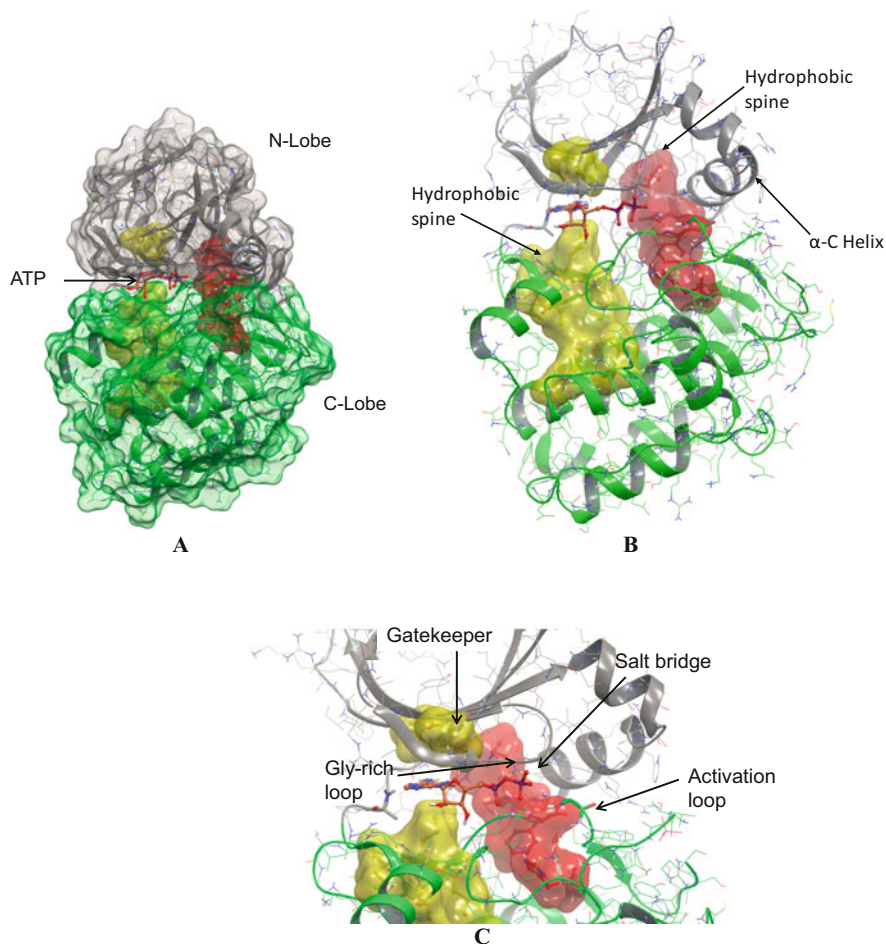


Fig. 1 General view of Aurora A kinase; (a) N-lobe is colored in grey and C-lobe in green. ATP is represented in ball and stick in its pocket at the interface between the two lobes; (b) surfaces of the residues forming the hydrophobic spines of Aurora A are colored in red and yellow. (c) Positions of the glycine-rich loop, activation loop, and gatekeeper (GK) residues are indicated

Figure 1a–c represents a general view of a kinase (Aurora A) for which key motifs and residues for activation and activity are highlighted:

Figure 2a, b describes a simplified view of a kinase active site where key residues and motifs for protein activation are depicted. These residues correspond to the general model of kinase activation reported by Taylor and coworkers [16]. The “N-lobe lysine” is the residue which is involved in a salt bridge with usually a glutamate residue from the α C- helix (“ α Cglutamate”) in a competent DFG-in conformation, whereas the “catlysine” from the catalytic loop interacts with the γ -phosphate of ATP to assist its transfer to the kinase substrate. The “phospho”residue”

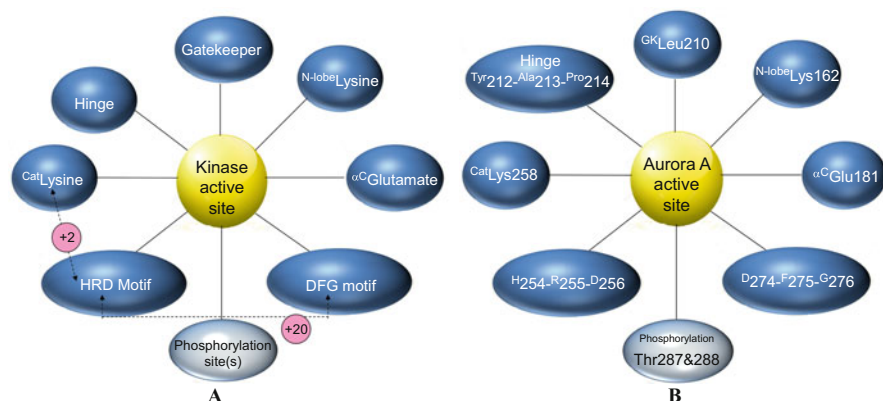


Fig. 2 (a) General kinase motif mapping (KMM), (b) KMM of Aurora A

corresponds to the phosphorylated residue in the activation loop. In general, the distances between these groups are conserved (numbers mentioned in pink in Fig. 2a). Figure 2b describes the ATP site of Aurora A in this schematic representation (Kinase Motif Map; KMM).

Recently, a chemogenetic study based on kinase sequence similarity and structure-activity relationship (SAR) analysis underlined 16 *privileged* residues in the active site that are recurrently involved in kinase protein stabilization and ligand binding [23]. In our ATP active site representation applied to Aurora A, the privileged motifs involved in protein ligand interactions are indicated in yellow and those involved in controlling the active vs inactive conformations balance in magenta (Fig. 3). The gatekeeper residue (Leu210) as well as two hinge residues (Tyr212, Pro214) are also privileged residues for ligand specificity. Interestingly, this analysis underlines the importance of hydrophobic residues which stabilize by packing the kinase active conformation and forming the so-called hydrophobic spine (Leu196 – α^C Gln185 – Phe275 – Leu208 – His254) [24].

It was originally thought that DFG-out related inhibitors would be more selective as this conformation has not been observed across the all kinome and has been publicized by the clinical success of Gleevec [25, 26]. Moreover this class of inhibitors is expected to be less impacted by micromolar concentrations of ATP in cells as they have shown non-competitive binding vs ATP in biochemical assays compared to active conformation directed ligands (DGF-in inhibitors) [8]. This selectivity trend has not been confirmed globally with DFG-out kinase inhibitors [27], but it has been shown that α -C helix-out inhibitors revealed exquisite selectivity profiles (e.g., MEK and HER2 inhibitors) [28, 29] albeit potentially at the expand of potency against oncogenic mutants, for which the inactive conformations are disfavored (e.g., lapatinib) [30].

We will describe in this chapter what were the medicinal chemistry strategies undertaken in our group to identify and develop selective kinase inhibitors for four

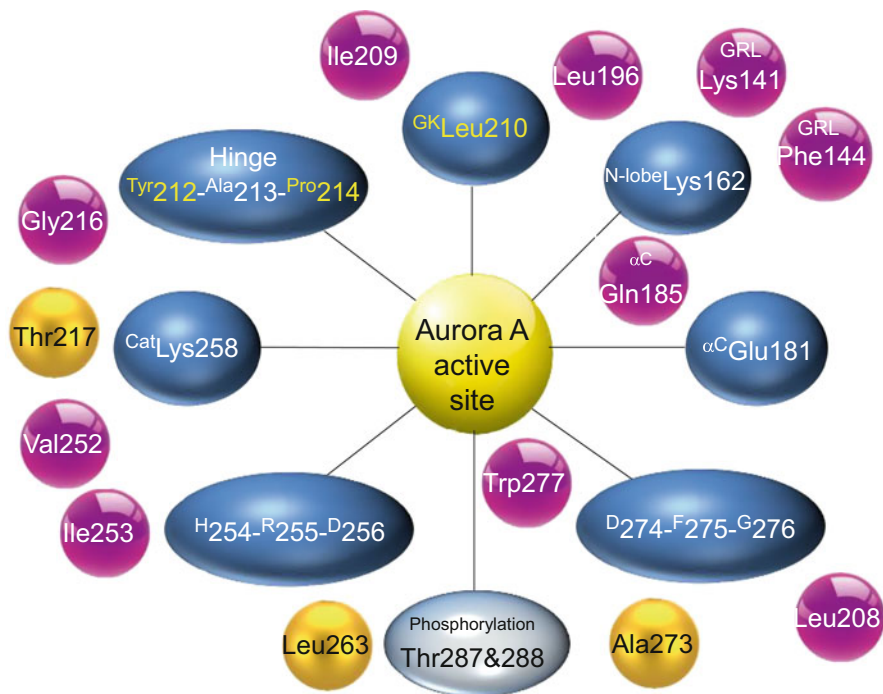


Fig. 3 KMM of Aurora A with *privileged* residues indicated

oncology projects, leveraging interactions with specific protein residues, active and inactive conformations, and stable/unstable water molecules in the ATP cleft.

2 Discovery of an Exquisite Selective Aurora Inhibitor as Neo-Cytotoxic Agent

The Aurora kinases exist as three isoforms (A, B, C), belong to the serine/threonine protein kinase family, and regulate cell division. The Aurora kinases are expressed and active predominantly during the G2/M phase of the cell cycle [31]. These kinases are involved in the control of the centrosome and nuclear cycles and have essential functions in mitotic processes such as chromosome condensation, spindle dynamics, kinetochore-microtubule interactions, chromosome orientation, and establishment of the metaphase plate. Each Aurora isoform has its own function during mitosis in line with its specific distinct localization, namely, the centrosomes and spindle poles for Aurora A and the centromeres and spindle mid-zone for Aurora B. Aurora A and Aurora B kinases are expressed in all dividing cells, whereas Aurora C kinase is mainly expressed in the testes and plays a role in spermatogenesis [32–34].

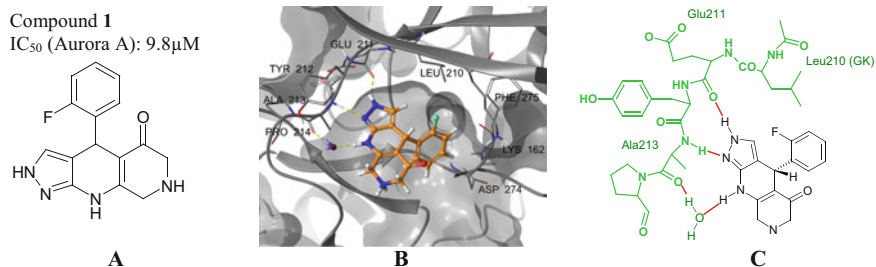
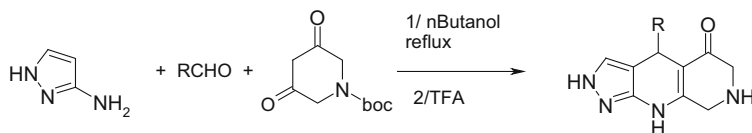


Fig. 4 Inhibition of Aurora A by compound **1**; (a) 2D structure of compound **1** and its activity on Aurora A; (b) X-ray structure of compound **1** (displayed with carbon atoms in orange) bound to Aurora A; surface of Aurora A ATP-pocket is displayed in grey. (c) 2D scheme of compound **1** (black) bound to Aurora A and a bridging water molecule (green). Hydrogen-bonds are represented as red lines

The Aurora kinases have been found aberrantly expressed in several solid tumors (bladder, breast, gastro-intestinal, liver, pancreatic, and thyroid) and in hematopoietic malignancies such as acute myeloid leukemia (AML), chronic myeloid leukemia (CML), multiple myeloma (MM) and lymphomas. Moreover, Aurora A and B overexpression has been associated with poor prognosis in ovarian carcinoma and non-small cell lung cancer, respectively. Also, *Aurora A* gene has been detected amplified in 50% colon, 25% ovarian, 12% breast, more than 90% pancreatic, and 50% bladder carcinomas. In tumors, Aurora A overexpression correlates with aneuploidy and Aurora B with genomic instability [34–36].

These observations have lent interest to this family of kinases as potential drug targets for the development of new anti-cancer therapies [37]. At the time we embarked in a discovery program to identify novel Aurora inhibitors, several compounds with various levels of selectivity either with respect to Aurora A vs Aurora B or regarding off-target kinases were advancing into preclinical phases or early clinical trials [38]. Our objective was to design and develop exquisitely selective inhibitors of the Aurora proteins in order to assess the intrinsic efficacy and tolerance of such neo-cytotoxic agents in relevant pharmacological tumor models.

Based on a pharmacophoric model established from publicly reported X-ray structures of Aurora A, about a million of internal compounds were screened in silico for their ability to match at least partially the model with the requirement to potentially interact with the hinge residues (e.g., Ala 213, Fig. 2b) [39]. After several runs of docking studies and probabilistic analysis, a set of 3,500 compounds was selected for assessing in vitro their inhibition potency of the Aurora kinase activity at 10 μM. Among the few chemical series which emerged in this assay with decent activity, our interest rapidly focused on the 1,2,4,6,7,8-hexahydro-5H-pyrazolo [3,4-b]-[1,7]naphthyridin-5 series represented by compound **1** which displayed hints of selectivity when tested at 20 μM against a panel of kinases (Fig. 4a). This chemical class was selected for further exploration despite modest affinity of **1** on Aurora A but considering a satisfactory ligand efficiency (LE = 0.33) and a



Scheme 1 Synthesis of a library of analogs of compound **1**, using a one-step three-component Hantzsch reaction

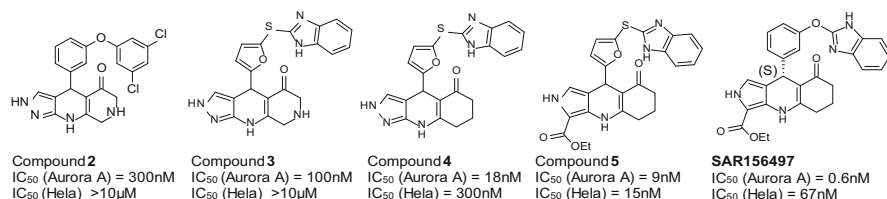


Fig. 5 2D structures of compounds from the tricyclic series, with their inhibitory activity on Aurora A as well as their activity in HeLa cell proliferation assay

promising selectivity profile. Co-crystallization trials were promptly initiated in order to define the binding mode of this rather unusual class of kinase inhibitors.

The 3D structure elucidation of **1** in complex with Aurora A protein highlighted the molecule in the *S*-configuration bound in the ATP site (Fig. 4b) and interacting with the hinge residue Ala213 via the central ring NH through a bridging water molecule and via the pyrazole moiety. Compound **1** developed an additional hydrogen bond with Glu211, at the vicinity of the gatekeeper residue, again with the pyrazole (Fig. 4c). Looking at the conformation of the complex, the DFG moiety was found positioned “mid-in / mid-out,” the phenylalanine side chain of Phe275 being oriented toward the *N*-lobe and in contact with the α C-helix, the latter being shifted compared to a canonical active conformation, and the salt bridge between the ^{Nlobe}Lys162 and the α C-helix^{Glu181} being disrupted. Therefore, the observed conformation of the complex with **1** was considered as non-competent or inactive [40].

As this chemical series is readily accessible in a one-step three-component Hantzsch reaction, a library of analogs of **1** was produced in a racemic form using various aldehydes (Scheme 1).

Extension of the aryl moiety on the tricyclic core turned out to produce more active derivatives (e.g., compounds **2** and **3** in Fig. 5) displaying also enhanced selectivity for Aurora A (IC₅₀ > 10 μM against a panel of about 30 kinases tested). Co-crystallized in Aurora A, compound **3** exhibiting the *S*-configuration adopted a similar binding mode compared to **1** at least regarding the tricyclic core in interactions with the hinge. However, the DFG motif was unequivocally oriented in the *in* configuration and the thio-benzimidazole group expanded into the hydrophobic back pocket behind the gatekeeper residue (Leu210). Interestingly, the benzimidazole moiety was engaged in a double interaction with ^{Nlobe}Lys162 and α C-helix^{Gln185}, a privileged residue, preventing the salt bridge formation (Fig. 6a) and the close

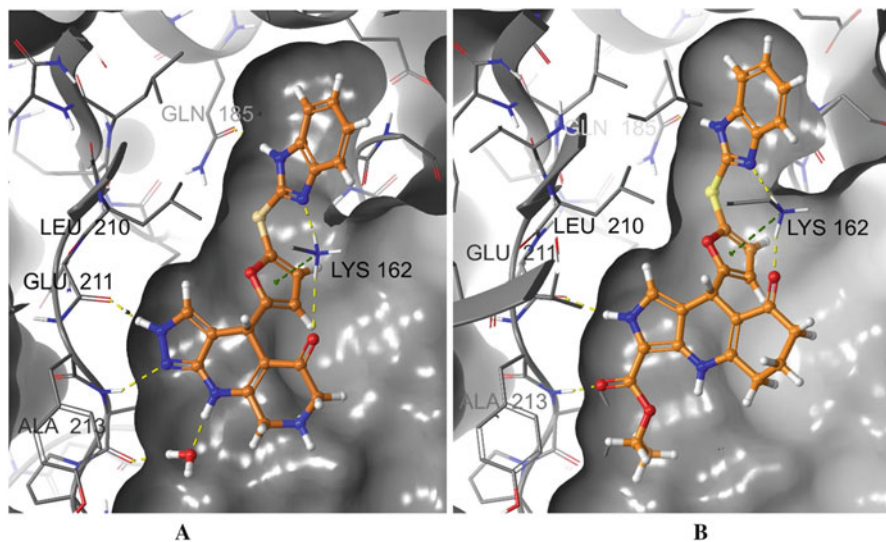


Fig. 6 (a) Compound **3** in Aurora A. (b) Compound (+)-**5** in Aurora A ($IC_{50} = 4$ nM)

contact of the αC -helix to the ATP cleft. This conformation called *αC -helix out* has been also reported to be the very specific inhibitory mechanism of lapatinib against Her2 and EGFR [30].

Despite decent potency vs Aurora A, compound **3** was devoid of any anti-proliferative activity when tested against a limited panel of cancer cell lines. Subsequent gain of affinity was obtained by removing the nitrogen atom in the pyridinone ring despite structural evidence of its involvement in an H-bond with a water molecule in the binding pocket. The resulting molecule (compound **4**, Fig. 5), a low double digit nanomolar Aurora A inhibitor, blocked Hela proliferation at 300 nM (IC_{50}). Compound **4** exhibited also a potent affinity for Aurora B ($IC_{50} = 5$ nM) and otherwise was shown to be totally inactive against other kinases tested (except Tie2, $IC_{50} = 3$ μ M).

In a second round of chemical optimization, the pyrazole moiety was modified, and the 2-ethoxycarbonyl-pyrrole group emerged as being the most productive substitution in terms of anti-proliferative potency in Hela cells (compound **5**, Fig. 5), whereas biochemical activity was only slightly improved compared to **4**. Compound **5** was resolved by chiral chromatography, and the dextrogyre enantiomer (+)-**5** (S-configuration) was identified as the active substance of the racemic mixture: Aurora A, $IC_{50} = 4$ nM; Aurora B, $IC_{50} = 2$ nM; and Hela cells, $IC_{50} = 2$ nM (the levogyre enantiomer was inactive). The binding mode of (+)-**5** in Aurora A was characterized to be very similar to the one observed for three but with two major differences. First, the hinge Ala213 NH was directly involved in an H-bond with the carbonyl of the carboxylate moiety (no water bridge). Second, the ^{Nlobe}Lys162 interaction with the benzimidazole-N was stabilized via a second interaction with a water molecule. Compound (+)-**5** was measured equipotent on the three Aurora

isoforms (Aurora C, $IC_{50} = 4$ nM) but otherwise totally inactive ($IC_{50} > 10$ μ M) on all other kinases tested. Our hypothesis to explain such high and rare level of selectivity shared by compounds **4**, **5**, and other analogs made in the series relies first on the fact that the α C-helix out conformation is not accessible to a broad ensemble of kinases for ligands/inhibitors [26]. Key determinants which would drive the occurrence of this inactive kinase conformation remain unclear but may be related to the gatekeeper size and the packing forces developed along the hydrophobic spine [41]. In the case of compounds **3** and **5** in complex with Aurora A, the benzimidazole core interacts with a glutamine residue (Gln185) localized in position “ α C-helix glutamate + 4,” a reported privileged residue/position. We analyzed among the kinome the occurrence of a glutamine in this position and found it rare at 2%.

Compound (+)-**5** was able to inhibit both Aurora A and Histone-H3 phosphorylation in HCT116 cell lines ($IC_{50} = 70$ and 10 nM, respectively), two relevant biomarkers of Aurora A and B inhibition to monitor pharmacodynamic modulation in vitro and in tumor models. Moreover, this compound displayed low nanomolar anti-proliferative activities against a large panel of cell lines and exhibited no toxicity on quiescent PBL cells providing evidence that targeting Aurora isoforms triggers specific and lethal effects on cancer cell lines but no damage on non-proliferative normal cells. Drug-likeness liabilities of compound (+)-**5** (Cyp inhibition, exposure in rats, hepatocyte clearance, and PDE3 inhibition) were then optimized to give rise to **SAR156497**, a molecule which has demonstrated a narrow therapeutic window when tested in a murine model of human colon adenocarcinoma xenograft [39].

3 Development of a Selective MET Kinase Inhibitor Active Against Oncogenic Mutants

MET is a tyrosine kinase which is involved in embryonic development and wound healing in normal cells. MET acts as a transmembrane receptor which is stimulated by the hepatocyte growth factor (HGF) inducing *in fine* cell proliferation, migration, and invasion [42]. Abnormal activation of the HGF-MET pathway has been frequently observed in human cancers in particular in solid tumors where MET protein is usually overexpressed [43]. Moreover, *MET* gene has been found amplified in 5–12% of gastric carcinoma, 2–13% of lung cancers, and 4–12% of colon-rectal carcinoma. Oncogenic mutations of the *MET* gene have been observed in multiple human cancer types (hepatocellular, papillary renal cell and head and neck carcinoma, etc.) leading to protein structure changes and activation [44]. Five major mutants of the kinase domain have been expressed in our group and tested for catalytic activity and have exhibited a four- to five-time enhancement of catalytic activity (Kcat) compared to the wild-type protein (internal data – Fig. 7a for mutation locations). Whereas Y1230H, Y1235D, L1195V, and H1094Y are mutated residues located at the vicinity of the ATP binding site (Figure 7b for the KMM representation), M1250T is remote to the ATP binding cleft and may influence catalytic

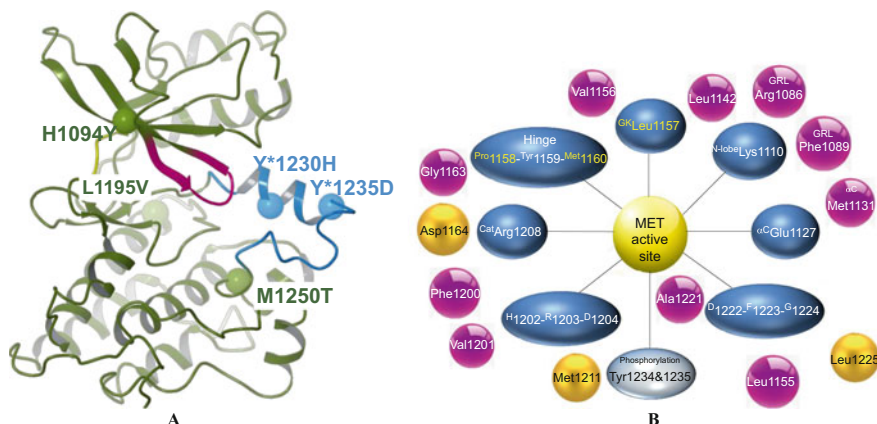
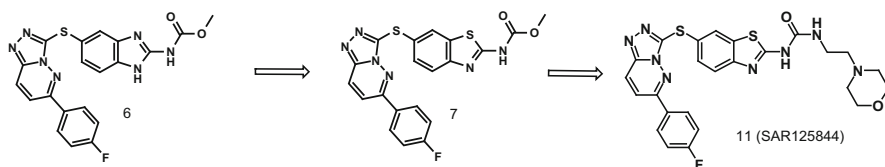


Fig. 7 (a, b) KMM of MET



Scheme 2 From hit to candidate

activity by allosteric effects [45]. MET activation has been reported to promote tumor initiation, metastasis, angiogenesis, and resistance to diverse therapies, including against anti-EGFR cancer agents [46].

To date, there is no selective MET inhibitor that is FDA-approved. Crizotinib (Xalkori) was originally tested in MET deregulated lung cancer patients but obtained its primary registration as ALK inhibitor in ALK translocation-positive NSCLC [47]. Several orally bioavailable MET tyrosine kinase inhibitors are currently in advanced clinical trials [48]. We will describe thereafter the discovery process which allowed the identification of **SAR125844**, an exquisite selective MET inhibitor investigated in phase II clinical trials for MET-amplified NSCLC patients (<https://clinicaltrials.gov/ct2/show/NCT01391533>).

From a two-step screen of a limited set of in house compounds, a hit (**cpd 6**, Scheme 2) was identified with low nanomolar potency against wild-type (WT) MET ($IC_{50} = 10$ nM), but this molecule also exhibited a marked affinity for tubulin, a major constituent of the cytoskeleton involved in DNA segregation, leading then to off-target cytotoxicity in non-MET-dependent tumor cell lines [49, 50].

Compound **6** displayed otherwise no activity ($IC_{50} > 10$ μ M) against a panel of kinases tested, in particular CDK9 a key player in cell cycle regulation and gene transcription [51]. This potent and selective MET inhibitor, obtained in a rather straightforward manner by compound collection screen, exhibited the

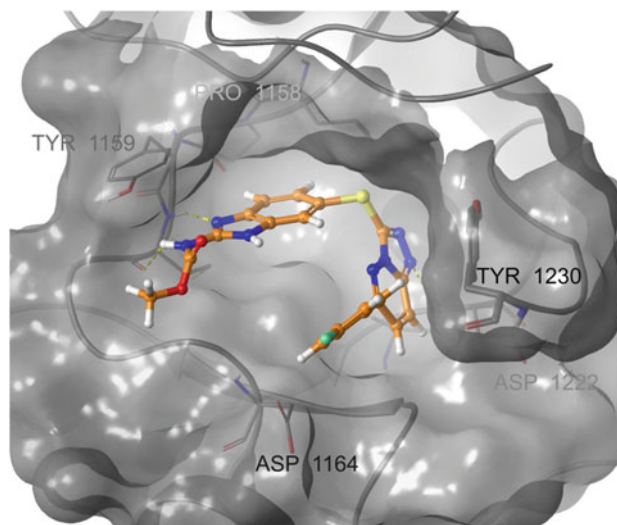
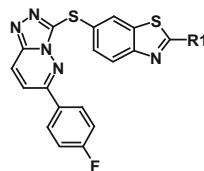


Fig. 8 Compound **6** (carbon atoms colored in orange) in MET ATP cleft

triazolopyridazine core, a chemical group introduced in this benzimidazole series in a historical anti-helminthic project developed in the 1980s in the company. Compound **6** could be co-crystallized in MET, and the 3D-structure of the complex was assessed. Structural analysis revealed compound **6** bound into the ATP pocket, developing in total three H-bonds, two with a hinge residue (Met1160), and one with the main-chain nitrogen atom of Asp1222 (DFG motif) via a nitrogen atom of the triazolopyridazine moiety. Moreover, the triazolopyridazine ring made a specific π - π interaction with Tyr1230 of the activation loop found in a non-competent conformation (Fig. 8). This specific binding mode involving Tyr1230 is believed to be a major driver of the selectivity for MET displayed by this chemical series and others [52]. Moreover, MET does not respect the general mode of kinase activation described by Taylor [16] since the salt bridge between Lys1110 and Glu1127 of the α -C Helix is disrupted (or not formed) as observed in the 3D structure of MET with a non-hydrolysable ATP analog (AMP-PNP) [53]. Instead α -C Helix Glu1127 interacts with Arg1227 of the A-loop which opens up an additional hydrophobic pocket exploited by ARQ197, a selective inhibitor of MET auto-phosphorylation [54]. In contrary to ARQ197, compound **6** did not disrupt the hydrophobic spine of MET formed by a stacking cascade of Leu1142, $^{\alpha\text{Helix}}$ Met1131, $^{\text{DFG}}$ Phe1223, and $^{\text{HRD}}$ His1202, but the α -C Helix was somewhat further displaced compared to the structure with AMP-PNP. The reported binding mode of **6** is shared with crizotinib, JNJ-38877605, SGX-523, and AMG-337, and other members of the so-called type I class of MET inhibitors [52].

The switch from the benzimidazole chemical scaffold to the benzothiazole core (compound **7**) dialed out affinity for tubulin and positive outcome in the Ames assay.

Fig. 9 2D representation of the common scaffold shared by compounds reported in Table 1



Subsequent incorporation of various chemical groups (amides, amines, carbamates, and ureas) in position 2 (R1, Fig. 9) of the benzothiazole scaffold gave rise to more potent compounds not only against WT MET but also vs the different mutants tested (Table 1).

In general, reduced affinity was measured vs the mutants tested compared to the WT protein which tolerated a broad range of substituents in this 2-position. Introduction of the morpholino-ethyl urea moiety led to the most active derivative of this sub-series in particular against the clinically relevant Y1230H mutant (cpd **11**; $IC_{50} = 204$ nM).

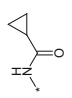
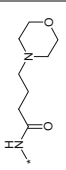
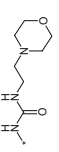
Attempts to co-crystallize compound **11** in WT MET turned out to be unsuccessful, but 3D co-structures were otherwise readily obtained with the selected MET mutants. Structural analysis of the three complexes with **11** revealed a very similar conformation (Fig. 10a), the ligand developing four conserved major hydrogen bonds in the ATP binding site, three with Met1160 and Lys1161 of the hinge, and one with Asp1222 of the DFG motif (Fig. 10b). However, the activation loop segment bearing residue 1,230 was not visible in any structure generated. Our hypothesis at least regarding Y1230H was that the strong π - π interaction observed in the WT protein between Tyr1230 and **11** was affected in the case of His1230 preventing stabilization of the activation loop and leading to reduced affinity for this mutant.

Potency against the Y1230H mutant could be significantly enhanced by modification of the substituent attached to the triazolopyridazine core. In particular replacement of the para-fluorophenyl moiety by a thiophene afforded the most potent derivative (**12**, Fig. 11a) vs Y1230H mutant ($IC_{50} = 23$ nM) which could be co-crystallized in the mutant protein. 3D co-structure analysis detected a clear positioning of the histidine residue (Fig. 11b), and the triazolopyridazine plane of **12** was twisted outward by $\sim 20^\circ$ compared to its position in the crystal structure of compound **6** in WT protein (Fig. 11c) [50].

High potency of **12** against MET Y1230H mutant could then be rationalized by more productive hydrophobic contacts between H1230 and the triazolopyridazine-thiophene segment which is planar compared to the skewed nature of the triazolopyridazine-p-fluorophenyl one.

Compound **11** was eventually selected as a candidate for development with respect to its eADME properties, its overall PK profile, and observed pharmacological effects in MET driven tumor models [55]. SAR125844 (**11**) displayed a favorable tolerance profile and preliminary evidence of antitumor activity in phase I

Table 1 Biochemical and cellular activities of compounds 8, 9, 10 and 11

Compound	R1	P-MET WT IC ₅₀ (nM)	MKN-45 proliferation IC ₅₀ (nM)	L1195V IC ₅₀ (nM)	M1250T IC ₅₀ (nM)	Y1230H IC ₅₀ (nM)	logD (pH 7.4)
8	NH ₂	10	81	9,000	245	>10,000	>4.6
9		3	7	61	13	883	4.7
10		6	12	318	93	1,172	4.3
11 (SAR125844)		4	7	64	6	204	4.2

P-MET WT: IC₅₀ measured using protein phosphorylation in a biochemical assay. MKN-45 Proliferation: IC₅₀ measured in proliferation assay using MKN-45 cell line. L1195V, M1250T and Y1230H: IC₅₀ measured using corresponding MET mutants in a biochemical assay. logD measured experimentally by high performance liquid chromatography (HPLC) (Xterra MS C18 column)

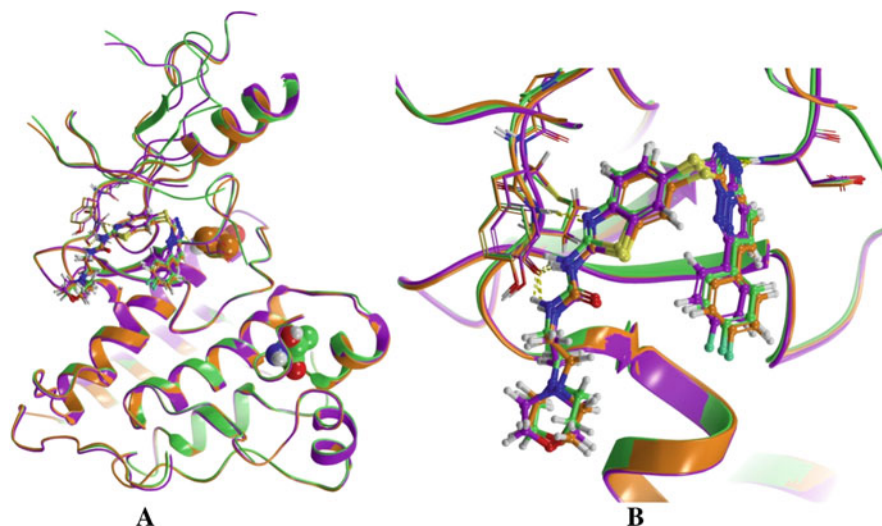


Fig. 10 Superimposition of co-crystal complexes of compound **11** bound to MET Y1230H (purple), MET L1195V (orange), and MET M1250T (green). (a): Mutated residues are displayed as CPK, when visible. (b): Focus on the ATP-binding pocket, highlighting a conserved binding conformation of compound **11** in the three mutant proteins

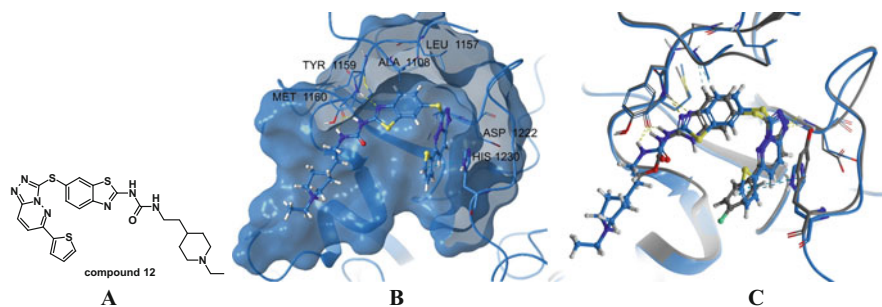


Fig. 11 (a) 2D structure of compound **12**. (b) Co-crystal of compound **12** bound to the ATP-binding pocket of MET Y1230H. (c) Superimposition of co-crystal complexes of compound **6** bound to MET WT (carbon atoms colored in grey) and of compound **12** bound to MET Y1230H (carbon atoms colored in blue). Residue 1,230 is on the right-hand part of the picture

patients which triggered the decision to evaluate the drug in a phase II clinical trial in MET-amplified NSCLC patients (NCT02435121) [56].

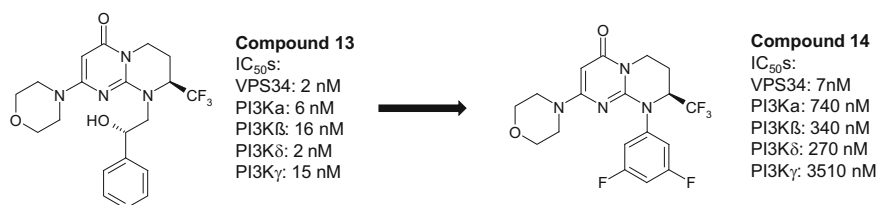
4 Design of Specific VPS34 Inhibitors for Autophagy Blockade in Tumors

VPS34 (also known as PIK3C3) is a lipid kinase of the class III PI3K (phosphoinositide 3-kinases) isoform which specifically catalyzes the phosphorylation of phosphatidylinositol (PtdIns) generating (PtdIns)3P [57]. VPS34 is the catalytic subunit of different complexes which associates the regulatory subunit Vps15 (also known as p150) for activity and several accessory subunits. Vps15 is myristoylated allowing the VPS34 protein complex to be anchored to intracellular membranes. Membrane-bound PtdIns3P binds to proteins which are involved in the formation of autophagosomes and participate also in endosomal trafficking from early to late endosomes [58, 59].

VPS34 plays an active role in the autophagy process by which cells adapt to protect themselves from metabolic stresses and hypoxic conditions. Autophagy is thought to be a process by which cancer cells develop resistance against chemotherapy and radiotherapy treatments. VPS34 has hence emerged as a new promising approach for cancer treatment as a single agent or in combination and recently as a target for insulin resistance in type 2 diabetes [60].

At the time we embarked in a drug discovery project in this field, no selective VPS34 inhibitors were known in the literature [61], and research studies were reported with pan PI3K inhibitors reflecting the high similarity in sequences between classes of PI3K (I-III) [62]. Using a phenotypic screen [63], the pyrimidinone hit **13** was identified with regard to its ability to inhibit (PtdIns)3P production in a transfected Hela cell line (IC_{50} , 1 nM). However, this molecule displayed a poor selective profile, being equally potent vs VPS34 than vs the four class I PI3K isoforms (Scheme 3) [64].

Further analog testing in the pyrimidinone series highlighted compound **14** as a more interesting starting point for chemical optimization, keeping the same level of potency vs VPS34 but with improved selectivity. Compound **14** could be co-crystallized in VPS34 protein, and the 3D structure of the complex was elucidated with satisfactory resolution (3 Å-Fig. 12a). Compound **14** interacted in the ATP site in a DFG-in conformation and developed key interactions with Phe684 (H-bond with the hinge), the N-lobe Lys636, and privileged residues, namely, Asp644 of the



Scheme 3 Selectivity profile of compounds **13** and **14**

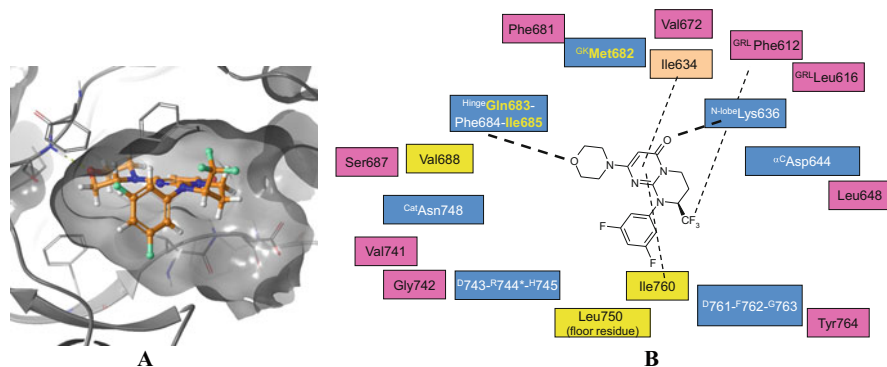
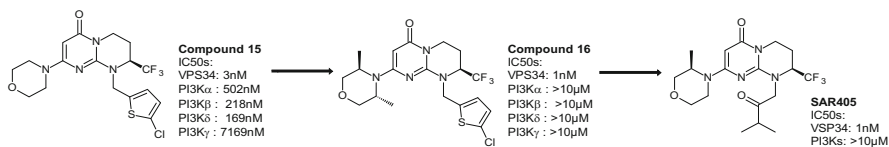


Fig. 12 (a) Compound **14** (carbon atoms colored in orange) in VPS34 ATP cleft, displaying a DFG-in conformation of the protein kinase. (b) Kinase motif map of VPS34 ATP site with cpd **14**. Of note, in VPS34 as in PI3Ks, the HRD motif is inverted (DRH), the ^{cat}Lys is mutated in ^{cat}Asn, and the α C-Glu replaced by a α C-Asp. The P-loop is poor in glycine residues therefore will not be referred as Gly-rich loop



Scheme 4 From hit to lead

α C-helix, the floor residue Leu750, the DFG-1 residue Ile760, and Phe612 in the P-loop (Fig. 12b).

Despite a significant impact of the lateral N-side chain structure on selectivity, it was not possible to totally dial out affinity vs PI3K δ in particular via chemical modifications at this position only (compound **14** and **15** profiles in Schemes 3 and 4). Therefore, we turned our attention to the morpholine hinge binding motif environment. There are few residues which differ in the active site of VPS34 vs the class I PI3Ks. In particular in the hinge region, both the gatekeeper and floor residues are mutated (Met vs Ile and Leu vs Met, respectively) offering potential levers for selectivity [64]. The introduction of two methyl groups on the morpholine gave rise to compound **16** exhibiting high potency on VPS34 and exquisite selectivity vs the PI3Ks and mTOR (Scheme 4).

Compound **16** was able to co-crystallize in VPS34, and a 3D structure segment is displayed in Fig. 13a. The shape of **16** positioned in the published X-ray structure of PI3K δ (PDB code, 2WXL, Fig. 13b) highlighted potential steric clashes near Ile825 (GK) on one hand and with Met900 (floor residue) on the other hand.

Multi-parametric optimization eventually led to the discovery of **SAR405** (Scheme 4) which affected vesicle trafficking and autophagy in cell lines and demonstrated sustained inhibition of the autophagy process in a murine tumor

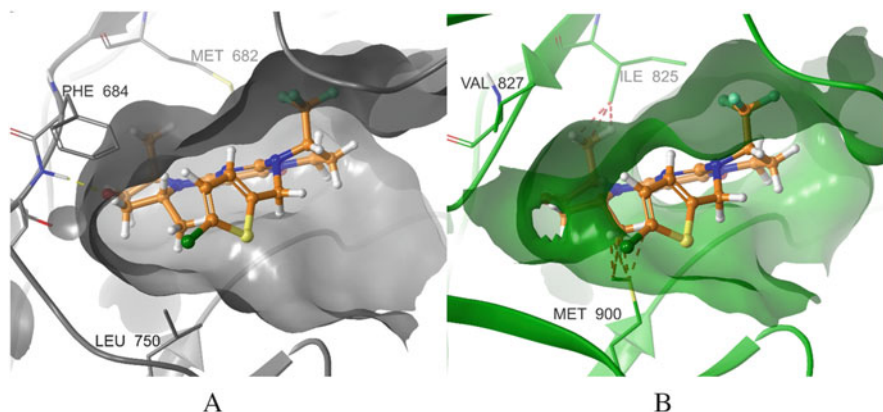


Fig. 13 (a) X-ray structure of compound **16** (displayed with carbon atoms in orange) bound to VPS34; surface of VPS34 ATP-binding pocket is displayed in grey. (b) Superimposition of co-crystal complex of compound **16** (carbon atoms colored in orange) bound to VPS34 and of X-ray structure of PI3K δ (PDB code 2WXL; protein carbon atoms and surface colored in green). VPS34 protein is not displayed. Steric clashes between compound **16** and residues Ile825 and Met900 of PI3K δ are depicted as red dotted lines

xenografted model [64, 65]. Moreover **SAR405** synergized with mTOR inhibitor everolimus for cell proliferation inhibition in renal carcinoma models [66].

5 PI3K β Inhibitor: Leveraging Water Molecules in the Active Site for Selectivity Enhancement

The class I PI3K lipid kinases are key mediators of the Akt pathway which they contribute to activate by phosphorylating the phosphatidylinositol-4,5-bisphosphate (PIP2) on the 3-position to form phosphatidylinositol-3,4,5-trisphosphate (PIP3) [67]. The class I PI3Ks comprises four isoforms PI3K α , PI3K β , PI3K δ , and PI3K γ which share high level of sequence identity. Whereas PI3K α , PI3K β , and PI3K δ (subclass IA members) can be activated by receptor tyrosine kinases or GPCRs, PI3K γ the single member of the subclass IB is activated by GPCRs. In addition, class IA PI3Ks are heterodimer enzymes composed of a p85 regulatory subunit and a p110 catalytic subunit harboring the kinase domain [68]. PIP3 then recruits PDK1 and Akt (PKB) at the membrane surface which allows phosphate transfer from PDK1 to Akt (on Thr308). Additional phosphorylation of Akt on Ser473 by mTORC2 results in full activation of Akt triggering downstream upregulation of effectors and elicits cellular processes as proliferation, angiogenesis, survival, and metabolism [69]. In normal cells, the Akt pathway is tightly regulated by the phosphatase and TENSin homologue (PTEN) which dephosphorylates PIP3 back into PIP2. In cancer cells, several activating genetic abnormalities have been detected in the Akt pathway such as gain of function mutations in *PIK3CA* gene, which encodes for the p110 α catalytic subunit of PI3K α , amplification of the *PIK3CA* gene, and deletion of the

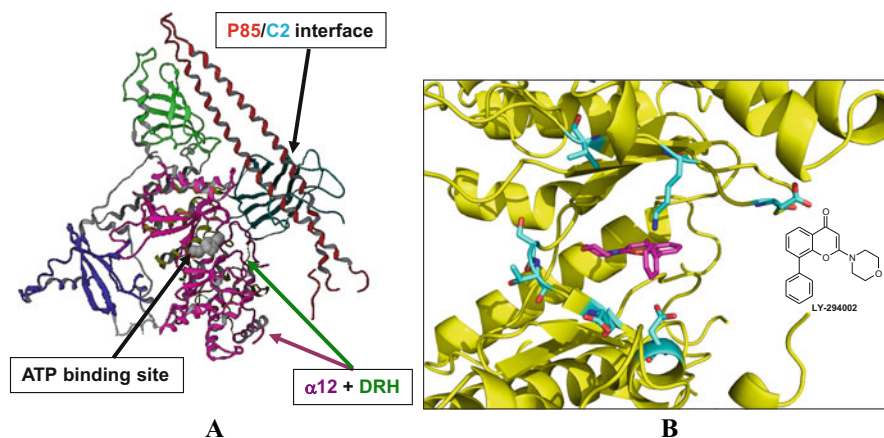


Fig. 14 (a) 3D view of p110 β /p85 interface. (b) LY-294002 docked in PI3K β active site (homology model)

tumor suppressor *PTEN* gene. Both *PIK3CA* somatic mutation and *PTEN* deletions are in general mutually exclusive [70]. *PTEN*-deficient cell lines have been demonstrated to depend on PI3K β activity as downregulation of the *PIK3CB* gene by shRNA led to cell growth and tumor growth inhibitions correlated with pAKT inhibition. In those cells, *PIK3CA* gene inhibition induced no effect regarding phosphorylation of AKT 473-residue [71].

As *PTEN* is deficient in many cancers including the most prevalent ones and those associated with the lowest survival rates (e.g., 23% occurrence in lung, 35% in colon, and 47% in gastric cancers) [72], it was relevant to engage a discovery program to identify selective PI3K β inhibitors, expecting a superior safety profile for such agents compared to the generation of pan-PI3K inhibitors which exhibited limiting adverse effects in clinical settings [73].

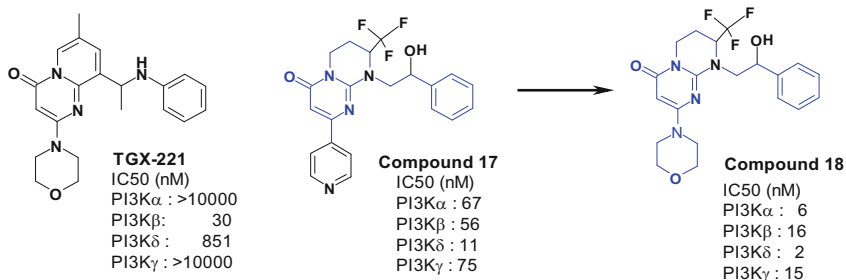
Our drug discovery strategy was to target the ATP site of PI3K β (p110 β) and to disregard other approaches such as protein-protein interactions inhibition. The disruption of the p110 β /p85 interface in the activated state of the protein complex via inhibition of the C2 (p110b) /iSH2 (p85) domains interaction [74] (Fig. 14a) was investigated but estimated to be of low probability of success due to computed limited drugability [75].

Sequence similarity analysis of the kinase domains of the four PI3K isoforms revealed that PI3K β shares 76% identity with PI3K δ , its closest isoform. Focusing on the ATP cleft per se, identity reaches 100% with PI3K α and PI3K δ . Only few residues differ across the four isoforms and are located at the ATP site entrance (Ser855, Thr856, Glu858, and Asp862) or in the P-loop (Lys777, Asp780, and Val789). These residues are highlighted in the PI3K β docking structure established in complex with LY-294002 [76], a well reported and widely used pan-PI3K inhibitor (Fig. 14b).

ligand protein interactions						
Kinase	GK	Hinge	Hinge	next to hinge	DFG-1	Floor residue
PI3K β	Ile851	Glu852	Val854	Glu858	Ile936	Met926
VPS34	Met682	Gln683	Ile685	Val688	Ile760	Leu750

active-inactive conformations control									
Kinase	hinge area	GK area	GK area	GRL	GRL	α Helix	DFG+1	HRD area	HRD area
PI3K β	Ser857	Val850	Cyst841	Met779	Met783	Leu817	His940	Ile917	Gly918
VPS34	Ser687	Phe681	Val672	Phe612	Leu616	Leu648	Tyr764	Val741	Gly742

Fig. 15 Comparative privileged residues of PI3K β vs VPS34. *GRL* glycine-rich loop

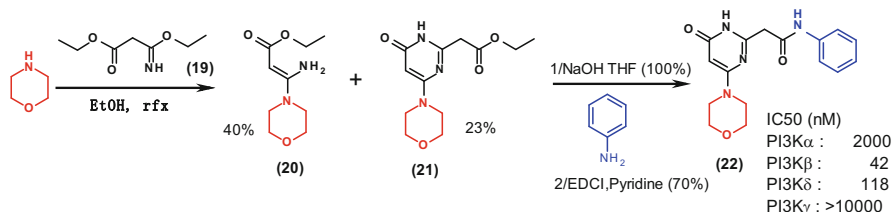


Scheme 5 Hit chemical exploration

It is worth noting that Glu858 is one of the privileged residues [23] of PI3K β (“next to hinge” residue) which is mutated in a valine (Val688) in VPS34 (Fig. 15). Overall, PI3K β and VPS34 share 27% identity and 40% homology with respect to the nature of these privileged residues (Fig. 15). It was therefore expected to identify PI3K β inhibitors with no off-target activity on VPS34 (and vice versa).

Rather than embarking in an *ab initio* drug design approach for hit finding, we decided to leverage high-throughput screens performed with our in-house compound collection on PI3K α and PI3K γ by testing resulting actives on PI3K β . Among them, our attention focused on compound **17**, a potent inhibitor of PI3K β (IC₅₀ = 56 nM) but also vs the other isoforms. Interestingly, compound **17** exhibited structural resemblance with TGX221 a publicly reported PI3K β selective inhibitor (Scheme 5). Tested against a panel of kinases, compound **17** showed potency against CDKs in particular and low nanomolar inhibition of VPS34 as a close analog of the aforementioned compounds **13–16**. Replacement of the pyridinone group on the bicyclic scaffold afforded compound **18**, still a pan-PI3K inhibitor but otherwise selective vs the other kinases tested, including the CDKs, VPS34, and mTOR, and except DNA-PK.

Further chemical exploration of this bicyclic pyrimidinone series did not really succeed in gaining selectivity towards PI3K β . Fortunately, in an attempt to synthesize the malonate derivative **20**, excess of reagent **19** offered the pyridinone **21** as a by-product which was then modified into anilide **22** to reflect TGX-221 structure (Scheme 6). To our delight, compound **22** turned out to be potent on PI3K β and reasonably selective vs PI3K δ [77].



Scheme 6 Chemical synthesis of compound 22

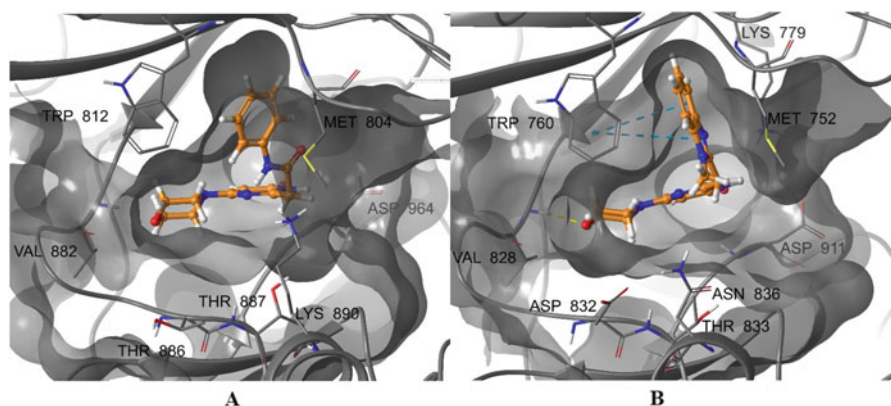
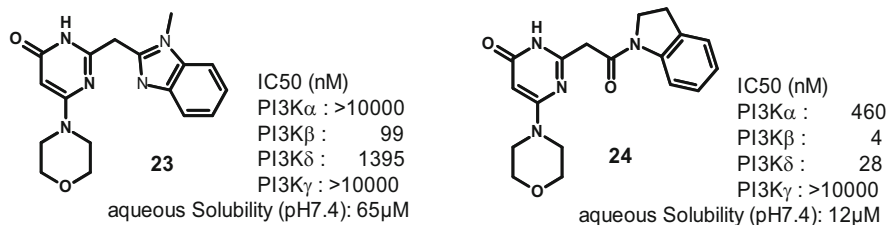


Fig. 16 (a) Compound **22** co-crystallized in PI3K γ . (b) Compound **23** co-crystallized in PI3K δ . Ligand carbon atoms are colored in orange

To rationalize the observed selectivity and potency, compound **22** was co-crystallized in PI3K γ , which served as structural platform at the time the compound was synthesized, despite no inhibitory activity measured on this isoform (IC₅₀ > 10 μ M). Interestingly compound **22** exhibited a different mode of binding compared to LY-294002, adopting a propeller shape as previously described for the selective PI3K δ inhibitor PIK-39 in complex also with PI3K γ despite again no activity on this isoform [78]. In the co-crystal, compound **22** interacted classically with the hinge Val854 NH residue via the morpholine oxygen, but more interestingly the phenyl group was projected towards the P-loop in the so-called selectivity pocket resulting from a movement of Met804 (Fig. 16a), a conserved residue across the PI3Ks.

Compound **22** and other anilide derivatives suffered from lack of in vivo stability due to rapid cleavage of the amide bond. We next generated a series of benzimidazoles derivatives and identified compound **23** as advanced lead for the project [77]. The 3D-structure of compound **23** in complex with PI3K δ could be obtained and confirmed the binding mode of **22** observed in PI3K γ . Similarly, the corresponding methionine residue of γ Met804 in the P-loop (δ Met752) changed its conformation compared to its position in the apo-structure, leaving space for the



Scheme 7 in vitro profile of compounds **23** vs **24**

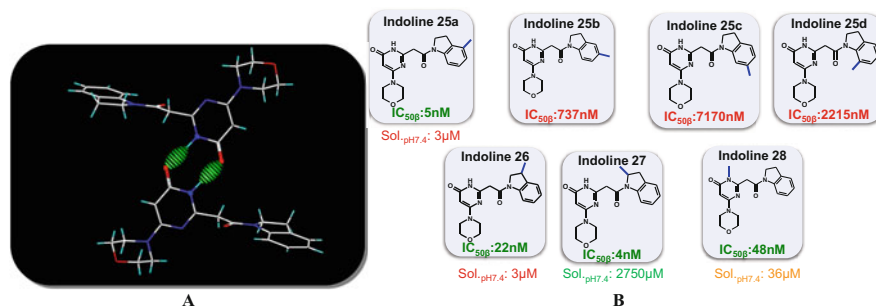
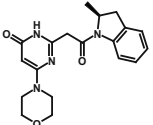
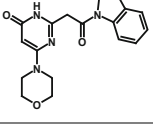


Fig. 17 (a) X-ray crystal structure of **24**. (b) Outcome of the methyl scan approach

methyl-benzimidazole moiety to bind in the created selectivity pocket delineated on the other hand by another conserved residue, namely, Trp760. However limited aqueous solubility and modest on-target potency precluded further development of compound **23** which chemically evolved then towards the more active but still poorly water-soluble pyrrolidine derivative **24** (Scheme 7). Improvement of potency on PI3K β for **24** was translated into potent pAkt inhibition in PTEN-deficient PC3 cell line, superior to **23** (IC₅₀ = 15 nM vs 65 nM). The indoline **24** structure is associated with a moderate experimental logP (1.4); therefore, the lack of solubility in the thermodynamic conditions tested was attributed to potentially high-energy packing forces in its solid form in line with the high melting point value measured with the produced batch (mp = 285°C).

The X-ray crystal structure of compound **24** was solved from single diffraction data. Crystal packing analysis underlined the formation of dimers via head-to-tail alignments through donor-acceptor N – H \cdots O contacts (2.74 Å) between pyrimidone moieties (Fig. 17a). Close interconnection of molecules was further favored both by indoline π -stacking and indoline/morpholine C – H \cdots π interactions. It was then postulated that solubility in the series could be enhanced by introduction of substituents (e.g., methyl group) which would disrupt such network of inter molecule interactions. We embarked then in methyl scan chemistry approach supported by molecular modeling calculations which highlighted several positions in the **24** chemical structures which would tolerate substitution.

Table 2 Biochemical activities of compounds (R)-**27** and (S)-**27** on five kinases, in nM

Compound	Structure	PI3K α (IC ₅₀)	PI3K β (IC ₅₀)	PI3K δ (IC ₅₀)	PI3K γ (IC ₅₀)	pAkt inh. PC3 (IC ₅₀)
(S)- 27		1,000	23	468	10,000	49
(R)- 27		569	6	6	3,315	12

Methylation of the phenyl ring was tolerated by the PI3K β binding site only in position 4 (indoline **25a**, Fig. 17b), but no improvement of solubility was noticed. Methylation of the pyrimidinone core (indoline **28**) was tolerated regarding activity, slightly increased solubility compared to **24**, but this avenue was dismissed since it introduced a metabolic hot spot. Methylation in position 3 had no effect in contrary to position 2 which brought an outstanding improvement of solubility. The racemic indoline **27** was separated into its two pure enantiomers, and another unexpected finding was obtained: the (R)-isomer-**27** was found equipotent on PI3K β and PI3K δ , whereas the (S)-isomer-**27** retained selectivity vs PI3K δ but at the expense of activity on PI3K β (Table 2).

Whereas PI3K β had been refractory to intensive efforts deployed in house and elsewhere to find conditions and constructs in order to obtain crystals of the kinase domain [74], we finally succeeded and reported for the first time the X-ray structure solved at 2.8 Å of a propeller shaped ligand ((S)-**27**) in complex with p110 β (<http://www.rcsb.org/structure/4BFR>). Moreover (S)-**27** could be also co-crystallized in PI3K δ (2.6 Å), and we realized that both co-structures were extremely similar (Fig. 18) despite one log difference in biochemical activity exhibited by (S)-**27** (Table 2) [79].

The two co-structures obtained were otherwise very consistent with those previously collected in the pyrimidinone series using PI3K γ as a surrogate protein (e.g., Fig. 16a) and for other publicly reported propeller-shaped selective ligands [80]. With respect to PI3K β , key and common observations were interaction of the morpholine moiety with the hinge region via the main-chain nitrogen of Val848, movements of the P-loop Trp781 and Met773 opening a specific pocket where the indoline moiety stacks.

From these findings emerged the following paradoxes:

1. A similar conformational change can occur across the different PI3K isoforms to create a specific pocket.
2. Biochemically inactive but propeller-shaped molecules can co-crystallize in PI3Ks and occupy the so-called selectivity pocket.

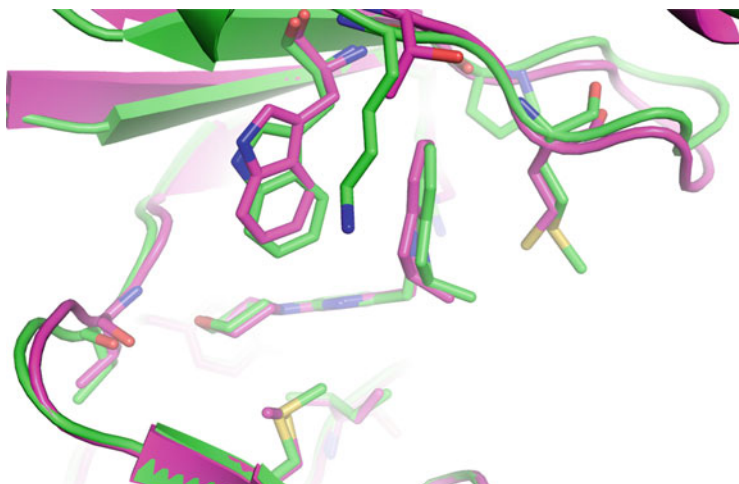


Fig. 18 3D-structure overlay of compound (S)-27 co-crystallized in PI3K β vs PI3K δ

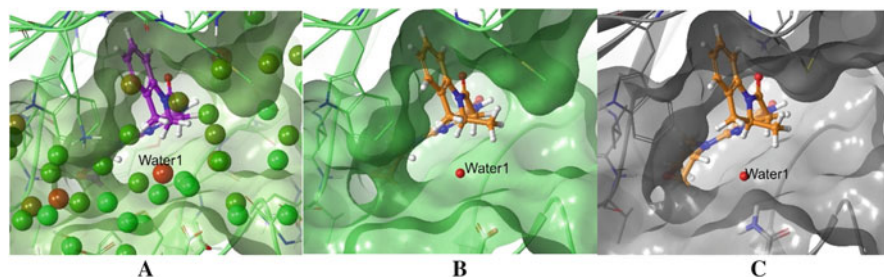


Fig. 19 (a) **24** in PI3K β . (b) (S)-**27** in PI3K β . (c) (S)-**27** in PI3K δ

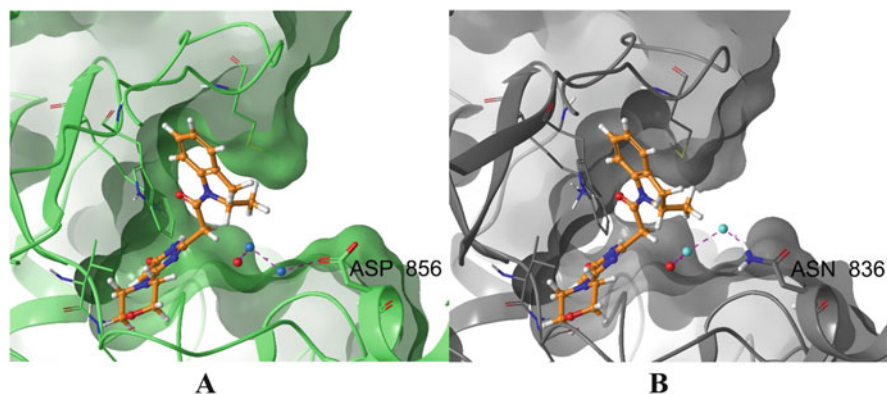
3. All the selectivity pocket residues in interaction with the propeller-shaped ligand are extremely conserved across the PI3K isoforms.

To tentatively rationalize at least the unintuitive observed selectivity profile of (S)-**27** vs (R)-**27**, we further explored the two 3D co-structures collected with (S)-**27** in PI3K β and PI3K δ and embarked in molecular dynamics simulations, solvent clustering, and statistical thermodynamic analysis using the WaterMap methodology [81] in order to investigate the network of water molecules at the vicinity of the ligand (<7 Å) and assess their respective entropy, enthalpy, and free energies [82]. With this algorithm, regions of high water density are identified as “hydration sites,” and their corresponding enthalpies and entropies are computed relative to bulk solvent using inhomogeneous solvation theory.

Using WaterMap calculations, a large number of water molecules were predicted to be present around the non-methylated ligand **24** (Fig. 19a), but one drew our attention as it was associated with high positive free energy (+6.0 kcal/mol) and

Table 3 Calculated free energies of binding in kcal/mol relative to **24** with WaterMap (WM)

Compound	$\Delta\Delta G$ WM PI3K β	$\Delta\Delta G$ WM PI3K δ
(S)- 27	-0.04	0.84
(R)- 27	-0.45	-3.59

**Fig. 20** Results of watermap calculations performed with (S)-**27** bound to PI3K β (A) and PI3K δ (B). Hydrogen-bond network through water molecules (blue spheres) between Water1 (red sphere) and ASP856 (in PI3K β) or ASN836 (PI3K δ) is depicted as magenta dashed lines

therefore considered highly unstable [83]. Interestingly, this water molecule (that we will call Water1) was computed to be located in proximity to the 2-position of the indoline core and equi-energetically present in PI3K δ (+5.8 kcal/mol). Visual inspection of the 3D structure established by WaterMap suggested that any substituent in the indoline 2-position with R or “down” stereochemistry would be perfectly suited for displacing Water1 leading to gain in free energy of ligand binding. WaterMap calculations with (S)-**27** recapitulated the same observation as for **24**; an unstable water molecule (Water1) is trapped by the (S)-ligand in the active site (Fig. 19b) decreasing its affinity (ΔG) vs the (R)-enantiomer which displaces it (Table 3). To reinforce the validity of this hypothesis, it is worth mentioning that computed free energies of binding were aligned in trends with the experimental ITC values collected (data not shown) not only for **24** and **27** but for a series of 2-substituted indoline analogs [83].

When applied to PI3K δ , Water1 was not only retrieved but also estimated to be even more instable (+6.7 kcal/mol vs +5.9 kcal/mol in the case of (S)-**27**). However, the respective free energy values are too similar to quantitatively explain the observed selectivity pattern of the two enantiomers. A favorable displacement of the water molecule in PI3K δ compared to PI3K β cannot solely explain why (R)-**27** is more potent and less selective.

To better assess the origin of this selectivity pattern, binding site water molecules and nearby residues in both PI3K β and PI3K δ were further analyzed. Water network originating from the unstable water molecule leads to a pair of residues that differ between the two isoforms. In PI3K β , Asp856 is connected to Water 1 through a

series of intermediate water molecules (Fig. 20a), whereas in PI3K δ , the equivalent residue is Asn836, which is also located at ~ 7 Å from the ligand and connected to Water1 via a similar network (Fig. 20b). Due to a more efficient charge transfer realized with Asp856 compared to the neutral Asn836, translated into more H-bonds to Water1, and shortest distances within the water network, PI3K β better tolerates the destabilizing influences of the methyl group in the (S)-configuration than PI3K δ , which encloses Water1 in a more hydrophobic environment, leading to the observed selectivity. Interestingly, this hypothesis reconnects to the privileged residue analysis [23] as Asp856 is one of them.

Compound (S)-27 became eventually SAR301260, a clinical development candidate tested in PTEN-deficient cancer patients [84].

6 Conclusions

Through the aforementioned projects which have been described, it was possible to identify and design very selective kinase inhibitors and dial out off-target affinity vs close kinase neighbors. If state-of-the art technologies were applied during the course of those projects (in biophysics, in modeling, etc.), serendipity in screens or in chemistry remained a significant contributor to these successful drug discovery programs. Moreover, exquisite selectivity was in certain circumstances rationalized a posteriori rather than guided (e.g., PI3K β). Still, the key protein elements or ligand properties which were identified to obtain and improve selectivity in one case or another have served subsequent kinase projects in our group and knowledge increased by experience for better efficiency. It is worth mentioning that other types of mechanisms of inhibition than acting directly in the conserved ATP cleft have been rarely explored or exploited in the kinase area [85, 86]. Only few kinases exhibit a true allosteric site (e.g., ABL) which could have been targeted to design a more specific generation of kinases inhibitors. In addition, to the best of our knowledge, approaches which were based on protein-protein interactions inhibition have failed to afford potent inhibitors except in the case of Akt [87]. Further investigations in new assay developments for hit-finding based, for example, on protein conformation changes [88] or in silico calculations to detect potential additional binding sites [89], should open new avenues for selective and specific kinase inhibitor discovery and development.

Compliance with Ethical Standards

Conflict of Interest: All authors are employees of Sanofi R&D and may hold stock in the same. All authors declare no conflict of interest.

Funding: All studies were funded only by Sanofi R&D.

Ethical Approval: This chapter does not contain any studies with human participants or animals performed by any of the authors.

Informed Consent: No human studies are reported; no informed consent required.

References

1. Manning G, Whyte DB, Martinez R, Hunter T, Sudarsanam S (2002) The protein kinase complement of the human genome. *Science* 298:1912–1934
2. Roskoski R (2018) FDA-approved protein kinase inhibitors. <http://www.brimr.org/PKI/PKIs.htm>
3. Monoclonal antibodies approved by the EMA and FDA for therapeutic use. <http://www.actip.org/products/monoclonal-antibodies-approved-by-the-ema-and-fda-for-therapeutic-use/>
4. Giordano S (2008) *Curr Med Chem* 15:422–432
5. Serrano C, George S (2014) Recent advances in the treatment of gastrointestinal stromal tumors. *Ther Adv Med Oncol* 6:115–127
6. Yan L, Rosen N, Arteaga C (2011) Targeted cancer therapies. *Chin J Cancer* 30:1–4
7. Jänne PA, Gray N, Settleman J (2009) Factors underlying sensitivity of cancers to small-molecule kinase inhibitors. *Nat Rev Drug Discov* 8:709–723
8. Knight ZA, Shokat KM (2005) Features of selective kinase inhibitors. *Chem Biol* 12:621–637
9. Schwartz PA, Murray BW (2011) Protein kinase biochemistry and drug discovery. *Bioorg Chem* 39:192–210
10. Morphy R (2010) Selectively nonselective kinase inhibition: striking the right balance. *J Med Chem* 53:1413–1437
11. Zhao Y, Adjei AA (2014) The clinical development of MEK inhibitors. *Nat Rev Clin Oncol* 11:385–400
12. Vogelstein B, Papadopoulos N, Velculescu VE, Zhou S, Diaz Jr LA, Kinzler KW (2013) Cancer genome landscapes. *Science* 339:1546–1558
13. Sullivan I, Planchard D (2017) Next-generation EGFR tyrosine kinase inhibitors for treating EGFR-mutant lung Cancer beyond first line. *Front Med*. <https://doi.org/10.3389/fmed.2016.00076>
14. Holderfield M, Deuker MM, McCormick F, McMahon M (2014) Targeting RAF kinases for cancer therapy: BRAF mutated melanoma and beyond. *Nat Rev Cancer* 14:455–467
15. Knighton DR et al (1991) Crystal structure of the catalytic subunit of cyclic adenosine monophosphate-dependent protein kinase. *Science* 253:407–414
16. Kornev AP, Haste NM, Taylor SS, Ten Eyck LF (2006) Surface comparison of active and inactive protein kinases identifies a conserved activation mechanism. *PNAS* 103:17783–17788
17. McClendon CL, Kornev AP, Gilson M, Taylor SS (2014) Dynamic architecture of a protein kinase. *PNAS* 111:E4623–E4631
18. Brewer MR, Yun CH, Lai D, Lemmon MA, Eck MJ, Pao W (2013) Mechanism for activation of mutated epidermal growth factor receptors in lung cancer. *PNAS* 110:E3595–E3604
19. Fratev FF, Jónsdóttir SO (2009) An *in silico* study of the molecular basis of B-RAF activation and conformational stability. *BMC Struct Biol* 9:1–17
20. Echeverria I, Liu Y, Gabelli SB, Amzel LM (2015) Oncogenic mutations weaken the interactions that stabilize the p110 α -p85 α heterodimer in phosphatidylinositol 3-kinase α . *FEBS J* 282:3528–3542
21. Peng W, Thomas EN, Mads HC (2015) FDA-approved small-molecule kinase inhibitors. *Trends Pharmacol Sci* 36:422–439
22. Wu P, Nielsen TE, Clausen MH (2016) Small-molecule kinase inhibitors: an analysis of FDA-approved drugs. *Drug Discov Today* 21:5–10
23. Martin E, Mukherjee P (2012) Kinase-kernel models: accurate *in silico* screening of 4 million compounds across the entire human kinome. *J Chem Inf Model* 52:156–170
24. Taylor SS, Kornev PA (2011) Protein kinases: evolution of dynamic regulatory proteins. *Trends Biochem Sci* 36:65–77
25. Zarrinkar PP et al (2008) A quantitative analysis of kinase inhibitor selectivity. *Nat Biotech* 26:127–132

26. Jacobs MD, Caron PR, Hare BJ (2008) Classifying protein kinase structures guides use of ligand-selectivity profiles to predict inactive conformations: structure of lck/imatinib complex. *Proteins* 70:1451–1460
27. Zarrinkar PP et al (2011) Comprehensive analysis of kinase inhibitor selectivity. *Nat Biotech* 29:1046–1051
28. Fabbro D, Cowan-Jacob SW, Moebitz H (2015) Ten things you should know about protein kinases. *Br J Pharmacol* 172:2675–2700
29. Palmieri L, Rastelli G (2013) α C helix displacement as a general approach for allosteric modulation of protein kinases. *Drug Discov Today* 18:407–414
30. Gilmer TM (2008) Impact of common epidermal growth factor receptor and HER2 variants on receptor activity and inhibition by Lapatinib. *Cancer Res* 68:571–579
31. Hochegger H, Hegarat N, Pereira-Leal JB (2013) Aurora at the pole and equator: overlapping functions of Aurora kinases in the mitotic spindle. *Open Biol.* <https://doi.org/10.1098/rsob.120185>
32. Saya H (2002) Roles of aurora A kinase in mitotic entry and G2 checkpoint in mammalian cells. *Genes Cells* 7:1173–1182
33. Lampson MA, Cheeseman IM (2011) Sensing centromere tension: aurora B and the regulation of kinetochore function. *Trends Cell Biol* 21:133–140
34. Quartuccio SM, Schindler K (2015) Functions of Aurora kinase C in meiosis and cancer. *Front Cell Dev Biol.* <https://doi.org/10.3389/fcell.2015.00050>
35. Katayama H, Brinkley WR, Sen S (2003) The Aurora kinases: role in cell transformation and tumorigenesis. *Cancer Metastasis Rev* 22:451–464
36. Goldenson B, Crispino JD (2015) The aurora kinases in cell cycle and leukemia. *Oncogene* 34:537–545
37. Tang A, Gao K, Chu L, Zhang R, Yang J, Zheng J (2017) Aurora kinases: novel therapy targets in cancers. *Oncotarget* 8(14):23937–23954
38. Keen N, Taylor S (2004) Aurora-kinase inhibitors as anticancer agents. *Nat Rev Cancer* 4:927–936
39. Carry JC, Clerc F, Minoux H et al (2015) SAR156497, an exquisitely selective inhibitor of aurora kinases. *J Med Chem* 58:362–375
40. Roskoski R (2016) Classification of small molecule protein kinase inhibitors based upon the structures of their drug-enzyme complexes. *Pharmacol Res* 103:26–48
41. Tong M, Seeliger MA (2015) Targeting conformational plasticity of protein kinases. *ACS Chem Biol* 10:190–200
42. Organ SL, Tsao MS (2011) An overview of the c-MET signaling pathway. *Ther Adv Med Oncol* 3(1 Suppl):S7–S19
43. Zhang J, Babic A (2016) Regulation of the MET oncogene: molecular mechanisms. *Carcinogenesis* 37:345–355
44. Tovar EA, Graveel CR (2017) MET in human cancer: germline and somatic mutations. *Ann Trans Med* 5(10):205. <https://doi.org/10.21037/atm.2017.03.64>
45. Dixit A, Torkamani A, Schork NJ, Verkhivker G (2009) Computational modeling of structurally conserved cancer mutations in the RET and MET kinases: the impact on protein structure, dynamics, and stability. *Biophys J* 96:858–874
46. Xu J, Wang J, Zhang S (2017) Mechanisms of resistance to irreversible epidermal growth factor receptor tyrosine kinase inhibitors and therapeutic strategies in non-small cell lung cancer. *Oncotarget* 8(52):90557–90578
47. Soria JC et al (2012) *ALK* translocation and crizotinib in non-small cell lung cancer: an evolving paradigm in oncology drug development. *Eur J Cancer* 48:961–973
48. Mo HN, Liu P (2017) Targeting *MET* in cancer therapy. *Chronic Dis Trans Med* 3(3):148–153
49. Schio L, Nemecek C, Ugolini T et al (2012) SAR125844: a potent and selective ATP-competitive inhibitor of MET kinase. *Cancer Res* 72(8, Suppl.1):2911
50. Schio L et al (2016) Discovery, pharmacokinetic and pharmacological properties of the potent and selective MET kinase inhibitor, 1-{6-[6-(4-Fluoro-phenyl)-[1,2,4]triazolo[4,3-b]pyridazin-

- 3-ylsulfanyl]-benzothiazol-2-yl]-3-(2-morpholin-4-yl-ethyl)-urea (SAR125844) *J. Med Chem* 59:7066–7074
51. Romano G, Giordano A (2008) Role of the cyclin-dependent kinase 9-related pathway in mammalian gene expression and human diseases. *Cell Cycle* 7(23):3664–3668
 52. Dussault I, Bellon SF (2009) From concept to reality: the long road to c-met and RON receptor tyrosine kinase inhibitors for the treatment of Cancer. *Anti Cancer Agents Med Chem* 9:221–229
 53. Komoto J, Yamada T, Takata Y, Markham GD, Takusagawa F (2004) Crystal structure of the S-Adenosylmethionine Synthetase ternary complex: a novel catalytic mechanism of S-Adenosylmethionine synthesis from ATP and met. *Biochemistry* 43:1821–1831
 54. Eathiraj S et al (2011) Discovery of a novel mode of protein kinase inhibition characterized by the mechanism of inhibition of human Mesenchymal-epithelial transition factor (c-met) protein autophosphorylation by ARQ 197. *J Biol Chem* 286(23):20666–20676
 55. Coumaran E, Goulaouic H (2015) Selective intravenous inhibitor of the MET tyrosine kinase SAR125844 inhibits tumor growth in MET-amplified Cancer. *Mol Cancer Ther* 14(2):384–394
 56. Angevin E et al (2017) A first-in-human phase I study of SAR125844, a selective MET tyrosine kinase inhibitor, in patients with advanced solid tumours with MET amplification. *Eur J Cancer* 87:131–139
 57. Lindmo K, Stenmark H (2006) Regulation of membrane traffic by phosphoinositide 3-kinases. *J Cell Sci* 119:605–614
 58. Backer JM (2016) The intricate regulation and complex functions of the class III phosphoinositide 3-kinase Vps34. *Biochem J* 473(15):2251–2271
 59. Stjepanovic G, Baskaran S, Mary G, Lin MG, Hurley JH (2017) Unveiling the role of VPS34 kinase domain dynamics in regulation of the autophagic PI3K complex. *Mol Cell Oncol* 4(6): e1367873
 60. Bilanges B (2017) Vps34 PI3-kinase inactivation enhances insulin sensitivity through reprogramming of mitochondrial metabolism. *Nat Commun* 8(1):1804. <https://doi.org/10.1038/s41467-017-01969-4>
 61. Honda A et al (2016) Potent, selective, and orally bioavailable inhibitors of VPS34 provide chemical tools to modulate autophagy in vivo. *ACS Med Chem Lett* 7:72–76
 62. Pasquier B (2016) Autophagy inhibitors. *Cell Mol Life Sci* 73:985–1001
 63. Peppard JV, Ronan B, Pasquier B (2014) Identifying small molecules which inhibit autophagy: a phenotypic screen using image-based high-content cell analysis. *Curr Chem Genom Trans Med* 8(Suppl-1, M2):3–15
 64. Pasquier B, El-Ahmad Y, Filoche-Rommé B et al (2015) Discovery of (2S)-8-[(3R)-3-Methylmorpholin-4-yl]-1-(3-methyl-2-oxobutyl)-2-(trifluoromethyl)-3,4-dihydro-2Hpyrimido [1,2-a]pyrimidin-6-one: a novel potent and selective inhibitor of Vps34 for the treatment of solid tumors. *J Med Chem* 58:376–400
 65. Pasquier B, Goulaouic H et al (2014) A highly potent and selective Vps34 inhibitor alters vesicle trafficking and autophagy. *Nat Chem Biol* 10:1013–1019
 66. Pasquier B (2015) SAR405, a PIK3C3/Vps34 inhibitor that prevents autophagy and synergizes with mTOR inhibition in tumor cells. *Autophagy* 11(4):725–726
 67. Kriplani N, Hermida MA, Brown ER, Leslie NR (2015) Class I PI3-kinases: function and evolution. *Adv Biol Regulation* 59:53–64
 68. Vadas O, Burke JE, Zhang X, Berndt A, Williams RL (2011) Structural basis for activation and inhibition of class I Phosphoinositide 3-kinases. *Sci Signal* 4(195):re2
 69. Yu JSL, Cui W (2016) Proliferation, survival and metabolism: the role of PI3K/AKT/mTOR signaling in pluripotency and cell fate determination. *Development* 143:3050–3060
 70. Millis SZ, Ikeda S, Reddy S, Gatalica Z, Kurzrock R (2016) Landscape of Phosphatidylinositol-3-kinase pathway alterations across 19784 diverse solid tumors. *JAMA Oncol* 2(12):1565–1573
 71. Lengauer C et al (2008) PTEN-deficient cancers depend on PIK3CB. *Proc Natl Acad Sci U S A* 105(35):13057–13062

72. Dillon LM, Miller TW (2014) Therapeutic targeting of cancers with loss of PTEN function. *Curr Drug Targets* 15(1):65–79
73. Greenwell IB, Ip A, Cohen JB (2017) PI3K inhibitors: understanding toxicity mechanisms and management. *Oncology (Williston Park)* 31(11):821–828
74. Williams RL (2011) Structure of lipid kinase p110b/p85b elucidates an unusual SH2-domain-mediated inhibitory mechanism. *Mol Cell* 41:567–578
75. Metz A, Ciglia E, Gohlke H (2012) Modulating protein-protein interactions: from structural determinants of binding to Druggability prediction to application. *Curr Pharm Des* 18:4630–4647
76. Vlahos CJ, Matter WF, Hui KY, Brown RF (1994) A specific inhibitor of phosphatidylinositol 3 kinase, 2-(4-Morpholinyl)-8-phenyl-4H-1-benzopyran-4-one (LY294002). *J Biol Chem* 269(7):5241–5248
77. Certal V, Halley F, Virone-Oddos A et al (2012) Discovery and optimization of new benzimidazole- and benzoxazole-pyrimidone selective PI3K β inhibitors for the treatment of phosphatase and TENSin homologue (PTEN)-deficient cancers. *J Med Chem* 55:4788–4805
78. Knight ZA, Williams RL, Shokat KM (2006) A pharmacological map of the PI3-K family defines a role for p110 α in insulin signaling. *Cell* 125(4):733–747
79. Certal V, Carry JC, Frank Halley F et al (2014) Discovery and optimization of pyrimidone indoline amide PI3K β inhibitors for the treatment of phosphatase and Tensin homologue (PTEN)-deficient cancers. *J Med Chem* 57:903–992
80. Somoza JR et al (2015) Structural, biochemical, and biophysical characterization of Idelalisib binding to Phosphoinositide 3-kinase δ . *JBC* 290(13):8439–8446
81. Robinson DD. WaterMap – theory and practical applications. <http://content.schrodinger.com/Training+Material/WM/Hsp90/WaterMap-orig.pdf>
82. Wang L, Berne BJ, Friesner RA (2011) Ligand binding to protein-binding pockets with wet and dry regions. *PNAS* 108(4):1326–1330
83. Robinson D, Bertrand T, Carry JC et al (2016) Differential water thermodynamics determine PI3K-Beta/Delta selectivity for solvent-exposed ligand modifications. *J Chem Inf Model* 56:886–894
84. Demers B et al (2018) First-in-human trial of the PI3K β -selective inhibitor SAR260301 in patients with advanced solid tumors. *Cancer* 124(2):315–324
85. Wu P, Clausen MH, Nielsen TE (2015) Allosteric small-molecule kinase inhibitors. *Pharmacol Ther* 156:59–68
86. Cowan-Jacob SW, Jahnke W, Knapp S (2014) Novel approaches for targeting kinases: allosteric inhibition, allosteric activation and pseudokinases. *Future Med Chem* 6(5):541–561
87. Cheng Y et al (2012) MK-2206, a novel allosteric inhibitor of Akt, synergizes with gefitinib against malignant glioma via modulating both autophagy and apoptosis. *Mol Cancer Ther* 11(1):154–164
88. Simard JR, Rauh R (2014) FLiK: a direct-binding assay for the identification and kinetic characterization of stabilizers of inactive kinase conformations. *Methods Enzymol* 548:147–171
89. Leis S, Schneider S, Zacharias M (2010) In Silico prediction of binding sites on proteins. *Curr Med Chem* 17:1550–1562

Exploiting Kinase Inhibitors for Cancer Treatment: An Overview of Clinical Results and Outlook



Athina Moschopoulou, Stefan Zwirner, Lars Zender, and Daniel Dauch

Contents

1	Introduction	126
2	EGFR Inhibitors	131
3	ALK Inhibitors	132
4	VEGFR Inhibitors	134
5	BCR-ABL Inhibitors	136
6	RAF Inhibitors	137
7	MEK Inhibitors	141
8	Next Clinical Developments	142
9	Challenges	143
	References	145

Abstract Mutated or dysregulated protein kinases represent major oncogenic drivers in cancer. Due to the general druggability of these potential oncoproteins, protein kinases have been regarded the most significant drug targets in cancer cells for the past three decades. Starting with the approval of imatinib for targeting BCR-ABL in leukemia positive for Philadelphia chromosome, a multitude of different kinase inhibitors have been developed and approved for the market so far. Additionally, many new compounds with increased efficacy and target specificity are under development and clinical testing. While several of these compounds allow for an efficient temporary treatment success in different tumor entities, long-term cancer control is often limited due to the development of therapy resistance. Thus, overcoming drug resistance in tumors represents a major challenge for successful cancer therapies in the future.

A. Moschopoulou, S. Zwirner, L. Zender (✉), and D. Dauch (✉)
Department of Medical Oncology and Pneumology, University Hospital Tuebingen, Eberhard Karls University Tuebingen, Tuebingen, Germany

German Cancer Research Consortium (DKTK), German Cancer Research Center (DKFZ), Heidelberg, Germany
e-mail: lars.zender@med.uni-tuebingen.de; daniel.dauch@med.uni-tuebingen.de

Keywords Cancer therapeutics, Kinase inhibitors, Protein kinases, Therapy resistance

Abbreviations

ALL	Acute lymphoblastic leukemia
CEL	Chronic eosinophilic leukemia
CLL	Chronic lymphoblastic leukemia
CML	Chronic myeloid leukemia
CNS	Central nervous system
CRC	Colorectal cancer
DFSP	Dermatofibrosarcoma protuberans
ER	Estrogen receptor
FDA	Food and Drug Administration
GI	Gastrointestinal
GIST	Gastrointestinal stromal tumor
HCC	Hepatocellular carcinoma
HES	Hypereosinophilic syndrome
MDS/MDP	Myelodysplastic/myeloproliferative diseases
NRY	Non-receptor protein-tyrosine kinase
NSCLC	Non-small cell lung carcinoma
PDAC	Pancreatic ductal adenocarcinoma
PH	Philadelphia chromosome
PNET	Primitive neuroectodermal tumor
RCC	Renal cell carcinoma
RY	Receptor protein-tyrosine kinase
S/T	Protein-serine/threonine protein kinase
SEGA	Subependymal giant cell astrocytoma
shRNA	Short hairpin RNA
T/Y	Threonine/tyrosine dual specificity protein kinase

1 Introduction

Over the past 20 years, research revealed that many diseases emerge from impairments in signal transduction. This insight has been used by scientists to unravel molecular mechanisms that drive complex diseases such as solid tumors, leukemias, systemic autoimmune diseases, and inflammatory diseases. Hence, biologists, chemists, physicians, and pharmacologists have focused their clinical research toward development of specific molecules targeting key signaling cascades of these diseases. To this point, most molecules aiming to this direction of treatment represented protein kinase inhibitors. Kinases are proteins that play a critical role in cellular signal transduction by phosphorylating downstream targets. Because dysregulation and mutations of protein kinases play major roles in human diseases, this family of

enzymes has become one of the most significant drug targets over the past three decades. It all started in 1978, when the protein kinase c-SRC was found to share high similarity to a protein from sarcoma virus and act as an oncogene [1]. In addition, studies in the early 1980s pointed out that hyperactivation of a protein kinase (protein kinase C) represents a key mechanism for tumor promotion [2]. The idea to target this group of enzymes therapeutically was also fueled by findings showing that naphthalene-sulphonamides were able to block kinases [3]. These molecules were used as a starting point to further synthesize drugs that inhibit protein kinases.

One of the key experiments for the development of kinase inhibitors was the crystallization of protein kinase A in 1991. Susan Taylor and colleagues revealed the structure of the kinase core for the very first time, giving insight into a key element of all kinases in the genome. This study demonstrated that residues involved in the binding of ATP were conserved among kinases [4, 5]. The crystal structure of PKA gave valuable information for the structural function of these enzymes. However, since core domains of kinases are highly conserved, the idea of selective inhibition of a protein kinase was also considered to be a major challenge.

Starting from the late 1980s, molecules targeting more than one kinase with different efficacies were developed. Some years before that, the only purely isolated tyrosine protein kinases were epidermal growth factor receptor (EGFR) and insulin receptor. The new molecules were 1,000-fold more potent against EGFR than against insulin receptor kinase. Interestingly, these drugs were found to be inactive against serine/threonine kinases [6]. Based on this evidence, scientists could then develop more inhibitors against these kinases that show structure/activity relationships.

Later on, new findings strengthened the idea of targeted kinase drug development. In particular, ATP mimics were found to selectively inhibit platelet-derived growth factor receptor (PDGFR), while they were not potent against other protein kinases. In addition, a study in the mid-1990s showed that quinoxalines are potent inhibitors of PDGFR though not able to interact with EGFR. Accordingly, quinazolines showed the opposite effect [7, 8]. Based on this finding, years later, Zeneca developed the inhibitor gefitinib that targets EGFR. Since 1988, when the first study showing targeted inhibition of the catalytic activity of EGFR was published, the number of protein kinase inhibitor agents developed climbed steadily. It is interesting to note that although EGFR and receptor tyrosine-protein kinase erbB-2 (HER2) share high homology, scientists were able to develop selective molecules against these targets with low cross-reaction already since 1993 [9].

A breakthrough was the first approval of a protein kinase inhibitor by the FDA (2001). This molecule was imatinib, firstly developed by Zeneca as a PDGFR inhibitor. Interestingly, it was later shown that the drug had also high efficacy against BCR-ABL, making it suitable for treatment of chronic myelogenous leukemia (CML) and acute lymphocytic leukemia (ALL) patients positive for Philadelphia chromosome [10, 11]. Since 2001, 48 kinase inhibitors have been approved to the market (Table 1) [12]. The vast majority are drugs against tyrosine protein kinases and receptors for the treatment of cancer. Only a few, ten of them, target serine/threonine kinases. The main difficulty of developing selective agents against serine/threonine kinases is the high similarity of the ATP-binding domain of these

Table 1 Approved protein kinase inhibitors (adapted from <http://www.brimr.org/PKI/PKIs.htm>)

Drug	Company	Known targets	Class	Disease	Year approved
Abemaciclib	Lilly	CDK4/6	S/T	Breast cancer	2017
Acalabrutinib	Acerta Pharma	BTK	NRY	Mantle cell lymphoma	2017
Afatinib	Boehringer Ingelheim	EGFR, ErbB2, ErbB4	RY	NSCLC	2013
Alectinib	Hoffmann-La Roche	ALK, RET	RY	NSCLC (ALK ⁺)	2015
Axitinib	Pfizer	VEGFR1/2/3, PDGFR β	RY	RCC	2012
Baricitinib	Lilly	JAK1/2	NRY	Rheumatoid arthritis	2018
Binimetinib	Array	MEK1/2	S/T	Melanoma	2018
Bosutinib	Pfizer	BCR-Abl, SRC, LYN, and HCK	NRY	CML	2012
Brigatinib	Ariad	ALK, ROS1, IGF-1R, Flt3, EGFR	RY	NSCLC (ALK ⁺)	2017
Cabozantinib	Exelixis	RET, MET, VEGFR1/2/3, KIT, TrkB, FLT3, AXL, TIE2	RY	RCC, HCC, medullary thyroid cancer	2012
Ceritinib	Novartis	ALK, IGF-1R, InsR, ROS1	RY	NSCLC, ALK ⁺ after crizotinib resistance	2014
Cobimetinib	Genentech	MEK1/2	T/Y	Melanoma with BRAF mutations together with vemurafenib	2015
Crizotinib	Pfizer	ALK, MET (HGFR), ROS1, MST1R	RY	NSCLC (ALK ⁺ or ROS1 ⁺)	2011
Dabrafenib	GSK	BRAF, BRAF ^{V600E} , CRAF	S/T	Melanoma, NSCLC (BRAF ^{V600E})	2013
Dacomitinib	Pfizer	EGFR family	RY	EGFR-mutant NSCLC	2018
Dasatinib	Bristol-Myers Squibb	BCR-ABL, EGFR, SRC, LCK, YES, FYN, KIT, EphA2, PDGFR β	NRY	CML	2006
Encorafenib	Array	BRAF	S/T	Melanoma	2018
Erlotinib	Genentech	EGFR	RY	NSCLC, pancreatic cancer	2004
Everolimus	Novartis	FKBP12/mTOR	S/T	Breast cancer (HER2 ⁻), PNET, RCC, angiomyolipoma, SEGA	2009
Fostamatinib	Rigel	SYK, spleen tyrosine kinase	RY	Thrombocytopenia	2018

Gefitinib	AstraZeneca	EGFR		RY	NSCLC	2003–2005, 2015
Gilertinib	Astellas	FLT3		RY	AML	2018
Ibrutinib	Pharmacyclics and J&J	Bruton tyrosine kinase		NR	Mantle cell lymphoma, CLL, lymphoplasmacytic lymphoma, marginal zone B-cell lymphoma	2013
Imatinib	Novartis	BCR-ABL, KIT, PDGFR		NR	CML, ALL (Ph ⁺), aggressive systemic mastocytosis, CEL, DFSP, HES, GIST, MDS/MDP	2001
Lapatinib	GSK	EGFR, ErbB2		RY	Breast cancer	2007
Larotrectinib	Bayer	TRK		RY	Solid tumors with NTRK gene fusion proteins	2018
Lenvatinib	Eisai	VEGFR1/2/3, PDGFR, FGFR, KIT, RET		RY	Differentiated thyroid cancer	2015
Lorlatinib	Pfizer	ALK		RY	NSCLC (ALK ⁺)	2018
Midostaurin	Novartis	FLT3, PDGFR, VEGFR2, PKC		RY	AML, mastocytosis, mast cell leukemia	2017
Neratinib	Puma	ErbB2/HER2		RY	Breast cancer (HER2 ⁺)	2017
Netarsudil	Aerie Pharm.	RRH kinase		NRS/T	Glaucoma	2018
Nilotinib	Novartis	BCR-ABL, PDGFR, DDR1		NR	CML (Ph ⁺)	2007
Nintedanib	Boehringer Ingelheim	FGFR1/2/3, PDGFR α/β , VEGFR1/2/3, Flt3		RY	Pulmonary fibrosis, idiopathic	2014
Osimertinib	AstraZeneca	EGFR T970M		RY	NSCLC	2015
Palbociclib	Parke-Davis	CDK4/6		S/T	Breast cancer (ER ⁺ /HER2 ⁺)	2015
Pazopanib	GSK	VEGFR1/2/3, PDGFR α/β , FGFR1/3, KIT, LCK, FMS, LTK		RY	RCC, soft tissue sarcomas	2009
Ponatinib	Ariad	BCR-Abl, BCR-ABL ^{T315I} , VEGFR, PDGFR, FGFR, EphR, SRC family kinases, kit, RET, TIE2, Flt3		NR	CML, ALL (Ph ⁺)	2012
Regorafenib	Bayer	VEGFR1/2/3, BCR-Abl, BRAF, BRAF (V600E), KIT, PDGFR α/β , RET, FGFR1/2, TIE2, EPH2A		RY	CRC, HCC, GIST	2012

(continued)

Table 1 (continued)

Drug	Company	Known targets	Class	Disease	Year approved
Ribociclib	Novartis	CDK4/6	S/T	Breast cancer	2017
Ruxolitinib	Incyte	JAK1/2	NRX	Myelofibrosis, polycythemia vera	2011
Sunitinib	Wyeth	FKBP/mTOR	S/T	Renal transplant, lymphangioleiomyomatosis	1999
Sorafenib	Onyx	VEGFR1/2/3, B-RAF1, BRAF ^{V600E} , KIT, FLT3, RET, p38, and PDGFRβ	RY	Thyroid cancer, differentiated HCC, RCC	2005
Sunitinib	Pfizer	PDGFRα/β, VEGFR1/2/3, KIT, FLT3, CSF-1R, AXL, RET	RY	RCC, GIST, pancreatic neuroendocrine tumors	2006
Temsirolimus	Wyeth	FKBP12/mTOR	S/T	RCC	2007
Tofacitinib	Pfizer	JAK3	NRX	Rheumatoid arthritis, psoriatic arthritis, ulcerative colitis	2012
Trametinib	GSK	MEK1/2	T/Y	Melanoma	2013
Vandetanib	AstraZeneca	RET, EGFRs, VEGFRs, BEK, TIE2, EphRs, SRC family kinases	RY	Thyroid cancer, medullary	2011
Vemurafenib	Genentech	BRAF ^{V600E} , RAF1	S/T	Melanoma (BRAF ^{V600E})	2011

enzymes. In addition, more serine/threonine kinases (420) than tyrosine kinases (90) were found in the human kinome. In the future, the use of different development strategies along with alternative targeting domains might extend the numbers of FDA-approved inhibitors [13, 14].

2 EGFR Inhibitors

The epidermal growth factor receptor (EGFR) is a transmembrane protein that acts as a receptor for ligands of the epidermal growth factor (EGF) family [15]. The *EGFR* gene is located at chromosome 7, and the encoding protein product encompasses 1,210 amino acids. EGFR is a member of the ErbB family, which is a family of four similar receptors with tyrosine kinase activity. The family consists of EGFR or HER1, HER2, HER3, and HER4. EGFR is a cell surface receptor and represents the starting point of signal transduction mechanisms controlling diverse cellular responses such as cell proliferation, migration, survival, and apoptosis [16]. Mutations and amplification of the *EGFR* gene can lead to overexpression of the receptor. This results in constant kinase activity and uncontrolled activation of downstream pathways. In breast cancer patients, the incidence of overexpressed *EGFR* is approximately 10–30% [17]. Apart from breast cancer, upregulated EGFR can also be found in several other epithelial tumor entities such as lung cancer, prostate cancer, and squamous carcinomas of head and neck [17–19] (Fig. 1).

In addition, deletion of *EGFR* can also be found in several malignancies. One of the most common deletions in the *EGFR* locus is EGFRvIII, where exons 2–7 of *EGFR* are deleted giving rise to a receptor lacking ligand-binding domain but remaining constantly active [20, 21]. Amplification of this mutant is present in gliomas such as glioblastomas with a frequency of 64% (grade IV) but also in head and neck squamous carcinomas and medulloblastomas [21, 22]. High expression of EGFR has been also correlated with short survival time of cancer patients [23].

Lapatinib is an inhibitor of both EGFR and Her2 receptor tyrosine kinases. It was approved in 2007 for treatment of breast cancer, non-small cell lung cancer (NSCLC), head and neck cancer, as well as gastric cancer. The use of lapatinib

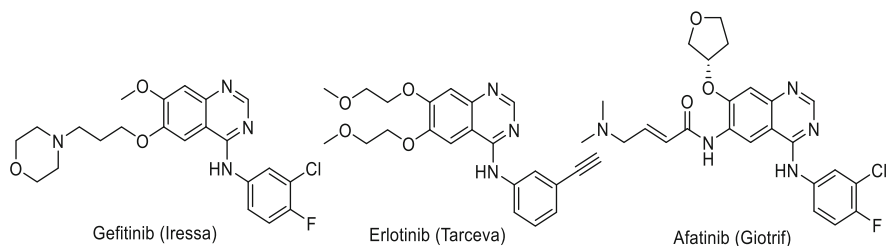


Fig. 1 Chemical structures of EGFR inhibitors

can inhibit the signaling of MAPK and PI3K pathways in patients with overexpressing EGFR and HER2. In particular, the response to lapatinib is linked to HER2 overexpression. The dual specificity of this drug results in inhibition of phosphorylation of AKT, RAF, and ERK. Interestingly, breast cancer patients positive for HER2 amplification with brain metastases are treated with lapatinib in combination with capecitabine for improvement of survival rates [24–27]. Gefitinib is an inhibitor targeting selectively EGFR (Fig. 1). Patients with locally advanced or metastatic NSCLC experienced beneficial outcome when treated with gefitinib [28]. In addition, treatment of EGFR mutation-positive NSCLC patients with gefitinib improved progression-free survival in comparison with chemotherapy. This was the first study that showed longer progression-free survival of patients treated with selective therapy compared to classic chemotherapy [29, 30]. Erlotinib (another kinase inhibitor targeting EGFR) is used for treatment of locally advanced or metastatic NSCLC (Fig. 1). A clinical study published in 2011 revealed that use of erlotinib prolongs survival of NSCLC patients, previously treated with first-line chemotherapy, leading to its approval for this use [31]. In addition, erlotinib combined with gemcitabine increases overall survival of patients with unresectable pancreatic cancer positive for mutant EGFR [32]. Despite providing therapeutic benefit, use of erlotinib has severe side effects such as breathing abnormalities, skin rash, diarrhea, and cough, and the recommended dosage is close to the maximum tolerated dose [33].

Afatinib is an irreversible inhibitor of ErbB family of kinase receptors (Fig. 1). As a first-line treatment of patients with lung adenocarcinoma carrying activating mutations in EGFR, afatinib increased progression-free survival but not overall survival, when compared to gefitinib [34]. In addition, the LUX-Lung 6 trial revealed that patients with advanced lung adenocarcinoma treated with afatinib had prolonged progression-free survival and time to treatment failure in comparison with those treated with gemcitabine in combination with cisplatin [35].

3 ALK Inhibitors

Anaplastic lymphoma kinase (ALK) is a tyrosine kinase receptor. In 1994, ALK was described for the first time as a component of a fusion protein derived from translocation t2;5 in anaplastic large cell lymphoma [36]. Several years later, the full length of ALK receptor tyrosine kinase was characterized. It consists of an extracellular ligand-binding domain, a transmembrane domain, and an intracellular kinase domain that shares high similarity with the insulin receptor (ER) [37, 38]. Although the physiological function of ALK is not completely revealed, it has been described to play a critical role in early embryo development and neural system development [38–41]. Furthermore, activation of ALK is involved in activation of PI3K-AKT, CRKL-C3G, MEKK2/3-MEK5-ERK5, JAK-STAT, and MAPK signaling pathways [38, 42–45]. Around 3–7% of NSCLC patients (usually non-smokers) have a particular mutation, where

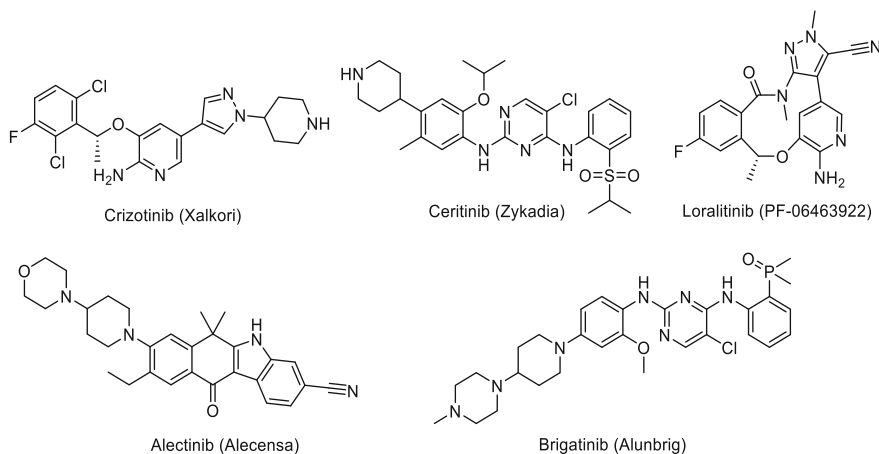


Fig. 2 Chemical structures of ALK inhibitors

echinoderm microtubule-associated protein-like 4 (EML4) gene is fused to ALK gene. This inversion of chromosome 2 results in the expression of the fusion protein EML4-ALK consisting of the N-terminal region of EML4 and the intracellular/kinase region of ALK [46, 47] (Fig. 2).

The first inhibitor of this category approved by FDA was crizotinib (2011) Fig. 2. Initially, it was developed as a c-Met inhibitor but is also able to target ALK, proto-oncogene tyrosine-protein kinase (ROS1), and hepatocyte growth factor receptor (HGFR) [48]. Profile 10,019 phase-I clinical trial and profile 100,513 showed significant objective response rates, prolonged progression-free survival, and median progression-free survival in pretreated ALK-positive (EML4-ALK) NSCLC patients [49, 50]. Based on this evidence, crizotinib received conditional approval for use also in Canada, in 2012. Subsequently, phase-III trials revealed superior median progression-free survival and greater reduction in symptoms related with lung cancer when treated with crizotinib compared to chemotherapy [51, 52]. The results from these studies led to full approval of crizotinib marking it as the “gold standard” of ALK-positive NSCLC.

Ceritinib represents a next-generation ALK inhibitor and showed a higher potency than first-generation inhibitors such as crizotinib (Fig. 2). Ceritinib showed a potency in inhibiting ALK-positive NSCLC that were previously treated and resistant to crizotinib [53]. This finding suggested potency in treatment of mutated and therapy-resistant ALK tumors. Indeed, phase-I ASCEND-1 trial resulted in significant overall response rates in patients pre-acquired with both identified and non-identified resistance mechanisms to crizotinib [54]. An ASCEND-2 phase-II trial showed beneficial response of ceritinib in patients pretreated with crizotinib or chemotherapy and with or without brain metastases [55]. These data resulted in the approval of ceritinib as the first-choice treatment for crizotinib-resistant, ALK-positive NSCLC patients in 2014. In addition, an ASCEND-5 phase-III trial confirmed superior response of ceritinib. In this trial, NSCLC patients with brain

metastases that were previously treated either with crizotinib or platinum-based chemotherapy were treated with ceritinib or chemotherapy [56]. Finally, ceritinib demonstrated potency against naive ALK-inhibitor NSCLC patients. The ASCEND-4 study revealed a median progression-free survival of 16.6 months of patients with advanced ALK-positive NSCLC treated with ceritinib versus 8.1 months of the chemotherapy-treated group [57]. The results from this study led to approval of ceritinib in 2017 by FDA as first-line treatment for patients with ALK-positive NSCLC [58]. Alectinib is another selective ALK inhibitor (Fig. 2). It was approved by FDA in 2015 for the treatment of NSCLC patients with acquired resistance to crizotinib (NP28673 and NP28761 phase-II clinical trials) [59, 60]. Later, the randomized phase-III clinical trial ALEX showed extended beneficial activity of alectinib in ALK-positive NSCLC patients. In particular, results demonstrated a superior progression-free survival rate of alectinib compared to crizotinib in naive ALK-inhibitor patients. In addition, alectinib was found to be less toxic and more active toward CNS. Only 12% of patients in the alectinib group showed a CNS progression event compared to 45% of the crizotinib group. Taking into account the previous results, FDA approved alectinib as first-line treatment of ALK-positive, metastatic NSCLC in 2017 [58, 61]. Latest additions to the ALK inhibitors' list include brigatinib and lorlatinib. Brigatinib is an ALK inhibitor used for NSCLC resistant to crizotinib (Fig. 2). It has received accelerated approval by the FDA in 2017 after phase-II clinical trial ALTA demonstrated significant results for the treatment of patients with progressed NSCLC [62, 63]. Lorlatinib was accepted for the same treatment in 2018 (Fig. 2). Both drugs demonstrate significant intracranial activity making them very potent in decreasing the formation of brain metastasis [63, 64]. Phase-III clinical trial CROWN is currently ongoing for comparison of lorlatinib with crizotinib as first-line treatments [58, 65].

4 VEGFR Inhibitors

More than 40 years ago, the hypothesis of targeting angiogenesis as a tumor therapy was established [66]. Although many factors are involved in mechanisms leading to blood vessel formation, activation of vascular endothelial growth factor (VEGF) pathways was described to be critical in pro-angiogenic signaling. Several types of solid cancers overexpress VEGF-A, making initially this protein to a highly relevant target for selective antiangiogenic therapeutic strategy [67, 68]. Another strategy for inhibiting angiogenesis is the blockage of tyrosine kinase activity of the corresponding receptors VEGFR1, VEGFR2, and VEGFR3. Many receptor tyrosine kinase inhibitors targeting VEGFR have been approved so far. Sorafenib, sunitinib, axitinib, regorafenib, pazopanib, vandetanib, cabozantinib, and lenvatinib are used for treatment of different solid carcinomas such as renal cell carcinoma (RCC), hepatocellular carcinoma (HCC), thyroid cancer, pancreatic neuroendocrine tumor, gastrointestinal stromal tumor (GIST), and metastatic colorectal cancer (CRC) (Fig. 3). Sorafenib and sunitinib represent pioneer kinase inhibitors for the inhibition

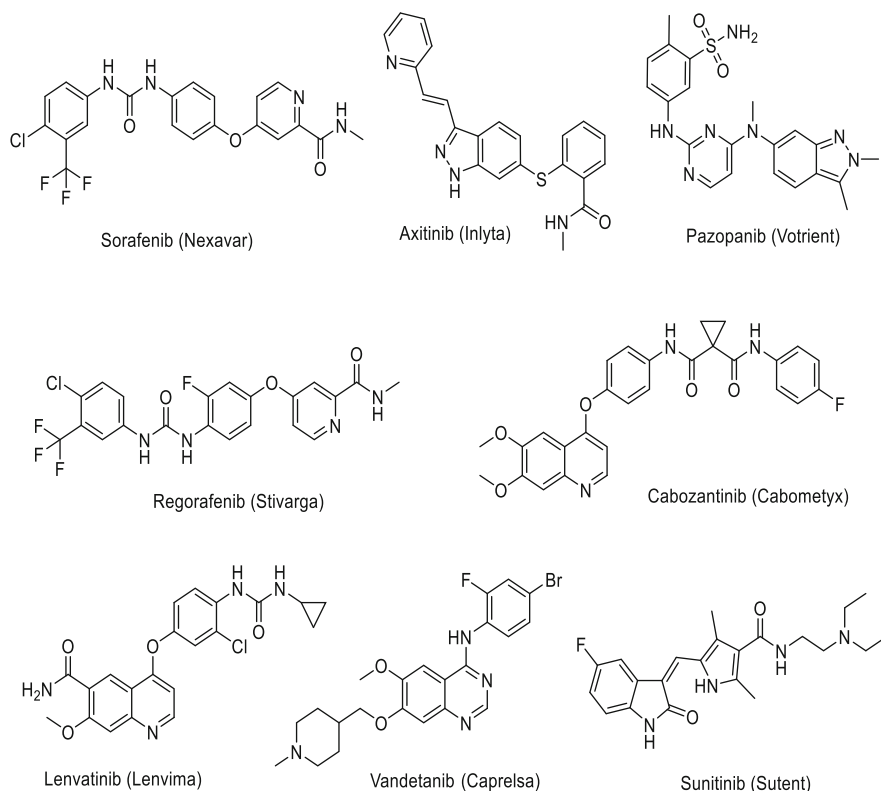


Fig. 3 Chemical structures of VEGFR inhibitors

of angiogenic signaling in cancer. These multikinase inhibitors were initially approved for the treatment of advanced renal cell carcinoma. The pivotal phase-III study TARGET resulted in significantly prolonged progression-free survival time of patients with resistant, advanced renal cell carcinoma when treated with sorafenib. Sunitinib showed similar results in the randomized phase-III trial, where it was compared as first-line treatment to subcutaneous injection of interferon- α for treatment of metastatic RCC. Patients of sunitinib group showed improvement in median progression-free survival and objective response rate [69–72]. Sorafenib and sunitinib have been also accepted by FDA for treatment of HCC and advanced pancreatic neuroendocrine tumors, respectively [73, 74] (Fig. 3).

Regorafenib was the first therapeutic agent to show improvement in the overall survival of patients with metastatic CRC, previously progressed on classic therapies [75]. Based on these results, regorafenib was approved by FDA in 2012 for treatment of metastatic CRC. Half a year later, regorafenib was also accepted for the treatment of advanced GIST [76]. Regorafenib also shows beneficial outcome when used as treatment of HCC, significantly longer overall survival in second-line HCC patients, leading to its approval by the FDA for this use in 2017 [77].

Second-generation VEGFR/multikinase inhibitors include pazopanib, cabozantinib, lenvatinib, axitinib, and vandetanib (Fig. 3). All of them have been approved by the FDA for the treatment of one or several cancer types including thyroid cancer, RCC, soft tissue sarcoma, and medullary thyroid cancer [78].

5 BCR-ABL Inhibitors

The ABL protein family consists of two members: c-ABL and ARG. Physiologically, c-ABL is involved in actin remodeling, cell adhesion, motility, DNA damage response, and microbial pathogen response. In several types of cancer, deregulation and uncontrolled expression of c-ABL kinase has been described [79, 80]. When phosphorylated, c-ABL induces activity of downstream targets, activating ERK5, RAC/JNK, and STAT 1/3 pathways. C-ABL is also a molecular component driving CML. Translocation of part of chromosome 9 to chromosome 22 (Philadelphia chromosome) leads to the expression of oncogenic fusion protein BCR-ABL [81] highlighting ABL is an important target for the development of selective inhibitors. Imatinib was the first kinase inhibitor to be approved by FDA (2001) (Fig. 4). It is an inhibitor of three different targets: ABL, mast/stem cell growth factor receptor (tyrosine kinase KIT or CD117), and PDGFR [82]. After phase-III clinical trial showed improved cytogenetic response rates of CML patients treated with imatinib, the drug was accepted for treatment of CML in blast, accelerated, and chronic phases [83]. Later, in 2002 and 2008, imatinib was approved also for treatment of GIST both for advanced, metastatic tumors and previously resected tumors [84, 85]. Unfortunately, imatinib treatment is not successful in around 30% of patients [86]. The reason is acquired resistance, based on either a reduced cellular uptake of the drug, an increased activity of efflux transporters, or point mutations leading to conformational changes of BCR-ABL and therefore to a reduced binding to imatinib. In addition, resistance is acquired by amplification and overexpression of *BCR-ABL* gene [87]. Second-generation ABL inhibitors such as nilotinib, dasatinib, and bosutinib were developed, in order to overcome mutation-related resistance (Fig. 4). They were all approved for the treatment of CML: nilotinib and dasatinib as first- or second-line treatment and bosutinib as second-line therapy [88]. Nilotinib showed highly promising results because it was potent against almost all mutations resulting in BCR-ABL-dependent resistance [89]. Dasatinib showed high potency in patients with chronic phase CML and a faster treatment response when it was compared to imatinib [90]. Due to its unique structure, dasatinib is also potent against some conformation-altering mutations of BCR-ABL [91, 92]. Bosutinib has a much different structure. It was initially designed as a SRC inhibitor but found to have activity against ABL [93]. Although bosutinib is not potent against major resistant mutants and does not have high selectivity for BCR-ABL, it has the benefit to be not sensitive to resistance efflux transporters and remains in the cells [94, 95]. Therefore, bosutinib is approved for second-line treatment of CML, while trials that test it as first-line treatment are ongoing [88, 96] (Fig. 4).

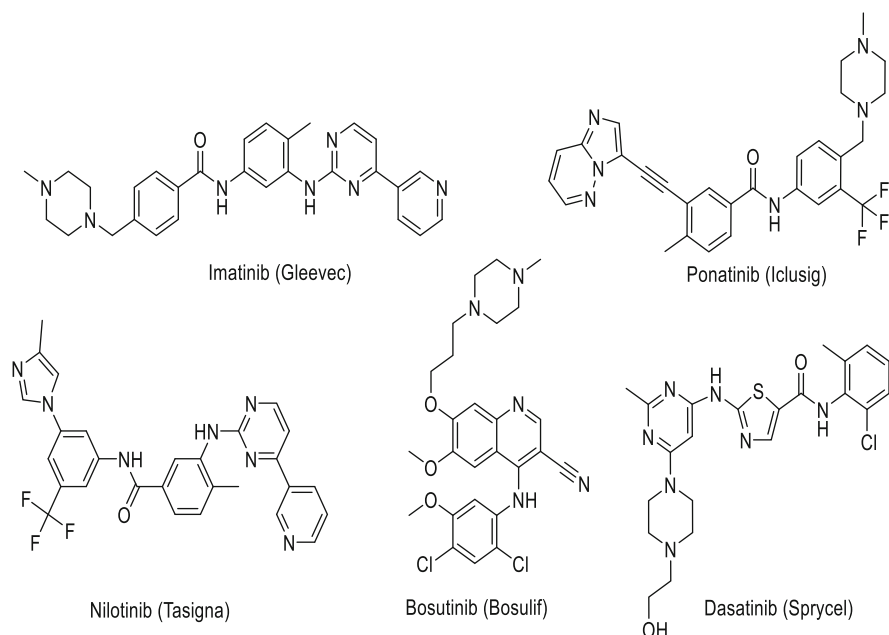


Fig. 4 Chemical structures of ABL inhibitors

The only approved third-generation inhibitor against ABL is ponatinib (Fig. 4). It is a dual SRC/ABL inhibitor that is accepted for the treatment of CML and Ph+ ALL. The structure of ponatinib was modified accordingly so that is highly potent against resistant mutants [97]. Clinically, it shows potency in the treatment of progressed and pretreated Ph+ leukemias. In addition, patients with resistant mutations also benefit from ponatinib treatment. In the corresponding study with 43 patients harboring the abovementioned characteristics, 98% showed a complete hematologic response and 72% a major cytogenetic response [98]. Finally, ponatinib has proven to be a valuable alternative to stem cell transplantation in patients with mutant, advance CML and Ph+ ALL [88, 99].

6 RAF Inhibitors

The RAS/MAPK pathway controls cell growth, proliferation, and survival in a broad range of different tumor entities. Activation of membrane-associated RAS proteins (KRAS, NRAS, HRAS) results in a recruitment of RAF proteins (ARAF, BRAF, and RAF1) leading to a phosphorylation of MEK1 and MEK2 which in turn phosphorylate and activate extracellular signal-regulated kinase (ERK1 and ERK2) (Fig. 5).

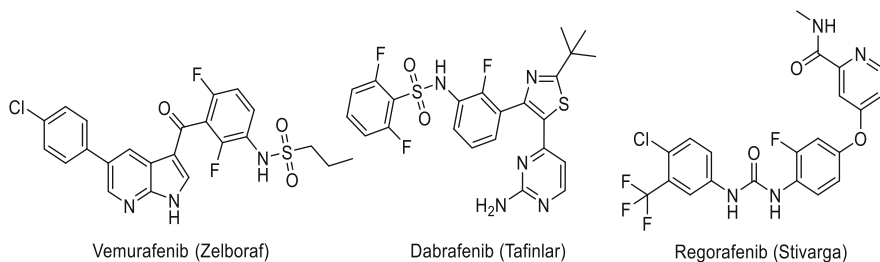


Fig. 5 Chemical structures of RAF inhibitors

RAS represents an important proto-oncogene and a major oncogenic driver. It was found mutated in around 30% of all human cancer entities [100]. Due to the fact that RAS proteins do not harbor any cavities for small molecule interaction, approaches to directly inhibit the function of RAS have not been successful so far. Therefore, the inhibition of RAS downstream factors such as RAF, MEK, and ERK has gained interest for the treatment of cancer [100].

RAF monomers are usually inactive, since the N-terminal domain of BRAF triggers autoinhibition [101, 102]. Upon activation, RAF forms homo- and heterodimers which induces downstream signaling to MEK. While physiological RAS activation induces MEK activation mainly via the formation of BRAF dimers [103], oncogenic RAS often triggers the formation of BRAF-RAF1 heterodimers [101, 104, 105].

BRAF mutations are present in 8% of all human tumors [106]. They were found in more than 50% of melanoma patients and were also identified in CRC (5–10%), hairy cell leukemia (~100%), thyroid carcinomas (25–45%), and, as a rare event, ovarian and lung cancer [106, 107]. Ninety percent of all BRAF mutations account for a substitution of valine with glutamic acid at position 600 (V600E) [100]. This mutation results in a constitutive kinase activity of BRAF monomers and protects BRAF from ERK-mediated negative feedback signaling [102].

The identification of BRAF mutations as oncogenic drivers led to intensified efforts in order to develop more selective and potent BRAF inhibitors. This work yielded in the development of vemurafenib (Zelboraf) and dabrafenib (Tafinlar) as FDA-approved drugs for the treatment of BRAF^{V600E}-mutated advanced melanoma [108–110] (Fig. 5).

Vemurafenib is a BRAF^{V600E} inhibitor with an IC₅₀ of 31 nM, which inhibits also BRAF proteins with other mutations (V600D, V600K, and V600R) as well as RAF1 (IC₅₀ = 48 nM) [109]. It shows only a low affinity to wild-type BRAF (IC₅₀ = 100 nM) [111]. In preclinical treatment studies, vemurafenib was effective in xenograft models of BRAF^{V600E}-mutated melanoma [108] and showed efficacy against BRAF-mutated melanoma cell lines [112].

Upon successful phase-I and phase-II clinical trials, a phase-III clinical trial of vemurafenib was initiated on 675 patients suffering from metastatic, BRAF^{V600E}-mutated melanomas (who did not receive any treatment before). This trial showed a median overall survival of 13.2 months for patients under vemurafenib treatment,

while patients under dacarbazine (as a control) showed only a survival of 9.9 months. Furthermore, vemurafenib resulted in a significant response in 48.4% of patients (in comparison with 5.5% in the dacarbazine-treated group) [113, 114].

Although vemurafenib was in general well tolerated by patients, several adverse symptoms were found upon treatment such as fatigue, nausea, alopecia, lymphopenia, neutropenia, headache, and diarrhea [113, 115–118].

Dabrafenib was shown to be in general a more potent Raf inhibitor than vemurafenib. It inhibits BRAF^{V600E} with an IC₅₀ of 0.8 nM, wild-type BRAF with an IC₅₀ of 3.2 nM, and RAF1 with an IC₅₀ of 5 nM [109, 119]. In preclinical assays, dabrafenib also showed efficacy against BRAF-mutated cell lines and reduced tumor development in xenograft melanoma mouse models [119]. A phase-III clinical trial of dabrafenib was performed in a total of 250 patients suffering from BRAF^{V600E}-mutated metastatic melanoma. While 187 patients received 150 mg dabrafenib twice per day, 63 patients received dacarbazine treatment [120]. In the dabrafenib-treated group, 6 patients (3%) showed a complete and 87 patients (47%) partial response, while 78 patients (42%) displayed a stable disease. In the dacarbazine group, one patient (2%) showed a complete and three patients (5%) partial response. A stable disease was seen in 30 patients (48%). The median progression-free survival in the dabrafenib group was 5.1 months, while dacarbazine-treated patients showed a progression-free survival rate of 2.7 months.

Side effects found often associated with dabrafenib treatment were pyrexia, headache, neutropenia, fatigue, thrombocytopenia, leukopenia, asthenia, hyponatremia, arthralgia, nausea, chills, myalgia, vomiting, diarrhea, and hair loss [108, 109, 117, 118, 120].

Overall, vemurafenib and dabrafenib induced initial therapeutic effects against BRAF^{V600} mutant melanomas. However, the long-term treatment success is limited due to the development of secondary resistance. Thus, most patients relapse after 1 year of treatment [121]. In addition, other tumor entities with BRAF^{V600E} mutation, such as colorectal, pancreatic, and thyroid cancer, mostly show a primary resistance to these drugs [122, 123]. It was hypothesized that long-term control of tumor development by these inhibitors is limited by the fact that they do not efficiently inhibit the dimerization of RAF and are partly unsuccessful in targeting BRAF and RAF1 dimers. Thus, BRAF homodimeric or BRAF-RAF1 heterodimeric signaling can trigger therapy resistance [100–102]. In addition, it was shown that therapy resistance of RAF inhibition can be also induced by the formation of different BRAF^{V600E} splice variants which can form resistant dimers [124].

Of note, RAF inhibitors were also applied in tumors without BRAF mutation. For example, the previously mentioned multikinase inhibitor sorafenib represents a RAF inhibitor and showed certain efficacy in the treatment of patients with HCC and RCC. Sorafenib was approved by the FDA for the treatment of these tumor types [125–129]. However, development of resistance against sorafenib is a frequent incident in treated patients.

Sorafenib inhibits RAF1 with an IC₅₀ of 6 nM, wild-type BRAF with an IC₅₀ of 25 nM, and BRAF^{V600E} with an IC₅₀ of 38 nM. Of note, it is hypothesized that the effect of sorafenib is based on a combined inhibition of RAF and other kinases such

as VEGFR. Sorafenib inhibits VEGFR1 with an IC_{50} of 26 nM and VEGFR2 with an $IC_{50} = 90$ nM. Other kinases that were found to be influenced by sorafenib are FLT-3 ($IC_{50} = 33$ nM), p38 ($IC_{50} = 38$ nM), RET ($IC_{50} = 47$ nM), c-KIT ($IC_{50} = 68$ nM), and FGFR1 ($IC_{50} = 580$ nM) [109, 126, 130]. A phase-III clinical trial testing sorafenib in advanced HCC (SHARP trial) was performed with 602 patients that were treated either with 400 mg sorafenib twice daily (299 patients) or with placebo (303 patients) [74, 129]. In that trial, 7 patients (2%) showed partial response, and 211 patients (71%) had a stable disease in the sorafenib group, whereas 2 patients (1%) showed partial response and 204 patients (67%) had a stable disease in placebo group. The median overall survival was 10.7 months upon sorafenib and 7.9 months upon placebo treatment. Median time to symptomatic progression was 4.1 months in the sorafenib group and 4.9 months in the placebo group. In addition, median time to radiological progression was 5.5 months in the sorafenib group and 2.8 months in the placebo group [109].

As mentioned before, phase-III clinical trials of sorafenib were also conducted against other tumor entities such as RCC and thyroid carcinoma [74, 128, 131]. In a trial against radioactive iodine refractory thyroid cancer (DECISION), 417 patients were treated either with 400 mg sorafenib twice per day (207 patients) or with placebo (210 patients) [132]. Sorafenib triggered a partial response in 12.2% of patients which was seen in only 0.5% of patients treated with the placebo. Furthermore, the sorafenib-treated group showed a median overall survival of 10.8 months compared to 5.8 months in the placebo-treated group.

Adverse effects associated with sorafenib were fatigue, anorexia, hypertension, nausea, vomiting, alopecia, flushing, constipation, voice change, diarrhea, headache, joint pain, pruritus, weight loss, hemorrhage (upper GI), neuropathy, stomatitis, hypophosphatemia, musculoskeletal pain, and abdominal pain [74, 109, 118, 125, 129, 132].

The molecular mechanisms for resistance against sorafenib are complex. It was shown that activation of p38alpha signaling during sorafenib therapy circumvents sorafenib-mediated inhibition of Raf in HCC. In line with this, inhibition of p38alpha improved the outcome of sorafenib in HCC mouse models [133].

For patients that show a progressive disease under sorafenib, recently the RAF inhibitor regorafenib (which targets also several other kinases, such as VEGFR, PDGFR) was approved by the FDA [77] (Fig. 5). In the RESORCE trial, 573 patients that progressed under sorafenib received either 160 mg regorafenib or placebo. The median survival under regorafenib was 10.6 months compared to 7.8 months under placebo treatment [77]. Furthermore, regorafenib was approved by the FDA for the treatment of metastatic colorectal cancer and advanced gastrointestinal stromal tumor (GIST) [75, 76].

7 MEK Inhibitors

The observation of therapy resistance and paradoxical ERK activation upon RAF inhibition resulted in increased effort to develop inhibitors targeting MEK. Several MEK inhibitors, such as refametinib, selumetinib, cobimetinib, and trametinib, have been tested in clinical trials for different tumor entities, e.g., NSCLC and melanoma [134, 135] (Fig. 6).

Also combination therapies of RAF and MEK inhibitors were tested and FDA approved and were able to further increase the treatment responses in melanoma patients [136]. In patients with metastatic melanoma, two phase-III trials were performed in order to test the combination of BRAF inhibitors and MEK inhibitors. In the COMBI-d trial, 423 patients with BRAF^{V600} mutations, which were not treated before, received either dabrafenib in combination with trametinib or dabrafenib alone [137]. The application of the combination therapy resulted in a 3-year overall survival of 44% compared to 32% in the group that received a dabrafenib monotherapy. Adverse effects of the trametinib and dabrafenib combination were pyrexia, fatigue, nausea, headache, diarrhea, rash, and arthralgia [137, 138].

In addition, also a combination of cobimetinib and vemurafenib was tested in 495 patients with untreated advanced BRAF^{V600}-mutated melanoma (coBRIM trial) [139]. In this trial, the 3-year rate of relapse-free survival was 58% in the group that received the combination therapy compared to 39% in the placebo group. The 3-year overall survival rate was 86% in the combination-therapy group compared to 77% in the placebo group [139].

In addition, different studies tested also the combination of RAF/MEK inhibitors with immunotherapies [140].

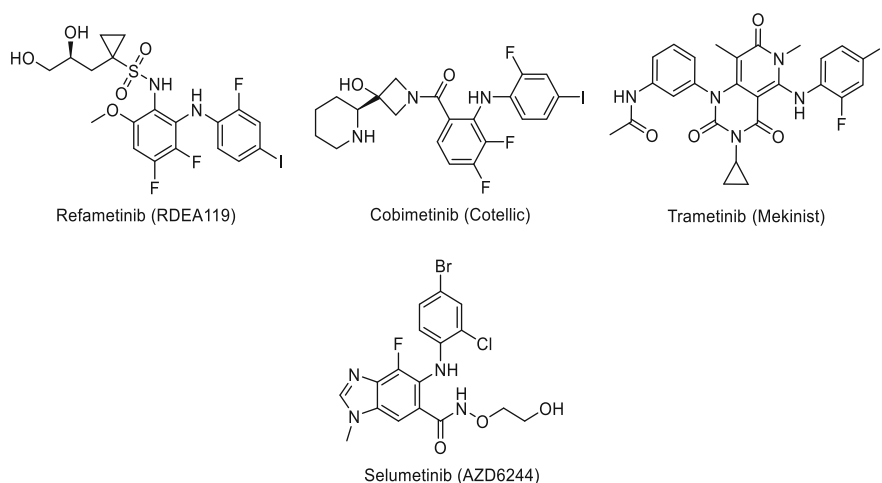


Fig. 6 Chemical structures of MEK inhibitors

8 Next Clinical Developments

The human genome encodes for over 500 kinases which gives ample scope for novel target finding and drug development in cancer therapy [141]. In addition to the 48 FDA-approved kinase inhibitors, a huge range of potential inhibitors are currently in clinical or preclinical trials. For example, clinical phase-I trials of compounds targeting nerve growth factor receptors [142], polo-like kinase 1 [143], phosphatidylinositol 4,5-bisphosphate 3-kinase delta and gamma [144], protein kinase B [145], focal adhesion kinase [146], casein kinase II [147], and Aurora kinases [148] were performed within the last years (Fig. 7).

Notably, the Aurora A kinase inhibitor alisertib could finish two clinical phase-II trials with promising responses in patients with neuroendocrine prostate cancer [NCT01799278] as well as advanced breast cancer and small cell carcinoma of the lung [NCT01045421] (Fig. 7). However, a phase-III trial in patients with relapsed/refractory peripheral T-cell lymphoma [NCT01482962] was announced to be discontinued based on a pre-specified interim analysis by Takeda.

In parallel, the research on PI3K and mTOR inhibiting compounds was heavily impelled in recent years [13]. In addition to idelalisib which was the first FDA-approved compound to inhibit a lipid kinase (PI3K δ isoform) [149, 150], in total seven dual PI3K/mTOR small molecule inhibitors are tested in advanced clinical trials [13] (Fig. 7). These comprise PKI587 (advanced solid malignancies) [151], quinacrine (various leukemias) [152, 153], GSK2126458 (colorectal, breast, NSCLC, and pancreatic cancer) [154], PF04691502 (breast cancer) [155], GDC0980 (mRC) [156], XL765 (breast cancer) [157], and NVP-BEZ235 (glioblastomas) [158].

The oral pan-PI3K inhibitor buparlisib which targets all four isoforms of class I PI3K was registered for three phase-III clinical trials against breast cancer. Buparlisib was tested in combination with fulvestrant in an advanced breast cancer study (Fig. 7). Due to the safety profile, the results do not endorse an expansion in this clinical setting [159, 160].

Interestingly, patients with a *PIK3CA* mutation have shown a median progression-free survival of 4.2 months (95% CI 2.8–6.7) after buparlisib treatment compared to 1.6 months (95% CI 1.4–2.8) in the placebo group. These results

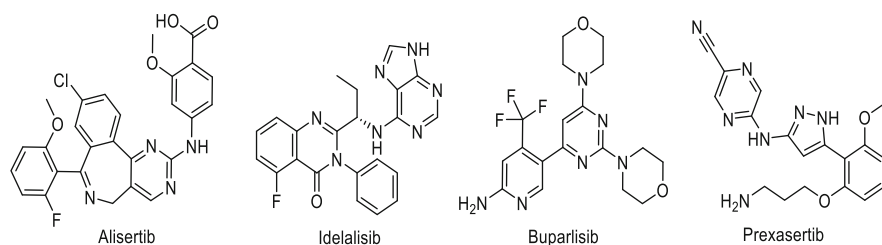


Fig. 7 Chemical structures of next clinical development

support the application of PI3K inhibitors combined with endocrine therapy in this genetic background [160].

Nearly all hallmarks of cancer can be targeted by approved protein kinase inhibitors. However, there are currently no FDA-accepted kinase inhibitors influencing genome instability and DNA damage response. The success story of olaparib, a Poly [ADP-ribose] polymerase 1 (PARP-1) inhibitor, underlines the high potential of small molecules in this field. In general, the incidence of DNA single- or double-strand breaks is mainly controlled by the network of ATR/ATM and CHK1/CHK2 signaling pathways leading to active DNA repair mechanisms and cell cycle checkpoint regulation [161]. At the moment, two different ATR inhibitors, AZD6738 and M6620, are tested in clinical phase-II trials with four and six studies. They are administered in prostate cancer, CLL, recurrent ovarian cancer, progressive metastatic gastric or gastroesophageal junction cancer, small cell lung carcinoma, as well as metastatic tumors including RCC, urothelial carcinoma, ovarian cancer, and PDAC [NCT03787680, NCT03328273, NCT03641313, NCT03517969, NCT03682289, NCT02595892, NCT02567409, NCT03462342, NCT02627443, NCT02487095].

Furthermore, checkpoint kinases are valid targets in DNA damage response. The CHK1/CHK2 inhibitor prexasertib is tested in small cell lung cancer, ovarian cancer, breast cancer, and prostate cancer in phase-II clinical trials [NCT02735980, NCT03414047, NCT02873975, NCT02203513] (Fig. 7).

In *BRCA* wild-type recurrent high-grade serous ovarian cancer, prexasertib could exhibit clinical activity and was in general well tolerated by treated patients [162]. Particularly patients with platinum-resistant or platinum-refractory cancer could profit here from further drug development [162].

9 Challenges

Beside numerous advances of kinase inhibitors, profound understanding of mechanisms *in vivo* is needed to overcome actual limitations in clinical oncology [13].

Secondary therapy resistance based on kinase mutations is an abundant phenomenon arising after kinase inhibition [163]. The diversity of such mutations among different kinases hampers the overall treatment success in cancer patients [164]. Acquired resistance is the most common resistance type caused by kinase inhibitors and relates to tumors that respond to therapy initially but show posterior resistance to permanent delivered therapy [13]. Secondary resistance can be induced by changes in the kinase gatekeeper residue since hydrophobic interactions in the sub-pocket are decisive for the inhibitor binding affinity [165, 166]. The gatekeeper residue interacts with Type I and Type II kinase inhibitors and sterically influences inhibitor binding to the hydrophobic region in the binding pocket [167]. In addition to gatekeeper mutations in BCR-ABL kinases inducing imatinib resistance, numerous other targets are affected by gatekeeper mutations [168–173]. A prominent example is the T790M mutation in EGFR kinase leading to boosted affinity toward

ATP that triggers resistance to quinazoline inhibitors as well as gefitinib and erlotinib [174–176]. To circumvent drug resistance in the clinic, structural optimization of small molecule inhibitors is required [13]. In case of mutated EGFR-induced resistance to gefitinib and erlotinib, newly developed EGFR inhibitors can covalently bind to the ATP-binding site of EGFR [177, 178]. That represents an example for highly selective inhibitors against mutated targets [13].

To further counter kinase inhibitor resistance, scientists break fresh ground with innovative strategies. In the context of gatekeeper mutations, currently developed inhibitors are going to accept varying amino acids at the gatekeeper mutation site [179, 180]. In a second approach, kinases will be targeted at alternative binding sites to avoid the ubiquitous ATP-binding pocket by a presumable unique cavity [181, 182]. Apart from that, also indirect kinase targeting via inhibition of kinase transformers would be a valid option to overcome resistance [183].

An additional clinical challenge represents the reduction or elimination of critical toxicities associated with kinase inhibitors, such as proteinuria, skin reactions, hypertension, or cardiotoxicity [184, 185].

Well-known examples are associated side effects of BCR-ABL inhibitors, including cytopenia, cardiotoxicity, and cardiac sequela. HER2 and ALK inhibition cause gastric problems and dermatological irregularities. EGFR inhibition is linked to dermatological issues, and VEGFR inhibition can trigger cardiotoxicity [186, 187].

To exclude toxicities triggered by off-target binding of the inhibitor, more specific therapeutic strategies are required. RNA interference is not only a powerful tool for specific gene knockdown in basic research, but it also raises expectations as a therapeutic approach to inhibit crucial players in cancer such as kinases [13]. However, since important drug targets cannot be efficiently eradicated by RNA interference so far, clinical resistance to kinase inhibitors will continue to be an important challenge to kinase-associated therapies [13, 188].

Altogether, the development of clinical relevant kinase inhibition has just started, but the rapid progress in the development of molecular technologies and engineering raises confidence for further success stories.

Compliance with Ethical Standards

Funding: L.Z. and D.D. are supported by the Deutsche Forschungsgemeinschaft (DFG, German Research Foundation) [FOR2314 (D.D., L.Z.), SFB-TR209 (D.D., L.Z.), SFB-TR240 (L.Z.), Gottfried Wilhelm Leibniz Program (L.Z.)], the Deutsche Forschungsgemeinschaft (DFG, German Research Foundation) under Germany's excellence strategy – EXC 2180 – 390900677 [Image Guided and Functionally Instructed Tumour Therapies (iFIT)], the *Landesstiftung Baden-Wuerttemberg* [*Improve CRC* (D.D., L.Z.)], the European Research Council [*CholangioConcept* (L.Z.)] and the German Center for Translational Cancer Research (DKTK).

Ethical Approval: This chapter does not contain any studies with human participants or animals performed by of the authors.

Informed Consent: All authors have given their consent to this book chapter.

Conflict of Interest: The authors declare no competing financial interests.

References

1. Collett MS, Erikson RL (1978) Protein kinase activity associated with the avian sarcoma virus SRC gene product. *Proc Natl Acad Sci* 75(4):2021–2024
2. Castagna M et al (1982) Direct activation of calcium-activated, phospholipid-dependent protein kinase by tumor-promoting phorbol esters. *J Biol Chem* 257(13):7847–7851
3. Hidaka H et al (1984) Isoquinolinesulfonamides, novel and potent inhibitors of cyclic nucleotide-dependent protein kinase and protein kinase C. *Biochemistry* 23(21):5036–5041
4. Knighton D et al (1991) Crystal structure of the catalytic subunit of cyclic adenosine monophosphate-dependent protein kinase. *Science* 253(5018):407–414
5. Zheng J et al (1993) Crystal structures of the myristylated catalytic subunit of cAMP-dependent protein kinase reveal open and closed conformations. *Protein Sci* 2(10):1559–1573
6. Yaish P et al (1988) Blocking of EGF-dependent cell proliferation by EGF receptor kinase inhibitors. *Science* 242(4880):933–935
7. Kovalenko M et al (1994) Selective platelet-derived growth factor receptor kinase blockers reverse *sis*-transformation. *Cancer Res* 54(23):6106–6114
8. Gazit A et al (1996) Tyrphostins. 5. Potent inhibitors of platelet-derived growth factor receptor tyrosine kinase: structure–activity relationships in quinoxalines, quinolines, and indole tyrphostins. *J Med Chem* 39(11):2170–2177
9. Oshero N et al (1993) Selective inhibition of the epidermal growth factor and HER2/neu receptors by tyrphostins. *J Biol Chem* 268(15):11134–11142
10. Levitzki A, Mishani E (2006) Tyrphostins and other tyrosine kinase inhibitors. *Annu Rev Biochem* 75(1):93–109
11. Hunter T (2007) Treatment for chronic myelogenous leukemia: the long road to imatinib. *J Clin Invest* 117(8):2036–2043
12. Roskoski R Jr (2020) FDA-approved protein kinase inhibitors. Blue Ridge Institute for Medical Research, Horse Shoe
13. Bhullar KS et al (2018) Kinase-targeted cancer therapies: progress, challenges and future directions. *Mol Cancer* 17(1):48
14. Manning G et al (2002) The protein kinase complement of the human genome. *Science* 298(5600):1912–1934
15. Herbst RS (2004) Review of epidermal growth factor receptor biology. *Int J Radiat Oncol Biol Phys* 59(2, Supplement):S21–S26
16. Oda K et al (2005) A comprehensive pathway map of epidermal growth factor receptor signaling. *Mol Syst Biol* 1:2005.0010
17. Lee HJ et al (2015) Prognostic and predictive values of EGFR overexpression and EGFR copy number alteration in HER2-positive breast cancer. *Br J Cancer* 112(1):103–111
18. Yang C-H et al (2015) EGFR over-expression in non-small cell lung cancers harboring EGFR mutations is associated with marked down-regulation of CD82. *Biochim Biophys Acta* 1852(7):1540–1549
19. Bossi P et al (2016) Prognostic and predictive value of EGFR in head and neck squamous cell carcinoma. *Oncotarget* 7(45):74362–74379
20. Gan HK, Cvriljevic AN, Johns TG (2013) The epidermal growth factor receptor variant III (EGFRvIII): where wild things are altered. *FEBS J* 280(21):5350–5370
21. An Z et al (2018) Epidermal growth factor receptor and EGFRvIII in glioblastoma: signaling pathways and targeted therapies. *Oncogene* 37(12):1561–1575
22. Han J et al (2015) CAR-engineered NK cells targeting wild-type EGFR and EGFRvIII enhance killing of glioblastoma and patient-derived glioblastoma stem cells. *Sci Rep* 5:11483
23. Sacher AG et al (2016) Prospective validation of rapid plasma genotyping for the detection of EGFR and KRAS mutations in advanced lung cancer. *JAMA Oncol* 2(8):1014–1022
24. De Silva N et al (2015) Molecular effects of Lapatinib in the treatment of HER2 overexpressing oesophago-gastric adenocarcinoma. *Br J Cancer* 113:1305

25. D'Amato V et al (2015) Mechanisms of lapatinib resistance in HER2-driven breast cancer. *Cancer Treat Rev* 41(10):877–883
26. Bachelot T et al (2013) Lapatinib plus capecitabine in patients with previously untreated brain metastases from HER2-positive metastatic breast cancer (LANDSCAPE): a single-group phase 2 study. *Lancet Oncol* 14(1):64–71
27. Long X-H et al (2014) Lapatinib alters the malignant phenotype of osteosarcoma cells via downregulation of the activity of the HER2-PI3K/AKT-FASN axis in vitro. *Oncol Rep* 31(1):328–334
28. Chen J-C et al (2014) Suppression of Dicer increases sensitivity to gefitinib in human lung cancer cells. *Ann Surg Oncol* 21(4):555–563
29. Mok TS et al (2009) Gefitinib or carboplatin–paclitaxel in pulmonary adenocarcinoma. *N Engl J Med* 361(10):947–957
30. Sim EHA et al (2018) Gefitinib for advanced non-small cell lung cancer. *Cochrane Database Syst Rev* 1:CD006847
31. Neal JW (2010) The SATURN trial: the value of maintenance erlotinib in patients with non-small-cell lung cancer. *Future Oncol* 6(12):1827–1832
32. Wang JP et al (2015) Erlotinib is effective in pancreatic cancer with epidermal growth factor receptor mutations: a randomized, open-label, prospective trial. *Oncotarget* 6(20):18162–18173
33. Cappuzzo F (2013) Erlotinib in the first-line treatment of non-small-cell lung cancer AU – D'Arcangelo, Manolo. *Expert Rev Anticancer Ther* 13(5):523–533
34. Paz-Ares L et al (2017) Afatinib versus gefitinib in patients with EGFR mutation-positive advanced non-small-cell lung cancer: overall survival data from the phase IIb LUX-Lung 7 trial. *Ann Oncol* 28(2):270–277
35. Wu YL et al (2013) LUX-Lung 6: a randomized, open-label, phase III study of afatinib (A) versus gemcitabine/cisplatin (GC) as first-line treatment for Asian patients (PTS) with EGFR mutation-positive (EGFR M+) advanced adenocarcinoma of the lung. *J Clin Oncol* 31(15_suppl):8016–8016
36. Morris S et al (1994) Fusion of a kinase gene, ALK, to a nucleolar protein gene, NPM, in non-Hodgkin's lymphoma. *Science* 263(5151):1281–1284
37. Morris SW et al (1997) ALK, the chromosome 2 gene locus altered by the t(2;5) in non-Hodgkin's lymphoma, encodes a novel neural receptor tyrosine kinase that is highly related to leukocyte tyrosine kinase (LTK). *Oncogene* 14:2175
38. Hallberg B, Palmer RH (2016) The role of the ALK receptor in cancer biology. *Ann Oncol* 27(suppl_3):iii4–iii15
39. Stute C et al (2004) Myoblast determination in the somatic and visceral mesoderm depends on Notch signalling as well as on *milliways(mil^{Alk})* as receptor for Jeb signalling. *Development* 131(4):743–754
40. Janoueix-Lerosey I et al (2018) The ALK receptor in sympathetic neuron development and neuroblastoma. *Cell Tissue Res* 372(2):325–337
41. Yao S et al (2013) Anaplastic lymphoma kinase is required for neurogenesis in the developing central nervous system of zebrafish. *PLoS One* 8(5):e63757
42. Yip PY (2015) Phosphatidylinositol 3-kinase-AKT-mammalian target of rapamycin (PI3K-Akt-mTOR) signaling pathway in non-small cell lung cancer. *Transl Lung Cancer Res* 4(2):165–176
43. An R et al (2016) CRKL mediates EML4-ALK signaling and is a potential therapeutic target for ALK-rearranged lung adenocarcinoma. *Oncotarget* 7(20):29199–29210
44. Umopathy G et al (2014) The kinase ALK stimulates the kinase ERK5 to promote the expression of the oncogene MYCN in neuroblastoma. *Sci Signal* 7(349):ra102
45. Hallberg B, Palmer RH (2013) Mechanistic insight into ALK receptor tyrosine kinase in human cancer biology. *Nat Rev Cancer* 13:685
46. Soda M et al (2007) Identification of the transforming EML4–ALK fusion gene in non-small-cell lung cancer. *Nature* 448:561

47. Hofman P (2017) ALK in non-small cell lung cancer (NSCLC) pathobiology, epidemiology, detection from tumor tissue and algorithm diagnosis in a daily practice. *Cancers* 9(8):107
48. Nwizu T et al (2011) Crizotinib (PF02341066) as a ALK/MET inhibitor – special emphasis as a therapeutic drug against lung cancer. *Drugs Future* 36(2):91–99
49. Kwak EL et al (2010) Anaplastic lymphoma kinase inhibition in non–small-cell lung cancer. *N Engl J Med* 363(18):1693–1703
50. Crinò L et al (2011) Initial phase II results with crizotinib in advanced ALK-positive non-small cell lung cancer (NSCLC): PROFILE 1005. *J Clin Oncol* 29(15_suppl):7514
51. Shaw AT et al (2013) Crizotinib versus chemotherapy in advanced ALK-positive lung cancer. *N Engl J Med* 368(25):2385–2394
52. Solomon BJ et al (2014) First-line crizotinib versus chemotherapy in ALK-positive lung cancer. *N Engl J Med* 371(23):2167–2177
53. Friboulet L et al (2014) The ALK inhibitor ceritinib overcomes crizotinib resistance in non-small cell lung cancer. *Cancer Discov* 4(6):662–673
54. Kim D-W et al (2016) Activity and safety of ceritinib in patients with ALK-rearranged non-small-cell lung cancer (ASCEND-1): updated results from the multicentre, open-label, phase 1 trial. *Lancet Oncol* 17(4):452–463
55. Crinò L et al (2016) Multicenter phase II study of whole-body and intracranial activity with ceritinib in patients with ALK-rearranged non–small-cell lung cancer previously treated with chemotherapy and crizotinib: results from ASCEND-2. *J Clin Oncol* 34(24):2866–2873
56. Bearz A et al (2016) Ceritinib vs chemotherapy (CT) in patients (pts) with advanced anaplastic lymphoma kinase (ALK)-rearranged (ALK+) non-small cell lung cancer (NSCLC) previously treated with CT and crizotinib (CRZ): results from the confirmatory phase 3 ASCEND-5 study. *Ann Oncol* 27(suppl_6):1–36
57. Soria J-C et al (2017) First-line ceritinib versus platinum-based chemotherapy in advanced ALK-rearranged non-small-cell lung cancer (ASCEND-4): a randomised, open-label, phase 3 study. *Lancet* 389(10072):917–929
58. Rothenstein JM, Chooback N (2018) ALK inhibitors, resistance development, clinical trials. *Curr Oncol* 25(Suppl 1):S59–S67
59. Zeaiter A et al (2016) Updated efficacy and safety from the global phase II NP28673 study of alectinib in patients (pts) with previously treated ALK+ non-small-cell lung cancer (NSCLC). *Ann Oncol* 27(suppl_6):1263P
60. Yang JC-H et al (2017) Pooled systemic efficacy and safety data from the pivotal phase II studies (NP28673 and NP28761) of alectinib in ALK-positive non-small cell lung cancer. *J Thorac Oncol* 12(10):1552–1560
61. Peters S et al (2017) Alectinib versus crizotinib in untreated ALK-positive non–small-cell lung cancer. *N Engl J Med* 377(9):829–838
62. Huang W-S et al (2016) Discovery of brigatinib (AP26113), a phosphine oxide-containing, potent, orally active inhibitor of anaplastic lymphoma kinase. *J Med Chem* 59(10):4948–4964
63. Kim D-W et al (2017) Brigatinib in patients with crizotinib-refractory anaplastic lymphoma kinase–positive non–small-cell lung cancer: a randomized, multicenter phase II trial. *J Clin Oncol* 35(22):2490–2498
64. Solomon B et al (2017) OA 05.06 phase 2 study of lorlatinib in patients with advanced ALK⁺/ROS1⁺ non-small-cell lung cancer. *J Thorac Oncol* 12(11):S1756
65. Solomon BJ et al (2018) Lorlatinib in patients with ALK-positive non-small-cell lung cancer: results from a global phase 2 study. *Lancet Oncol* 19(12):1654–1667
66. Folkman J (1971) Tumor angiogenesis: therapeutic implications. *N Engl J Med* 285(21):1182–1186
67. Ferrara N, Gerber H-P, LeCouter J (2003) The biology of VEGF and its receptors. *Nat Med* 9:669
68. Ferrara N (2002) VEGF and the quest for tumour angiogenesis factors. *Nat Rev Cancer* 2:795
69. Di Lorenzo G et al (2010) Third-line sorafenib after sequential therapy with sunitinib and mtor inhibitors in metastatic renal cell carcinoma. *Eur Urol* 58(6):906–911

70. Motzer RJ et al (2007) Sunitinib versus interferon alfa in metastatic renal-cell carcinoma. *N Engl J Med* 356(2):115–124
71. Carducci MA et al (2015) Atrasentan in patients with advanced renal cell carcinoma: a phase 2 trial of the ECOG-ACRIN Cancer Research Group (E6800). *Clin Genitourin Cancer* 13(6):531–539.e1
72. Bhargava P, Robinson MO (2011) Development of second-generation VEGFR tyrosine kinase inhibitors: current status. *Curr Oncol Rep* 13(2):103–111
73. Raymond E et al (2011) Sunitinib malate for the treatment of pancreatic neuroendocrine tumors. *N Engl J Med* 364(6):501–513
74. Llovet JM et al (2008) Sorafenib in advanced hepatocellular carcinoma. *N Engl J Med* 359(4):378–390
75. Grothey A et al (2013) Regorafenib monotherapy for previously treated metastatic colorectal cancer (CORRECT): an international, multicentre, randomised, placebo-controlled, phase 3 trial. *Lancet* 381(9863):303–312
76. Demetri GD et al (2013) Efficacy and safety of regorafenib for advanced gastrointestinal stromal tumours after failure of imatinib and sunitinib (GRID): an international, multicentre, randomised, placebo-controlled, phase 3 trial. *Lancet* 381(9863):295–302
77. Bruix J et al (2017) Regorafenib for patients with hepatocellular carcinoma who progressed on sorafenib treatment (RESORCE): a randomised, double-blind, placebo-controlled, phase 3 trial. *Lancet* 389(10064):56–66
78. Zirlik K, Duyster J (2018) Anti-angiogenics: current situation and future perspectives. *Oncol Res Treat* 41(4):166–171
79. Srinivasan D, Plattner R (2006) Activation of Abl tyrosine kinases promotes invasion of aggressive breast cancer cells. *Cancer Res* 66(11):5648–5655
80. Sirvent A et al (2007) The tyrosine kinase Abl is required for Src-transforming activity in mouse fibroblasts and human breast cancer cells. *Oncogene* 26:7313
81. Mgbemena VE (2014) Re-evaluating the role of BCR/ABL in chronic myelogenous leukemia AU – Ross, Theodora S. *Mol Cell Oncol* 1(3):e963450
82. Schenone S et al (2015) Analogs, formulations and derivatives of imatinib: a patent review AU – Musumeci, Francesca. *Expert Opin Ther Pat* 25(12):1411–1421
83. Cohen MH et al (2002) Approval summary for imatinib mesylate capsules in the treatment of chronic myelogenous leukemia. *Clin Cancer Res* 8(5):935–942
84. Dematteo RP et al (2009) Adjuvant imatinib mesylate after resection of localised, primary gastrointestinal stromal tumour: a randomised, double-blind, placebo-controlled trial. *Lancet* 373(9669):1097–1104
85. Dagher R et al (2002) Approval summary. Imatinib mesylate in the treatment of metastatic and/or unresectable malignant gastrointestinal stromal tumors. *Clin Cancer Res* 8(10):3034–3038
86. Hasford J et al (2011) Predicting complete cytogenetic response and subsequent progression-free survival in 2060 patients with CML on imatinib treatment: the EUTOS score. *Blood* 118(3):686–692
87. Hochhaus A et al (2002) Molecular and chromosomal mechanisms of resistance to imatinib (STI571) therapy. *Leukemia* 16:2190
88. Rossari F, Minutolo F, Orciuolo E (2018) Past, present, and future of Bcr-Abl inhibitors: from chemical development to clinical efficacy. *J Hematol Oncol* 11(1):84–84
89. Kantarjian HM et al (2011) Nilotinib versus imatinib for the treatment of patients with newly diagnosed chronic phase, Philadelphia chromosome-positive, chronic myeloid leukaemia: 24-month minimum follow-up of the phase 3 randomised ENESTnd trial. *Lancet Oncol* 12(9):841–851
90. Kantarjian HM et al (2012) Dasatinib or imatinib in newly diagnosed chronic-phase chronic myeloid leukemia: 2-year follow-up from a randomized phase 3 trial (DASISION). *Blood* 119(5):1123–1129

91. Skora L et al (2013) NMR reveals the allosteric opening and closing of Abelson tyrosine kinase by ATP-site and myristoyl pocket inhibitors. *Proc Natl Acad Sci* 110(47):E4437–E4445
92. Shah NP et al (2004) Overriding imatinib resistance with a novel ABL kinase inhibitor. *Science* 305(5682):399–401
93. Boschelli DH et al (2001) Optimization of 4-Phenylamino-3-quinolinecarbonitriles as potent inhibitors of Src kinase activity. *J Med Chem* 44(23):3965–3977
94. Boschelli F, Arndt K, Gambacorti-Passerini C (2010) Bosutinib: a review of preclinical studies in chronic myelogenous leukaemia. *Eur J Cancer* 46(10):1781–1789
95. Redaelli S et al (2009) Activity of bosutinib, dasatinib, and nilotinib against 18 imatinib-resistant BCR/ABL mutants. *J Clin Oncol* 27(3):469–471
96. Cortes JE et al (2017) Bosutinib versus imatinib for newly diagnosed chronic myeloid leukemia: results from the randomized BFORE trial. *J Clin Oncol* 36(3):231–237
97. Huang W-S et al (2010) Discovery of 3-[2-(Imidazo[1,2-b]pyridazin-3-yl)ethyl]-4-methyl-N-{4-[(4-methylpiperazin-1-yl)methyl]-3-(trifluoromethyl)phenyl}benzamide (AP24534), a potent, orally active pan-inhibitor of breakpoint cluster region-abelson (BCR-ABL) kinase including the T315I gatekeeper mutant. *J Med Chem* 53(12):4701–4719
98. Cortes JE et al (2012) Ponatinib in refractory Philadelphia chromosome-positive leukemias. *N Engl J Med* 367(22):2075–2088
99. Nicolini FE et al (2015) The impact of ponatinib versus allogeneic stem cell transplant (SCT) on outcomes in patients with chronic myeloid leukemia (CML) or Philadelphia chromosome-positive acute lymphoblastic leukemia (Ph+ ALL) with the T315I mutation. *Blood* 126(23):480–480
100. Samatar AA, Poulidakos PI (2014) Targeting RAS-ERK signalling in cancer: promises and challenges. *Nat Rev Drug Discov* 13(12):928–942
101. Agianian B, Gavathiotis E (2018) Current insights of BRAF inhibitors in cancer. *J Med Chem* 61(14):5775–5793
102. Lavoie H, Therrien M (2015) Regulation of RAF protein kinases in ERK signalling. *Nat Rev Mol Cell Biol* 16(5):281–298
103. Roring M et al (2012) Distinct requirement for an intact dimer interface in wild-type, V600E and kinase-dead B-Raf signalling. *EMBO J* 31(11):2629–2647
104. Rajakulendran T et al (2009) A dimerization-dependent mechanism drives RAF catalytic activation. *Nature* 461(7263):542–545
105. Heidorn SJ et al (2010) Kinase-dead BRAF and oncogenic RAS cooperate to drive tumor progression through CRAF. *Cell* 140(2):209–221
106. Davies H et al (2002) Mutations of the BRAF gene in human cancer. *Nature* 417(6892):949–954
107. Schubbert S, Shannon K, Bollag G (2007) Hyperactive Ras in developmental disorders and cancer. *Nat Rev Cancer* 7(4):295–308
108. Zamboni A et al (2012) Small molecule inhibitors of BRAF in clinical trials. *Bioorg Med Chem Lett* 22(2):789–792
109. Rahman MA et al (2014) BRAF inhibitors: from the laboratory to clinical trials. *Crit Rev Oncol Hematol* 90(3):220–232
110. Alcalá AM, Flaherty KT (2012) BRAF inhibitors for the treatment of metastatic melanoma: clinical trials and mechanisms of resistance. *Clin Cancer Res* 18(1):33–39
111. Bollag G et al (2010) Clinical efficacy of a RAF inhibitor needs broad target blockade in BRAF-mutant melanoma. *Nature* 467(7315):596–599
112. Tap WD et al (2010) Pharmacodynamic characterization of the efficacy signals due to selective BRAF inhibition with PLX4032 in malignant melanoma. *Neoplasia* 12(8):637–649
113. Chapman PB et al (2011) Improved survival with vemurafenib in melanoma with BRAF V600E mutation. *N Engl J Med* 364(26):2507–2516
114. da Rocha Dias S et al (2013) The European Medicines Agency review of vemurafenib (Zelboraf(R)) for the treatment of adult patients with BRAF V600 mutation-positive

- unresectable or metastatic melanoma: summary of the scientific assessment of the Committee for Medicinal Products for Human Use. *Eur J Cancer* 49(7):1654–1661
115. Flaherty KT et al (2010) Inhibition of mutated, activated BRAF in metastatic melanoma. *N Engl J Med* 363(9):809–819
 116. Ravnán MC, Mátalka MS (2012) Vemurafenib in patients with BRAF V600E mutation-positive advanced melanoma. *Clin Ther* 34(7):1474–1486
 117. Mattei PL et al (2013) Cutaneous effects of BRAF inhibitor therapy: a case series. *Ann Oncol* 24(2):530–537
 118. Anforth R, Fernandez-Penas P, Long GV (2013) Cutaneous toxicities of RAF inhibitors. *Lancet Oncol* 14(1):e11–e18
 119. Gibney GT, Zager JS (2013) Clinical development of dabrafenib in BRAF mutant melanoma and other malignancies. *Expert Opin Drug Metab Toxicol* 9(7):893–899
 120. Hauschild A et al (2012) Dabrafenib in BRAF-mutated metastatic melanoma: a multicentre, open-label, phase 3 randomised controlled trial. *Lancet* 380(9839):358–365
 121. Zhang W (2015) BRAF inhibitors: the current and the future. *Curr Opin Pharmacol* 23:68–73
 122. Barras D (2015) BRAF mutation in colorectal cancer: an update. *Biomark Cancer* 7(Suppl 1):9–12
 123. Witkiewicz AK et al (2015) Whole-exome sequencing of pancreatic cancer defines genetic diversity and therapeutic targets. *Nat Commun* 6:6744
 124. Poulidakos PI et al (2011) RAF inhibitor resistance is mediated by dimerization of aberrantly spliced BRAF(V600E). *Nature* 480(7377):387–390
 125. Eisen T et al (2006) Sorafenib in advanced melanoma: a phase II randomised discontinuation trial analysis. *Br J Cancer* 95(5):581–586
 126. Wilhelm SM et al (2004) BAY 43-9006 exhibits broad spectrum oral antitumor activity and targets the RAF/MEK/ERK pathway and receptor tyrosine kinases involved in tumor progression and angiogenesis. *Cancer Res* 64(19):7099–7109
 127. Rimassa L et al (2013) A phase II randomized dose escalation trial of sorafenib in patients with advanced hepatocellular carcinoma. *Oncologist* 18(4):379–380
 128. Escudier B et al (2009) Sorafenib for treatment of renal cell carcinoma: final efficacy and safety results of the phase III treatment approaches in renal cancer global evaluation trial. *J Clin Oncol* 27(20):3312–3318
 129. Rimassa L, Santoro A (2009) Sorafenib therapy in advanced hepatocellular carcinoma: the SHARP trial. *Expert Rev Anticancer Ther* 9(6):739–745
 130. Wilhelm S et al (2006) Discovery and development of sorafenib: a multikinase inhibitor for treating cancer. *Nat Rev Drug Discov* 5(10):835–844
 131. Brose MS et al (2011) Rationale and design of decision: a double-blind, randomized, placebo-controlled phase III trial evaluating the efficacy and safety of sorafenib in patients with locally advanced or metastatic radioactive iodine (RAI)-refractory, differentiated thyroid cancer. *BMC Cancer* 11:349
 132. Brose MS et al (2014) Sorafenib in radioactive iodine-refractory, locally advanced or metastatic differentiated thyroid cancer: a randomised, double-blind, phase 3 trial. *Lancet* 384(9940):319–328
 133. Rudalska R et al (2014) In vivo RNAi screening identifies a mechanism of sorafenib resistance in liver cancer. *Nat Med* 20(10):1138–1146
 134. Janne PA et al (2017) Selumetinib plus docetaxel compared with docetaxel alone and progression-free survival in patients with KRAS-mutant advanced non-small cell lung cancer: the SELECT-1 randomized clinical trial. *JAMA* 317(18):1844–1853
 135. Kim C, Giaccone G (2018) MEK inhibitors under development for treatment of non-small-cell lung cancer. *Expert Opin Investig Drugs* 27(1):17–30
 136. Moriceau G et al (2015) Tunable-combinatorial mechanisms of acquired resistance limit the efficacy of BRAF/MEK cotargeting but result in melanoma drug addiction. *Cancer Cell* 27(2):240–256

137. Long GV et al (2017) Dabrafenib plus trametinib versus dabrafenib monotherapy in patients with metastatic BRAF V600E/K-mutant melanoma: long-term survival and safety analysis of a phase 3 study. *Ann Oncol* 28(7):1631–1639
138. Long GV et al (2017) Adjuvant dabrafenib plus trametinib in stage III BRAF-mutated melanoma. *N Engl J Med* 377(19):1813–1823
139. Ascierto PA et al (2016) Cobimetinib combined with vemurafenib in advanced BRAF(V600)-mutant melanoma (coBRIM): updated efficacy results from a randomised, double-blind, phase 3 trial. *Lancet Oncol* 17(9):1248–1260
140. Griffin M et al (2017) BRAF inhibitors: resistance and the promise of combination treatments for melanoma. *Oncotarget* 8(44):78174–78192
141. Faivre S, Kroemer G, Raymond E (2006) Current development of mTOR inhibitors as anticancer agents. *Nat Rev Drug Discov* 5:671
142. Anagnostopoulou V et al (2013) Differential effects of dehydroepiandrosterone and testosterone in prostate and colon cancer cell apoptosis: the role of nerve growth factor (NGF) receptors. *Endocrinology* 154:2446
143. WeiSz L, Efferth T (2012) Polo-like kinase 1 as target for cancer therapy. *Exp Hematol Oncol* 1:38
144. Akinleye A et al (2013) Phosphatidylinositol 3-kinase (PI3K) inhibitors as cancer therapeutics. *J Hematol Oncol* 6:88
145. Fayard E et al (2011) Protein kinase B (PKB/Akt), a key mediator of the PI3K signaling pathway. In: *Phosphoinositide 3-kinase in health and disease*. Springer, New York, pp 31–56
146. Cance WG et al (2013) Disrupting the scaffold to improve focal adhesion kinase-targeted cancer therapeutics. *Sci Signal* 6:pe10
147. Ahmed K et al (2015) Targeting CK2 for cancer therapy using a nanomedicine approach. In: *Protein kinase CK2 cellular function in normal and disease states*. Springer, New York, pp 299–315
148. Hilton JF, Shapiro GI (2014) Aurora kinase inhibition as an anticancer strategy. *J Clin Oncol* 32:57
149. Jones JA et al (2017) Efficacy and safety of idelalisib in combination with ofatumumab for previously treated chronic lymphocytic leukaemia: an open-label, randomised phase 3 trial. *Lancet Haematol* 4(3):e114–e126
150. Pandey R, Kapur R (2018) Kinase inhibitors in clinical practice: an expanding world. *J Allergy Clin Immunol* 141(2):522–524
151. Shapiro GI et al (2015) First-in-human study of PF-05212384 (PKI-587), a small-molecule, intravenous, dual inhibitor of PI3K and mTOR in patients with advanced cancer. *Clin Cancer Res* 21(8):1888–1895
152. Eriksson A et al (2015) Drug screen in patient cells suggests quinacrine to be repositioned for treatment of acute myeloid leukemia. *Blood Cancer J* 5:e307
153. Haik S et al (2014) Doxycycline in Creutzfeldt-Jakob disease: a phase 2, randomised, double-blind, placebo-controlled trial. *Lancet Neurol* 13:150
154. Bedard PL et al (2014) Abstract CT205: a phase I dose-escalation study of trametinib (T) in combination with continuous or intermittent GSK2126458 (GSK458) in patients (pts) with advanced solid tumors. *Cancer Res* 74:CT205
155. Dowsett M et al (2012) Phase II randomized study of pre-operative pf-04691502 plus letrozole compared with letrozole (L) in patients with estrogen receptor-positive, HER2-negative early breast cancer (BC). *Ann Oncol* 23:44
156. Powles T et al (2014) A randomized phase II study of GDC-0980 versus everolimus in metastatic renal cell carcinoma (mRCC) patients (pts) after VEGF-targeted therapy (VEGF-TT). *J Clin Oncol* 32(15_suppl):4525
157. Yu P et al (2014) Characterization of the activity of the PI3K/mTOR inhibitor XL765 (SAR245409) in tumor models with diverse genetic alterations affecting the PI3K pathway. *Mol Cancer Ther* 13:1078

158. Mukherjee B et al (2012) The dual PI3K/mTOR inhibitor NVP-BEZ235 is a potent inhibitor of ATM-and DNA-PKCs-mediated DNA damage responses. *Neoplasia* 14:34
159. Bauer TM, Patel MR, Infante JR (2015) Targeting PI3 kinase in cancer. *Pharmacol Ther* 146:53–60
160. Di Leo A et al (2018) Buparlisib plus fulvestrant in postmenopausal women with hormone-receptor-positive, HER2-negative, advanced breast cancer progressing on or after mTOR inhibition (BELLE-3): a randomised, double-blind, placebo-controlled, phase 3 trial. *Lancet Oncol* 19(1):87–100
161. Manic G et al (2015) Trial watch: targeting ATM-CHEK2 and ATR-CHEK1 pathways for anticancer therapy. *Mol Cell Oncol* 2(4):e1012976
162. Lee J-M et al (2018) Prexasertib, a cell cycle checkpoint kinase 1 and 2 inhibitor, in *BRCA* wild-type recurrent high-grade serous ovarian cancer: a first-in-class proof-of-concept phase 2 study. *Lancet Oncol* 19(2):207–215
163. Wilson TR et al (2012) Widespread potential for growth-factor-driven resistance to anticancer kinase inhibitors. *Nature* 487:505
164. Lito P, Rosen N, Solit DB (2013) Tumor adaptation and resistance to RAF inhibitors. *Nat Med* 19:1401
165. Chell V et al (2013) Tumour cell responses to new fibroblast growth factor receptor tyrosine kinase inhibitors and identification of a gatekeeper mutation in FGFR3 as a mechanism of acquired resistance. *Oncogene* 32:3059
166. Foguel D et al (2014) The importance of a gatekeeper residue on the aggregation of transthyretin implications for transthyretin-related amyloidoses. *J Biol Chem* 289(41):28324–28337
167. Liu Y, Gray NS (2006) Rational design of inhibitors that bind to inactive kinase conformations. *Nat Chem Biol* 2:358–364
168. Gibbons DL et al (2012) The rise and fall of gatekeeper mutations? The BCR-ABL1 T315I paradigm. *Cancer* 118:293
169. Heinrich MC et al (2006) Molecular correlates of imatinib resistance in gastrointestinal stromal tumors. *J Clin Oncol* 24:4764
170. Metzgeroth G et al (2012) Limited clinical activity of nilotinib and sorafenib in FIP1L1-PDGFR α positive chronic eosinophilic leukemia with imatinib-resistant T674I mutation. *Leukemia* 26:162
171. Nishikawa S et al (2018) Selective gene amplification to detect the T790M mutation in plasma from patients with advanced non-small cell lung cancer (NSCLC) who have developed epidermal growth factor receptor tyrosine kinase inhibitor (EGFR-TKI) resistance. *J Thorac Dis* 10(3):1431–1439
172. Pauwels D, Sweron B, Cools J (2012) The N676D and G697R mutations in the kinase domain of FLT3 confer resistance to the inhibitor AC220. *Haematologica* 97:1773
173. Xavier CP et al (2009) Luteolin, quercetin and ursolic acid are potent inhibitors of proliferation and inducers of apoptosis in both KRAS and BRAF mutated human colorectal cancer cells. *Cancer Lett* 281:162
174. Kobayashi S et al (2005) EGFR mutation and resistance of non-small-cell lung cancer to gefitinib. *N Engl J Med* 352:786
175. Pao W et al (2005) Acquired resistance of lung adenocarcinomas to gefitinib or erlotinib is associated with a second mutation in the EGFR kinase domain. *PLoS Med* 2:e73
176. Yun CH et al (2008) The T790M mutation in EGFR kinase causes drug resistance by increasing the affinity for ATP. *Proc Natl Acad Sci* 105:2070
177. Heymach JV et al (2006) Epidermal growth factor receptor inhibitors in development for the treatment of non-small cell lung cancer. *Clin Cancer Res* 12:4441s
178. Kwak EL et al (2005) Irreversible inhibitors of the EGF receptor may circumvent acquired resistance to gefitinib. *Proc Natl Acad Sci U S A* 102:7665
179. Modugno M et al (2007) Crystal structure of the T315I Abl mutant in complex with the aurora kinases inhibitor PHA-739358. *Cancer Res* 67:7987

180. Weisberg E et al (2005) Characterization of AMN107, a selective inhibitor of native and mutant Bcr-Abl. *Cancer Cell* 7:129
181. Gumireddy K et al (2005) A non-ATP-competitive inhibitor of BCR-ABL overrides imatinib resistance. *Proc Natl Acad Sci U S A* 102:1992
182. Gumireddy K et al (2005) ON01910, a non-ATP-competitive small molecule inhibitor of Plk1, is a potent anticancer agent. *Cancer Cell* 7:275
183. Copland M et al (2008) BMS-214662 potently induces apoptosis of chronic myeloid leukemia stem and progenitor cells and synergizes with tyrosine kinase inhibitors. *Blood* 111:2843
184. Orphanos GS, Ioannidis GN, Ardavanis AG (2009) Cardiotoxicity induced by tyrosine kinase inhibitors. *Acta Oncol* 48:964
185. Shah DR, Shah RR, Morganroth J (2013) Tyrosine kinase inhibitors: their on-target toxicities as potential indicators of efficacy. *Drug Saf* 36:413
186. Mayor S (2006) Targeting cardiovascular complications. *Lancet Oncol* 7:282
187. Moslehi JJ, Deininger M (2015) Tyrosine kinase inhibitor-associated cardiovascular toxicity in chronic myeloid leukemia. *J Clin Oncol* 33:4210
188. Bernards R, Brummelkamp TR, Beijersbergen RL (2006) shRNA libraries and their use in cancer genetics. *Nat Methods* 3:701

Case Study on Receptor Tyrosine Kinases EGFR, VEGFR, and PDGFR



Lídia Moreira Lima, Maria Leticia de Castro Barbosa,
Daniel Nascimento do Amaral, and Eliezer J. Barreiro

Contents

1	Receptor Tyrosine Kinases and Inhibitors	156
2	Epidermal Growth Factor Receptor (EGFR)	158
2.1	FDA-Approved EGFR Inhibitors	159
2.2	Development of 4-Anilinoquinazolines as EGFR Inhibitors	159
2.3	EGFR Inhibitors for Non-small Cell Lung Cancer (NSCLC) Treatment	166
2.4	Second-Generation EGFRi and the Strategy to Circumvent Resistance Development Mediated by EGFR T790M Mutation	167
3	Vascular Endothelial Growth Factor Receptors (VEGFRs)	171
3.1	VEGF and Angiogenesis	172
3.2	VEGFR-2 Structural Characteristics	173
3.3	VEGFR Inhibitors	173
3.4	Lenvatinib Story Case	177
4	Platelet-Derived Growth Factor Receptor (PDGFR)	182
4.1	PDGFR and Tumorigenesis	183
4.2	PDGFR Role in Several Tumor Types	183
4.3	PDGFR Inhibitors	185
5	Epilogue	192
	References	192

Abstract Receptor tyrosine kinases (RTKs) are cell-surface proteins that trigger key cellular responses, such as survival, proliferation, differentiation, migration, and cell-cycle control. As increased activity, abundance, and/or cellular distribution of wild-type and mutant forms of RTKs is often associated with tumor establishment, growth, and progression, several drugs directed to clinically relevant RTKs have entered the pharmaceutical market since the beginning of the twenty-first century, representing innovative approaches for cancer treatment. The modulation strategies include small-molecule tyrosine kinase inhibitors (TKIs), targeting the ATP-binding

L. M. Lima, M. L. de Castro Barbosa, D. N. do Amaral, and E. J. Barreiro (✉)
Instituto Nacional de Ciência e Tecnologia de Fármacos e Medicamentos (INCT-INOFAR),
Laboratório de Avaliação e Síntese de Substâncias Bioativas (LASSBio®), Universidade
Federal do Rio de Janeiro, Rio de Janeiro, Brazil
e-mail: ejbarreiro@ccsdecania.ufrj.br

site of the intracellular TK domain, and monoclonal antibodies directed to the extracellular domain, interfering with RTK activation and/or marking RTK-expressing cells for destruction by the immune system. Even though these drugs clearly represented an impressive breakthrough in the therapy of RTK-addicted tumors, resistance development and detection of refractory tumors have given rise to novel therapeutic challenges, pushing the drug discovery process forward. This chapter focuses particularly on the discussion of several case studies on the development of small-molecule tyrosine kinase inhibitors (TKIs) directed to EGFR, VEGFR, and PDGFR, clinically relevant RTKs, and the subset of advances in this field.

Keywords Cancer, Epidermal growth factor receptor (EGFR), Platelet-derived growth factor receptor (PDGFR), Receptor tyrosine kinases (RTKs), Tyrosine kinase inhibitors (TKIs), Vascular endothelial growth factor receptor (VEGFR)

1 Receptor Tyrosine Kinases and Inhibitors

Receptor tyrosine kinases (RTKs) are cell-surface proteins that trigger key cellular responses, such as survival, proliferation, differentiation, migration, and cell-cycle control [1, 2]. All RTKs belonging to 20 subfamilies encoded by human genome share a common structural architecture, comprising an extracellular (EC) agonist-binding domain, a single transmembrane helix, and a cytoplasmic subunit with a juxtamembrane (JM) region and a tyrosine kinase (TK) domain, which is in turn subdivided into the ATP-binding region (TK1) and the phosphotransferase region (TK2) [1, 3, 4].

Particularly the TK domain is responsible for transferring the terminal phosphate of adenosine triphosphate (ATP) to the corresponding substrates. This catalytic domain contains a typical bilobal architecture connected by the so-called hinge region, located in the cleft between these two lobes (Fig. 1). The adenine core of ATP forms two hydrogen bonds with the *hinge* amino acid backbone, while the phosphate and ribose groups of ATP are directed to the solvent-accessible surface area through a hydrophilic channel, while the side chain of the so-called gatekeeper residue defines the total volume of the ATP-binding pocket among different kinases [5–7]. The conformational topology of the glycine-rich region (GXGXXG) in the *N*-lobe, also known as flexible phosphate-binding loop (P-loop), is considered to be a structurally determinant factor for the pocket configuration. Moreover, kinases present an activation loop (A-loop), which starts with a flexible conserved amino acid sequence Asp-Phe-Gly (DFG). Since the A-loop has flexible variations in size and sequence, its conformation is critical for modulating kinase catalytic activity [6, 8].

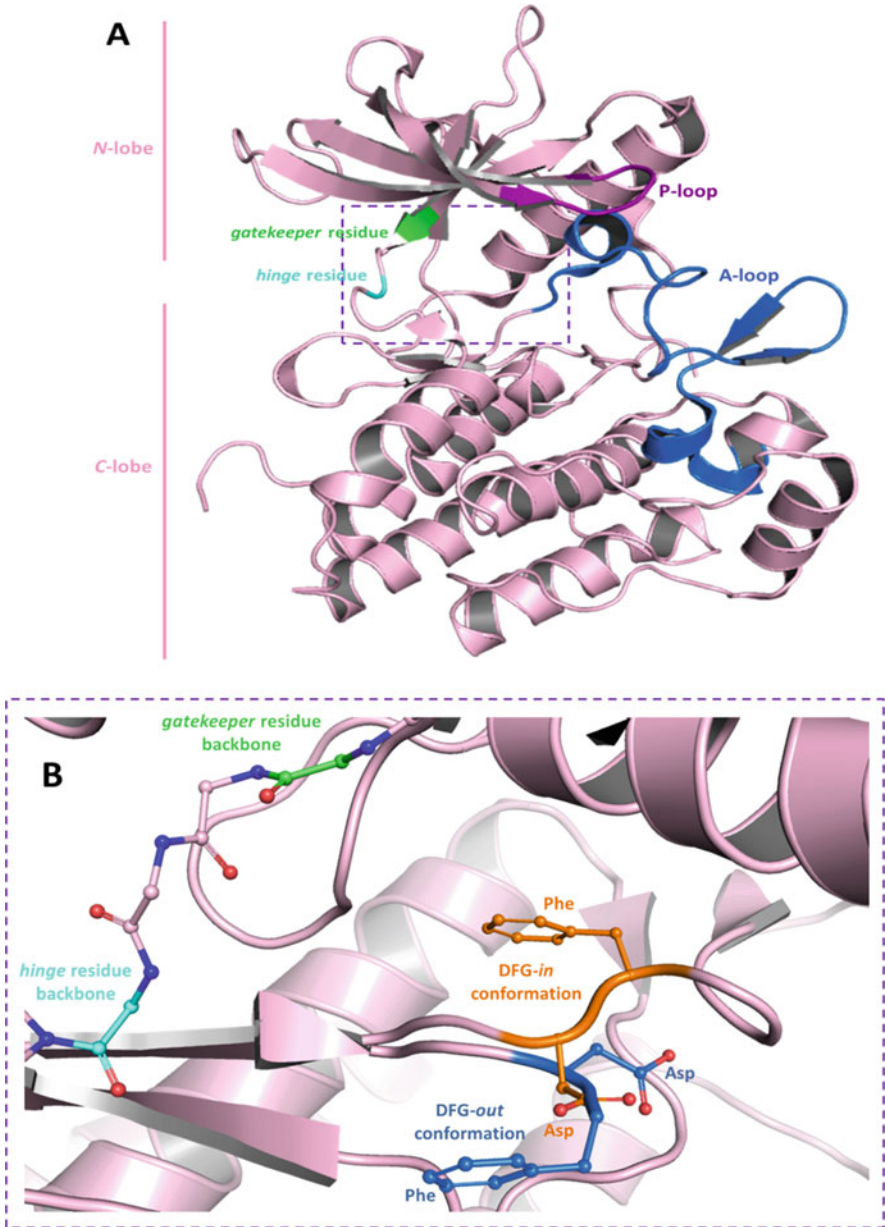


Fig. 1 (a) Tyrosine kinase domain with a typical bilobal architecture connected by the so-called hinge region, located in the cleft between the *N*-lobe and the *C*-lobe. (b) Kinase ATP-binding pocket with the conserved amino acid sequence Asp-Phe-Gly (DFG) in the active *DFG-in* and the inactive *DFG-out* conformations. The backbones of *hinge* and *gatekeeper* residues are also highlighted

The active DFG-*in* conformation of a kinase is characterized by the conserved DFG Asp residue facing the ATP-binding site. This Asp coordinates to Mg^{2+} ions, forming a bridge contact with the ATP's triphosphate group, while the side chain of the Phe residue is contained in a hydrophobic adjacent pocket (Fig. 1) [5, 7].

In turn, in the so-called DFG-*out* conformation, the side chain of Asp is placed away from the ATP pocket through a rearrangement of the DFG loop, preventing ATP binding and prompting the phenyl ring to leave the aforementioned adjacent hydrophobic pocket (Fig. 1) [5, 9].

Several cancer types are associated with genetic modifications or abnormalities in RTKs, resulting in increased activity, abundance, and/or cellular distribution. Therefore, many efforts have been dedicated to the search of novel drugs able to block or attenuate RTK signaling pathways, with a number of RTK inhibitors already approved by the US Food and Drug Administration (FDA) [2, 7, 10].

The modulation strategies include small-molecule tyrosine kinase inhibitors (TKIs), targeting the ATP-binding site of the intracellular TK domain [7, 10], and monoclonal antibodies directed to the extracellular domain, interfering with RTK activation and/or marking RTK-expressing cells for destruction by the immune system [1].

TKIs can be, in turn, subdivided according to their preferential interactions with active DFG-*in* or inactive DFG-*out* target conformations. Type I TKIs interact in and around the ATP-binding region of the target in a DFG-*in* conformation, performing hydrogen bonds with the *hinge* residue and additional hydrophobic and electrostatic interactions with the adjacent amino acid residues, which can differ between the TK family members [11]. In contrast, type II TKIs bind and stabilize the inactive DFG-*out* conformation of the target RTK, not only interacting with the ATP-binding site but also occupying the adjacent hydrophobic pocket available in this conformation as an allosteric binding site (Fig. 1) [6, 7]. This chapter focuses particularly on the discussion of several case studies on the development of small-molecule tyrosine kinase inhibitors (TKIs) directed to clinically relevant RTKs and the subset of advances in this field.

2 Epidermal Growth Factor Receptor (EGFR)

Epidermal growth factor receptor (EGFR, ErbB-1, HER-1) is a RTK member of the ErbB receptor family, which is related to cellular growth, differentiation, and survival. The other members of the ErbB RTK family are ErbB-2 (HER-2), ErbB-3 (HER-3), and ErbB-4 (HER-4) [12, 13]. The EGFR activation process is initiated by extracellular ligand recognition, inducing receptor dimerization with formation of homodimers of EGFR or heterodimers between EGFR and other ErbB family members [14, 15], among which ErbB-2 (HER-2) is the most common EGFR heterodimerization partner [16].

Ligands of the EGFR extracellular binding domain comprise epidermal growth factor (EGF), transforming growth factor alpha ($TGF-\alpha$), amphiregulin (AR), epigen

(EP), β -cellulin (BTC), heparin-binding EGF (HB-EGF), and epiregulin (EPR) [17, 18], and the main signaling pathways triggered by EGFR activation are PI3K/AKT and MAPK and indirectly IL-6-mediated STAT activation [19, 20].

Deregulation of EGFR activity is associated with more aggressive epidermal tumors, e.g., lungs, pancreas, breast, colon, and head and neck, and with poor prognosis [21, 22], usually as a consequence of receptor overexpression, ligand overproduction, and/or constitutive receptor activation due to point mutations or other genetic alterations [23–27].

In this context, scientific efforts were extensively dedicated to enable the pharmacologic modulation of EGFR activity through the inhibition of its catalytic domain with small molecular weight TKIs. Subsequent approval of several drugs from this class by FDA demonstrated their clinical efficacy in different tumor types [28]. However, challenges for the near future of this therapeutic strategy have also emerged, as discussed throughout this chapter.

2.1 FDA-Approved EGFR Inhibitors

Currently six small molecular weight TKI drugs (1–6) are approved by FDA for treating patients with tumors related to EGFR-deregulated activity (Fig. 2) [7, 10]. Gefitinib (1; ZD1819; Iressa™; AstraZeneca), erlotinib (2; CP-258,774; Tarceva™; Roche), and afatinib (5; BIBW2992; Giotrif™; Boehringer Ingelheim) are approved by FDA for treatment of patients with non-small cell lung cancer (NSCLC). In late 2015, osimertinib (6; AZD9291; Tagrisso™; AstraZeneca) was approved as breakthrough therapy to treat NSCLC with no clinical benefits from prior EGFR TKIs [29].

Lapatinib (3, GW572016; Tykerb™; GlaxoSmithKline) has as a primary indication for the treatment of breast cancer patients with HER-2 overexpression and with no response to first choice drugs. In turn, vandetanib (4, ZD6474; Caprelsa™; AstraZeneca) is approved to treat medullary thyroid cancer [30–32].

The 4-anilinoquinazoline moiety has been extensively explored for the last decades in TKI drug discovery projects, especially for EGFR inhibition [33]. Noticeably, five of six approved EGFR TKI drugs have in common this privileged scaffold in their chemical structure (Fig. 2).

2.2 Development of 4-Anilinoquinazolines as EGFR Inhibitors

The history of the development of 4-anilinoquinazoline derivatives as EGFR inhibitors begins in the 1990s during research efforts undertaken at Zeneca Pharmaceuticals. Through a virtual screening approach using Zeneca Company Compound

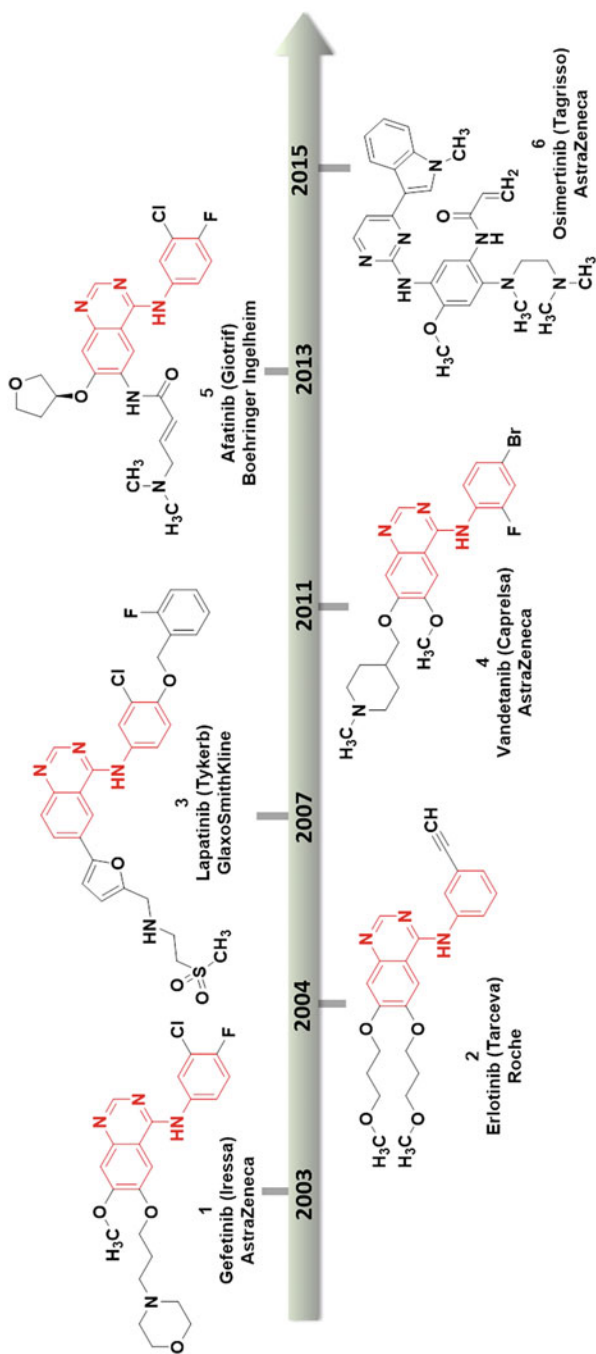


Fig. 2 FDA-approved small-molecule EGFR inhibitors 1-6. Noticeably, five of six approved EGFR TKI drugs have in common the privileged 4-aminoquinazoline scaffold highlighted in red

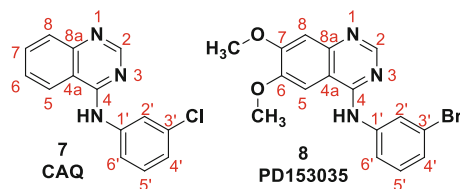


Fig. 3 First examples of 4-anilinoquinazoline EGFR inhibitors described in literature during the 1990s: 4-(3-chloroanilino)quinazoline (**7**, CAQ) from Zeneca Pharmaceuticals and PD153035 (**8**) from Parke Davis Laboratory

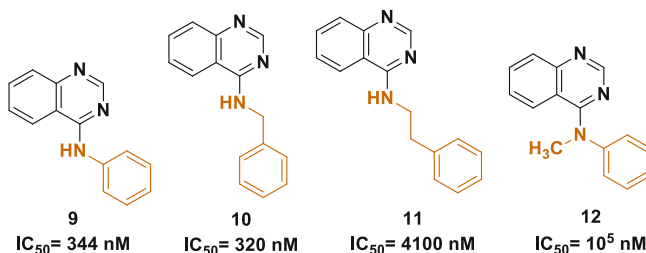


Fig. 4 The influence of substituents at quinazoline carbon 4 (C4), highlighted in orange, on EGFR inhibitory activity

Collection, researchers were able to identify compound 4-(3-chloroanilino)quinazoline (**7**, CAQ) as an ATP-competitive inhibitor with high affinity to EGFR ($K_i = 16$ nM) (Fig. 3) [34].

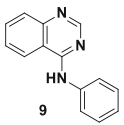
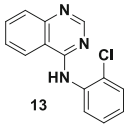
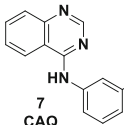
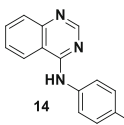
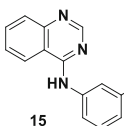
Simultaneously, researchers from Parke Davis Laboratory described compound PD153035 (**8**; Fig. 3) as a highly potent ATP-competitive EGFR inhibitor ($IC_{50} = 30$ pM) presenting an outstanding selectivity profile against other tyrosine kinases, e.g., platelet-derived growth factor receptor (PDGFR), fibroblast growth factor receptor (FGFR), insulin receptor (IR), and colony-stimulating factor-1 receptor (CSF-1R) [35].

As selectivity represents a major concern in the development of ATP-competitive protein kinase (PK) inhibitors, these data shed light on a brand-new world, where potent and selective compounds would be able to be designed and developed for treating disorders related to the deregulation of these proteins.

During the following years, the structure-activity relationship (SAR) of 4-anilinoquinazolines for EGFR inhibition and their selectivity against other kinases were better understood through a ligand-based drug design (LBDD) approach.

Rewcastle and colleagues studied the influence of substituents at quinazoline carbon 4 (C4) for the EGFR inhibitory activity (Fig. 4), exploring the homologation strategy of molecular modification. The aniline (**9**) and benzylamine (**10**) derivatives are equipotent EGFR inhibitors, while phenylethylamine derivative **11** is about ten times less potent. By contrast, the *N*-methylated derivative **12** loses its EGFR inhibitory potency, demonstrating the requirement of a secondary amino group in the anilinoquinazoline moiety [36].

Table 1 Enzymatic and cellular EGFR inhibitory potencies for the selected 4-anilinoquinazoline derivatives [37]

Compound	IC ₅₀ (μM)	EGF-stimulated KB cells (μM)	Basal EGF-stimulated KB cells (μM)	KB cellular selectivity
 9	0.55	12.5	38	3.04
 13	1	>12.5	25	not determined
 7 CAQ	0.04	1.2	15	12.5
 14	0.5	3.6	6	1.67
 15	0.02	0.8	12.5	15.6

Subsequently, Wakeling and coworkers described the influence of substituents in the aniline moiety on EGFR inhibition (Table 1), based on enzymatic and cellular assays. The determination of cellular activity in EGF-dependent cells and selectivity against EGF-non-dependent cells was performed through the inhibition of KB cell line proliferation when stimulated and non-stimulated by EGF [37].

Among the chlorine-substituted derivatives (**7**, **13**, **14**), the most potent compound is the previously described *meta*-chloro analogue (**7**, CAQ). Moreover, the *meta*-bromo derivative **15** was identified in the KB cell line assay as the most potent and selective from this series (Table 1) [37].

Intending to explore the role of nitrogen atoms in the heteroaromatic core, several nitrogen-containing bicyclic aromatic systems with the *meta*-bromo-aniline substituent were also evaluated for EGFR inhibition (Fig. 5). The 4-anilinoquinazoline moiety was identified as an ideal heteroaromatic bicyclic system, suggesting that the particular substitution pattern is favorable for interaction with the target protein and that electronic aspects might also be considered once the electron density of the N1 atom differs between the quinazoline, quinoline, isoquinoline, cinnoline, phthalazine, benzo[*d*][1,2,3]triazine, and quinoxaline bicyclic systems [36].

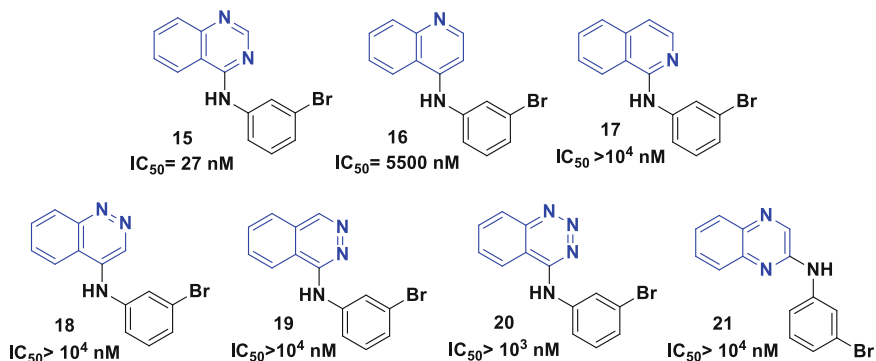


Fig. 5 The influence of heteroaromatic bicyclic systems, highlighted in blue, on the EGFR inhibitory activity

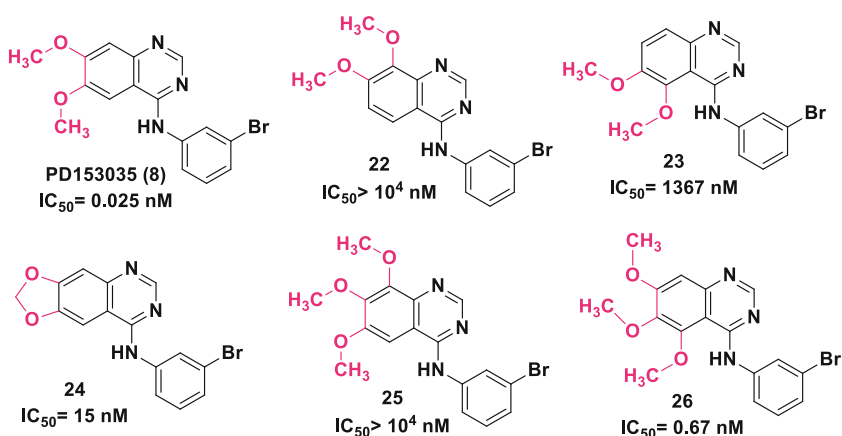


Fig. 6 The influence of alkoxy substituents in the quinazoline moiety, highlighted in magenta, on EGFR inhibition

The substitution pattern of the quinazoline core was also explored. Initially, monosubstituted and disubstituted derivatives bearing nitro, amino, and methoxy groups were evaluated, highlighting the impressive potency of the 6,7-dimethoxy analogue PD153035 (**8**; $IC_{50} = 29 \text{ pM}$) in comparison with other monosubstituted and disubstituted members of the congener series [36, 38]. An additional study with dimethoxy, methylenedioxy, and trimethoxy derivatives proved the pivotal role of 6,7-dialkoxy groups as substituents in the quinazoline moiety for EGFR inhibition (Fig. 6) [39].

It is important to keep in mind that subtle modifications in the chemical structure of protein kinase inhibitors (PKIs) might affect not only the potency for the target kinase but also the selectivity of compounds toward the kinase. For instance, methylation of the aniline nitrogen of derivative **27** led to a loss of EGFR (~80

Fig. 7 Methylation of the aniline nitrogen in the 4-anilinoquinazoline moiety affects the inhibitory potency and the selectivity profile among different kinases

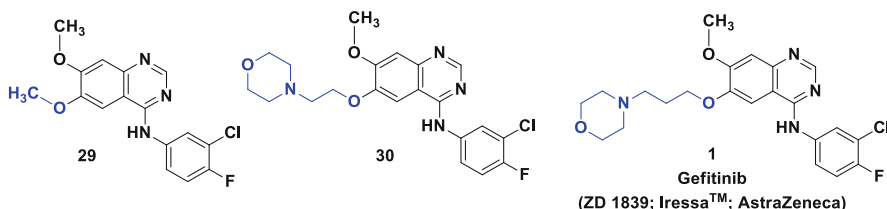
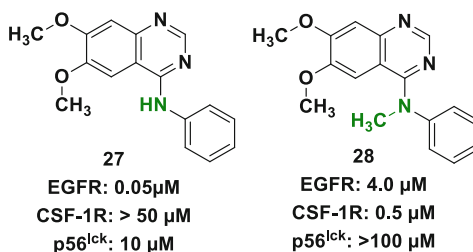


Fig. 8 Structural modifications performed in C6 alkoxy substituent of the EGFR inhibitor **29** in order to improve physical-chemical properties and optimize oral bioavailability, originating from gefitinib (**1**; ZD1819; IressaTM; AstraZeneca) as the first EGFR inhibitor approved for clinical use in EGFR-addicted tumors

times) and p56^{lck} (more than 10 times) inhibitory potencies, but, on the other hand, the *N*-methyl analogue **28** gained significant potency on CSF-1R (Fig. 7) [40–42].

Gefitinib (**1**; ZD1819; IressaTM; AstraZeneca; Fig. 2), the first EGFR inhibitor approved for clinical use in EGFR-addicted tumors, was discovered in a research effort for clinical development of novel 4-anilinoquinazoline derivatives with adequate oral bioavailability for once-a-day administration [43].

Aiming to optimize the pharmacokinetics of the already described 6,7-dimethoxy-4-anilinoquinazoline inhibitor **29**, modifications in the C6 substituent were performed in order to improve physical-chemical properties (Fig. 8). Derivative **29** presents satisfactory metabolic stability with reduced clearance in mice and high in vitro potency in enzymatic ($IC_{50} = 9$ nM) and cellular assays (EGF-stimulated KB cells $IC_{50} = 80$ nM).

The introduction of a *para*-fluorine is a well-known strategy to improve metabolic stability of bioactive compounds and clinical candidates, protecting the C4 position from aromatic hydroxylation and ensuring a lower metabolic lability [44, 45].

It is important to mention that during hit-to-lead optimization other parameters besides potency are considered for the selection of the best compound for further clinical development, including oral bioavailability, distribution, clearance, and metabolic stability. In this context, even though more potent EGFR inhibitors were known, derivative **29** was selected for additional SAR studies, considering adequate plasmatic concentrations achieved 6 and 24 h after oral administration [43].

Among all C6-modified alkoxy derivatives, those bearing a cyclic morpholine side chain were equipotent in the enzymatic assay (**30** $IC_{50} = 20$ nM and

1 ($IC_{50} = 23$ nM), presenting the most promising results from the series. However, compound ZD1839 (**1**) with a longer spacer in the C6 side chain was selected as this analogue presented high and sustained blood concentration after oral administration and was more potent than **30** in the cellular assay ($IC_{50} = 80 \times 380$ nM, respectively; Fig. 8) [43].

Preclinical studies confirmed the antitumor efficacy of ZD1919 (**1**), later named gefitinib (IressaTM), in animal xenograft models, and early phase I clinical trials established the adequate oral bioavailability of **1** in a once-a-day dose regimen [46].

Since EGFR crystallographic data were not yet available, Palmer and colleagues constructed an *in silico* structural model [47] using as background the previous SAR studies and the crystal structure of a cAMP-dependent protein kinase [48]. According to this model, the 4-anilinoquinazoline derivatives would interact with the EGFR-ATP-binding site through hydrogen bonds with specific amino acid residues and nonpolar interactions within a hydrophobic pocket at the *hinge* region neighborhood. H-bonds between the *hinge* methionine residue 793 (M793) and the quinazoline N1 atom and between the side chain of the *gatekeeper* threonine residue 790 (T790) and the quinazoline N3 atom were suggested. In turn, the aniline moiety would fit into a hydrophobic pocket non-occupied by ATP, and this particular interaction was supposed to confer selectivity for EGFR inhibition within the kinome [47].

Analyses of previous results also indicated that a polar interaction with M793 would be more important than one with T790 residue, as the 4-anilinoquinoline derivative **16** presented significant EGFR inhibitory activity while the 2-anilinoisoquinoline derivative **17** did not (Fig. 5).

Five years later, in 2002, a co-crystallized structure of EGFR with a 4-anilinoquinazoline inhibitor was finally obtained and elucidated. Erlotinib (**2**; CP-258,774; TarcevaTM; Roche, Fig. 2), the inhibitor present in the mentioned crystal structure (Protein Data Bank code: 1M17), was originally described in 1997 as a potent and selective ATP-competitive EGFR inhibitor (EGFRi) [49].

Compound **2** has an acetylene group at the *meta* position of the aniline ring, which is twisted in an angle of 42° in relation to the quinazoline moiety and is placed inside a hydrophobic pocket in the binding region, performing nonpolar interactions with T790, K745, and L788 amino acid residues. As already anticipated by Palmer [47], the quinazoline N1 acts as a hydrogen bond acceptor to the amide hydrogen of the M793 residue backbone. Additionally, the quinazoline N3 atom interacts with the side chain of the *gatekeeper* residue T790 through a water-bridged H-bond, and both C6 and C7 substituents are directed to a solvent-exposed region in the outer area of the protein [50] (Fig. 9).

Gefitinib (**1**; ZD1819; IressaTM; AstraZeneca) and erlotinib (**2**; CP-258,774; TarcevaTM; Roche) were initially approved in 2003 and 2004, respectively, as third-line therapies for patients with metastatic or advanced NSCLC who did not respond to chemotherapy with docetaxel and platinum-based antineoplastic drugs [51–53]. These EGFRi are currently being approved as first-line therapies for treatment of metastatic NSCLC characterized by the occurrence of EGFR-activating mutations.

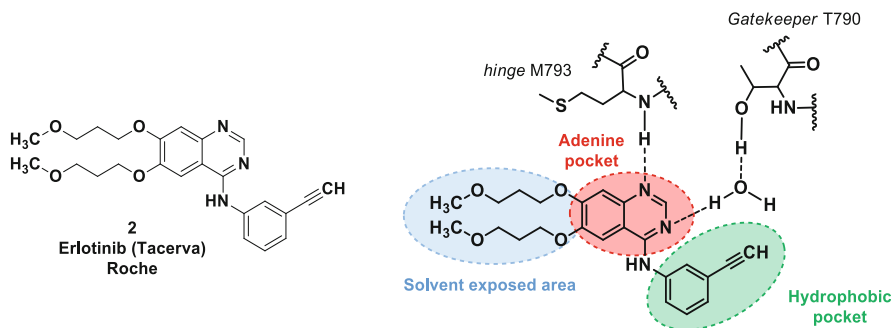


Fig. 9 Binding mode of erlotinib (**2**; CP-258,774; Tarceva™; Roche) to the EGFR kinase domain elucidated by co-crystallization with the target protein

2.3 EGFR Inhibitors for Non-small Cell Lung Cancer (NSCLC) Treatment

The 4-anilinoquinazoline EGFRi gefitinib (**1**) and erlotinib (**2**) represented an impressive innovation in NSCLC therapy. However, clinical responses differ significantly among the treated patients. Over the last years, clinical data have demonstrated a clear connection between therapy responsiveness to first-generation EGFRi and the existence of mutations in this protein [54].

EGFR mutations may be beneficial for treatment when associated with enhanced response rates and antitumor efficacy but may also be deleterious when related to drug resistance and clinical inefficacy [55]. For this reason, genetic diagnostic testing has become an important tool for the identification of patients tending to be more responsive to a specific EGFRi [56, 57].

Among NSCLC patients, only 10–20% respond to EGFRi first-generation drugs. The most common EGFR genetic alterations associated with a better clinical outcome are the point mutation L858R in exon 21, with the change of a leucine for an arginine residue, and the amino acid deletion 746–750 in exon 19 [55, 58]. First-generation EGFRi present higher affinity for EGFR_{L858R} and EGFR_{del747-750} than for EGFR wild-type (EGFR_{wt}), and NSCLC patients harboring these mutations consequently show a better treatment response to these drugs [59, 60].

Moreover, after 10–14 months of treatment, initially responsive patients usually become resistant to these drugs. A single-point mutation in the *gatekeeper* threonine residue to a methionine (T790M) and an EGFR_{L858R/T790M} double-mutant form are commonly associated with this acquired resistance. The T790M-mutated EGFR is more frequent in advanced tumors and can be observed in approximately 60% of resistant patients [61, 62]. It is worth mentioning that *gatekeeper* mutations of other protein kinases, e.g., Abl (T315I), PDGFRA (T674I), c-KIT (T670I), and ALK (L1196M), have already been described as common causes for clinical resistance to inhibitors [63, 64].

Several studies were performed in an attempt to elucidate the precise molecular reason behind the resistance development in T790M-mutated EGFR. Initially, the loss of affinity observed for EGFRi gefitinib (**1**) and erlotinib (**2**) was associated with steric constraints in the binding pocket due to the substitution of the smaller threonine by the bulkier methionine residue, hampering a proper interaction with the ATP-binding site [65]. However, crystallographic data revealed no significant differences in the crystal structures of gefitinib (**1**) co-crystallized with EGFR_{wt} and EGFR_{L858R/T790M}. These experimental results weakened the steric clash hypothesis [66].

Subsequently, Yun and colleagues demonstrated that the lower potency of gefitinib (**1**) and erlotinib (**2**) for EGFR_{T790M} inhibition was actually a consequence of an altered enzymatic kinetic. These authors clearly showed that ATP has a higher affinity for EGFR_{wt} and EGFR_{T790M} when compared to the sensible EGFR_{L858R}-mutated form. Consequently, competitive reversible inhibitors, e.g., gefitinib (**1**) and erlotinib (**2**), have shorter residence times and are easily displaced by ATP in the clinical nonresponsive EGFR variants. On the other hand, as ATP has a lower affinity for EGFR_{L858R}, first-generation EGFRi result in a better clinical outcome for patients harboring this EGFR mutation [60].

Moreover, these data indicate that NSCLC patients harboring EGFR_{T790M} or EGFR_{L858R/T790M} are not expected to respond adequately to treatment with first-generation EGFRi drugs, highlighting the critical need for the discovery of novel inhibitors active against these mutated forms [62, 67, 68].

2.4 Second-Generation EGFRi and the Strategy to Circumvent Resistance Development Mediated by EGFR T790M Mutation

Some years after the first reports of acquired resistance to gefitinib (**1**) mediated by EGFR_{T790M} mutation, Kwak and coworkers suggested the benefits of designing irreversible EGFRi to overcome this issue, due to their ability to inhibit diverse EGFR mutant forms, including EGFR_{T90M} [69]. The proposed irreversible inhibition would take place in two steps, comprising the formation of an initial reversible ligand-receptor complex, through complementary molecular recognition and induced fit of the ligand to the target protein, followed by a reaction between an electrophilic group in the structure of the EGFRi and a nucleophilic amino acid to generate a covalent bond. Usually, the nucleophilic amino acid contains a hydroxyl or thiol side chain, while the electrophilic site consists of a reactive chemical scaffold placed in a strategic position in the ligand structure after considering the chemical reactivity of the nucleophile and the topology of the target binding site [70–72].

The longer residence time observed for covalent inhibitors would be enough to inactivate the target protein until its de novo synthesis, allowing wider dosage intervals. Moreover, permanent inhibition of EGFR mutant forms and slow

Table 2 Alignment of a primary amino acid sequence fragment among ErbB family members, highlighting the cysteine residue conserved in EGFR (ErbB-1), HER-2 (ErbB-2), and HER-4 (ErbB-4)

ErbB-1	I ⁷⁸⁹	T	Q	L	M	P	F	G	C ⁷⁹⁷	L	L	D	Y ⁸⁰¹
ErbB-2	V ⁷⁹⁷	T	Q	L	M	P	Y	G	C ⁸⁰⁵	L	L	D	H ⁸⁰⁹
ErbB-3	V ⁷⁶⁷	T	Q	Y	L	P	L	G	S ⁷⁷⁵	L	L	D	H ⁷⁷⁹
ErbB-4	V ⁷⁹⁵	T	Q	L	M	P	H	G	C ⁸⁰³	L	L	E	Y ⁸⁰⁷

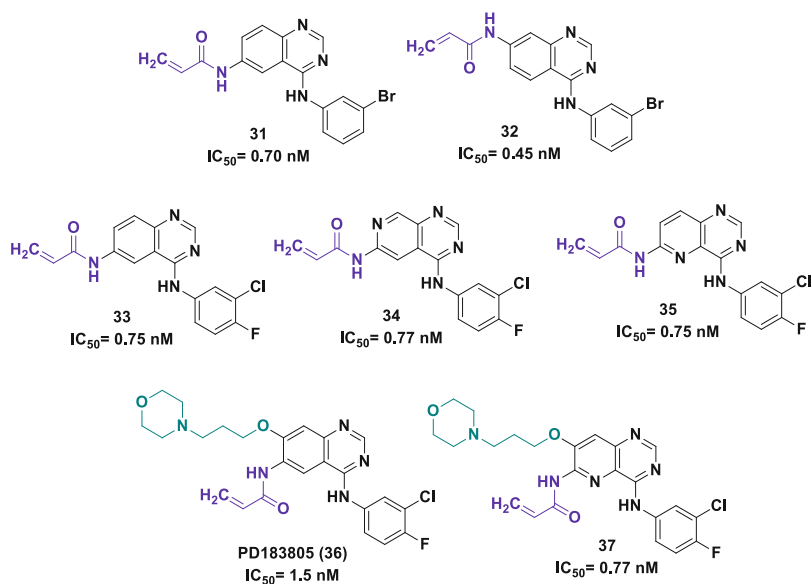


Fig. 10 First examples of EGFR covalent inhibitors described in literature by [77] (31–32), [78] (33–35), and [79] (36–37). The covalent binding acrylamide moiety is highlighted in purple and the solubilizing basic propoxymorpholine substituent in green

resistance development were expected to be relevant advantages of EGFR covalent irreversible inhibitors over ATP-competitive reversible inhibitors [73–75].

At that moment, the easy access to crystallographic data of EGFR_{wt} and mutant forms provided the basis for planning novel irreversible EGFRi through the structure-based drug design (SBDD) approach. Careful analysis of EGFR primary amino acid sequence and of its ATP-binding site tridimensional structure indicated the possibility of exploring a specific cysteine residue at position 797 (C797) for the design of selective covalent inhibitors, as C797 is not conserved among other protein kinase families. Actually, only EGFR (ErbB-1), HER-2 (ErbB-2), and HER-4 (ErbB-4) present this cysteine residue in an analogue position around the *hinge* region, and the proposed covalent inhibitors were expected to inhibit these ErbB family members, according to the data depicted in Table 2 [76].

At the end of the 1990s, Fry's research group described for the first time EGFR covalent inhibitors (Fig. 10) demonstrating their inhibitory mechanism by using

washout experiments, mass spectrometry, and mutagenesis assays [77]. Among the synthesized derivatives, PD168393 (**31**), substituted with an acrylamide moiety at quinazoline C6, presented an IC_{50} of 0.70 nM and a faster EGFR kinetic inactivation in comparison with the C7-substituted regioisomer **32**, which had shown a similar inhibitory potency ($IC_{50} = 0.45$ nM).

Additionally, even though covalent inhibitors usually raise some questions concerning selectivity, safety, and the possibility of adduct formation with off-targets, PD168393 (**31**) was demonstrated to be selective for EGFR, showing no inhibitory activity against several other PKs, e.g., platelet-derived growth factor receptor (PDGFR), fibroblast growth factor receptor (FGFR), protein kinase C (PKC), and insulin receptor [78].

Subsequently, a novel series of quinazoline (**33**) and pyrido[*d*]pyrimidine (**34–35**) EGFR covalent inhibitors was described (Fig. 10), and despite the similar enzymatic inhibitory potencies, the quinazoline derivative **33** showed selectivity to inhibit the proliferation of A431 cell line, which overexpresses EGFR, while pyrido[*d*]pyrimidine derivatives **34–35** were equipotent or even selective to the MDA-MD-435 cell line, overexpressing HER-2. Compound **33** presented promising preclinical results in tumor xenograft animal models, but solubility issues had hampered its clinical development considering the relevance of this molecular property for pharmacokinetics and in vivo activity [78]. To overcome these issues, the same research group in Parke Davis Laboratory designed novel EGFR covalent inhibitors bearing basic moieties at quinazoline C7, which would be easily protonated in vivo, keeping the acrylamide moiety at C6 [79].

According to enzymatic and cellular assays, the propoxymorpholine substituent (**36–37**) was identified as the most promising among the evaluated structural modifications (Fig. 10). The pyrido[*d*]pyrimidine derivative **37** showed lower hydrolysis stability and a higher reactivity to glutathione in comparison with quinazoline **36**. The more stable and less reactive derivative **36** also demonstrated a higher potency both in cellular and mouse xenograft models [79]. Compound PD183805 (**36**), later named canertinib, was then selected for clinical development as a pan-ErbB family covalent inhibitor, but it was discontinued during phase II clinical trials due to unacceptable skin toxicity [80].

Simultaneously, researchers from Wyeth Pharmaceuticals were working on a series of compounds harboring basic sites at the C6 substituent close to the covalent reactive group (Fig. 11) aiming to optimize their aqueous solubility [81]. Moreover, the basic tertiary amines at quinazoline C6 would act as in situ catalysts for cysteine side chain thiol group deprotonation improving the reactivity of this atom to covalent bond formation; and a protonated basic group would increase, by inductive effect, the electrophilicity of the β -carbonyl nucleophilic carbon [82].

Several tertiary amines linked to butynamides (**38**), crotonamide (**39**) and butenamide (**40**) were evaluated in enzymatic and cellular assays [81]. According to the oncogene addiction phenomenon, which describes the dependency of certain tumor cells on a specific oncogenic protein, if the corresponding target or signaling pathway is inhibited, an antiproliferative effect would be observed [83]. The cellular assays employed A431 EGFR overexpressing cells; SKBR3 HER-2 overexpressing

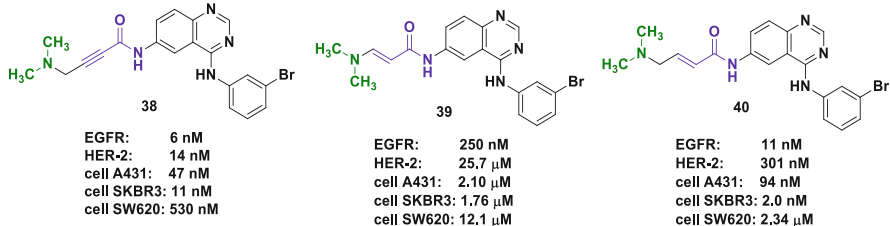


Fig. 11 EGFR covalent inhibitors (**38–40**) developed by Wyeth Pharmaceuticals. The covalent binding moiety is highlighted in purple and the solubilizing basic substituent in green

cells, which also overexpress EGFR to a lower extent; and the SW620 cell line. The inhibitory potency against SW620 tumor cells, with no alteration in EGFR and HER-2 expression rates, was used as a cytotoxic selectivity parameter [81]. For this reason, the TK inhibitors **38–40** were expected to inhibit selectively the EGFR and/or HER-2 overexpressing cell lines (Fig. 11).

Butenamide **40** was chosen as the inhibitor with best potency and selectivity combination. This derivative was evaluated in mouse xenograft models based on A431 tumor cell line, presenting high efficacy after oral administration. Structural optimization gave rise to afatinib (**5**; BIBW2992; GiotrifTM; Boehringer Ingelheim), which is 100 times more potent than gefitinib (**1**) for inhibition of the clinical resistant EGFR_{L858R/T790M} mutant form [84]. This drug is a pan-ErbB inhibitor with significant activity on EGFR_{wt} and EGFR mutant forms. Phase I clinical data detected as major adverse effects skin rash, acne, and diarrhea, also observed for first-generation EGFRi as a result of EGFR_{wt} inhibition [85–87].

As you would expect for a covalent inhibitor, experimental data showed that when the crotonamide double bond of drug **5** was replaced by a simple bond, generating derivative BI37781 (**41**), a significant loss of potency against EGFR_{L858R/T790M}, HER-2, and HER-4 was observed (Fig. 12) [88].

Afatinib (**5**; BIBW2992; GiotrifTM; Boehringer Ingelheim) was approved in 2013 for treatment of NSCLC patients expressing EGFR mutant forms. This drug represented a breakthrough in NSCLC treatment as the first 4-anilinoquinazoline derivative bearing an electrophilic reactive group able to form a covalent bond with a cysteine residue conserved in EGFR, HER-2, and HER-4. However, this compound frequently induces adverse effects related to EGFR_{wt} covalent inhibition, such as skin rash and diarrhea [89, 90].

In late 2015, a new covalent inhibitor, osimertinib (**6**; AZD9291; TagrissoTM; AstraZeneca), was approved by FDA for the treatment of NSCLC patients resistant to first- and second-generation drugs. This novel EGFRi, classified as third-generation, is supposed to induce less adverse skin effects, acting as a selective inhibitor of EGFR-harboring T790M mutation [91, 92].

As life is not a bed of roses, a point mutation at cysteine residue 797 (C797S) has recently been described in NSCLC patients [93]. This C797S mutation abolishes the antitumor efficacy of second- and third-generation EGFRi that act through covalent inactivation of EGFR. On the other hand, novel mutant selective competitive and

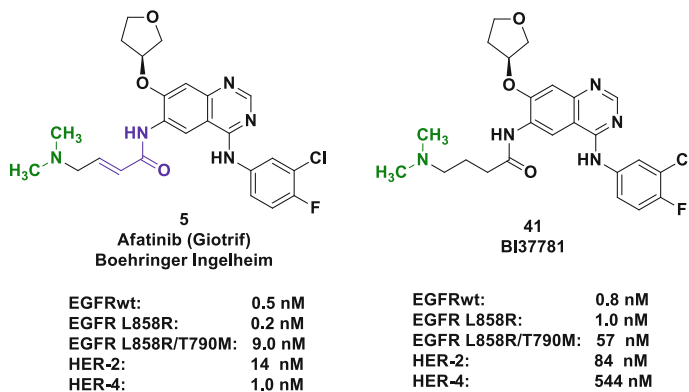


Fig. 12 ErbB covalent inhibitor afatinib (**5**) and the corresponding analogue (**41**) without the crotonamide double bond. The covalent binding moiety is highlighted in purple and the solubilizing basic substituent in green

allosteric EGFRi have recently been described and are currently being considered as the new promises for a short future in the fight against NSCLC [94–96]. Since the approval of the first EGFR inhibitor, gefitinib (**1**; ZD1819; Iressa™; AstraZeneca), in 2003, time has shown that the therapeutic challenges for EGFR inhibition keep changing and pushing the drug discovery process into a new direction.

3 Vascular Endothelial Growth Factor Receptors (VEGFRs)

Vascular endothelial growth factor receptors (VEGFRs) are RTKs implicated in vascular development, angiogenesis, and lymphangiogenesis, which are activated by their natural ligands, i.e., the vascular endothelial growth factors (VEGFs). VEGFRs are classified as VEGFR-1, VEGFR-2, and VEGFR-3, differing from each other in their cellular roles, distribution, and ligand-specific recognition [6].

VEGFR-1, also known as FMS-like tyrosine kinase 1 (Flt-1), is expressed in the cell surface of blood endothelial cells, as well as in monocytes and hematopoietic and smooth muscle cells. VEGFR-1 activation mediates hematopoietic precursors' recruitment and monocytes' and macrophages' migration, playing an important role in early inflammation. For this reason, VEGFR-1 signaling is considered as crucial for rheumatoid arthritis progression [6, 97].

Subtype VEGFR-2, also known as kinase insert domain receptor (KDR) or fetal liver kinase (Flk-1), is expressed in vascular endothelial cells, megakaryocytes, and neuronal and hematopoietic stem cells. VEGFR-2 is a key regulator of vasculogenesis during embryonic development and of angiogenic processes during adult life, participating in wound healing, diabetic retinopathy, rheumatoid arthritis, psoriasis, inflammatory disorders, tumor growth, and metastasis [6, 97].

In turn, VEGFR-3, also known as Flt-4, is located on lymphendothelial cells, inducing proliferation and survival [98–100].

3.1 *VEGF and Angiogenesis*

Tumor growth and metastatic dissemination demand previous formation of new blood vessels from an existing vascular network, in a process known as angiogenesis. As a consequence of neovascularization, solid tumor cells receive the oxygen and nutrients necessary for their survival and growth and also become able to migrate through blood circulation, establishing distant metastases [101, 102].

Under physiologic conditions, especially during the female reproductive cycle and wound healing, a fine balance between pro-angiogenic and antiangiogenic factors takes place. On the other hand, pathological angiogenesis can be found in several diseases, such as rheumatoid arthritis, age-related macular degeneration, proliferative diabetic retinopathy, atherosclerosis, and postischemic vascularization of the myocardium. Mainly in solid tumors, the dynamic balance between pro- and antiangiogenic factors is disrupted, with a clear overexpression of pro-angiogenic mediators, providing an ideal condition for neovascularization and tumor metastasis. Therefore, the inhibition of angiogenesis is well-established as a promising strategy in the development of novel antitumor drugs [103–105].

Fibroblast growth factors (FGFs), platelet-derived growth factors (PDGFs), tumor necrosis factor alpha (TNF- α), angiogenin, cyclooxygenase-2 (COX-2), interleukin-8 (IL-8), neptine, and vascular endothelial growth factors (VEGFs) are known positive modulators of angiogenesis. Among them, VEGFs are highlighted as the most important, being implicated in physiologic and pathological angiogenesis [104, 106]. VEGF expression and release are regulated by environmental factors, such as hypoxia and pH; by other growth factors, such as PDGF, TNF- α , transforming growth factor- β , and insulin-like growth factor-1, among others; by cytokines, such as IL-6 and IL-1; and by hormones, such as estrogen. VEGF overexpression has been associated with poor prognosis and progression of several tumor types, e.g., renal cell carcinoma; colorectal, gastric, and pancreatic carcinomas; breast, prostate, and lung cancers; and melanoma [104, 107].

The VEGFs family comprises six structurally related proteins: VEGF-A, VEGF-B, VEGF-C, VEGF-D, VEGF-E, and the placental growth factor (PlGF). VEGF-A, usually mentioned only as VEGF, is the most important growth factor among this family and represents the most potent pro-angiogenic endothelial chemoattractant released by cancer cells [108], mediating this effect mainly by VEGFR-2 activation [97].

3.2 VEGFR-2 Structural Characteristics

First isolated by Terman and colleagues in 1991, VEGFR-2 belongs to the 7-Ig/5-Ig RTK superfamily, being closely related to previously described class III RTKs, e.g., platelet-derived growth factor receptors (PDGFRs), colony-stimulating factor-1 receptor (CSF-1R), and c-KIT receptor [109]. The human VEGFR-2 gene encodes a full-length protein of 1,356 amino acids, comprising an extracellular (EC) domain with seven immunoglobulin-like (7-Ig) motifs, a short transmembrane (TM) helix, and the cytoplasmic subunit. VEGFR-2 is originally translated as a 150 kDa protein, giving rise to the mature 230 kDa form located in the cell surface after a series of glycosylations [6, 109–113].

Ligand binding induces receptor dimerization and autophosphorylation of specific intracellular tyrosine residues (Fig. 13), culminating in VEGFR-2 activation and cell signaling through the intracellular tyrosine kinase (TK) domain. Several intracellular proteins are phosphorylated by this RTK, including phospholipase C γ (PLC γ), phosphatidylinositol 3-kinase (PI3K), p38 mitogen-activated protein kinase (p38 MAPK), and Ras protein. These signaling proteins trigger downstream pathways that result in increased endothelial cell proliferation, migration, and survival and vascular permeability, culminating in angiogenesis [6, 109–113].

3.3 VEGFR Inhibitors

The assumption that solid tumors are not able to grow beyond 2 mm in diameter and are not able to spread to distant sites without developing a vascular supply, provided by angiogenesis, has indicated the relevance of VEGFR inhibitors (VEGFRi) as therapeutic tools for cancer treatment. In fact, the efficacy of VEGFRi has been demonstrated in several preclinical models and in human clinical trials. As previously mentioned, therapeutic approaches to block the VEGF/VEGFR signaling pathway include those designed against the extracellular ligand-binding domains of VEGFR, such as monoclonal antibodies, and the small-molecule tyrosine kinase inhibitors (TKIs) [10, 114, 115]. From the perspective of this chapter, only the latter approach, i.e., VEGFR TKIs, will be discussed.

The resolution of co-crystal structures of small-molecule TKIs with VEGFR-2 has provided clear structural evidence regarding their general binding mode, guiding the further design of novel VEGFR-2 inhibitors. In general, the majority of known VEGFR-2 TKIs bind to the kinase domain through three key hydrogen bonds with specific amino acid residues, i.e., the backbone NH of *hinge* residue Cys 919; the backbone NH of Asp 1046 of the conserved DFG motif; and the side chain carboxylate of Glu 885. Moreover, a lipophilic pocket defined by residues Ile 888, Leu 889, Ile 898, Val 899, Leu 1019, and Ile 1044 is usually involved in hydrophobic interactions with ligands' nonpolar subunits. Finally, hydrophilic contacts with a solvent-exposed region can also be observed for those inhibitors bearing

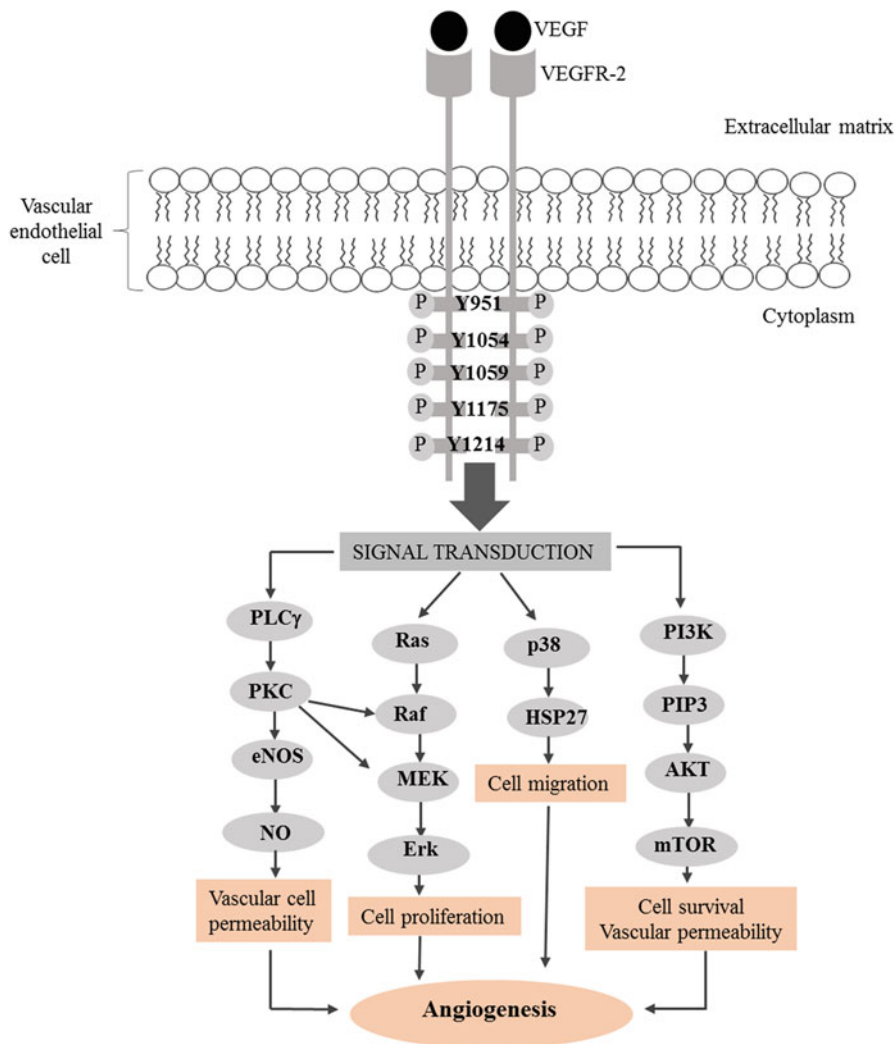


Fig. 13 Simplified signal transduction pathway mediated by VEGF-A binding to VEGFR-2, inducing receptor dimerization and autophosphorylation of specific intracellular tyrosine residues. *PLC γ* phospholipase C- γ , *PKC* protein kinase C, *eNOS* endothelial nitric oxide synthase, *NO* nitric oxide, *Ras* rat sarcoma (it is a small GTPase), *Raf* rapidly accelerated fibrosarcoma, *MEK* MAPK/ERK kinase, *ERK* extracellular regulated kinases, *p38* p38 mitogen-activated protein kinase, *HSP27* heat-shock protein 27, *PI3K* phosphoinositide 3-kinase, *PIP3* phosphatidylinositol (3,4,5)-trisphosphate, *AKT* Protein kinase B (PKB) (also known as Akt), *mTOR* mammalian target of rapamycin

a long terminal solubilizing chain, such as in the structure of nintedanib (48; Fig. 14) [6, 116, 117].

It is worth mentioning that all approved VEGFR inhibitors in clinical use (Table 3), and many others in different stages of drug development, present weak

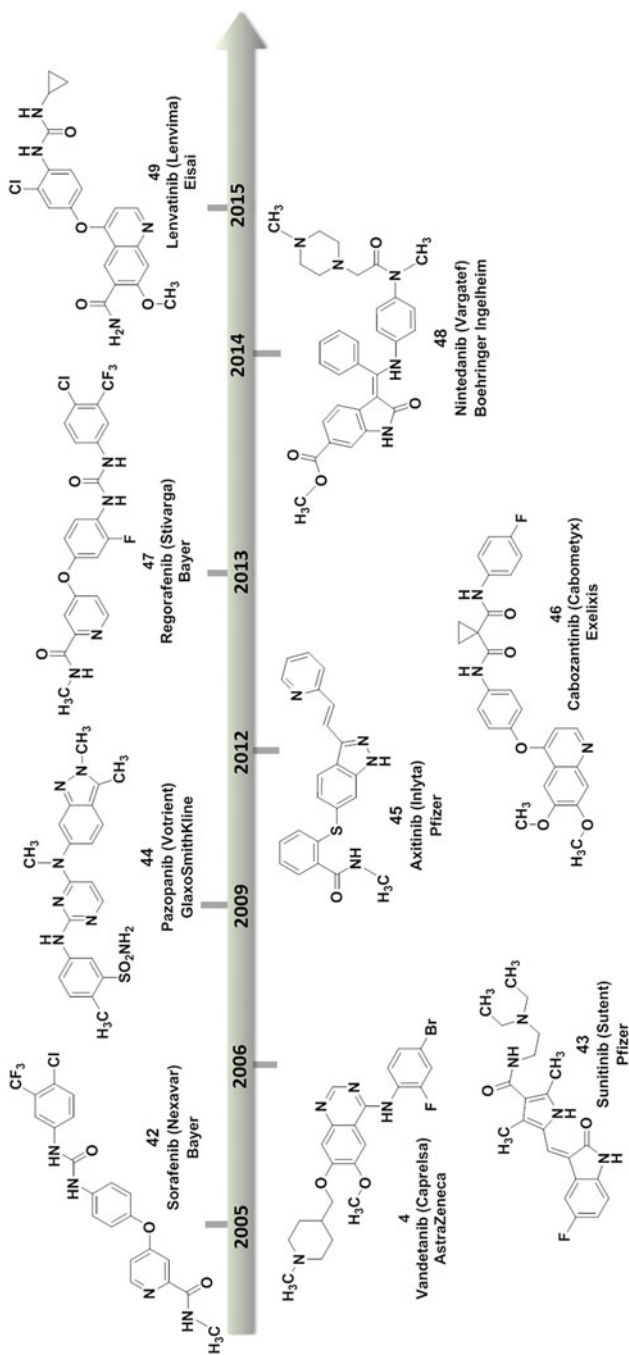


Fig. 14 FDA-approved small-molecule VEGFR inhibitors **4** and **42–49**

Table 3 Small-molecule VEGFR TKIs approved by FDA and their IC₅₀ values against VEGFR subtypes

Drug	Company	Main targets	Inhibitory profile against VEGFR subtypes (IC ₅₀ in nM)		
			VEGFR-1	VEGFR-2	VEGFR-3
Sorafenib	Bayer/Onyx	VEGFR, c-KIT, Raf, PDGFR-β	26	90	20
Sunitinib	Pfizer	VEGFR, c-KIT, Raf, PDGFR, Flt3, CSR-1F	15	38	30
Pazopanib	GSK	VEGFR, c-KIT, PDGFR, FGFR, c-Fms	10	30	47
Vandetanib	AstraZeneca	VEGFR, EGFR	1,600	40	100
Nintedanib	Boehringer Ingelheim	VEGFR, FGFR PDGFR	34	21	13
Axitinib	Pfizer	VEGFR, c-KIT, PDGFR-β	1.2	0.25	0.29
Cabozantinib	Exelixis	VEGFR-2, Met, Ret, c-KIT Flt-3, Tie2	N.D.	0.035	N.D.
Regorafenib	Bayer	VEGFR, c-KIT, RET, Raf-1 PDGFRβ	13	4.2	46
Lenvatinib	Eisai	VEGFR, RET, PDGFR, FGFR, c-KIT	22	4	5.2

to moderate selectivity among VEGFR subtypes (VEGFR-1, VEGFR-2, and VEGFR-3), with exception of cabozantinib (**46**, Fig. 14), a potent and selective inhibitor of VEGFR-2 (Table 3) [7, 10, 118, 119]. Nevertheless, VEGFR subtype selectivity is not considered an essential requirement for clinical efficacy and safety. In fact, VEGFR-2 and VEGFR-3 dual inhibition is considered strategic to prevent blood and lymphangiogenesis, respectively. Furthermore, known VEGFR TKIs are usually not selective against other tyrosine kinases closely related to VEGFR-2, such as PDGFRs, CSF1R, and c-KIT receptors (Table 3), and are commonly referred to as multi-kinase inhibitors.

As can be noted from structures depicted in Figs. 14 and 15, different heterocyclic scaffolds are employed in the development of new VEGFR TKI drug candidates, including quinazolines, quinolines, pyrimidines, pyridines, indolinones, indazoles, pyrrolo-triazines, pyridazines, and quinolinones, and these rings are usually involved in the hydrogen bond interaction with the *hinge* amino acid residue. These scaffolds are properly decorated with the introduction of substituents able to perform complementary interactions with specific amino acid residues in the ATP-binding site of VEGFRs, exploring the *hinge* region (adenine pocket), the DFG sequence, the hydrophobic adjacent pockets, and the solvent-exposed region.

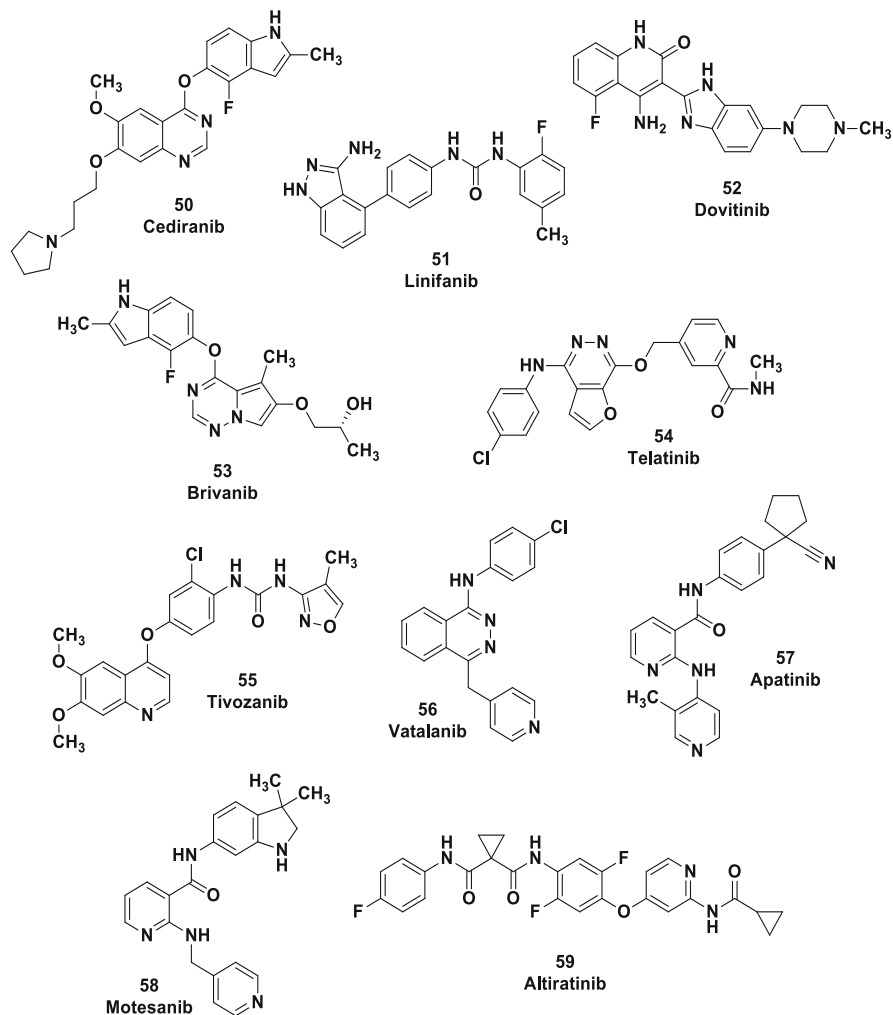


Fig. 15 Examples of VEGFR TKIs on clinical trials as anticancer drug candidates

3.4 Lenvatinib Story Case

Lenvatinib (**49**; E7080; LenvimaTM; Eisai; Fig. 15) is the most recent VEGFR TKI approved by FDA for clinical use in cancer treatment. This drug actually consists an oral multi-kinase inhibitor that selectively inhibits VEGFR 1–3 and other pro-angiogenic and prooncogenic receptor tyrosine kinases, including fibroblast growth factor receptors 1–4 (FGFR1-4), platelet-derived growth factor receptor- α (PDGFR- α), c-KIT, and RET. Compound **49** is a quinoline-functionalized derivative belonging to the general formula depicted in Fig. 16, which was first described as a

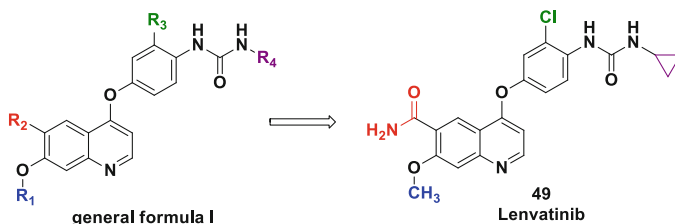


Fig. 16 General formula I of a quinoline-functionalized congener series, highlighting the VEGFR TKI lenvatinib (**49**) able to inhibit tube formation from vascular endothelial cells stimulated by VEGF, FGF2, or HGF

VEGFR TKI able to inhibit tube formation from vascular endothelial cells stimulated by VEGF, FGF2, or HGF [120].

Lenvatinib (**49**) was granted Orphan Drug Designation for thyroid cancer by the health authorities in Japan in 2012, followed by Europe and the USA in 2013. The first application for marketing authorization was submitted in Japan in June 2014. In 2015, US FDA approved lenvatinib (**49**) for treatment of patients with locally recurrent or metastatic, progressive, radioactive iodine-refractory differentiated thyroid cancer. More recently, in 2016, FDA approved this drug in combination with everolimus, an mTOR inhibitor, for treatment of advanced renal cell carcinoma.

3.4.1 3D Structure and Kinetic Profile

The X-ray analysis of the crystal structure of VEGFR-2-lenvatinib complex, at a resolution of 1.57 Å, demonstrated that lenvatinib (**49**) binds to VEGFR-2 in a DFG-*in* conformation, characterizing a particular binding mode for this inhibitor in comparison with known VEGFR-2 type II TKIs, which bind and stabilize the inactive DFG-*out* conformation of the target RTKs, such as sorafenib (**42**) and regorafenib (**47**).

The binding site of drug **49** is situated in the hinge region, i.e., in the cleft between *N*-terminal and the *C*-terminal lobes (Fig. 1). This inhibitor completely occupies the adenine ring-binding site (Fig. 17), performing a strong hydrogen bond between the backbone NH of *hinge* residue Cys 919 and the nitrogen of the quinoline ring. Additional hydrogen bonds between the urea subunit and the backbone of Asp1046 and the side chain of Glu885 are observed, as well as between the amide group linked to the quinoline scaffold and Asn923, in this case bridged by water molecules (Fig. 17) [121].

It is important to notice that in the VEGFR-2-lenvatinib complex (Fig. 17), the small cyclopropyl substituent of the urea moiety is performing a CH- π interaction with the phenyl ring of the DFG Phe1047 residue, this interaction being essential for the favored recognition in a VEGFR-2 DFG-*in* conformation. Other urea type II inhibitors, such as sorafenib (**42**) and regorafenib (**47**), present larger aromatic

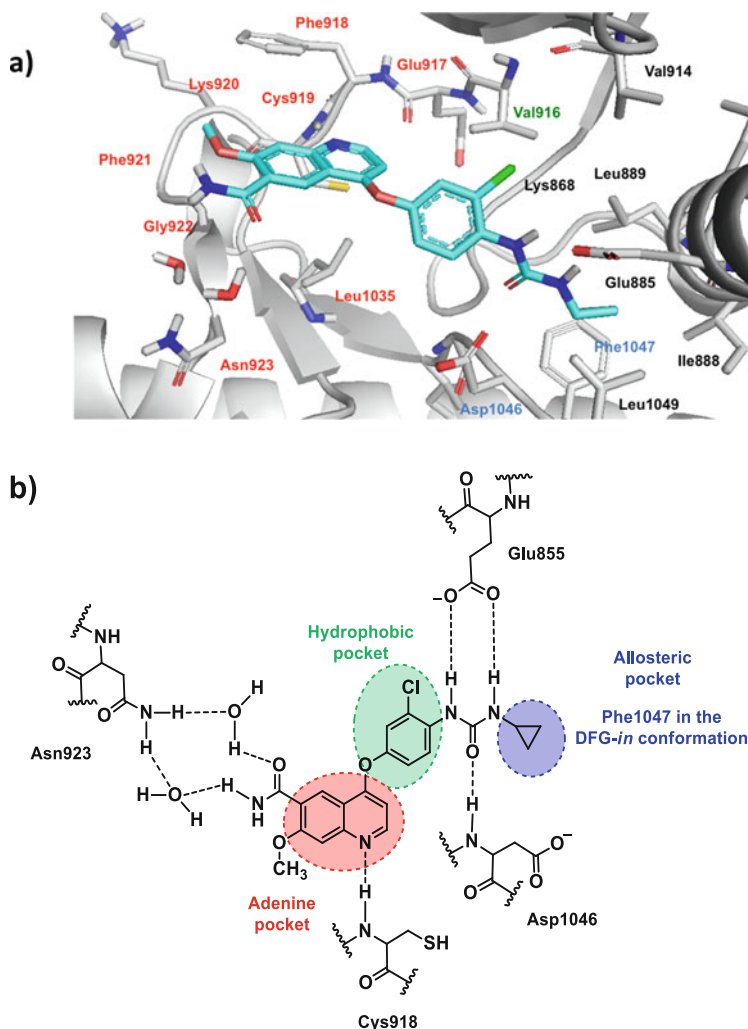


Fig. 17 Binding mode of lenvatinib (**49**) with the target kinase VEGFR-2 (PDB code: 3WZD). (a) Crystal structure with residues from ATP-binding site indicated in red, DFG residues blue colored, and gatekeeper residue in green. (b) Simplified representation of VEGFR-2-levatinib complementary interactions

substituents in the urea moiety, inducing a favored recognition in a VEGFR-2 DFG-out conformation with the phenyl ring of Phe1047 located outside of the adjacent hydrophobic pocket.

Kinetics studies revealed a dissociation constant (K_d) of 2.1 ± 0.1 nmol/L between lenvatinib (**49**) and VEGFR-2 and a residence time of 17 ± 2 min. When compared to sunitinib (**43**), a classical VEGFR-2 type I TKI, with a residence time < 2.9 min, compound **49** clearly shows a prolonged residence time and a faster

association rate ($k_{on} = 4.8 \times 10^5 \pm 1.4 \times 10^4$). This experimental evidence demonstrated that this compound doesn't fit in the classical type I or type II inhibitor definition, presenting a distinct binding mode able to interact with the neighboring allosteric pocket of VEGFR-2 in a DFG-*in* conformation [121, 122].

3.4.2 Pharmacokinetic Profile

Lenvatinib (**49**) is rapidly absorbed (t_{max} is typically 1–4 h post-dose), and co-administration with food slows the rate (t_{max} is delayed by 2 h), but not the extent, of absorption. The drug is extensively metabolized, and in vitro and in vivo studies have shown this drug to be eliminated via both liver and kidney, primarily by excretion in bile, with a half-life of approximately 28 h and oral clearance of 4.2–7.1 L/h [123, 124]. Although earlier in vitro studies indicated that oxidative metabolism of lenvatinib (**49**) would be primarily be mediated by CYP3A4, this does not appear to be a major pathway involved in drug clearance, since no significant changes were observed in the metabolism profile of healthy volunteers concomitantly treated with ketoconazole, a potent and specific inhibitor of CYP3A4 [125].

Lenvatinib (**49**) demonstrated high (98–99%) binding to human plasma proteins, mainly albumin, in vitro and a blood-to-plasma concentration ratio that ranged from 0.589 to 0.608. It is considered a substrate for P-glycoprotein (P-gp) and breast cancer-resistant protein (BCRP), but not for organic anion transporters (OAT1 and OAT3), organic anion transporting polypeptides (OATP1B1 and OAT1B3), organic cation transporters (OCT1 and OCT2), or the bile salt export pump. Moreover, this drug presents a low potential for drug-drug interactions based on clinical studies [126].

3.4.3 Pharmacodynamic Profile

As already mentioned, lenvatinib (**49**) is a potent multi-kinase inhibitor. The most sensitive kinases, with half-maximal inhibitory concentration (IC₅₀) values below 10 nM, include VEGF receptors (VEGFR 1–3) and RET. The second most sensitive group includes FGF receptors (FGFR1-4), PDGFR- α , and c-KIT with IC₅₀ values below 100 nM (Table 4). All targets are typical pro-angiogenic and oncogenic pathway-related receptor tyrosine kinases (RTKs). This drug potently inhibits VEGF-driven KDR phosphorylation in human umbilical vein endothelial cells (HUVECs) and inhibits VEGF-driven HUVEC proliferation and tube formation. Lenvatinib (**49**) exhibited weak direct antiproliferative activity in vitro against several human cancer cell lines, showing a typical response for an antiangiogenic agent. However, this drug presents potent antitumor activity against a number of human cancer cell lines in mouse xenograft models which is clearly mediated via angiogenesis inhibition [120, 127–129].

Table 4 Receptor tyrosine kinases as drug targets for lenvatinib (**49**)

Kinase	IC ₅₀ (nM)
VEGFR-3 (FLT4)	2.3
VEGFR-2 (KDR)	3.0
VEGFR-1 (FLT1)	4.6
RET	6.4
FGFR-2	27
PDGFR- α	29
FGFR-4	43
FGFR-3	52
FGFR-1	61
c-KIT	85

IC₅₀ half-maximal inhibitory concentration, *FGFR* fibroblast growth factor receptor, *PDGFR- α* platelet-derived growth factor receptor alpha, *VEGFR* vascular endothelial growth factor receptor, *RET* rearranged during transfection (the receptor for GDNF family ligands), *c-KIT* a transmembrane protein with tyrosine kinase activity encoded by the oncogene *c-kit*, also referred to as stem cell factor receptor or CD117

Lenvatinib (**49**) has demonstrated antiangiogenic and/or antitumor properties in preclinical *in vitro* and *in vivo* studies, showing promising anticancer activity in 11 human thyroid cancer xenograft models derived from the following human cell lines: (a) differentiated thyroid cancer (DTC) – the most prevalent type of thyroid cancer; (b) medullary thyroid cancer (MTC); and (c) anaplastic thyroid cancer (ATC) – one of the most deadly human diseases with prevalence below 2%. The broad antitumor activity observed for most of the human thyroid cancer models is attributed to the potent antiangiogenic effect, as a result of a multiple inhibition of RTKs that play an essential role in the development of tumor-dependent angiogenesis, e.g., VEGFR-2, PDGFR, and FGFR [128, 129].

Particularly, the efficacy of lenvatinib (**49**) in patients with radioiodine-refractory differentiated thyroid cancer (RR-DTC) was established based on a randomized, double-blind, multinational phase III SELECT study, in which this anticancer drug significantly improved median progression-free survival (PFS) and the overall response rate when compared with placebo. The beneficial effect of lenvatinib (**49**) on PFS was also seen across all pre-specified subgroups including those based on sex, race, geographic region, prior or no prior VEGF-targeted therapy, age (aged ≤ 65 or > 65 years), histological (sub)type, and baseline TSH level [130, 131]. Taken together, these clinical findings validate lenvatinib (**49**) as an oral active multi-kinase inhibitor with potential to modify the role of systemic treatment in the management of patients with radioiodine-refractory thyroid cancer, representing an exciting therapeutic option to RR-DTC treatment.

3.4.4 Safety Profile

The safety and tolerability profiles observed for orally administered lenvatinib (**49**) in the SELECT clinical study were consistent with those of VEGF-VEGFR-targeted therapies and mostly manageable through dose modifications and standard clinical interventions [123, 130, 131].

Most frequent treatment-related adverse events (TRAEs) occurred in 75.9% of lenvatinib (**49**) recipients versus 9.9% of placebo recipients including hypertension, proteinuria, diarrhea, fatigue or asthenia, decreased appetite, decrease in bodyweight, nausea, and stomatitis. In the SELECT trial, the incidence of grade ≥ 3 TRAEs in the lenvatinib-treated group was as follows: hypertension (42.9%); proteinuria (10.0%); arterial thromboembolic effects (2.7%); venous thromboembolic effects (3.8%); renal failure (including acute renal failure; 1.9%); hepatic failure (0.4%); gastrointestinal fistula (0.8%); and corrected QT prolongation (1.5%). Dose interruptions and reduction of lenvatinib (**49**) were most commonly due to diarrhea (22.6% of patients), hypertension (19.9%), and proteinuria (18.8%); discontinuation of treatment was most commonly due to development of hypertension (1.1%) and asthenia (1.1%) [128, 130].

4 Platelet-Derived Growth Factor Receptor (PDGFR)

The platelet-derived growth factor (PDGF) family consists of four polypeptide members (A–D) that can generate disulfide-bonded homodimers or the heterodimer PDGF-AB [132]. PDGF dimers bind to the platelet-derived growth factor receptor subtypes PDGFR- α and PDGFR- β , inducing receptor dimerization and culminating in intracellular autophosphorylation and activation [133].

PDGFRs belong to the 7-Ig/5-Ig RTK superfamily, being characterized by an extracellular (EC) domain containing five immunoglobulin-like (5-Ig) motifs typical from the type III subclass of RTKs [3, 4].

PDGF-AA, AB, BB, and CC are able to bind to receptor $\alpha\alpha$ -homodimers; PDGF-BB and DD to receptor $\beta\beta$ -homodimers; and PDGF-AB, BB, CC, and DD to receptor $\alpha\beta$ heterodimers [133]. The platelet-derived growth factor (PDGF) isoforms and their receptors (PDGFRs) play key roles in the regulation of several cellular processes, e.g., survival, growth, and motility of mesenchymal cells, such as fibroblasts, pericytes, and smooth muscle cells; embryonal development; as well as tissue repair and homeostasis in adults [133, 134].

PDGFR- α signaling is mainly related to the development of several tissues and organs, e.g., the lungs, intestine, skin, kidney, bones, and neuroprotective tissues. On the other hand, PDGFR- β signaling is recognized as essential for early hematopoiesis and blood vessel formation [135]. During angiogenesis, the recruitment of pericytes, which represent the cells in charge of supporting and stabilizing the vasculature, is mainly driven by activation of PDGFR- β [134]. This receptor also

induces vascular endothelial growth factor (VEGF) expression [136]. Furthermore, both PDGFR- α and PDGFR- β are related to the development of novel lymphatic vessels [134].

4.1 PDGFR and Tumorigenesis

PDGFs and their receptors (PDGFRs) act as important mediators of tumor growth and invasion through direct effects on tumor cells, as well as on their surrounding microenvironment [132]. PDGFs are largely produced by different types of solid tumors, inducing stroma formation and angiogenesis in order to ensure nutrient and oxygen supplies [137]. Several tumors are associated with genetic alterations that culminate in constitutive activation of PDGFRs. The overexpression of these RTKs can be detected directly in tumor cells or in tumor-associated pericytes and stroma cells [134]. PDGFR- β expression by pericytes mediates their recruitment and proper integration in tumor vessels [137].

Moreover, the higher expression and activation of PDGFRs in solid tumors contribute to an increase in the interstitial fluid pressure (IFP), causing tumor interstitial hypertension (TIH), which reduces the permeability from the capillary into tissue, thus decreasing the diffusion of anticancer drugs [136, 137].

Consequently, PDGFR inhibition is considered a promising therapeutic approach for anticancer treatment, as it is supposed to control tumor growth by directly targeting tumor cells and by decreasing angiogenesis, and is also associated with higher chemotherapy delivery and exposure [133, 134, 136].

4.2 PDGFR Role in Several Tumor Types

Prominent expression of PDGFs and PDGFR- α in human glioma cells suggests the relevance of this signaling pathway in gliomagenesis and disease progression [132]. Simultaneous expression of PDGFR- α/β was detected in around 60% of human colorectal carcinoma samples [138, 139]. High stromal expression of PDGFR- β is also observed in breast cancer and associated with tumor aggressiveness and poor prognosis [138, 140]. Additionally, PDGFR- β is frequently upregulated in primary and metastatic prostate cancer cells [133].

Moreover, PDGFR gain-of-function mutations and derived fusion proteins are implicated in several tumor types. Suzuki and coworkers demonstrated that PDGFR- β carrying the gain-of-function mutation D849N in the activation loop accelerates the establishment of B16 melanoma in a murine model of this disease [137]. These PDGFR genetic alterations and their role in myeloid malignancies and gastrointestinal stromal tumors (GISTs) represent the most relevant examples described in scientific literature so far.

4.2.1 Myeloid Malignancies

Myeloid malignancies are stem cell-derived clonal disorders and comprise three different categories: acute myeloid leukemia (AML), myelodysplastic syndrome (MDS), and myeloproliferative neoplasms (MPN). Both PDGFR- α (gene PDGFRA located on chromosome 4q12) and β (gene PDGFRB located on chromosome 5q31–q32) are linked to myeloid malignancies [141]. In 1994, a fusion protein containing the tyrosine kinase domain of PDGFR- β (*tel*-PDGFR β) was associated with a subtype of MDS, i.e., the chronic myelomonocytic leukemia (CMML) [141, 142]. Later, in 2003, a fusion of the Fip1-like 1 (FIP1L1) gene to the PDGFRA gene generated by an interstitial deletion on chromosome 4q12 was identified as a marker of the hypereosinophilic syndrome, a rare hematologic disorder with sustained overproduction of eosinophils in the bone marrow [143]. Moreover, the FIP1L1-PDGFR- α fusion gene was also identified in rare cases of acute myeloid leukemia and T-cell acute lymphoblastic leukemia [144]. The generated fusion protein FIP1L1-PDGFR- α is constitutively activated [143].

4.2.2 Gastrointestinal Stromal Tumors (GISTs)

Gastrointestinal stromal tumors (GISTs) are the most common mesenchymal tumors of the gastrointestinal tract, most of them (~80%) presenting activating mutations in the c-KIT receptor tyrosine kinase [145–147]. Around 50% of GISTs are metastatic, usually to liver or peritoneum [148]. In 2003, a study from Heinrich and coworkers demonstrated that around 40% of GISTs lacking c-KIT mutations present activation mutations in a related receptor tyrosine kinase, i.e., PDGFR- α , indicating that mutations in these RTKs represent mutually exclusive oncogenic mechanisms in GISTs. Moreover, these authors concluded that tumors expressing c-KIT or PDGFR- α oncoproteins were indistinguishable regarding the activation of downstream signaling pathways [147, 149].

Among PDGFRA-mutated patients, the most common mutation (~60%) was located in the exon 18, producing an activation loop with a valine instead of the conserved aspartic acid at codon 842 (PDGFR- α D842V) [145, 147, 149]. Another gain-of-function mutation of PDGFR- α in GIST was described by Hirota et al. [150], comprising the substitution of Val-561 to Asp (PDGFR- α V561D) at the juxtamembrane domain (exon 12). These authors also demonstrated that mutated PDGFR- α D842V and V561D represent constitutively activated forms of this RTK [150]. From then on, several other PDGFR- α mutations affecting the activation loop (exon 18), the juxtamembrane domain (exon 12), or the tyrosine kinase domain (exon 14) have been described for GIST patients [145].

4.3 PDGFR Inhibitors

Considering the relevance of the PDGFR pathway for tumor establishment, growth, and aggressiveness, the development of PDGFR inhibitors has become a promising therapeutic approach in cancer treatment. This inhibition is achieved by three main strategies, i.e., antagonism with specific antibodies directed to the protein extracellular (EC) domain; sequestration of PDGF isoforms by soluble extracellular parts of the receptors, preventing their binding to cellular PDGFRs; and direct inhibition of the enzymatic activity by the well-known TKIs [133].

Several potent inhibitors of PDGFR kinase activity are available for therapeutic use (Fig. 18) or under preclinical and clinical evaluation [7, 10]. Up to now, none of the approved inhibitors are highly selective for this target, but, in turn, they inhibit several structurally related tyrosine kinases, showing particular selectivity profiles depending on their binding modes to the TK domain [3, 133].

The first PDGFR inhibitor approved for clinical use was imatinib (**60**), which also inhibits the stem cell receptor c-KIT and Abl kinases. However, imatinib (**60**) treatment in PDGFR-dependent tumors has recurrently been associated with primary and secondary resistance and disease progression. Second-line drugs include approved multi-kinase inhibitors, such as sorafenib (**42**) and sunitinib (**43**) (Fig. 18). For instance, sunitinib (**43**, SU11248; Sutent™; Pfizer) was approved by FDA in 2006 for imatinib-refractory GIST patients, although not all imatinib-resistant patients benefit from this drug [3, 148, 151].

Moreover, considering the relevance of PDGFRs as therapeutic targets for cancer treatment, selective drug candidates rationally designed to act as PDGFR inhibitors are under development in ongoing clinical trials. The most advanced prototype is crenolanib (**63**; Fig. 20), a TKI designed to target PDGFR α/β [152] which is currently in clinical development for acute myeloid leukemia (AML), gastrointestinal stromal tumor (GIST), and glioma treatments [11].

4.3.1 Imatinib: The First PDGFR TKI

Imatinib (**60**, STI571; Glivec™ or Gleevec™; Novartis) is a small-molecule tyrosine kinase inhibitor (TKI) belonging to the 2-phenylaminopyrimidine chemical class [3, 153]. It was originally described by Druker and colleagues in 1996 as a potent inhibitor of the fusion BCR-ABL oncoprotein, which is associated with chronic myeloid leukemia (CML) and other types of Philadelphia chromosome-positive leukemias [4, 153, 154]. Therefore, this drug received its first approval by FDA in 2001 for treatment of CML [3, 155]. Later, the receptor tyrosine kinases (RTKs) PDGFR- α , PDGFR- β , and KIT were also found to be potently inhibited by **60**, resulting in an additional approval of this drug in 2002 for advanced GISTs, taking into account the important role of KIT and PDGFR in the pathogenesis of this type of cancer [3, 4, 155]. Several other therapeutic uses were further established for

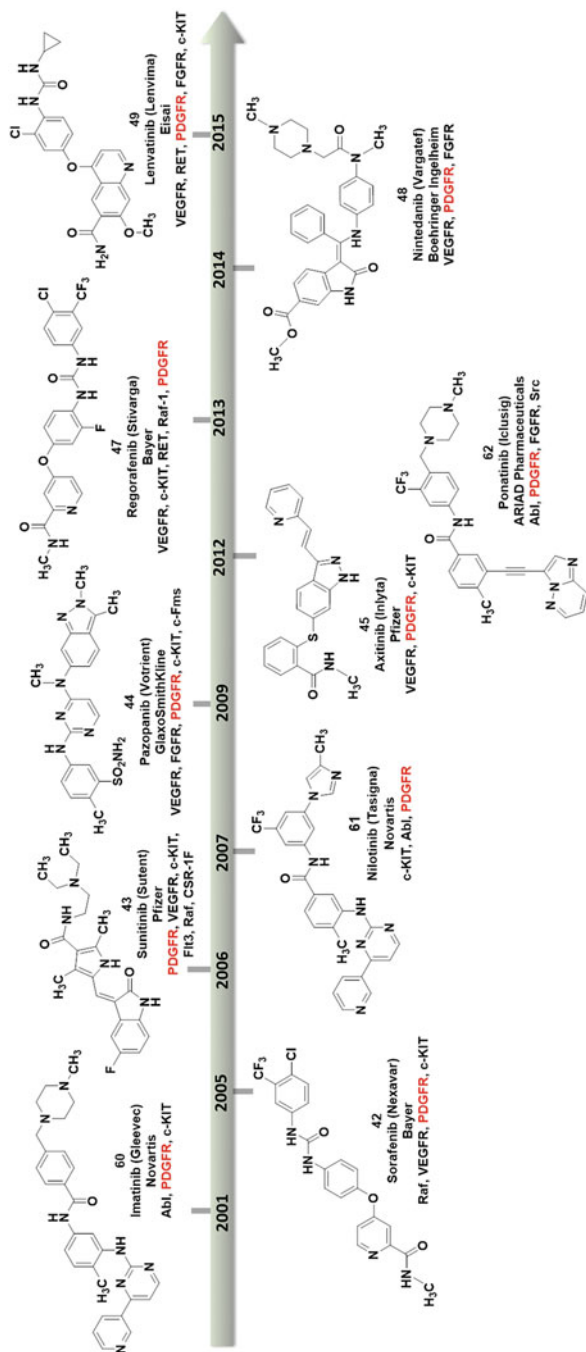


Fig. 18 FDA-approved small-molecule PDGFR inhibitors **42–45**, **47–49**, and **60–62**

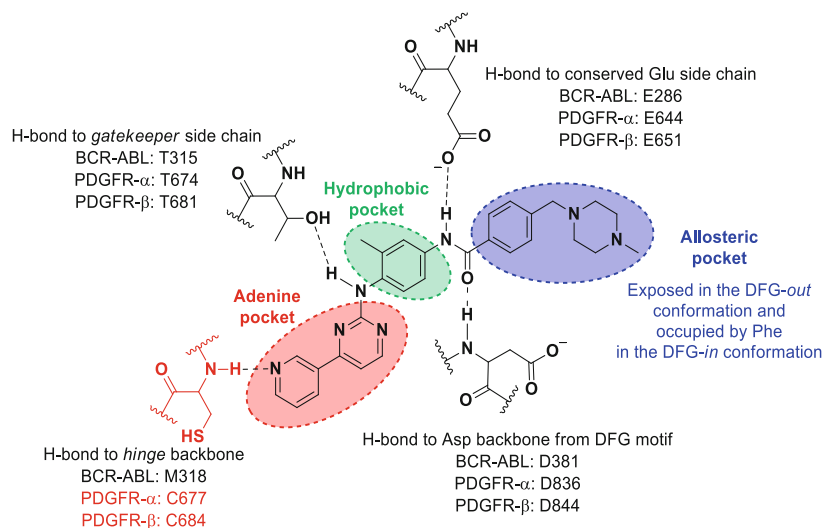


Fig. 19 Predicted binding mode of imatinib (**60**) with the target kinases PDGFR- α and PDGFR- β , based on previous NMR and crystallographic results for the inhibition of BCR-ABL

imatinib (**60**), an innovative drug for clinical management of tumors with constitutively activated forms of the target TKs, i.e., c-ABL, c-KIT, or PDGFR- α/β [153].

No co-crystallized structure of imatinib (**60**) with PDGFR- α or β has been reported. However, it is possible to predict the binding mode of drug **60** to these targets based on previous NMR and crystallographic results for the inhibition of BCR-ABL and c-KIT (Fig. 19). This drug acts as a type II TKI by binding and stabilizing the inactive DFG-out conformation of the target TKs. Imatinib (**1**) explores the ATP-binding site (Fig. 19), interacting via hydrogen bond with the *hinge* residue, and performs hydrophobic interactions with an adjacent allosteric pocket exposed in the DFG-out conformation, establishing additional electrostatic interactions with the Asp of the DFG motif and with a conserved Glu residue located in the adjacent helix C [7, 8, 156].

Considering the favored binding of **60** to the DFG-out conformation (Figs. 1 and 19), equilibrium imbalance between these conformations due to mutations in the activation loop can result in primary or secondary resistance [4, 153].

Two main cellular mechanisms are associated with imatinib resistance, including gene amplification and mutations [153]. The most common PDGFRA D842V mutation observed in GIST patients causes a shift in equilibrium favoring the active DFG-in conformation and an increase of the affinity for ATP [5], and these patients typically relapse to imatinib (**60**) treatment [145, 157].

Moreover, the use of imatinib (**60**) as clinical inhibitor of the fusion oncoprotein FIP1L1-PDGFR- α in hypereosinophilic syndrome is correlated with the emergence of the secondary resistant mutation T674I in the *gatekeeper* amino acid residue [143, 144]. The mutated T674I FIP1L1-PDGFR- α loses a hydrogen bond between

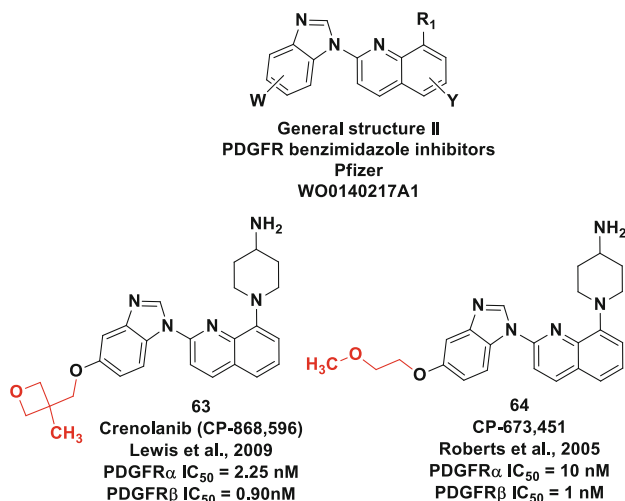


Fig. 20 Benzimidazole series of PDGFR inhibitors described originally by Pfizer as potent antiproliferative and antiangiogenic agents, highlighting the most promising derivatives crenolanib (**63**, CP-868,596) and CP-673,451 (**64**), with their corresponding inhibitory potencies

the aminopyrimidine moiety and the *gatekeeper* residue, and the binding site becomes too narrow to accommodate the ligand due to introduction of the larger isoleucine side chain [4, 145, 153]. This mutation is analogous to the T315I substitution in BCR-ABL, classically associated with secondary resistance development in CML patients (Fig. 19) [4].

For that reason, nature and location of PDGFR oncogenic mutations will translate in different prognoses, influencing tumor aggressiveness and the expected clinical response to imatinib (**60**) treatment [146].

It is worthy of note that imatinib (**60**) represented an impressive breakthrough in the therapy of PDGFR-addicted tumors. However, considering resistance development and refractory tumors, an urgent need for novel and alternative therapeutic strategies has emerged [157].

4.3.2 Crenolanib: A Novel PDGFR Inhibitor Drug Candidate

Crenolanib (**63**, CP-868,596; AROG Pharmaceuticals; Fig. 20) is an orally bioavailable benzimidazole tyrosine kinase inhibitor (TKI) designed as highly selective modulator of TKRs PDGFR- α and β (K_d = 3.2 nM, IC₅₀ = 2.25 nM and K_d = 2.1 nM; IC₅₀ = 0.9 nM, respectively) [11, 134, 158]. Subsequently, it was demonstrated that this compound also acts as a potent inhibitor of the FMS-like tyrosine kinase 3 (FLT3; K_d = 0.7 nM) [158, 159]. Crenolanib (**63**) is currently recognized as a highly selective inhibitor of class III RTKs PDGFR- α , PDGFR- β , and FLT-3, presenting a weaker inhibition for the other members of this RTK class;

i.e., c-KIT ($K_d = 78$ nM) and CFS-1R ($K_d = 30$ nM) [11, 158]. On the other hand, crenolanib (**63**) does not inhibit any other known tyrosine or serine/threonine kinase at clinically achievable concentrations [134, 158].

This class of benzimidazole TKIs (Fig. 20) was first described by Pfizer in 2001 (WO0140217A1) as antiproliferative and antiangiogenic agents, showing IC_{50} values in the nanomolar range for PDGFR- β inhibition. Although no structure-activity relationship is described for this series, the most promising derivatives from this research effort, i.e., crenolanib (**63**, CP-868,596) [134] and CP-673,451 (**64**) [160], clearly share common structural features and similar inhibitory potencies against PDGFRs, differing exclusively in the ether side chain (Fig. 20).

The promising antiangiogenic properties and adequate safety and pharmacokinetic profiles described for crenolanib (**63**) during preclinical studies encouraged further clinical trials. Phase I clinical evaluation of crenolanib (**63**) in humans indicates an optimal and well-tolerated dose regimen of 100 mg twice daily, with nausea and vomiting as the most frequent adverse effects, which are, however, mitigated by concomitant food ingestion [134]. AROG Pharmaceuticals licensed this drug candidate from Pfizer in April 2010.

Crenolanib (**63**) is currently undergoing multiple phase II and III clinical trials, as a single agent or in combination with known antitumor drugs, for acute myeloid leukemia (AML, NCT01522469, NCT01657682, NCT02400281), gastrointestinal stromal tumor (GIST; NCT01243346, NCT02847429), and glioma treatments (NCT01229644, NCT01393912) [11, 136, 158].

Biochemical studies clearly demonstrated that this prototype acts as a type I TKI, presenting greater affinity to the target kinases' active states. For instance, crenolanib (**63**) showed tenfold higher affinity to active FLT3 ($K_d = 0.7$ nM) versus auto-inhibited FLT3 ($K_d = 6.7$ nM) [11].

Considering that active states are often derived from the gain-of-function mutations of PDGFR-encoding genes, crenolanib (**63**) represents a promising alternative for patients with PDGFR mutations, especially those that render the kinase domain constitutively phosphorylated, causing acquired resistance to imatinib (**60**) and other type II TKIs, such as sorafenib (**42**) and nilotinib (**61**) [11, 152].

In this context, crenolanib (**63**) was described by Heinrich and colleagues as the most potent PDGFR- α D842V kinase inhibitor identified so far, with an IC_{50} in a range of 10 nM, being at least 100-fold more potent than imatinib (**60**). Moreover, the prototype retained its inhibitory activity when the gatekeeper T674I mutation was added to the D842V mutated protein. Similar to the biochemical assay results, compound **63** was significantly more potent ($IC_{50} = 22$ nM) than imatinib (**60**; $IC_{50} = 1,510$ nM) against BaF3 D842V cell line proliferation [158].

Moreover, this highly selective inhibitor of class III RTKs is expected to show reduced toxicity in comparison with other nonselective multi-kinase inhibitors, demonstrating that type I inhibitors are not necessarily associated with lack of selectivity [152]. However, the exact molecular reasons for this impressive selectivity profile remain yet to be elucidated. Representing the first example of a potent and highly selective type I TKI, crenolanib (**63**) may characterize a novel breakthrough in target therapy in cancer [159].

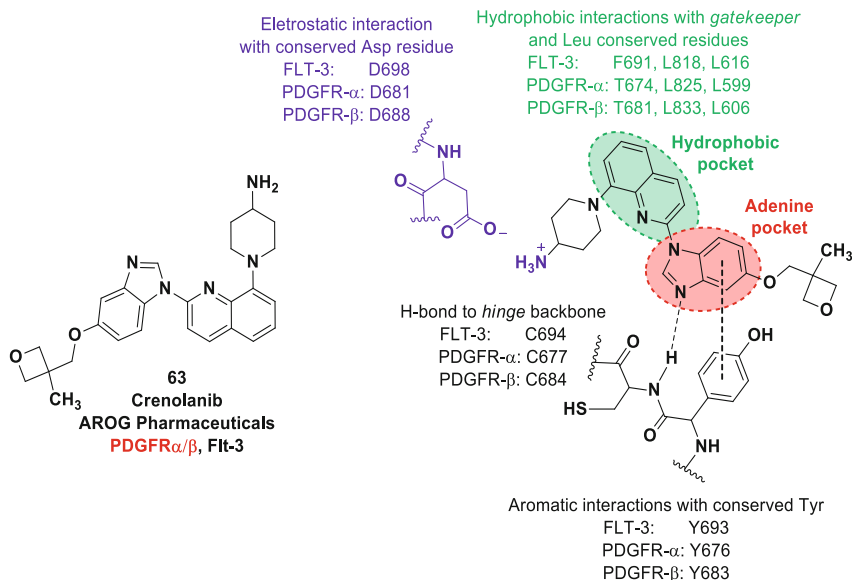


Fig. 21 Predicted binding mode of crenolanib (**63**) with the target kinases PDGFR- α and PDGFR- β , based on previous docking studies for the interaction of this compound with FLT-3

Despite the well-described biochemical results indicating that crenolanib (**63**) acts as a type I inhibitor, up to now no co-crystallized structure of this prototype with any of the target RTKs has been reported. Smith and coworkers performed a docking study to predict the binding mode of compound **63** to FLT-3. According to their results, crenolanib benzimidazole nitrogen interacts via hydrogen bond with the *hinge* residue Cys-694, and the aromatic bicyclic rings fit into a hydrophobic pocket that includes Leu-616, Phe-691, Tyr-693, and Leu-818, with the quinoline ring performing aromatic interactions with *gatekeeper* Phe-691 and the benzimidazole ring with Tyr-693. It is noteworthy that these authors also report a relevant electrostatic interaction between the positively charged amino group in the piperidine moiety and the Asp-698 residue [159]. A similar binding mode is expected for the other members of class III 5-Ig RTKs, including PDGFR- α/β (Fig. 21).

Considering the unusual highly selective profile of this type I TKI, it is interesting to observe whether the mentioned amino acid residues are conserved among the class III 5-Ig RTKs in comparison with other tyrosine kinases outside this specific class. Taking into account the results depicted in Fig. 22, one can notice that the ionic interaction between the prototype and the Asp-698 residue is conserved for all the class III 5-Ig RTKs, though this is not the case for the other analyzed kinases, suggesting a clear role of this amino acid-mediated interaction for the selectivity among the evaluated targets. However, further achievement of a crystal structure with the target enzymes may bring new light into this hypothesis.

In this context, the drug candidate crenolanib (**63**) could be clearly considered a next-generation type I RTK inhibitor with a novel chemical framework and a unique

FLT3	614 <u>KV</u> <u>L</u> GS 618	690 <u>I</u> <u>F</u> <u>E</u> <u>Y</u> <u>C</u> <u>C</u> <u>Y</u> <u>G</u> D 698	818 <u>L</u> <u>V</u> <u>T</u> <u>H</u> <u>G</u> <u>K</u> <u>V</u> <u>V</u> <u>K</u> <u>I</u> <u>C</u> <u>D</u> <u>F</u> <u>G</u> 831
PDGFR- α	597 <u>R</u> <u>V</u> <u>L</u> GS 601	673 <u>I</u> <u>T</u> <u>E</u> <u>Y</u> <u>C</u> <u>F</u> <u>Y</u> <u>G</u> D 681	825 <u>L</u> <u>L</u> <u>A</u> <u>Q</u> <u>G</u> <u>K</u> <u>I</u> <u>V</u> <u>K</u> <u>I</u> <u>C</u> <u>D</u> <u>F</u> <u>G</u> 838
PDGFR- β	604 <u>R</u> <u>T</u> <u>L</u> GS 608	680 <u>I</u> <u>T</u> <u>E</u> <u>Y</u> <u>C</u> <u>R</u> <u>Y</u> <u>G</u> D 688	833 <u>L</u> <u>I</u> <u>C</u> <u>E</u> <u>G</u> <u>K</u> <u>L</u> <u>V</u> <u>K</u> <u>I</u> <u>C</u> <u>D</u> <u>F</u> <u>G</u> 846
KIT	593 <u>K</u> <u>T</u> <u>L</u> GA 597	669 <u>I</u> <u>T</u> <u>E</u> <u>Y</u> <u>C</u> <u>C</u> <u>Y</u> <u>G</u> D 677	799 <u>L</u> <u>L</u> <u>T</u> <u>H</u> <u>G</u> <u>R</u> <u>I</u> <u>T</u> <u>K</u> <u>I</u> <u>C</u> <u>D</u> <u>F</u> <u>G</u> 812
VEGFR-I	831 <u>K</u> <u>S</u> <u>L</u> GR 835	908 <u>I</u> <u>V</u> <u>E</u> <u>Y</u> <u>C</u> <u>K</u> <u>Y</u> <u>G</u> N 916	1029 <u>L</u> <u>L</u> <u>S</u> <u>E</u> <u>N</u> <u>N</u> <u>V</u> <u>V</u> <u>K</u> <u>I</u> <u>C</u> <u>D</u> <u>F</u> <u>G</u> 1042
VEGFR-II	838 <u>K</u> <u>P</u> <u>L</u> GR 842	915 <u>I</u> <u>V</u> <u>E</u> <u>E</u> <u>C</u> <u>K</u> <u>F</u> <u>G</u> N 923	1035 <u>L</u> <u>L</u> <u>S</u> <u>E</u> <u>K</u> <u>N</u> <u>V</u> <u>V</u> <u>K</u> <u>I</u> <u>C</u> <u>D</u> <u>F</u> <u>G</u> 1048
EGFR	716 <u>K</u> <u>V</u> <u>L</u> GS 720	789 <u>I</u> <u>T</u> <u>Q</u> <u>L</u> <u>M</u> <u>P</u> <u>F</u> <u>G</u> C 797	844 <u>L</u> <u>V</u> <u>K</u> <u>T</u> <u>P</u> <u>Q</u> <u>H</u> <u>V</u> <u>K</u> <u>I</u> <u>T</u> <u>D</u> <u>F</u> <u>G</u> 857
FGFR-1	482 <u>K</u> <u>P</u> <u>L</u> GE 486	560 <u>I</u> <u>V</u> <u>E</u> <u>Y</u> <u>A</u> <u>S</u> <u>K</u> <u>G</u> N 568	630 <u>L</u> <u>V</u> <u>T</u> <u>E</u> <u>D</u> <u>N</u> <u>V</u> <u>M</u> <u>K</u> <u>I</u> <u>A</u> <u>D</u> <u>F</u> <u>G</u> 643
ABL	246 <u>H</u> <u>K</u> <u>L</u> GG 250	314 <u>I</u> <u>T</u> <u>E</u> <u>F</u> <u>M</u> <u>T</u> <u>Y</u> <u>G</u> N 322	370 <u>L</u> <u>V</u> <u>G</u> <u>E</u> <u>N</u> <u>H</u> <u>L</u> <u>V</u> <u>K</u> <u>V</u> <u>A</u> <u>D</u> <u>F</u> <u>G</u> 383

	<i>gatekeeper</i>			<i>hinge</i>		
FLT3	L616	F691	Y693	C694	D698	L818
PDGFR-α	L599	T674	Y676	C677	D681	L825
PDGFR-β	L606	T681	Y683	C684	D688	L833
KIT	L595	T670	Y672	C673	D677	L799
VEGFR-I	L833	V909	Y911	C912	N916	L1029
VEGFR-II	L840	V916	F918	C919	N923	L1035
EGFR	L718	T790	L792	M793	C797	L844
FGFR-1	L484	V561	Y563	A564	N568	L630
ABL	L248	T315	F317	M318	N322	L370

Fig. 22 Sequence alignment and the modification of amino acid residues described as important for crenolanib (**63**) recognition by FLT-3 in comparison with other relevant tyrosine kinases (TKs). For all the class III 5-Ig RTKs, highlighted in green, the Asp amino acid residue involved in the ionic electrostatic interaction with the charged amino group of drug candidate **63** is conserved. The amino acid residues from FLT-3 are highlighted in brown, as well as those conserved in other PKs

binding mode, showing favored inhibition of active phosphorylated class III 5-Ig RTKs, comprising wild-type and mutant forms of the target proteins PDGFR- α , PDGFR- β , and FLT3.

5 Epilogue

As increased activity, abundance, and/or cellular distribution of wild-type and mutant forms of RTKs is often associated with tumor establishment, growth, and progression, small-molecule TKIs directed to clinically relevant RTKs have entered the pharmaceutical market since the beginning of the twenty-first century, representing innovative drugs for cancer treatment.

Their clinical use is based in the oncogene addiction phenomenon, which describes the dependency of certain tumor cells on a specific oncogenic protein. Even though these drugs clearly represented an impressive breakthrough in the therapy of RTK-addicted tumors, resistance development and detection of refractory tumors have given rise to novel therapeutic challenges, pushing the drug discovery process forward.

The valley of death between preclinical assays and clinical practice is gradually becoming narrower as a result of constant collaboration and exchange of information from the bed to the bench and back, aiming to better understand the drug resistance molecular mechanisms and to plan innovative inhibitors able to overcome the unexpected clinical challenges.

One thing is certain, “drugs on demand” to attend to a limited group of patients is a growing therapeutic principle in the field, and the near future will bring exciting novelties concerning tumor resistance development, individualized therapies, selection of responsive patients, and the development of new clinical candidates.

Compliance with Ethical Standards

Funding: This study was funded by INCT-INOFAR (CNPq#465.249/2014-0; FAPERJ#E-26/010.000090/2018)

Conflict of Interest: Authors (LML; MLCB; DNA; EJB) declare that they have no conflict of interest.

Ethical Approval: This article does not contain any studies with human participants or animals performed by any of the authors.

References

1. Lemmon MA, Schlessinger J (2010) Cell signaling by receptor tyrosine kinases. *Cell* 141:1117–1134. <https://doi.org/10.1016/j.cell.2010.06.011>
2. Wagner JP, Wolf-Yadlin A, Sevecka M et al (2013) Receptor tyrosine kinases fall into distinct classes based on their inferred signaling networks. *Sci Signal* 6:ra58
3. Bayraktar UD, Bayraktar S, Rocha-Lima CM (2010) Molecular basis and management of gastrointestinal stromal tumours. *World J Gastroenterol* 16:2726–2734. <https://doi.org/10.3748/wjg.v16.i22.2726>

4. Guida T, Anaganti S, Provitera L et al (2007) Sorafenib inhibits imatinib-resistant KIT and platelet-derived growth factor receptor beta gatekeeper mutants. *Clin Cancer Res* 13:3363–3369. <https://doi.org/10.1158/1078-0432.CCR-06-2667>
5. Liang L, Yan X-E, Yin Y, Yun C-H (2016) Structural and biochemical studies of the PDGFRA kinase domain. *Biochem Biophys Res Commun* 477:667–672. <https://doi.org/10.1016/j.bbrc.2016.06.117>
6. Shi L, Zhou J, Wu J et al (2016) Anti-angiogenic therapy: strategies to develop potent VEGFR-2 tyrosine kinase inhibitors and future prospect. *Curr Med Chem* 23:1000–1040
7. Wu P, Nielsen TE, Clausen MH (2015) FDA-approved small-molecule kinase inhibitors. *Trends Pharmacol Sci* 36:422–439. <https://doi.org/10.1016/j.tips.2015.04.005>
8. Vajpai N, Strauss A, Fendrich G et al (2008) Solution conformations and dynamics of ABL kinase-inhibitor complexes determined by NMR substantiate the different binding modes of imatinib/nilotinib and dasatinib. *J Biol Chem* 283:18292–18302. <https://doi.org/10.1074/jbc.M801337200>
9. Dietrich J, Hulme C, Hurley LH (2010) The design, synthesis, and evaluation of 8 hybrid DFG-out allosteric kinase inhibitors: a structural analysis of the binding interactions of Gleevec, Nexavar, and BIRB-796. *Bioorg Med Chem* 18:5738–5748. <https://doi.org/10.1016/j.bmc.2010.05.063>
10. Wu P, Nielsen TE, Clausen MH (2016) Small-molecule kinase inhibitors: an analysis of FDA-approved drugs. *Drug Discov Today* 21:5–10. <https://doi.org/10.1016/j.drudis.2015.07.008>
11. Muralidhara C, Ramachandran A, Jain VK (2012) Abstract 3683: Crenolanib, a novel type I, mutant-specific inhibitor of class III receptor tyrosine kinases, preferentially binds to phosphorylated kinases. *Cancer Res* 72:3683–3683. <https://doi.org/10.1158/1538-7445.AM2012-3683>
12. Bazley LA, Gullick WJ (2005) The epidermal growth factor receptor family. *Endocr Relat Cancer* 12:17–28. <https://doi.org/10.1677/erc.1.01032>
13. Wieduwilt MJ, Moasser MM (2008) The epidermal growth factor receptor family: biology driving targeted therapeutics. *Cell Mol Life Sci* 65:1566–1584. <https://doi.org/10.1007/s00018-008-7440-8>
14. Tebbutt N, Pedersen MW, Johns TG (2013) Targeting the ERBB family in cancer: couples therapy. *Nat Rev Cancer* 13:663–673. <https://doi.org/10.1038/nrc3559>
15. Zhang H, Berezov A, Wang Q et al (2007) ErbB receptors: from oncogenes to targeted cancer therapies. *J Clin Invest* 117:2051–2058
16. Graus-Porta D, Beerli RR, Daly JM, Hynes NE (1997) ErbB-2, the preferred heterodimerization partner of all ErbB receptors, is a mediator of lateral signaling. *EMBO J* 16:1647–1655. <https://doi.org/10.1093/emboj/16.7.1647>
17. Hynes NE, MacDonald G (2009) ErbB receptors and signaling pathways in cancer. *Curr Opin Cell Biol* 21:177–184
18. Nyati M, Morgan M, Feng F, Lawrence T (2006) Integration of EGFR inhibitors with radiochemotherapy. *Nat Rev Cancer* 6:876–885. <https://doi.org/10.1038/nrc1953>
19. Gao S, Mark K, Leslie K (2007) Mutations in the EGFR kinase domain mediate STAT3 activation via IL-6 production in human lung adenocarcinomas. *J Clin Invest* 117:3846–3856. <https://doi.org/10.1172/JCI31871.3846>
20. Wang Q, Greene MI (2008) Mechanisms of resistance to ErbB-targeted cancer therapeutics. *J Clin Invest* 118:2389–2392. <https://doi.org/10.1172/JCI36260>
21. Hickey K, Grehan D, Reid IM et al (1994) Expression of epidermal growth factor receptor and proliferating cell nuclear antigen predicts response of esophageal squamous cell carcinoma to chemoradiotherapy. *Cancer* 74:1693–1698. [https://doi.org/10.1002/1097-0142\(19940915\)74:6<1693::AID-CNCR2820740609>3.0.CO;2-#](https://doi.org/10.1002/1097-0142(19940915)74:6<1693::AID-CNCR2820740609>3.0.CO;2-#)
22. Liu B, Bernard B, Wu JH (2006) Impact of EGFR point mutations on the sensitivity to gefitinib : insights from comparative structural analyses and molecular dynamics simulations. *Proteins Struct Funct Bioinf* 65:331–346. <https://doi.org/10.1002/prot>

23. Abella JV, Park M (2009) Breakdown of endocytosis in the oncogenic activation of receptor tyrosine kinases. *Am J Physiol Endocrinol Metab* 296:E973–E984. <https://doi.org/10.1152/ajpendo.90857.2008>
24. Meierjohann S, Hufnagel A, Wende E et al (2010) MMP13 mediates cell cycle progression in melanocytes and melanoma cells: in vitro studies of migration and proliferation. *Mol Cancer* 9:201. <https://doi.org/10.1186/1476-4598-9-201>
25. Mendelsohn J (2001) The epidermal growth factor receptor as a target for cancer therapy. *Endocr Relat Cancer* 8:3–9
26. Pines G, Huang PH, Zwang Y et al (2010) EGFRvIV: a previously uncharacterized oncogenic mutant reveals a kinase autoinhibitory mechanism. *Oncogene* 29:5850–5860. <https://doi.org/10.1038/onc.2010.313>
27. Umekita Y, Ohi Y, Sagara Y, Yoshida H (2000) Co-expression of epidermal growth factor receptor and transforming growth factor- α predicts worse prognosis in breast-cancer patients. *Int J Cancer* 89:484–487. [https://doi.org/10.1002/1097-0215\(20001120\)89:6<484::AID-IJC3>3.0.CO;2-S](https://doi.org/10.1002/1097-0215(20001120)89:6<484::AID-IJC3>3.0.CO;2-S)
28. Chong CR, Jänne PA (2013) The quest to overcome resistance to EGFR-targeted therapies in cancer. *Nat Med* 19:1389–1400. <https://doi.org/10.1038/nm.3388>
29. Nawaz K, Webster RM (2016) The non-small-cell lung cancer drug market. *Nat Rev Drug Discov* 15:229–230. <https://doi.org/10.1038/nrd.2016.42>
30. Dienstmann R, De Dosso S, Felip E, Tabernero J (2012) Drug development to overcome resistance to EGFR inhibitors in lung and colorectal cancer. *Mol Oncol* 6:15–26
31. Moreira C, Kaklamani V (2010) Lapatinib and breast cancer: current indications and outlook for the future. *Expert Rev Anticancer Ther* 10:1171–1182. <https://doi.org/10.1586/era.10.113>
32. Ton GN, Banaszynski ME, Kolesar JM (2013) Vandetanib: a novel targeted therapy for the treatment of metastatic or locally advanced medullary thyroid cancer. *Am J Health Syst Pharm* 70:849–855
33. Woodburn JR (1999) The epidermal growth factor receptor and its inhibition in cancer therapy. *Pharmacol Ther* 82:241–250. [https://doi.org/10.1016/S0163-7258\(98\)00045-X](https://doi.org/10.1016/S0163-7258(98)00045-X)
34. Ward WHJ, Cook PN, Slater AM et al (1994) Epidermal growth factor receptor tyrosine kinase. *Biochem Pharmacol* 48:659–666. [https://doi.org/10.1016/0006-2952\(94\)90042-6](https://doi.org/10.1016/0006-2952(94)90042-6)
35. Fry DW, Kraker AJ, McMichael A et al (1994) A specific inhibitor of the epidermal growth factor receptor tyrosine kinase. *Science* 265:1093–1095. <https://doi.org/10.1126/science.8066447>
36. Rewcastle GW, Denny WA, Bridges AJ et al (1995) Synthesis and structure-activity relationships for 4-[(phenylmethyl) amino]- and 4-(phenylamino) quinazolines as potent adenosine 5'-triphosphate binding site inhibitors of the tyrosine kinase domain of the epidermal growth factor receptor. *J Med Chem* 38:3482–3487
37. Wakeling AE, Barker AJ, Davies DH et al (1996) Specific inhibition of epidermal growth factor receptor tyrosine kinase by 4-anilinoquinazolines A.E. *Breast Cancer Res Treat* 38:67–73
38. Denny WA, Rewcastle GW, Bridges AJ et al (1996) Structure-activity relationships for 4-anilinoquinazolines as potent inhibitors at the ATP binding site of the epidermal growth factor receptor in vitro. *Clin Exp Pharmacol Physiol* 23:424–427
39. Bridges AJ, Zhou H, Cody DR et al (1996) Tyrosine kinase inhibitors 8. An unusually steep structure-activity relationship for analogues of 4-(3-bromoanilino)-6,7-dimethoxyquinazoline (PD 153035), a potent inhibitor of the epidermal growth factor receptor. *J Med Chem* 39:267–276
40. Barreiro EJ, Kümmerle AE, Fraga CAM (2011) The methylation effect in medicinal chemistry. *Chem Rev* 111:5215–5246
41. Myers MR, Setzer N, Spada AP et al (1997) The synthesis and SAR of new 4-(N-alkyl-N-phenyl)amino-6,7-dimethoxyquinazolines and 4-(N-alkyl-N-phenyl)amino-pyrazolo[3,4-d]pyrimidines, inhibitors of CSF-1R tyrosine kinase activity. *Bioorg Med Chem Lett* 7:421–424

42. Myers MR, Setzer NN, Spada AP et al (1997) The preparation and SAR of 4-(anilino), 4-(phenoxy), and 4-(thiophenoxy)-quinazolines: inhibitors of p56(lck) and EGF-R tyrosine kinase activity. *Bioorg Med Chem Lett* 7:417–420. [https://doi.org/10.1016/S0960-894X\(97\)00034-6](https://doi.org/10.1016/S0960-894X(97)00034-6)
43. Barker AJ, Gibson KH, Grundy W et al (2001) Studies leading to the identification of ZD1839 (Iressa): an orally active, selective epidermal growth factor receptor tyrosine kinase inhibitor targeted to the treatment of cancer. *Bioorg Med Chem Lett* 11:1911–1914. [https://doi.org/10.1016/S0960-894X\(01\)00344-4](https://doi.org/10.1016/S0960-894X(01)00344-4)
44. Böhm H-J, Banner D, Bendels S et al (2004) Fluorine in medicinal chemistry. *Chembiochem* 5:637–643. <https://doi.org/10.1002/cbic.200301023>
45. Gillis EP, Eastman KJ, Hill MD et al (2015) Applications of fluorine in medicinal chemistry. *J Med Chem* 58:8315–8359. <https://doi.org/10.1021/acs.jmedchem.5b00258>
46. Woodburn JR (1998) EGF receptor tyrosine kinase inhibitors as anti-cancer agents – pre-clinical and early clinical profile of ZD 1839. *Cell Mol Biol Lett* 3:348–349
47. Palmer BD, Trumpf-Kallmeyer S, Fry DW et al (1997) Tyrosine kinase inhibitors. 11. Soluble analogues of pyrrolo- and pyrazoloquinazolines as epidermal growth factor receptor inhibitors: synthesis, biological evaluation, and modeling of the mode of binding. *J Med Chem* 40:1519–1529. <https://doi.org/10.1021/jm960789h>
48. Zheng J, Trafny EA, Knighton DR et al (1993) 2.2 angstrom refined crystal structure of the catalytic subunit of cAMP-dependent protein kinase complexed with MnATP and a peptide inhibitor. *Acta Crystallogr D Biol Crystallogr* 49:362–365
49. Moyer JD, Barbacci EG, Iwata KK et al (1997) Induction of apoptosis and cell cycle arrest by CP-358,774, an inhibitor of epidermal growth factor receptor tyrosine kinase. *Cancer Res* 57:4838–4848
50. Stamos J, Sliwkowski MX, Eigenbrot C (2002) Structure of the epidermal growth factor receptor kinase domain alone and in complex with a 4-anilinoquinazoline inhibitor. *J Biol Chem* 277:46265–46272. <https://doi.org/10.1074/jbc.M207135200>
51. Cohen MH (2003) FDA drug approval summary: Gefitinib (ZD1839) (Iressa(R)) tablets. *Oncologist* 8:303–306. <https://doi.org/10.1634/theoncologist.8-4-303>
52. Cohen M, Johnson J, Chen Y et al (2005) FDA drug approval summary: Erlotinib (Tarceva®) tablets. *Oncologist* 10:461–466
53. Herbst RS, Fukuoka M, Baselga J (2004) Gefitinib – a novel targeted approach to treating cancer. *Nat Rev Cancer* 4:956–965. <https://doi.org/10.1038/nrc1506>
54. Juchum M, Gunther M, Laufer SA (2014) Fighting cancer drug resistance: opportunities and challenges for mutation-specific EGFR inhibitors. *Drug Resist Updat* 20:12–28. <https://doi.org/10.1016/j.drug.2015.05.002>
55. Ohashi K, Maruvka YE, Michor F, Pao W (2013) Epidermal growth factor receptor tyrosine kinase inhibitor-resistant disease. *J Clin Oncol* 31:1070–1080
56. Fridlyand J, Simon RM, Walrath JC et al (2013) Considerations for the successful co-development of targeted cancer therapies and companion diagnostics. *Nat Rev Drug Discov* 12:743–755. <https://doi.org/10.1038/nrd4101>
57. Vargas AJ, Harris CC (2016) Biomarker development in the precision medicine era: lung cancer as a case study. *Nat Rev Cancer* 16:525–537. <https://doi.org/10.1038/nrc.2016.56>
58. Lynch TJ, Bell DW, Sordella R et al (2004) Activating mutations in the epidermal growth factor receptor underlying responsiveness of non-small-cell lung cancer to gefitinib. *N Engl J Med* 350:2129–2139. <https://doi.org/10.1056/NEJMoa1109400>
59. Laufer S, Bajorath J (2015) Advancing the kinase field: new targets and second generation inhibitors. *J Med Chem* 58:1. <https://doi.org/10.1021/jm5018708>
60. Yun C, Mengwasser KE, Toms AV et al (2008) The T790M mutation in EGFR kinase causes drug resistance by increasing the affinity for ATP. *Proc Natl Acad Sci U S A* 105:2070–2075. <https://doi.org/10.1073/pnas.0709662105>
61. Ma C, Wei S, Song Y (2011) T790M and acquired resistance of EGFR TKI: a literature review of clinical reports. *J Thorac Dis* 3:10–18

62. Oxnard GR, Arcila ME, Chmielecki J et al (2011) New strategies in overcoming acquired resistance to epidermal growth factor receptor tyrosine kinase inhibitors in lung cancer. *Clin Cancer Res* 17:5530–5537. <https://doi.org/10.1158/1078-0432.CCR-10-2571>
63. Bikker JA, Brooijmans N, Wissner A, Mansour TS (2009) Kinase domain mutations in cancer: implications for small molecule drug design strategies. *J Med Chem* 52:1493–1509
64. Holohan C, Van Schaeybroeck S, Longley DB, Johnston PG (2013) Cancer drug resistance: an evolving paradigm. *Nat Rev Cancer* 13:714–726. <https://doi.org/10.1038/nrc3599>
65. Godin-Heymann N, Ulkus L, Brannigan BW et al (2008) The T790M “gatekeeper” mutation in EGFR mediates resistance to low concentrations of an irreversible EGFR inhibitor. *Mol Cancer Ther* 7:874–879. <https://doi.org/10.1158/1535-7163.MCT-07-2387>
66. Gajiwala KS, Feng J, Ferre R et al (2013) Insights into the aberrant activity of mutant EGFR kinase domain and drug recognition. *Structure* 21:209–219. <https://doi.org/10.1016/j.str.2012.11.014>
67. Doebele RC, Oton AB, Peled N et al (2010) New strategies to overcome limitations of reversible EGFR tyrosine kinase inhibitor therapy in non-small cell lung cancer. *Lung Cancer* 69:1–12. <https://doi.org/10.1016/j.lungcan.2009.12.009>
68. Zhou W, Ercan D, Chen L et al (2009) Novel mutant-selective EGFR kinase inhibitors against EGFR T790M. *Nature* 462:1070–1074. <https://doi.org/10.1038/nature08622>
69. Kwak EL, Sordella R, Bell DW et al (2005) Irreversible inhibitors of the EGF receptor may circumvent acquired resistance to gefitinib. *Proc Natl Acad Sci U S A* 102:7665–7670. <https://doi.org/10.1073/pnas.0502860102>
70. Liu Q, Sabnis Y, Zhao Z et al (2013) Developing irreversible inhibitors of the protein kinase cysteinome. *Chem Biol* 20:146–159. <https://doi.org/10.1016/j.chembiol.2012.12.006>
71. Mah R, Thomas JR, Shafer CM (2014) Drug discovery considerations in the development of covalent inhibitors. *Bioorg Med Chem Lett* 24:33–39
72. Singh J, Petter RC, Baillie TA, Whitty A (2011) The resurgence of covalent drugs. *Nat Rev Drug Discov* 10:307–317. <https://doi.org/10.1038/nrd3410>
73. Barf T, Kaptein A (2012) Irreversible protein kinase inhibitors: balancing the benefits and risks. *J Med Chem* 55:6243–6262. <https://doi.org/10.1021/jm3003203>
74. Kalgutkar AS, Dalvie DK (2012) Drug discovery for a new generation of covalent drugs. *Expert Opin Drug Discovery* 7:561–581. <https://doi.org/10.1517/17460441.2012.688744>
75. Levitzki A (2013) Tyrosine kinase inhibitors: views of selectivity, sensitivity, and clinical performance. *Annu Rev Pharmacol Toxicol* 53:161–185. <https://doi.org/10.1146/annurev-pharmtox-011112-140341>
76. Singh J, Dobrusin EM, Fry DW et al (1997) Structure-based design of a potent, selective, and irreversible inhibitor of the catalytic domain of the erbB receptor subfamily of protein tyrosine kinases. *J Med Chem* 40:1130–1135. <https://doi.org/10.1021/jm960380s>
77. Fry DW, Bridges AJ, Denny WA et al (1998) Specific, irreversible inactivation of the epidermal growth factor receptor and erbB2, by a new class of tyrosine kinase inhibitor. *Proc Natl Acad Sci U S A* 95:12022–12027. <https://doi.org/10.1073/pnas.95.20.12022>
78. Smaill JB, Palmer BD, Rewcastle GW et al (1999) 4-(Phenylamino)pyrido[d]pyrimidine acrylamides as irreversible inhibitors of the ATP binding site of the epidermal growth factor receptor. *J Med Chem* 42:1803–1815
79. Smaill JB, Rewcastle GW, Loo JA et al (2000) Tyrosine kinase inhibitors. 17. Irreversible inhibitors of the epidermal growth factor receptor: 4-(phenylamino)quinazoline- and 4-(phenylamino)pyrido[3,2-d]pyrimidine-6-acrylamides bearing additional solubilizing functions. *J Med Chem* 43:1380–1397. <https://doi.org/10.1021/jm990482t>
80. Williams R (2008) Discontinued drugs in 2006: oncology drugs. *Expert Opin Investig Drugs* 17:269–283. <https://doi.org/10.1517/13543784.17.3.269>
81. Tsou HR, Mamuya N, Johnson BD et al (2001) 6-Substituted-4-(3-bromophenylamino)quinazolines as putative irreversible inhibitors of the epidermal growth factor receptor (EGFR) and human epidermal growth factor receptor (HER-2) tyrosine kinases with enhanced antitumour activity. *J Med Chem* 44:2719–2734. <https://doi.org/10.1021/jm0005555>

82. Carmi C, Lodola A, Rivara S et al (2011) Epidermal growth factor receptor irreversible inhibitors: chemical exploration of the cysteine-trap portion. *Mini Rev Med Chem* 11:1019–1030. <https://doi.org/10.2174/138955711797247725>
83. Weinstein IB, Joe AK (2006) Mechanisms of disease: oncogene addiction – a rationale for molecular targeting in cancer therapy. *Nat Clin Pract Oncol* 3:448–457. <https://doi.org/10.1038/ncponc0558>
84. Li D, Ambrogio L, Shimamura T et al (2008) BIBW2992, an irreversible EGFR/HER2 inhibitor highly effective in preclinical lung cancer models. *Oncogene* 27:4702–4711. <https://doi.org/10.1038/onc.2008.109>
85. Eskens FALM, Mom CH, Planting AST et al (2008) A phase I dose escalation study of BIBW 2992, an irreversible dual inhibitor of epidermal growth factor receptor 1 (EGFR) and 2 (HER2) tyrosine kinase in a 2-week on, 2-week off schedule in patients with advanced solid tumours. *Br J Cancer* 98:80–85. <https://doi.org/10.1038/sj.bjc.6604108>
86. Fiala O, Pesek M, Finek J et al (2013) Skin rash as useful marker of erlotinib efficacy in NSCLC and its impact on clinical practice. *Neoplasma* 60:26–32. https://doi.org/10.4149/neo_2013_004
87. Giordano P, Manzo A, Montanino A et al (2016) Afatinib: an overview of its clinical development in non-small-cell lung cancer and other tumours. *Crit Rev Oncol Hematol* 97:143–151
88. Solca F, Dahl G, Zoepfel A et al (2012) Target binding properties and cellular activity of afatinib (BIBW 2992), an irreversible ErbB family blocker. *J Pharmacol Exp Ther* 343:342–350. <https://doi.org/10.1124/jpet.112.197756>
89. Miller VA, Hirsh V, Cadranel J et al (2012) Afatinib versus placebo for patients with advanced, metastatic non-small-cell lung cancer after failure of erlotinib, gefitinib, or both, and one or two lines of chemotherapy (LUX-Lung 1): a phase 2b/3 randomised trial. *Lancet Oncol* 13:528–538. [https://doi.org/10.1016/S1470-2045\(12\)70087-6](https://doi.org/10.1016/S1470-2045(12)70087-6)
90. Sanderson K (2013) Irreversible kinase inhibitors gain traction. *Nat Rev Drug Discov* 12:649–651. <https://doi.org/10.1038/nrd4103>
91. Cross DAE, Ashton SE, Ghorghiu S et al (2014) AZD9291, an irreversible EGFR TKI, overcomes T790M-mediated resistance to EGFR inhibitors in lung cancer. *Cancer Discov* 4:1046–1061. <https://doi.org/10.1158/2159-8290.CD-14-0337>
92. Smit EF, Baas P (2015) Lung cancer in 2015: bypassing checkpoints, overcoming resistance, and honing in on new targets. *Nat Rev Clin Oncol* 13:75–76. <https://doi.org/10.1038/nrclinonc.2015.223>
93. Thress KS, Paweletz CP, Felip E et al (2015) Acquired EGFR C797S mutation mediates resistance to AZD9291 in non-small cell lung cancer harboring EGFR T790M. *Nat Med* 21:560–562. <https://doi.org/10.1038/nm.3854>
94. Hanan EJ, Eigenbrot C, Bryan MC et al (2014) Discovery of selective and non-covalent diaminopyrimidine based inhibitors of EGFR containing the T790M resistance mutation. *J Med Chem* 57:10176. <https://doi.org/10.1021/jm501578n>
95. Heald R, Bowman KK, Bryan MC et al (2015) Noncovalent mutant selective epidermal growth factor receptor inhibitors: a lead optimization case study. *J Med Chem* 58:8877–8895. <https://doi.org/10.1021/acs.jmedchem.5b01412>
96. Jia Y, Yun C-H, Park E et al (2016) Overcoming EGFR(T790M) and EGFR(C797S) resistance with mutant-selective allosteric inhibitors. *Nature* 534:129–132. <https://doi.org/10.1038/nature17960>
97. Holmes K, Roberts OL, Thomas AM, Cross MJ (2007) Vascular endothelial growth factor receptor-2: structure, function, intracellular signalling and therapeutic inhibition. *Cell Signal* 19:2003–2012. <https://doi.org/10.1016/j.cellsig.2007.05.013>
98. Ferrara N, Gerber HP, LeCouter J (2003) The biology of VEGF and its receptors. *Nat Med* 9:669–676. <https://doi.org/10.1038/nm0603-669>

99. Shibuya M (2011) Vascular endothelial growth factor (VEGF) and its receptor (VEGFR) signaling in angiogenesis: a crucial target for anti- and pro-Angiogenic therapies. *Genes Cancer* 2:1097–1105. <https://doi.org/10.1177/1947601911423031>
100. Takahashi S (2011) Vascular endothelial growth factor (VEGF), VEGF receptors and their inhibitors for antiangiogenic tumour therapy. *Biol Pharm Bull* 34:1785–1788. <https://doi.org/10.1248/bpb.34.1785>
101. Adams RH, Alitalo K (2007) Molecular regulation of angiogenesis and lymphangiogenesis. *Nat Rev Mol Cell Biol* 8:464–478. <https://doi.org/10.1038/nrm2183>
102. Bergers G, Benjamin LE (2003) Tumourigenesis and the angiogenic switch. *Nat Rev Cancer* 3:401–410. <https://doi.org/10.1038/nrc1093>
103. Carmeliet P (2005) Angiogenesis in life, disease and medicine. *Nature* 438:932–936. <https://doi.org/10.1038/nature04478>
104. Hoeben A, Landuyt B, Highley MS et al (2004) Vascular endothelial growth factor and angiogenesis. *Pharmacol Rev* 56:549–580. <https://doi.org/10.1124/pr.56.4.3.549>
105. Schenone S, Bondavalli F, Botta M (2007) Antiangiogenic agents: an update on small molecule VEGFR inhibitors. *Curr Med Chem* 14:2495–2516. <https://doi.org/10.2174/092986707782023622>
106. Moreira IS, Fernandes PA, Ramos MJ (2007) Vascular endothelial growth factor (VEGF) inhibition – a critical review. *Anti Cancer Agents Med Chem* 7:223–245
107. Lee SH, Jeong D, Han Y-S, Baek MJ (2015) Pivotal role of vascular endothelial growth factor pathway in tumour angiogenesis. *Ann Surg Treat Res* 89:1–8. <https://doi.org/10.4174/astr.2015.89.1.1>
108. Holmes DIR, Zachary I (2005) The vascular endothelial growth factor (VEGF) family: angiogenic factors in health and disease. *Genome Biol* 6:209. <https://doi.org/10.1186/gb-2005-6-2-209>
109. Terman BI, Carrion ME, Kovacs E et al (1991) Identification of a new endothelial cell growth factor receptor tyrosine kinase. *Oncogene* 6:1677–1683. <https://doi.org/10.1383/surg.23.2.37.60352>
110. Dougher-Vermazen M, Hulmes JD, Böhlen P, Terman BI (1994) Biological activity and phosphorylation sites of the bacterially expressed cytosolic domain of the KDR VEGF-receptor. *Biochem Biophys Res Commun* 205:728–738
111. Fuh G, Li B, Crowley C et al (1998) Requirements for binding and signaling of the kinase domain receptor for vascular endothelial growth factor. *J Biol Chem* 273:11197–11204. <https://doi.org/10.1074/jbc.273.18.11197>
112. Roskoski R (2008) VEGF receptor protein-tyrosine kinases: structure and regulation. *Biochem Biophys Res Commun* 375:287–291
113. Simons M, Gordon E, Claesson-Welsh L (2016) Mechanisms and regulation of endothelial VEGF receptor signalling. *Nat Rev Mol Cell Biol* 17:611–625. <https://doi.org/10.1038/nrm.2016.87>
114. Youssoufian H, Hicklin DJ, Rowinsky EK (2007) Review: monoclonal antibodies to the vascular endothelial growth factor receptor-2 in cancer therapy. *Clin Cancer Res* 13:5544s–5548s. <https://doi.org/10.1158/1078-0432.CCR-07-1107>
115. Sitohy B, Nagy JA, Dvorak HF (2012) Anti-VEGF/VEGFR therapy for cancer: reassessing the target. *Cancer Res* 72:1909–1914. <https://doi.org/10.1158/0008-5472.CAN-11-3406>
116. Xu D, Wang T-L, Sun L-P, You Q-D (2011) Recent progress of small molecular VEGFR inhibitors as anticancer agents. *Mini Rev Med Chem* 11:18–31. <https://doi.org/10.2174/138955711793564015>
117. Zhang J, Shan Y, Pan X, He L (2011) Recent advances in antiangiogenic agents with VEGFR as target. *Mini Rev Med Chem* 11:920–946. <https://doi.org/10.2174/138955711797068355>
118. Sharma PS, Sharma R, Tyagi T (2011) VEGF/VEGFR pathway inhibitors as anti-angiogenic agents: present and future. *Curr Cancer Drug Targets* 11:624–653

119. Zhang C, Tan C, Ding H et al (2012) Selective VEGFR inhibitors for anticancer therapeutics in clinical use and clinical trials. *Curr Pharm Des* 18:2921–2935. <https://doi.org/10.2174/138161212800672732>
120. Matsui J, Yamamoto Y, Funahashi Y et al (2008) E7080, a novel inhibitor that targets multiple kinases, has potent antitumor activities against stem cell factor producing human small cell lung cancer H146, based on angiogenesis inhibition. *Int J Cancer* 122:664–671. <https://doi.org/10.1002/ijc.23131>
121. Okamoto K, Ikemori-Kawada M, Jestel A et al (2014) Distinct binding mode of multikinase inhibitor lenvatinib revealed by biochemical characterization. *ACS Med Chem Lett* 6:89–94. <https://doi.org/10.1021/ml500394m>
122. Roskoski R (2016) Classification of small molecule protein kinase inhibitors based upon the structures of their drug-enzyme complexes. *Pharmacol Res* 103:26–48. <https://doi.org/10.1016/j.phrs.2015.10.021>
123. Boss DS, Glen H, Beijnen JH et al (2012) A phase I study of E7080, a multitargeted tyrosine kinase inhibitor, in patients with advanced solid tumours. *Br J Cancer* 106:1598–1604. <https://doi.org/10.1038/bjc.2012.154>
124. Inoue K, Mizuo H, Kawaguchi S et al (2014) Oxidative metabolic pathway of lenvatinib mediated by aldehyde oxidase. *Drug Metab Dispos* 42:1326–1333. <https://doi.org/10.1124/dmd.114.058073>
125. Shumaker R, Aluri J, Fan J et al (2015) Effects of ketoconazole on the pharmacokinetics of lenvatinib (E7080) in healthy participants. *Clin Pharmacol Drug Dev* 4:155–160. <https://doi.org/10.1002/cpdd.140>
126. Shumaker RC, Aluri J, Fan J et al (2014) Effect of rifampicin on the pharmacokinetics of lenvatinib in healthy adults. *Clin Drug Investig* 34:651–659. <https://doi.org/10.1007/s40261-014-0217-y>
127. Matsui J, Funahashi Y, Uenaka T et al (2008) Multi-kinase inhibitor E7080 suppresses lymph node and lung metastases of human mammary breast tumour MDA-MB-231 via inhibition of vascular endothelial growth factor-receptor (VEGF-R) 2 and VEGF-R3 kinase. *Clin Cancer Res* 14:5459–5465. <https://doi.org/10.1158/1078-0432.CCR-07-5270>
128. Scott LJ (2015) Lenvatinib: first global approval. *Drugs* 75:553–560
129. Tohyama O, Matsui J, Kodama K et al (2014) Antitumour activity of lenvatinib (E7080): an angiogenesis inhibitor that targets multiple receptor tyrosine kinases in preclinical human thyroid Cancer models. *J Thyroid Res* 2014:1–13. <https://doi.org/10.1155/2014/638747>. ID 638747
130. Frampton JE (2016) Lenvatinib: a review in refractory thyroid Cancer. *Target Oncol* 11:115–122
131. Schlumberger M, Tahara M, Wirth LJ et al (2015) Lenvatinib versus placebo in radioiodine-refractory thyroid Cancer. *N Engl J Med* 372:621–630. <https://doi.org/10.1056/NEJMoa1406470>
132. Cao Y (2013) Multifarious functions of PDGFs and PDGFRs in tumour growth and metastasis. *Trends Mol Med* 19:460–473. <https://doi.org/10.1016/j.molmed.2013.05.002>
133. Heldin C-H (2013) Targeting the PDGF signaling pathway in tumour treatment. *Cell Commun Signal* 11:97. <https://doi.org/10.1186/1478-811X-11-97>
134. Lewis NL, Lewis LD, Eder JP et al (2009) Phase I study of the safety, tolerability, and pharmacokinetics of oral CP-868,596, a highly specific platelet-derived growth factor receptor tyrosine kinase inhibitor in patients with advanced cancers. *J Clin Oncol* 27:5262–5269. <https://doi.org/10.1200/JCO.2009.21.8487>
135. Chen P-HH, Chen X, He X (2013) Platelet-derived growth factors and their receptors: structural and functional perspectives. *Biochim Biophys Acta* 1834:2176–2186. <https://doi.org/10.1016/j.bbapap.2012.10.015>
136. Michael M, Vlahovic G, Khamly K et al (2010) Phase Ib study of CP-868,596, a PDGFR inhibitor, combined with docetaxel with or without axitinib, a VEGFR inhibitor. *Br J Cancer* 103:1554–1561. <https://doi.org/10.1038/sj.bjc.6605941>

137. Suzuki S, Heldin C, Heuchel RL (2007) Platelet-derived growth factor receptor-beta, carrying the activating mutation D849N, accelerates the establishment of B16 melanoma. *BMC Cancer* 7:224. <https://doi.org/10.1186/1471-2407-7-224>
138. Estevez-Garcia P, Castaño A, Martín AC et al (2012) PDGFR α / β and VEGFR2 polymorphisms in colorectal cancer: incidence and implications in clinical outcome. *BMC Cancer* 12:514. <https://doi.org/10.1186/1471-2407-12-514>
139. Wehler T, Frerichs K, Graf C et al (2008) PDGFR α / β expression correlates with the metastatic behavior of human colorectal cancer: a possible rationale for a molecular targeting strategy. *Oncol Rep* 19:697–704. <https://doi.org/10.3892/or.19.3.697>
140. Paulsson J, Sjoblom T, Micke P et al (2009) Prognostic significance of stromal platelet-derived growth factor beta-receptor expression in human breast cancer. *Am J Pathol* 175:334–341. <https://doi.org/10.2353/ajpath.2009.081030>
141. Tefferi A (2009) Molecular drug targets in myeloproliferative neoplasms: mutant ABL1, JAK2, MPL, KIT, PDGFRA, PDGFRB and FGFR1. *J Cell Mol Med* 13:215–237. <https://doi.org/10.1111/j.1582-4934.2008.00559.x>
142. Golub TR, Barker GF, Lovett M, Gary Gilliland D (1994) Fusion of PDGF receptor B to a novel ets-like gene, tel, in chronic myelomonocytic leukemia with t(5;12) chromosomal translocation. *Cell* 77:307–316. [https://doi.org/10.1016/0092-8674\(94\)90322-0](https://doi.org/10.1016/0092-8674(94)90322-0)
143. Cools J, DeAngelo DJ, Gotlib J et al (2003) A tyrosine kinase created by fusion of the PDGFRA and FIP1L1 genes as a therapeutic target of imatinib in idiopathic hypereosinophilic syndrome. *N Engl J Med* 348:1201–1214
144. Lierman E, Michaux L, Beullens E et al (2009) FIP1L1-PDGFRalpha D842V, a novel panresistant mutant, emerging after treatment of FIP1L1-PDGFRalpha T674I eosinophilic leukemia with single agent sorafenib. *Leukemia* 23:845–851. <https://doi.org/10.1038/leu.2009.2>
145. Corless CL, Schroeder A, Griffith D et al (2005) PDGFRA mutations in gastrointestinal stromal tumours: frequency, spectrum and in vitro sensitivity to imatinib. *J Clin Oncol* 23:5357–5364. <https://doi.org/10.1200/JCO.2005.14.068>
146. Debiec-Rychter M, Dumez H, Judson I et al (2004) Use of c-KIT/PDGFR α mutational analysis to predict the clinical response to imatinib in patients with advanced gastrointestinal stromal tumours entered on phase I and II studies of the EORTC soft tissue and bone sarcoma group. *Eur J Cancer* 40:689–695. <https://doi.org/10.1016/j.ejca.2003.11.025>
147. Heinrich MC, Corless CL, Duensing A et al (2003) PDGFRA activating mutations in gastrointestinal stromal tumours. *Science* 299:708–711
148. Boyar MS, Taub RN (2007) New strategies for treating GIST when imatinib fails. *Cancer Investig* 25:328–335. <https://doi.org/10.1080/07357900701206273>
149. Heinrich MC, Corless CL, Demetri GD et al (2003) Kinase mutations and imatinib response in patients with metastatic gastrointestinal stromal tumour. *J Clin Oncol* 21:4342–4349. <https://doi.org/10.1200/JCO.2003.04.190>
150. Hirota S, Ohashi A, Nishida T et al (2003) Gain-of-function mutations of platelet-derived growth factor receptor alpha gene in gastrointestinal stromal tumours. *Gastroenterology* 125:660–667. [https://doi.org/10.1016/S0016-5085\(03\)01046-1](https://doi.org/10.1016/S0016-5085(03)01046-1)
151. Kim EJ, Zalupski MM (2011) Systemic therapy for advanced gastrointestinal stromal tumours: beyond imatinib. *J Surg Oncol* 104:901–906. <https://doi.org/10.1002/jso.21872>
152. Wang P, Song L, Ge H et al (2014) Crenolanib, a PDGFR inhibitor, suppresses lung cancer cell proliferation and inhibits tumour growth in vivo. *Onco Targets Ther* 7:1761–1768
153. Gambacorti-Passerini CB, Gunby RH, Piazza R et al (2003) Molecular mechanisms of resistance to imatinib in Philadelphia-chromosome-positive leukaemias. *Lancet Oncol* 4:75–85. [https://doi.org/10.1016/S1470-2045\(03\)00979-3](https://doi.org/10.1016/S1470-2045(03)00979-3)
154. Druker BJ, Tamura S, Buchdunger E et al (1996) Effects of a selective inhibitor of the abl tyrosine kinase on the growth of Bcr-Abl positive cells. *Nat Med* 2:561–566. <https://doi.org/10.1038/nm0596-561>

155. Gschwind A, Fischer OM, Ullrich A (2004) The discovery of receptor tyrosine kinases: targets for cancer therapy. *Nat Rev Cancer* 4:361–370. <https://doi.org/10.1038/nrc1360>
156. von Bubnoff N, Gorantla SP, Engh RA et al (2011) The low frequency of clinical resistance to PDGFR inhibitors in myeloid neoplasms with abnormalities of PDGFRA might be related to the limited repertoire of possible PDGFRA kinase domain mutations in vitro. *Oncogene* 30:933–943. <https://doi.org/10.1038/onc.2010.476>
157. Weisberg E, Wright RD, Jiang J et al (2006) Effects of PKC412, Nilotinib, and Imatinib against GIST-associated PDGFRA mutants with differential Imatinib sensitivity. *Gastroenterology* 131:1734–1742. <https://doi.org/10.1053/j.gastro.2006.09.017>
158. Heinrich MC, Griffith D, McKinley A et al (2012) Crenolanib inhibits the drug-resistant PDGFRA D842V mutation associated with imatinib-resistant gastrointestinal stromal tumours. *Clin Cancer Res* 18:4375–4384. <https://doi.org/10.1158/1078-0432.CCR-12-0625>
159. Smith CC, Lasater EA, Lin KC et al (2014) Crenolanib is a selective type I pan-FLT3 inhibitor. *Proc Natl Acad Sci U S A* 111:5319–5324. <https://doi.org/10.1073/pnas.1320661111>
160. Roberts WG, Whalen PM, Soderstrom E et al (2005) Antiangiogenic and antitumour activity of a selective PDGFR tyrosine kinase inhibitor, CP-673,451. *Cancer Res* 65:957–966

Inhibitors of c-Jun N-Terminal Kinase 3



Pierre Koch

Contents

1	Introduction	204
2	Reversible Inhibitors	208
2.1	Prototypical JNK Inhibitor SP600125	208
2.2	Aminopyrimidines	208
2.3	2-Alkylsulfanyl-5-(pyridin-4-yl)imidazoles	210
2.4	Aminopyrazole Derivatives	213
3	Covalent Inhibitors	215
3.1	Aminopyrimidine-Based Covalent Inhibitors	215
3.2	Pyridinylimidazole-Based Covalent Inhibitors	218
4	Conclusion	221
	References	221

Abstract The serine/threonine kinase c-Jun N-terminal kinase (JNK) 3 is implicated in the pathogenesis of various disorders ranging from neurodegenerative diseases to inflammation, metabolic disease, diabetes, liver diseases, and cancer. Although the number of publications reporting on JNK3 inhibitors has been decreasing in the last few years, this enzyme still constitutes an attractive target. Within the last years, significant progress in the design of JNK3 inhibitors displaying good to excellent selectivity versus other protein kinases has been achieved. However, the development of a JNK-isoform-selective JNK3 inhibitor, which may serve as a tool compound in animal studies to further evaluate the role of JNK3 as a therapeutic target, is highly desirable. This chapter summarizes the progress in the development of reversible and irreversible inhibitors of JNK3.

Keywords c-Jun N-terminal kinase 3, Covalent inhibitors, JNK3, MAP kinase family, Reversible inhibitors, Selectivity

P. Koch (✉)

Department of Pharmaceutical and Medicinal Chemistry, Institute of Pharmaceutical Sciences,
Eberhard Karls Universität Tübingen, Tübingen, Germany
e-mail: pierre.koch@uni-tuebingen.de

Abbreviations

AP	Activation protein
ATF	Activating transcription factor
CYP450	Cytochrome P450
EGFR	Epidermal growth factor receptor kinase
JNK	c-Jun N-terminal kinase
MAP	Mitogen-activated protein
SAPK	Stress-activated protein kinases
SAR	Structure-activity relationships

1 Introduction

The c-Jun N-terminal kinases (JNKs) are serine/threonine kinases belonging to the family of mitogen-activated protein (MAP) kinases. First members of this enzyme class were discovered in the early 1990s and originally termed as stress-activated protein kinases (SAPKs). Three different isoforms with molecular weights ranging from 46 to 55 kDa have been classified within this group, namely, JNK1 (also known as SAPK- γ /MAPK8), JNK2 (SAPK- α /MAPK9), and JNK3 (SAPK- β /MAPK10), which are encoded by the three distinct genes *jnk1*, *jnk2*, and *jnk3*, respectively [1, 2].

The JNKs are activated by different forms of cellular stress via the classical MAP kinase signaling cascade by tandem phosphorylation by two upstream kinases, in detail by a MAP kinase kinase and by MAP kinase kinases 4 or 7 (Fig. 1) [4]. Activated JNK can phosphorylate a broad subset of downstream targets including both transcription factors and nonnuclear substrates [3].

Phosphorylation of c-Jun, which takes part in the formation of the activation protein (AP)-1, increases the transcriptional activity of this complex. An analogous effect derives from the phosphorylation of the activating transcription factor (ATF)-2, which modifies gene expression through the formation of dimers with members of the Jun family [5]. Besides these two well-characterized pathways, JNKs can also act on additional nuclear targets, thereby modulating their effects on gene transcription (Fig. 1). Furthermore, the members of the JNK family phosphorylate cytosolic and mitochondrial substrates resulting in a modification of their functionality or in the regulation of their stability [3].

Due to diverse downstream targets, the JNKs are involved in various physiological functions. These kinases are implicated in the regulation of cell survival/apoptosis in response to external stimuli. The role of JNKs in cell death has been described as bivalent, since it depends on the entity of the stimulus and on the signal integration with additional pathways.

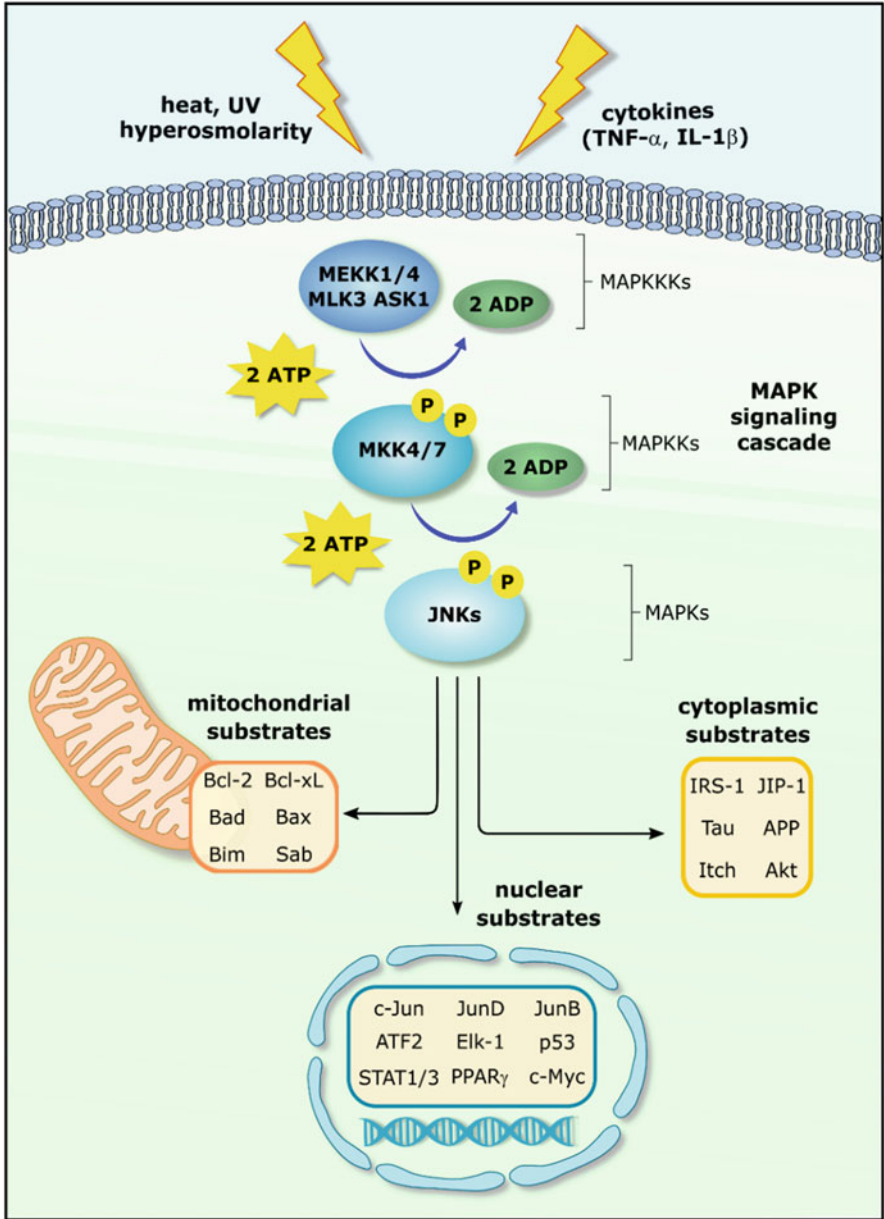


Fig. 1 Representation of the different substrates of JNK. The figure was realized using the information from Bogoyevitch and Kobe [3]

Whereas JNK1 and JNK2 are present in all cells and tissues of the human body, JNK3 is almost exclusively expressed in the brain and to a lesser extent in the testis and heart. The deregulation of JNK3 is linked to several disorders ranging from neurodegenerative diseases, like Parkinson's and Alzheimer's disease, to inflammation, metabolic diseases, diabetes, liver diseases, and cancer [6–8].

Nevertheless, the design of isoform-selective JNK inhibitors is very challenging as JNK1, JNK2, and JNK3 share more than 80% sequence identity. In particular, the sequence comprising the ATP-binding site or the surrounding area is highly conserved among the isoforms (Fig. 2). In these regions, the JNK3 displays 98% and 95% similarity to JNK1 and JNK2, respectively.

The JNK3 has become an attractive therapeutic target. Several inhibitors targeting this enzyme have been reported from both pharmaceutical industry and academia in the last two decades. However, there are only few reported examples of JNK3 inhibitors that display selectivity versus the other JNK isoforms. For reviews about inhibitors of the JNKs, see Koch et al. [9] and Gehringer et al. [10]

A limited number of small molecule inhibitors of JNKs have been investigated in clinical trials (Table 1). Most of them are ATP-competitive inhibitors (GL5001, CC-401, and CC-930) showing no intra-JNK selectivity. The structure as well as the mechanism of action of CC-90001 is undisclosed. Nevertheless, no JNK3 inhibitor has been launched into the market yet. The phase II clinical trial studies of CC-401 and CC-930 were terminated because of an unfavorable benefit/risk profile.

An alternative strategy to target the JNKs is represented by the retro-inverso peptide inhibitor XG-102 (formerly referred to as AM-111) developed by Xigen SA [11, 12]. While tanzisertib, bentamipimod, and CC-401 are classical type I inhibitors

	Glycine rich loop								N-lobe (1)		
JNK1	I32	G33	S34	G35	A36	Q37	G38	I39	A53	I54	K55
JNK2	I32	G33	S34	G35	A36	Q37	G38	I39	A53	V54	K55
JNK3	I70	G71	S72	G73	A74	Q75	G76	I77	A91	I92	K93

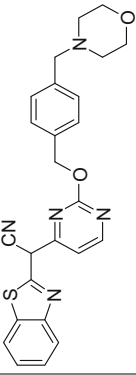
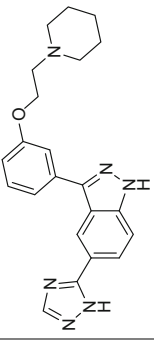
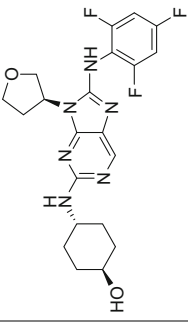
	C-helix				N-lobe (2)			
JNK1	R69	E73	L74	M77	I86	L88	I106	V107
JNK2	R69	E73	L74	L77	I86	L88	L106	V107
JNK3	R107	E111	L112	M115	I124	L126	L144	V145

	Hinge-region							C-lobe		
JNK1	M108	E109	L110	M111	D112	A113	N114	C116	D151	K153
JNK2	M108	E109	L110	M111	D112	A113	N114	C116	D151	K153
JNK3	M146	E147	L148	M149	D150	A151	N152	C154	D189	K191

	C-lobe (continued)					DFG-motif			
JNK1	P154	S155	N156	I157	V158	L168	D169	F170	G171
JNK2	P154	S155	N156	I157	V158	L168	D169	F170	G171
JNK3	P192	S193	N194	I195	V196	L206	D207	F208	G209

Fig. 2 Sequence alignment of JNK1, JNK2, and JNK3 in the catalytic cleft and adjacent area. Differences in amino acid sequence in the N-lobe and C-helix are highlighted

Table 1 Status of small molecule JNK inhibitors in clinical trials

Name	Structure	Company	Most advanced phase/indication	Status (year)
AS602801 GL5001 bentamapimod		PregLem SA	Phase II/inflammatory endometriosis	Completed (2013) ^a
CC-401		Celgene corporation	Phase I/refractory acute myelogenous leukemia	Terminated (2006) ^a
CC-930 tanzisertib		Celgene corporation	Phase II/pulmonary fibrosis Phase II/discoid lupus	Terminated (2012) ^a Terminated (2016) ^a
CC-90001	Undisclosed	Celgene corporation	Phase II/idiopathic pulmonary fibrosis	Ongoing/recruiting (2017) ^b

Data were obtained from the webpage <https://clinicaltrials.gov> (Accessed on October 29, 2018)

^aStudy completion date

^bStudy start date

Fig. 3 Amino acid sequence of D-retro-inverso peptide inhibitor XG-102

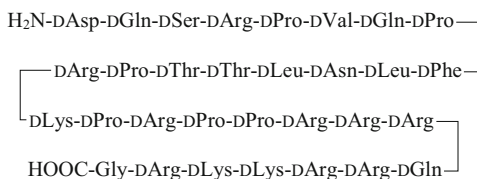
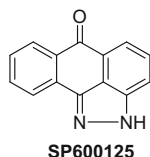


Fig. 4 Structure and biological activities of SP600125. Biological data are taken from Bennet et al. [13]



IC ₅₀ (JNK3) =	40 nM
IC ₅₀ (JNK2) =	40 nM
IC ₅₀ (JNK1) =	90 nM
IC ₅₀ (p38 α) =	>10,000 nM

binding reversibly to the ATP-binding site, the retro-inverso peptide inhibitor XG-102 occupies the docking site of the JIP scaffold protein. XG-102 consists of 30 D-configured amino acids and 1 glycine residue (Fig. 3). Clinical phase III trials for treatment of hearing loss as well as for post-cataract surgery inflammation and pain were recently completed for this peptide inhibitor.

2 Reversible Inhibitors

2.1 Prototypical JNK Inhibitor SP600125

One of the first reported small molecule JNK3 inhibitors is 1,9-pyrazoloanthrone (SP600125), an ATP-competitive pan-JNK inhibitor developed by Celgene (Fig. 4) [13]. SP600125 was one of the first JNK inhibitors displaying selectivity versus the related p38 α MAP kinase, which is also a member of the MAP kinase family. Although SP600125 has been described to be lacking selectivity within the kinome [14, 15], it is a widely used reference compound in biological JNK assays [16–18]. SP600125 binds to the ATP-binding site of the JNKs and forms two hydrogen bond interactions with the hinge region. The N1-atom accepts a hydrogen bond from the backbone amide group of Met111 (JNK1 numbering), and the NH group at the 2-position acts as a hydrogen bond donor toward the backbone carbonyl group of Glu109 (JNK1 numbering). In addition, SP600125 is surrounded by hydrophobic residues in the adenine-binding region of the enzyme [15].

2.2 Aminopyrimidines

Aminopyrimidine derivatives as potent inhibitors of the JNKs have been reported from different research groups [19–24]. In contrast to previous studies, LoGrasso and coworkers focused on brain-penetrant JNK-selective aminopyrimidines with

promising cellular potency. Their aminopyrimidine series comprised about 500 compounds and 12 examples, all showing no inhibition toward p38 α MAP kinase at a test concentration of 20 μ M, were further profiled [24]. Compound **1** represents the most potent inhibitor of this series displaying IC₅₀ values in the low nanomolar range against JNK3 and JNK1 (Fig. 5). Aminopyrimidine **1** showed moderate cellular activity. It inhibits the phosphorylation of c-Jun in INS-1 cells with an IC₅₀ value of 210 nM. However, compound **1** is not able to penetrate into the brain. Although being less potent in the in vitro enzyme assay, compound **2** showed an increased cell penetration profile resulting in a strong inhibition of cellular c-Jun phosphorylation (IC₅₀ = 54 nM) and promising pharmacokinetic properties [24]. Inhibitor **2** is able to cross the blood-brain barrier (brain/plasma ratio = 75%) and possesses good oral bioavailability in rats (*F* = 45%). However, its plasma protein binding in different species (mouse, rat, dog, monkey, and human) is high (>92%). The metabolic stability of **2** in liver microsomes is reasonable. When dosed at 1 mg/kg (iv) in in vivo studies in rats, aminopyrimidine **2** has a favorable PK profile with a half-life of 2.4 h and a clearance of 20 mL/min/kg. Furthermore, inhibitor **2** lowers the generation of reactive oxygen species in INS-1 cells. However, aminopyrimidine **2** displays a high affinity toward the cytochrome P450 (CYP450) isoforms 2C9, 3A4, and 1A2 (>70% inhibition at a tested concentration of 10 μ M).

The X-ray crystal structure of aminopyrimidine **2** bound to JNK3 (PDB code: 3KVX) revealed an unexpected binding mode [24]. Although the 2-aminopyrimidine motif is a typical hinge-binding motif present in numerous kinase inhibitors, inhibitor **2** does not form any hydrogen bond interactions with the enzyme. It binds in the ATP-binding site of JNK3 with a highly planar arrangement of the aromatic rings (Fig. 6). Compared to another X-ray structure published by the same group (PDB code: 1PMN) [26], the glycine-rich loop was collapsed toward the active site by 2.5 Å. The compression of the binding pocket might be the driver of selectivity.

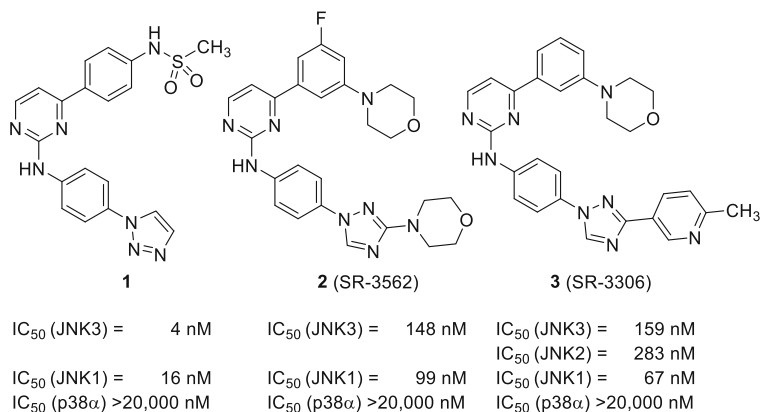


Fig. 5 Structure and biological data of aminopyrimidines **1–3**. Biological data are taken from Kamenecka et al. [24] and Chambers et al. [25]

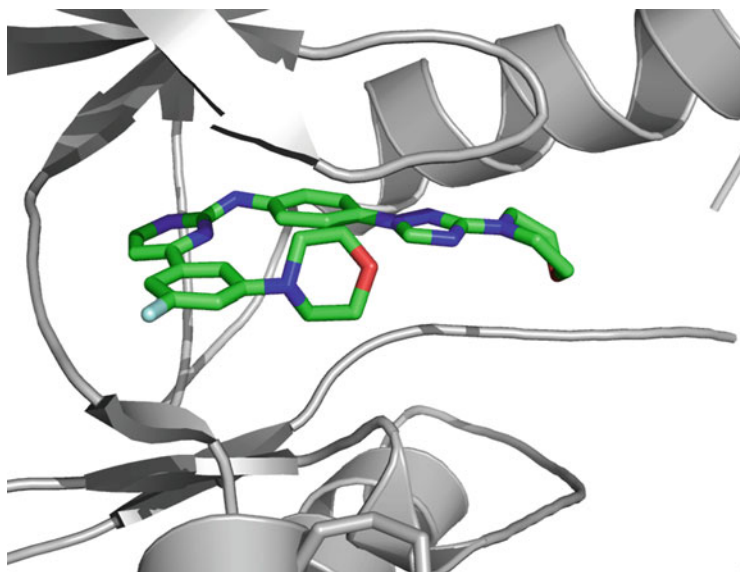


Fig. 6 X-ray crystal structure of **2** bound to JNK3. The protein backbone is displayed as cartoon in gray. The compound is highlighted as sticks

Another example of the aminopyrimidinyl-based JNK inhibitors is compound **3** (SR-3306) (Fig. 5) [25]. Compared to inhibitor **2**, pan-JNK inhibitor **3** lacks the fluoro substituent on one of the benzene rings, and the morpholino moiety at the triazole moiety is replaced by a methylpyridine. In terms of JNK3 inhibition in the biochemical activity assay, compound **3** is an equipotent inhibitor as compound **2**. However, in the cellular assay, JNK inhibitor **3** showed a fourfold reduced activity ($IC_{50} = 216$ nM) than **2**. Pyrimidinylamine **3** possesses a moderate selectivity. At a test concentration of 3 μ M, compound **3** inhibited 35 out of the tested 347 kinases. Additionally, compound **3** showed a clean human ether-à-go-go-related gene (hERG) ($IC_{50} > 30$ μ M) as well as CYP profile ($IC_{50} > 50$ μ M against 1A2, 2A6, 2B6, 2C8, 2C9, 2C19, 2D6, 2E1, and 3A4 isoenzymes). Furthermore, inhibitor **3** is able to cross the blood-brain barrier (plasma/brain ratio: 30–40%).

Inhibitor **3** displayed a neuroprotective effect in different in vitro and in vivo models of Parkinson's disease [25, 27] and effectively protects against ischemia/reperfusion injury in rats at a test concentration of 5 mg/kg [28].

2.3 2-Alkylsulfanyl-5-(pyridin-4-yl)imidazoles

2-Alkylsulfanyl-4-(4-fluorophenyl)-5-(pyridin-4-yl)imidazoles are a prominent class of kinase inhibitors and can be considered as open analogs of the early lead p38 α MAP kinase inhibitor SKF86002 [29] developed by researchers from

Smith, Kline & French Laboratories (Fig. 7). In different target hopping approaches, several compounds of this class served as lead structures for the design of (selective) inhibitors of other protein kinases not belonging to the family of MAP kinases, e.g., the epidermal growth factor receptor kinase (EGFR) [30, 31], as well as the protein kinases CK1 δ and CK1 ϵ [32].

Using a rational structure-based design approach, a series of different reversible and covalent JNK inhibitors was established [33, 34]. In case of the reversible series [33], pyridinylimidazole-based p38 α MAP kinase inhibitor LN950 [35, 36] that also shows moderate affinity toward JNK3 (IC₅₀ = 181 nM) [33] served as lead structure. With the aim to improve the inhibition of JNK3 for this class of compounds and simultaneously erase their initial p38 α MAP kinase inhibition, a broad series of derivatives was generated, and structure-activity relationships (SAR) were established. The lead compound was extensively modified keeping the putative hinge-binding motif (2-aminopyridine) constant in all analogs (Fig. 8). Structural modifications included (bio)isosteric replacement of the five-membered core scaffold as well as variations in the imidazole N-substitution pattern. The 4-fluorophenyl ring located in the hydrophobic region I was replaced by other substituted phenyl rings, by cycloalkyl rings, as well as by (branched) alkyl groups. Moreover, different substituents at the pyridine-C2 position interacting with the hydrophobic region II were probed. Modifications in this position included branched aliphatic moieties as well as (substituted) carbocyclic and phenyl rings.

As general SARs, aryl moieties at the pyridine-C2 position were better tolerated by JNK3 than by p38 α MAP kinase. A major contribution in shifting inhibitory activity from p38 α MAP kinase to JNK3 was achieved by modifying the 4-fluorophenyl ring at the imidazole C4-position. Replacement of this moiety by a small methyl group (compound **6**) resulted in a complete loss of p38 α MAP kinase activity, whereas only a slight decrease in JNK3 affinity was observed.

As the central core, a 2,4,5-substituted imidazole ring is the most favored one in terms of improving both JNK3 inhibitory activity and selectivity over p38 α MAP kinase. Alkylation of the imidazole nitrogen atom either vicinal (compound **7**) or distal (compound **8**) to the pyridinyl substituent resulted in a decrease of JNK3 inhibitory activities.

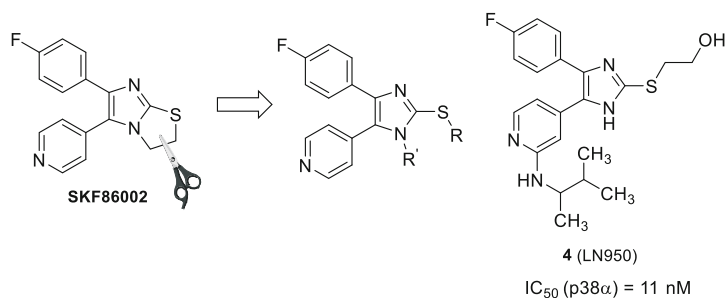


Fig. 7 Derivation of 2-alkylsulfanylimidazoles from SKF86002 as well as structure and biological data of p38 α MAP kinase inhibitor LN950

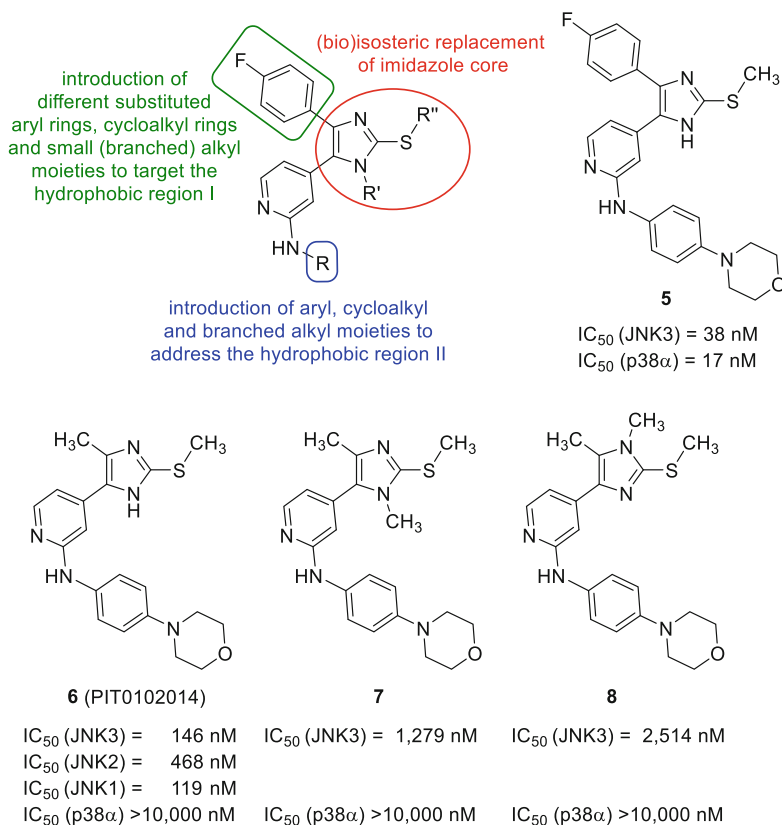


Fig. 8 Structural modifications of the lead structure and structures as well as biological data of the most potent reversible JNK inhibitor PIT0102014 of this series. Biological data are taken from Ansideri et al. [33]

The most promising inhibitor of this series (compound **6**) displays IC_{50} values in the low triple-digit nanomolar range for JNK1 and JNK3 and shows a slight selectivity against the JNK2 isoform (Fig. 8).

The binding mode of pyridinylimidazole **6** at the target kinase was confirmed by X-ray crystallography (PDB code: 6EKD) (Fig. 9). This example represents the first reported crystal structure of a 2-alkylsulfanyl-5-(pyridin-4-yl)imidazole in complex with JNK3. The inhibitor molecule shows a typical type I teardrop binding mode. The hinge-binding motif (2-aminopyridine) of **6** forms – as expected – two hydrogen bond interactions with the backbone of Met149. The methyl substituent on the imidazole-C4 position is pointing toward the hydrophobic region I. A water-mediated hydrogen bond network exists around the imidazole core. The imidazole-N3 atom (distal from the pyridine ring) is not interacting with the conserved Lys93 side chain via a direct hydrogen bond. This interaction was observed to be mediated by two water molecules. Additionally, the imidazole-N1 atom (adjacent to the pyridine ring) is also involved in a water-mediated hydrogen bond to Asn152.

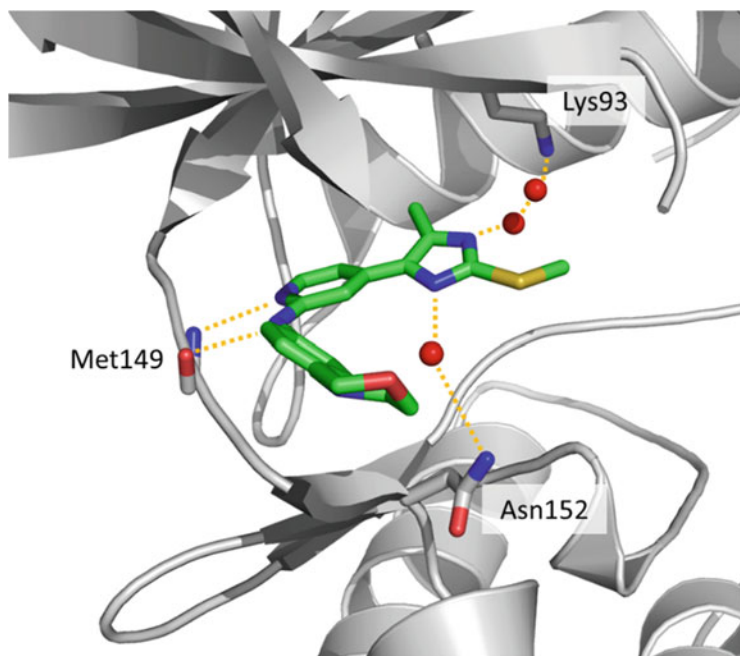


Fig. 9 Crystal structure of inhibitor **6** (PIT0102014) bound to JNK3 (PDB entry: 6EKD). The protein backbone is displayed as cartoon in gray. The compound and selected amino acids are highlighted as sticks. Water molecules are represented as red spheres, and hydrogen bonds are shown as yellow dashed lines

Pyridinylimidazole **6** was evaluated further pharmacologically. This inhibitor is metabolically stable in human liver microsomes, and it possesses only low to moderate affinity toward four out of five tested pharmacologically relevant cytochrome P450 isoenzymes as well as toward hERG channels [33].

2.4 Aminopyrazole Derivatives

In another study, LoGrasso, Feng, and coworkers reported about a series of aminopyrazole-based JNK3 inhibitors, which show high isoform selectivity over JNK1 and in some cases also versus JNK2 (Fig. 10) [37].

Starting from lead compound SR-4326, a large SAR study comprising derivatives with modifications on the urea moiety as well as on the amide moiety was generated.

Replacement of the methylpyridine moiety present in SR-4326 by a pyrrolidinylpyrazole moiety resulted in aminopyrazole **10** showing a subnanomolar IC_{50} value in the JNK3 activity assay as well as a good intra-JNK selectivity (Fig. 10). JNK3 inhibitor **10** displays a more than 500- and 200-fold selectivity over JNK1 and JNK2, respectively. However, data from a selectivity screening of **10** has not been reported so far.

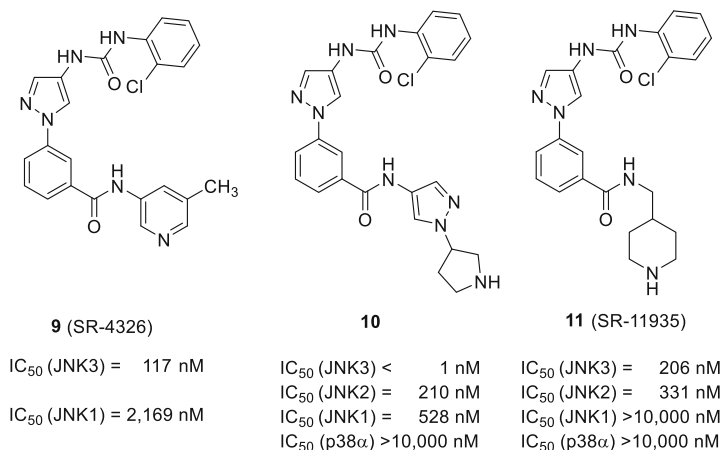


Fig. 10 Structural modifications of the lead structure **9** (SR-4326) and structures as well as biological data of inhibitors **10** and **11** (SR-11935) of this series. Biological data are taken from Zheng et al. [37]

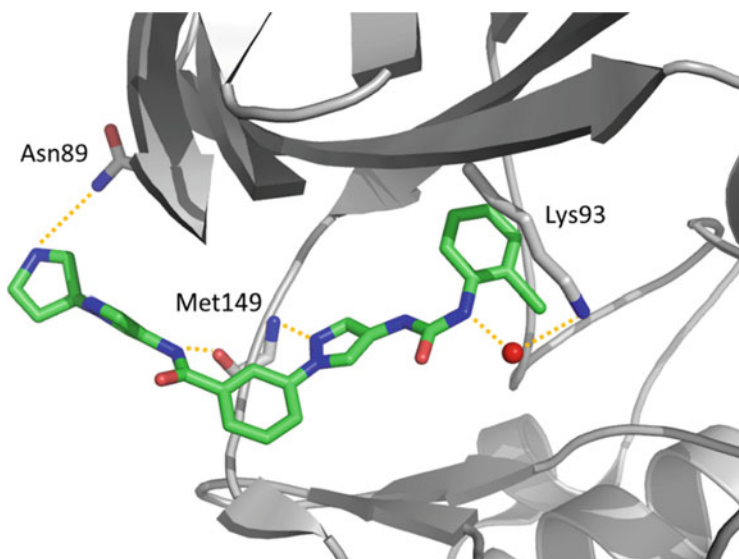


Fig. 11 X-ray structure of inhibitor **10** in complex with JNK3 (PDB code: 4WHZ). The protein backbone is displayed as cartoon in gray. The compound and selected amino acids are highlighted as sticks. Hydrogen bonds are shown as yellow dashed lines

The binding mode of JNK-isoform-selective inhibitor **10** within the ATP-binding site of JNK3 was determined by X-ray experiments (Fig. 11). The *R*-enantiomer of **10** forms several hydrogen bond interactions with JNK3. The chloro-substituted phenyl ring is located in the hydrophobic region I. The N2 atom of the central pyrazole accepts a hydrogen bond from the NH group of Met149 of the hinge region.

A second hydrogen bond toward the backbone of Met149 (carbonyl group) was observed. In this case, the amide NH group serves as a hydrogen bond donor. A water-mediated hydrogen bond interaction is formed between the NH group of the urea group (next to the aniline) and the amino group of the Lys93 side chain. An additional hydrogen bond is established between the NH group of the pyrrolidine ring and Asn89.

Several dual JNK2/3 inhibitors of the aminopyrazole series have also been reported in the same publication [37]. In the biochemical assay, SR-11935 shows a greater than 50-fold isoform selectivity versus JNK1 and potent activity in different cell-based assays in SHSY5Y cells. At a test concentration of 10 μ M, SR-11935 displays a good kinome selectivity. However, in this high-throughput screening method, a high affinity for JNK1 was observed. SR-11935 penetrates into the brain (plasma/brain ratio of \sim 2:1) showing both good solubility and good DMPK properties. Moreover, this inhibitor displays good microsomal stability, when incubated with human or mice liver microsomes as well as no affinity toward CYP450 isoforms 1A2, 2C9, 2D6, and 3A4. In addition, SR-11935 potently inhibits mitochondrial dysfunction and is noncytotoxic.

3 Covalent Inhibitors

The design of covalent kinase inhibitors has resurged [38–40]. In total, a number of six covalent kinase inhibitors were introduced to the market from 2013 to 2018 (Fig. 12). All these inhibitors possess an α,β -unsaturated amide as electrophilic moiety, which targets the side chain of a non-catalytic cysteine residue in the proximity of the ATP-binding site.

As illustrated in the sequence alignment of the JNKs (Fig. 2), all three JNK isoforms possess a cysteine (Cys114 in JNK1/2 numbering; Cys154 in JNK3 numbering) located in the C-lobe adjacent to the hinge region. In this position, this cysteine is unique within the kinome and can be targeted by an inhibitor bearing an electrophilic warhead in a suitable position to form a covalent bond.

3.1 Aminopyrimidine-Based Covalent Inhibitors

The first covalent inhibitors of JNK3 were reported in 2012 by Gray and coworkers [18]. In search for covalent type II inhibitors of the c-Kit and PDGFR kinases, the imatinib-derived pan-JNK inhibitor JNK-IN-1 (Fig. 13) was discovered.

A selectivity screening of JNK-IN-1 versus 400 kinases revealed, at a test concentration of 10 μ M, besides binding to the classical imatinib targets (Abl, c-Kit and DDR1/2), also a strong binding to all three JNK isoforms. Determination of the biochemical IC_{50} values against the latter kinases revealed JNK-IN-1 to be a moderate inhibitor of all three JNK isoforms.

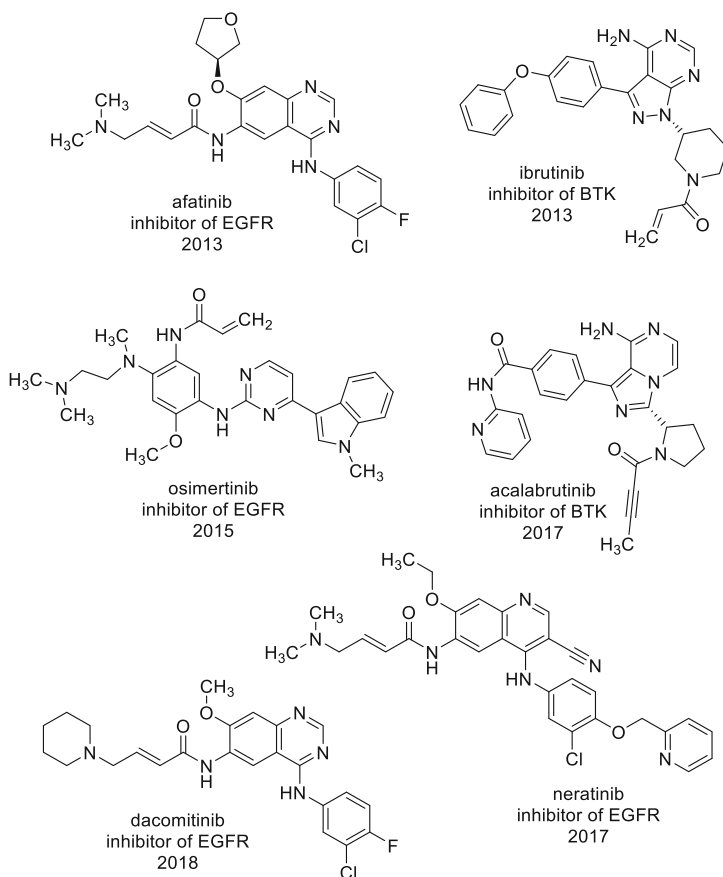


Fig. 12 Structures, their target kinase, and the year of their FDA approval of the covalent kinase inhibitors afatinib, ibrutinib, osimertinib, acalabrutinib, dacomitinib, and neratinib

Using a structure-based design, a series of analogs was established, and the pan-JNK inhibitor JNK-IN-1 was further optimized regarding its inhibitory activity. Removing the methyl group of the benzene ring at the pyrimidine-C2-amino position and changing the substitution pattern on both benzene rings in the linker bearing the electrophilic warhead resulted in compound JNK-IN-7. This potential covalent inhibitor displayed IC_{50} values in the low single-digit nanomolar range for JNK1 and JNK2 as well as in the subnanomolar range for JNK3 (1 h incubation). In case of JNK3, JNK-IN-7 shows a 1,000-fold higher activity compared to parent compound JNK-IN-1. JNK-IN-7 also inhibits c-Jun phosphorylation in HeLa and A375 cells with IC_{50} values of 130 nM and 244 nM, respectively [18].

The X-ray structure of JNK-IN-7 in complex with JNK3 (PDB code: 3V6S) (Fig. 14) reveals that this covalent inhibitor has a different binding mode in the ATP-binding site of JNK3 than imatinib in Abl kinase (PDB code: 1IEP) (Fig. 15) [41].

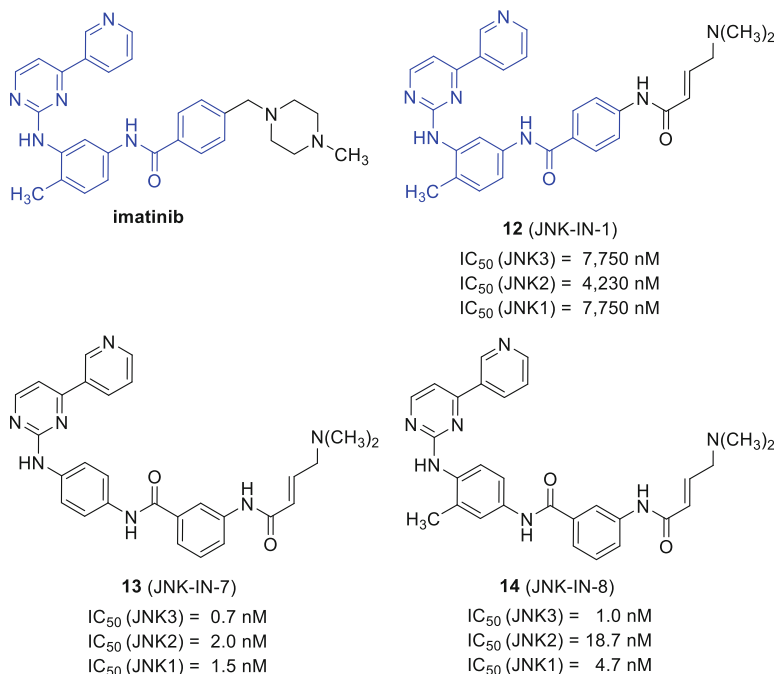


Fig. 13 Structures and biological data (after 1 h of incubation) of irreversible JNK inhibitors based on the imatinib scaffold. Structural similarities of imatinib present in **12** (JNK-IN-1) are highlighted in blue color. Biological data are taken from Zhang et al. [18]

JNK-IN-7 binds to JNK3 in a type I binding mode with the kinase in the active DFG-in conformation. The covalent link between the electrophilic arylamide and the side chain of Cys154 was also unambiguously revealed. The classical hinge-binding motif (pyrimidinylamine) interacts with the backbone of Met149 via two hydrogen bonds [18].

Imatinib shows a typical type II inhibitor binding mode targeting the inactive DFG-out conformation of Abl kinase. The pyrimidinylamine moiety does not interact via hydrogen bonds with the hinge region. Instead, the nitrogen atom of the 3-pyridinyl moiety accepts a hydrogen bond from the backbone N-H of Met318 (Fig. 15) [41].

In vitro kinase screening against a panel of 442 kinases revealed a very good selectivity for JNK-IN-7. Within this panel, this covalent inhibitor bound or inhibited eight other protein kinases with a K_D or IC_{50} value of 100 nM or lower besides the JNKs.

Reintroduction of the methyl group on the phenyl ring in *ortho*-position to the pyridine-C2-amino moiety on JNK-IN-7 resulted in JNK-IN-8. This inhibitor displays almost the same inhibitory activity for the JNK3 as JNK-IN-7 yet showing a significantly improved selectivity profile for JNK3 within the JNK family as well as against the rest of the kinome [18].

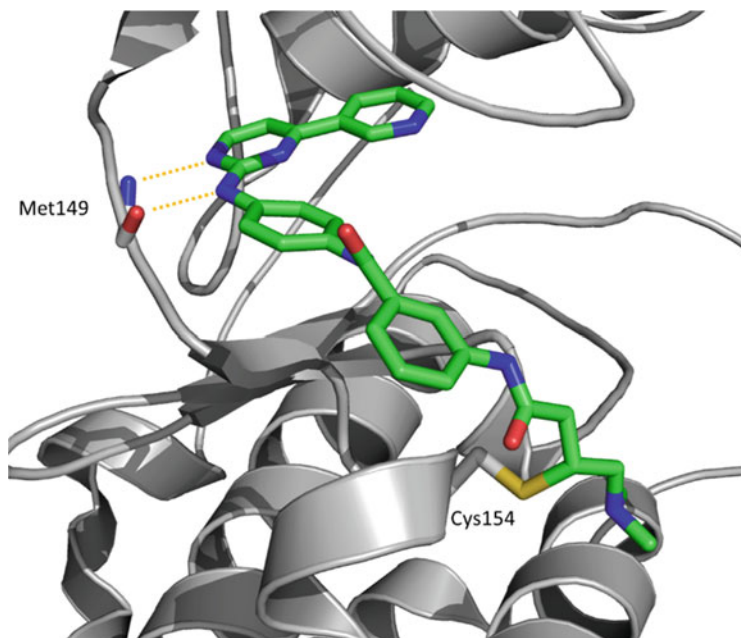


Fig. 14 X-ray structure of JNK-IN-7 in complex with JNK3 (PDB code: 3V6S). The protein backbone is displayed as cartoon in gray. The compound and selected amino acids are highlighted as sticks. Hydrogen bonds are shown as yellow dashed lines

However, in cell-based assays, JNK-IN-8 shows slightly lower inhibitory activity compared to JNK-IN-7 (IC_{50} values of 486 nM and 333 nM in Hela and A375 cells, respectively) [18]. In a panel of 442 different protein kinases (also including mutants), JNK-IN-8 only bound to two Kit mutants (V559D and V557D,T650I). In a cellular kinase profiling versus distinct protein kinases, JNK-IN-8 exclusively inhibited JNK1,2,3. Due to its excellent selectivity profile, the covalent pan-JNK-inhibitor JNK-IN-8 was selected by the chemical probes portal as a tool compound to further investigate the role of JNK1/2/3 inhibition (www.chemicalprobesportal.org). However, the same portal recommends using JNK-IN-8 along with validated JNK inhibitors as a positive control.

3.2 *Pyridinylimidazole-Based Covalent Inhibitors*

The concept of covalently targeting the JNK3 was also transferred to the reversible JNK inhibitors of the 2-alkylsulfanyl-5-(pyridin-4-yl)imidazole series, which are already optimized to interact with different regions in the ATP-binding site of JNK3 (see Sect. 2.3) [34]. For targeting the mentioned cysteine side chain in the JNKs, the electrophilic warhead was attached to the pyridine-C2-amino function via a suitable linker (Fig. 16).

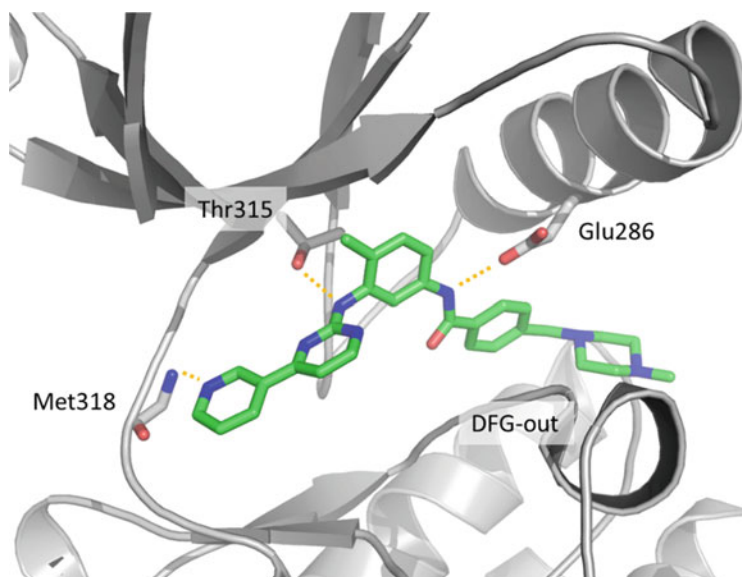


Fig. 15 X-ray structure of imatinib bound to Abl kinase (PDB code: 1IEP). The compound and selected amino acids are highlighted as sticks. Hydrogen bonds are shown as yellow dashed lines

An acrylamide was chosen as an electrophilic warhead due to the fact that α,β -unsaturated carbonyl groups are soft electrophiles. On the one side, the acrylamide preferentially reacts with the soft thiol present in the side chain of Cys154. On the other side, acrylamides are less reactive than α,β -unsaturated esters as well as α,β -unsaturated ketones, thereby reducing possible side reactions with thiol groups present in other intracellular proteins.

Potential covalent inhibitors bearing different linkers consisting of two phenyl rings connected by an amide bond were synthesized wherein the linker length and geometry was varied (Fig. 16). The contribution of the covalent bond formation to the inhibitory activity was estimated by comparing the activity of the potential irreversible inhibitors with the one of the corresponding saturated analogs [34].

The linker, consisting of a *para*-substitution pattern on the phenyl ring connected to the pyridine-C2-amino position as well as a *meta*-substitution pattern on the second phenyl ring bearing the acrylamide moiety, showed to have the appropriate length and properties to place the reactive electrophile in optimal position to form the covalent bond with the Cys154 side chain. The resulting covalent inhibitor PIT0104026 inhibits JNK3 in the low nanomolar range and possesses an approximately 1,000-fold selectivity versus the p38 α MAP kinase. The irreversible binding mode of PIT0104026 was confirmed by mass shift experiments. This covalent inhibitor displays a good selectivity. In a screening versus a panel of 410 kinases, 15 kinases including JNK1,2,3 were inhibited at a test concentration of 1 μ M [34].

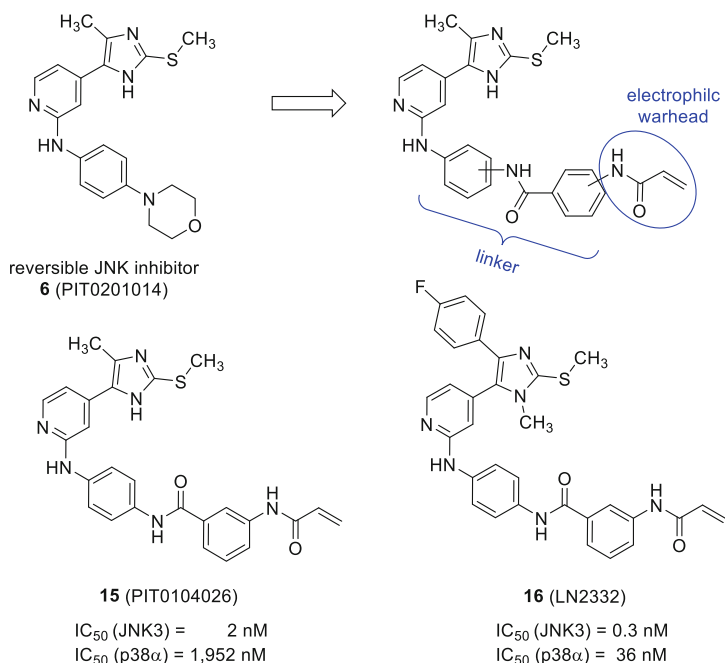


Fig. 16 Design of pyridinylimidazole-based irreversible JNK inhibitors as well as structures and biological data (after 50 min (JNK3) or 60 min (p38 α) of incubation) of covalent JNK inhibitors **15** (PIT0104026) and **16** (LN2332). Biological data are taken from Muth et al. [34]

The inhibitory potency as well as the selectivity of PIT0104026 was further improved by targeting the hydrophobic region I (the so-called selectivity pocket) of the enzyme with a 4-fluorophenyl ring as well as by introducing a methyl substituent on the imidazole nitrogen atom distal to the 4-fluorophenyl moiety. The resulting inhibitor LN2332 shows inhibition of JNK3 in the picomolar range (Fig. 16) [34].

A mass shift corresponding to the molecular weight of LN2332 was detected after its incubation with JNK3 followed by liquid chromatography-mass spectrometry. Since neither the incubation of the saturated counterpart of LN2332 nor the incubation of LN2332 with a JNK3-C154A-mutant resulted in a mass shift, the covalent binding mode of LN2332 with the Cys154 side chain was unambiguously proven.

Further pharmacological profiling identified LN2332 as a promising covalent pan-JNK inhibitor since it remained metabolically stable when exposed to human liver microsomes. LN2332 shows no unpredictable side reactions to other thiol-containing enzymes and has an excellent selectivity profile. In a panel of 410 protein kinases, LN2332 inhibits at a tested concentration of 0.5 μ M – besides all three JNK isoforms – only three other protein kinases (Tie-2, MAPKAP2, and CK-1 δ). However, cellular data of LN2332 have not been reported so far.

4 Conclusion

Numerous very potent reversible and irreversible small molecule JNK3 inhibitors displaying IC_{50} values down to the subnanomolar range have been reported within the last years. The binding modes for most of these inhibitors were determined by X-ray experiments. Several examples of recently published JNK3 inhibitors are showing very good to excellent selectivity within the kinome. Most of the discussed inhibitors display no or only low affinity versus non-JNK members of the MAP kinase family.

Moreover, some JNK3 inhibitors displaying intra-JNK selectivity have been reported. Within the class of aminopyrazole-derived reversible inhibitors, several examples of JNK2/3 inhibitors, e.g., SR-11935, showing selectivity versus JNK1 have been reported. Among them, aminopyrazole **10** represents the first reported potent JNK3 inhibitor showing very good JNK-isoform selectivity. However, its kinome-wide selectivity has not been reported.

The targeting of the thiol group present in the non-conserved Cys154, which is located adjacent to the ATP-binding site in JNK3, by electrophilic warheads resulted in the very potent irreversible pan-JNK inhibitors LN2332 and JNK-IN-8. Both compounds show an excellent selectivity within the human kinome. The latter covalent inhibitor, which is also active in cellular assays, is the only available high-quality kinase probe for JNK1/2/3 so far and might be used to further investigate the role of the JNKs in various disorders.

Acknowledgments Many thanks to Dr. Francesco Ansideri and Stanislav Andreev for helpful discussions. Dr. Ansideri is also acknowledged for providing Fig. 1. Kristina Schmidt is gratefully acknowledged for proofreading of the manuscript.

Compliance with Ethical Standards

Conflict of Interest: Author declares that he has no conflict of interest.

Ethical approval: This article does not contain any studies with human participants performed by the author.

References

1. Barr RK, Bogoyevitch MA (2001) The c-Jun N-terminal protein kinase family of mitogen-activated protein kinases (JNK MAPKs). *Int J Biochem Cell B* 33:1047–1063. [https://doi.org/10.1016/S1357-2725\(01\)00093-0](https://doi.org/10.1016/S1357-2725(01)00093-0)
2. Bogoyevitch MA (2006) The isoform-specific functions of the c-Jun N-terminal kinases (JNKs): differences revealed by gene targeting. *BioEssays* 28:923–934. <https://doi.org/10.1002/bies.20458>
3. Bogoyevitch MA, Kobe B (2006) Uses for JNK: the many and varied substrates of the c-Jun N-terminal kinases. *Microbiol Mol Biol Rev* 70:1061. <https://doi.org/10.1128/MMBR.00025-06>

4. Davis RJ (2000) Signal transduction by the JNK group of MAP kinases. *Cell* 103:239–252. [https://doi.org/10.1016/S0092-8674\(00\)00116-1](https://doi.org/10.1016/S0092-8674(00)00116-1)
5. Hess J, Angel P, Schorpp-Kistner M (2004) AP-1 subunits: quarrel and harmony among siblings. *J Cell Sci* 117:5965–5973. <https://doi.org/10.1242/jcs.01589>
6. Mehan S, Meena H, Sharma D, Sankhla R (2011) JNK: a stress-activated protein kinase therapeutic strategies and involvement in Alzheimer's and various neurodegenerative abnormalities. *J Mol Neurosci* 43:376–390. <https://doi.org/10.1007/s12031-010-9454-6>
7. Resnick L, Fennell M (2004) Targeting JNK3 for the treatment of neurodegenerative disorders. *Drug Discov Today* 9:932–939. [https://doi.org/10.1016/S1359-6446\(04\)03251-9](https://doi.org/10.1016/S1359-6446(04)03251-9)
8. Manning AM, Davis RJ (2003) Targeting JNK for therapeutic benefit: from JunK to gold? *Nat Rev Drug Discov* 2:554–565. <https://doi.org/10.1038/nrd1132>
9. Koch P, Gehringer M, Laufer SA (2015) Inhibitors of c-Jun N-terminal kinases: an update. *J Med Chem* 58:72–95. <https://doi.org/10.1021/jm501212r>
10. Gehringer M, Muth F, Koch P, Laufer SA (2015) c-Jun N-terminal kinase inhibitors: a patent review (2010–2014). *Expert Opin Ther Pat* 25:849–872. <https://doi.org/10.1517/13543776.2015.1039984>
11. Barkdull GC, Hondarrague Y, Meyer T, Harris JP, Keithley EM (2007) AM-111 reduces hearing loss in a Guinea pig model of acute labyrinthitis. *Laryngoscope* 117:2174–2182. <https://doi.org/10.1097/MLG.0b013e3181461f92>
12. Coleman JKM, Littlesunday C, Jackson R, Meyer T (2007) AM-111 protects against permanent hearing loss from impulse noise trauma. *Hearing Res* 226:70–78. <https://doi.org/10.1016/j.heares.2006.05.006>
13. Bennett BL, Sasaki DT, Murray BW, O'Leary EC, Sakata ST, Xu WM, Leisten JC, Motiwala A, Pierce S, Satoh Y, Bhagwat SS, Manning AM, Anderson DW (2001) SP600125, an anthrapyrazolone inhibitor of Jun N-terminal kinase. *P Natl Acad Sci USA* 98:13681–13686. <https://doi.org/10.1073/pnas.251194298>
14. Fabian MA, Biggs WH, Treiber DK, Atteridge CE, Azimioara MD, Benedetti MG, Carter TA, Ciceri P, Edeen PT, Floyd M, Ford JM, Galvin M, Gerlach JL, Grotzfeld RM, Herrgard S, Insko DE, Insko MA, Lai AG, Lelias JM, Mehta SA, Milanov ZV, Velasco AM, Wodicka LM, Patel HK, Zarrinkar PP, Lockhart DJ (2005) A small molecule-kinase interaction map for clinical kinase inhibitors. *Nat Biotechnol* 23:329–336. <https://doi.org/10.1038/nbt1068>
15. Heo Y-S, Kim SK, Seo CI, Kim YK, Sung B-J, Lee HS, Lee JI, Park S-Y, Kim JH, Hwang KY, Hyun Y-L, Jeon YH, Ro S, Cho JM, Lee TG, Yang C-H (2004) Structural basis for the selective inhibition of JNK1 by the scaffolding protein JIP1 and SP600125. *EMBO J* 23:2185–2195. <https://doi.org/10.1038/sj.emboj.7600212>
16. Goettert M, Luik S, Graesser R, Laufer SA (2011) A direct ELISA assay for quantitative determination of the inhibitory potency of small molecules inhibitors for JNK3. *J Pharm Biomed Anal* 55:236–240. <https://doi.org/10.1016/j.jpba.2011.01.014>
17. Feng YB, Chambers JW, Iqbal S, Koenig M, Park H, Cherry L, Hernandez P, Figuera-Losada M, LoGrasso PV (2013) A small molecule bidentate-binding dual inhibitor probe of the LRRK2 and JNK kinases. *ACS Chem Biol* 8:1747–1754. <https://doi.org/10.1021/cb3006165>
18. Zhang T, Inesta-Vaquera F, Niepel M, Zhang JM, Ficarro SB, Machleidt T, Xie T, Marto JA, Kim N, Sim T, Laughlin JD, Park H, LoGrasso PV, Patricelli M, Nomanbhoy TK, Sorger PK, Alessi DR, Gray NS (2012) Discovery of potent and selective covalent inhibitors of JNK. *Chem Biol* 19:140–154. <https://doi.org/10.1016/j.chembiol.2011.11.010>
19. Alam M, Beevers RE, Ceska T, Davenport RJ, Dickson KM, Fortunato M, Gowers L, Haughan AF, James LA, Jones MW, Kinsella N, Lowe C, Meissner JWG, Nicolas AL, Perry BG, Phillips DJ, Pitt WR, Platt A, Ratcliffe AJ, Sharpe A, Tait LJ (2007) Synthesis and SAR of aminopyrimidines as novel c-Jun N-terminal kinase (JNK) inhibitors. *Bioorg Med Chem Lett* 17:3463–3467. <https://doi.org/10.1016/j.bmcl.2009.03.023>

20. Humphries PS, Lafontaine JA, Agree CS, Alexander D, Chen P, Do QQT, Li LLY, Lunney EA, Rajapakse RJ, Siegel K, Timofeevski SL, Wang TL, Wilhite DM (2009) Synthesis and SAR of 4-substituted-2-aminopyrimidines as novel c-Jun N-terminal kinase (JNK) inhibitors. *Bioorg Med Chem Lett* 19:2099–2102. <https://doi.org/10.1016/j.bmcl.2009.03.023>
21. Song XY, Chen WM, Lin L, Ruiz CH, Cameron MD, Duckett DR, Kamenecka TM (2011) Synthesis and SAR of 2-phenoxy pyridines as novel c-Jun N-terminal kinase inhibitors. *Bioorg Med Chem Lett* 21:7072–7075. <https://doi.org/10.1016/j.bmcl.2011.09.090>
22. Song X, He Y, Koenig M, Shin Y, Noël R, Chen W, Ling YY, Feurstein D, Lin L, Ruiz CH, Cameron MD, Duckett DR, Kamenecka TM (2012) Synthesis and SAR of 2,4-diaminopyrimidines as potent c-Jun N-terminal kinase inhibitors. *Med Chem Commun* 3:238–243. <https://doi.org/10.1039/C1MD00219H>
23. Palmer WS, Alam M, Arzeno HB, Chang KC, Dunn JP, Goldstein DM, Gong LY, Goyal B, Hermann JC, Hogg JH, Hsieh G, Jahangir A, Janson C, Jin S, Kamlott RU, Kuglstatter A, Lukacs C, Michoud C, Niu LH, Reuter DC, Shao A, Silva T, Trejo-Martin TA, Stein K, Tan YC, Tivitmahaisoon P, Tran P, Wagner P, Weller P, Wu SY (2013) Development of amino-pyrimidine inhibitors of c-Jun N-terminal kinase (JNK): kinase profiling guided optimization of a 1,2,3-benzotriazole lead. *Bioorg Med Chem Lett* 23:1486–1492. <https://doi.org/10.1016/j.bmcl.2012.12.047>
24. Kamenecka T, Jiang R, Song XY, Duckett D, Chen WM, Ling YY, Habel J, Laughlin JD, Chambers J, Figuera-Losada M, Cameron MD, Lin L, Ruiz CH, LoGrasso PV (2010) Synthesis, biological evaluation, X-ray structure, and pharmacokinetics of aminopyrimidine c-Jun-N-terminal kinase (JNK) inhibitors. *J Med Chem* 53:419–431. <https://doi.org/10.1021/jm901351f>
25. Chambers JW, Pachori A, Howard S, Ganno M, Hansen D, Kamenecka T, Song XY, Duckett D, Chen WM, Ling YY, Cherry L, Cameron MD, Lin L, Ruiz CH, LoGrasso P (2011) Small molecule c-Jun-N-terminal kinase inhibitors protect dopaminergic neurons in a model of Parkinson's disease. *ACS Chem Neurosci* 2:198–206. <https://doi.org/10.1021/cn100109k>
26. Scapin G, Patel SB, Lisnock J, Becker JW, LoGrasso PV (2003) The structure of JNK3 in complex with small molecule inhibitors: structural basis for potency and selectivity. *Chem Biol* 10:705–712. [https://doi.org/10.1016/S1074-5521\(03\)00159-5](https://doi.org/10.1016/S1074-5521(03)00159-5)
27. Crocker CE, Khan S, Cameron MD, Robertson HA, Robertson GS, LoGrasso P (2011) JNK inhibition protects dopamine neurons and provides behavioral improvement in a rat 6-hydroxydopamine model of Parkinson's disease. *ACS Chem Neurosci* 2:207–212. <https://doi.org/10.1021/cn1001107>
28. Chambers JW, Pachori A, Howard S, Iqbal S, LoGrasso PV (2013) Inhibition of JNK mitochondrial localization and signaling is protective against ischemia/reperfusion injury in rats. *J Biol Chem* 288:4000–4011. <https://doi.org/10.1074/jbc.M112.406777>
29. Griswold DE, Marshall PJ, Webb EF, Godfrey R, Newton J, DiMartino MJ, Sarau HM, Gleason JG, Poste G, Hanna N (1987) SK&F 86002: a structurally novel anti-inflammatory agent that inhibits lipoxygenase- and cyclooxygenase-mediated metabolism of arachidonic acid. *Biochem Pharmacol* 36:3463–3470. [https://doi.org/10.1016/0006-2952\(87\)90327-3](https://doi.org/10.1016/0006-2952(87)90327-3)
30. Günther M, Juchum M, Kelter G, Fiebig H, Laufer S (2016) Lung cancer: EGFR inhibitors with low nanomolar activity against a therapy-resistant L858R/T790M/C797S mutant. *Angew Chem Int Ed* 55:10890–10894. <https://doi.org/10.1002/anie.201603736>
31. Günther M, Lategahn J, Juchum M, Döring E, Keul M, Engel J, Tumbrink HL, Rauh D, Laufer S (2017) Trisubstituted pyridinylimidazoles as potent inhibitors of the clinically resistant L858R/T790M/C797S EGFR mutant: targeting of both hydrophobic regions and the phosphate binding site. *J Med Chem* 60:5613–5637. <https://doi.org/10.1021/acs.jmedchem.7b00316>
32. Halekotte J, Witt L, Ianes C, Krüger M, Bührmann M, Rauh D, Pichlo C, Brunstein C, Luxenburger A, Baumann U, Knippschild U, Bischof J, Peifer C (2017) Optimized

- 4,5-diarylimidazoles as potent/selective inhibitors of protein kinase CK1 δ and their structural relation to p38 α MAPK. *Molecules* 22:522. <https://doi.org/10.3390/molecules22040522>
33. Ansideri F, Macedo JT, Eitel M, El-Gokha A, Zinad DS, Scarpellini C, Kudolo M, Schollmeyer D, Boeckler FM, Blaum BS, Laufer SA, Koch P (2018) Structural optimization of a Pyridinylimidazole scaffold: shifting the selectivity from p38 α mitogen-activated protein kinase to c-Jun N-terminal kinase 3. *ACS Omega* 3:7809–7831. <https://doi.org/10.1021/acsomega.8b00668>
 34. Muth F, El-Gokha A, Ansideri F, Eitel M, Döring E, Sievers-Engler A, Lange A, Boeckler FM, Lämmerhofer M, Koch P, Laufer SA (2017) Tri- and tetrasubstituted pyridinylimidazoles as covalent inhibitors of c-Jun N-terminal kinase 3. *J Med Chem* 60:594–607. <https://doi.org/10.1021/acs.jmedchem.6b01180>
 35. Koch P, Bäuerlein C, Jank H, Laufer S (2008) Activated Protein (MAP) kinase: synthesis and biological testing of 2-Alkylsulfanyl-, 4(5)-aryl-, 5(4)-Heteroaryl-substituted Imidazoles. *J Med Chem* 51:5630–5640. <https://doi.org/10.1021/jm800373t>
 36. El-Gokha A, Laufer SA, Koch P (2015) An optimized and versatile synthesis to pyridinylimidazole-type p38 α mitogen activated protein kinase inhibitors. *Org Biomol Chem* 13:10699–10704. <https://doi.org/10.1039/c5ob01505g>
 37. Zheng K, Iqbal S, Hernandez P, Park HJ, LoGrasso PV, Feng Y (2014) Design and synthesis of highly potent and isoform selective JNK3 inhibitors: SAR studies on aminopyrazole derivatives. *J Med Chem* 57:10013–10030. <https://doi.org/10.1021/jm501256y>
 38. Singh J, Petter RC, Baillie TA, Whitty A (2011) The resurgence of covalent drugs. *Nat Rev Drug Discov* 10:307–317. <https://doi.org/10.1038/nrd3410>
 39. Liu QS, Sabnis Y, Zhao Z, Zhang TH, Buhrlage SJ, Jones LH, Gray NS (2013) Developing irreversible inhibitors of the protein kinase cysteinome. *Chem Biol* 20:146–159. <https://doi.org/10.1016/j.chembiol.2012.12.006>
 40. Chaikuad A, Koch P, Laufer SA, Knapp S (2018) The cysteinome of protein kinases as a target in drug development. *Angew Chem Int Ed* 57:4372–4385. <https://doi.org/10.1002/anie.201707875>
 41. Nagar B, Bornmann WG, Pellicena P, Schindler T, Veach DR, Miller WT, Clarkson B, Kuriyan J (2002) Crystal structures of the kinase domain of c-Abl in complex with the small molecule inhibitors PD173955 and imatinib (STI-571). *Cancer Res* 62:4236–4243

Covalent Janus Kinase 3 Inhibitors



Matthias Gehringer and Michael Forster

Contents

1	JAK3 and the Janus Kinase Family	226
2	Covalent JAK3 Inhibitors	231
3	Summary	251
	References	252

Abstract During the past decade, covalent targeting has experienced a revival, especially in the kinase field. Addressing non-conserved cysteine residues by targeted covalent inhibitors has enabled the design of ligands with high selectivity in the kinome and has led to five currently approved drugs (1–5; early September 2018). Covalent inhibition was also the prime strategy for the selective targeting of JAK3, a member of the Janus kinase (JAK) family of non-receptor tyrosine kinases. JAKs are key regulators of the immune system. However, while the function of JAK3 is mainly limited to immune signaling, the remaining three JAK family members also fulfill other essential functions outside the immune system. Therefore, JAK3 has long been discussed as a promising target for the treatment of inflammatory and autoimmune disorders with limited side effects. Until recently, however, the development of sufficiently JAK3-selective small molecules was impeded by the high similarity of the JAKs' ATP binding pockets. Addressing Cys909, which is a serine in the other JAK family members, with electrophilic warheads, has recently enabled the generation of JAK3 inhibitors with unprecedented selectivity in the JAK family and the kinome. These compounds have now paved the way for the in-depth examination of JAK3-dependent signaling in cells and in vivo. Current research efforts culminated in the development of PF-06651600, a phase II clinical candidate from Pfizer under investigation for the treatment of rheumatoid arthritis, inflammatory bowel disease, and alopecia areata.

M. Gehringer (✉) and M. Forster

Department of Pharmaceutical and Medicinal Chemistry, Institute of Pharmaceutical Sciences,
Eberhard Karls University Tuebingen, Tuebingen, Germany

e-mail: Matthias.gehringer@uni-tuebingen.de; Michael.forster@uni-tuebingen.de

In this chapter, the history of covalent JAK3 inhibitors will be reviewed followed by the detailed discussion of case studies on how covalent targeting of Cys909 enabled isoform- and kinome-wide selectivity for this promising therapeutic target.

Keywords Chemical probes, Covalent inhibitors, Covalent-reversible inhibitors, Cysteine targeting, Inflammation, Isoform selectivity, Janus kinase 3

1 JAK3 and the Janus Kinase Family

Although covalent kinase inhibitors have mostly been used in oncology so far, the covalent inhibition of kinases regulating immune response is currently under investigation for the treatment of inflammatory and autoimmune disorders [1]. In this context, substantial efforts have been made to selectively address Janus kinase (JAK) 3, a member of the JAK family of non-receptor tyrosine kinases [2]. JAKs are composed of seven domains termed Janus homology domains (JH1–7, see Fig. 1a). The name Janus kinase arose from the JAKs' domain structure featuring a pseudokinase domain (JH2) adjacent to the catalytic domain (JH1), representing the two faces of the Roman god Janus [3, 4]. All four members of this kinase family, JAK1–3 and tyrosine kinase (TYK) 2, are involved in immune signaling via the JAK–STAT (signal transducers and activators of transcription) pathway. JAKs are the intracellular effectors of type I and II cytokine receptors, which are devoid of intrinsic kinase activity [5]. They associate with the intracellular receptor domains where they signal as homo- and heterodimers or heterotrimers. Upon receptor activation, a conformational change positions the JAKs near to each other promoting cross-phosphorylation and thereby activation (Fig. 1b). The fully active JAKs phosphorylate the receptor to enable the recruitment of STAT proteins via the receptor's SH2 domains. The STATs are subsequently phosphorylated by the JAKs. This phosphorylation event promotes STAT dimerization and translocation to the nucleus where the STAT proteins function as transcription factors [4]. JAK3 only associates with cytokine receptors featuring the interleukin-2 receptor subunit gamma, also termed common gamma chain (γ_c), i.e., interleukin (IL)-2, IL-4, IL-7, IL-9, IL-15, and IL-21 receptors [6, 7]. At these receptors, JAK3 functions exclusively as a heterodimeric pair with JAK1. In contrast, all heterodimeric combinations of JAK1, JAK2, and TYK2 are possible, and even heterotrimeric combinations of the latter JAKs as well as homodimeric JAK2 pairs occur at certain receptor types [4]. Moreover, JAK3 expression is mainly limited to hematopoietic and epithelial cells highlighting the restricted and specific role of JAK3 compared to other Janus kinases [8, 9].

Inactivation of JAK3 by loss-of-function mutations leads to a pathology called JAK3-SCID (severe combined immunodeficiency), which is characterized by a lack of T cells and NK cells and the presence of nonfunctional B cells [10].

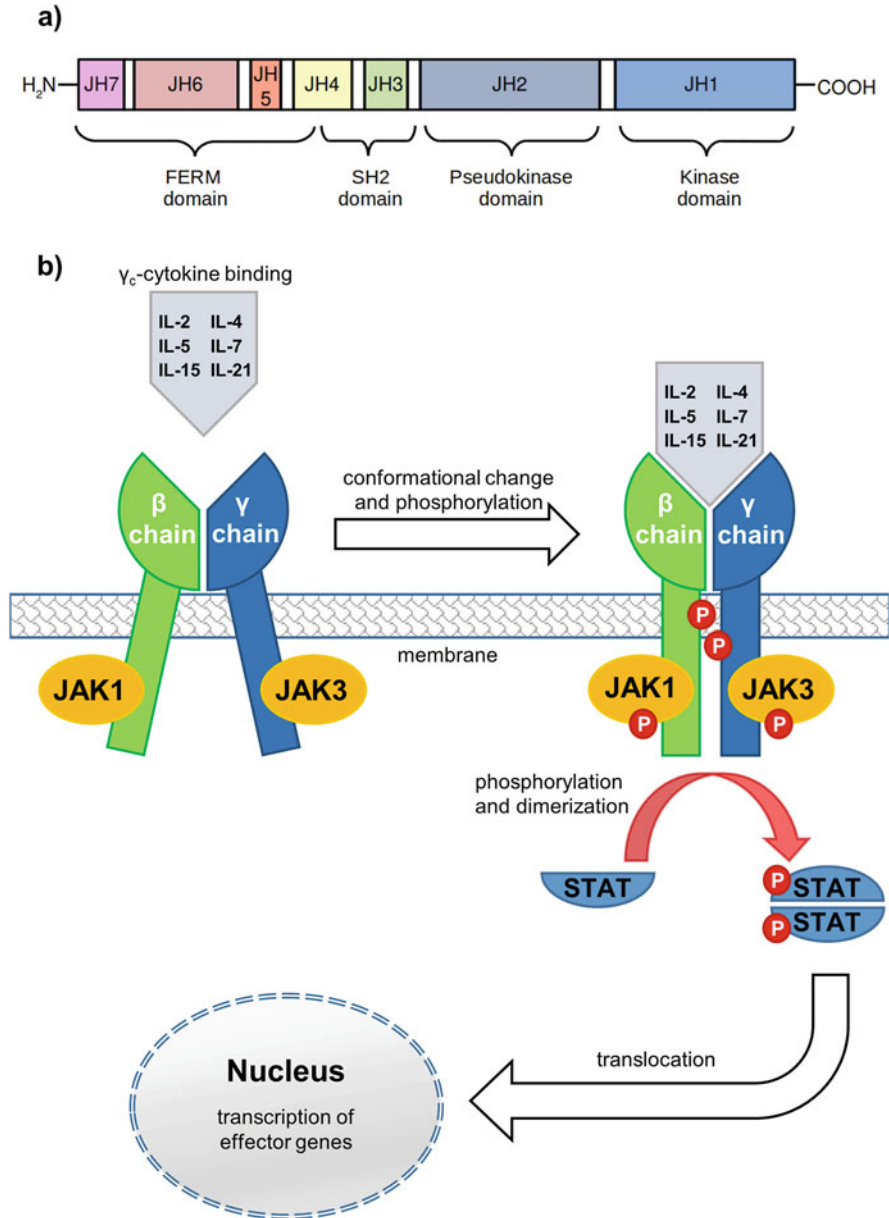


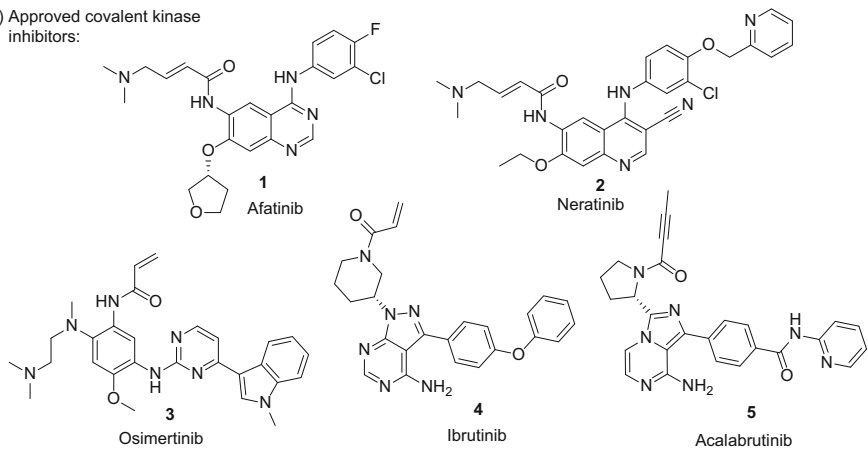
Fig. 1 (a) Domain structure of the Janus kinases. The C-terminal JH1 domain represents the catalytically active kinase domain, while the JH2 domain is a structurally similar pseudokinase domain with regulatory function. The JH3 and JH4 domains possess a Src homology 2 (SH2)-like structure, and JH5–JH7 constitute a FERM (four-point-one, ezrin, radixin, moesin) homology domain. (b) Schematic depiction of the JAK-STAT pathway (adopted from Forster et al. [2])

A similar phenotype is observed in JAK3-deficient mice [11] and in a genetic disorder called X-linked severe combined immunodeficiency (X-SCID), in which the *IL2RG* gene is mutated [12]. However, although the impaired function of the JAK3- γ_c complex severely compromises immune response, these effects are mainly limited to the immune system suggesting JAK3 as a promising target for the treatment of inflammatory and autoimmune disorders with few side effects [13].

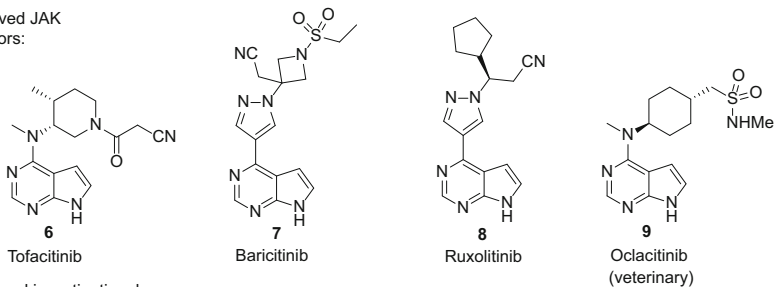
Although significant effort has recently been made to design selective covalent JAK3 inhibitors, none of these compounds has been approved so far (for an overview of approved covalent kinase inhibitors 1–5, see Fig. 2a). However, several non-covalent JAK inhibitors with varying degrees of selectivity within the JAK family and the kinome have gained approval or are in late-stage clinical trials (Fig. 2b, c). The first JAK inhibitor that had been under clinical investigation was CP-690,550 (tofacitinib, 6) [14], a compound developed by the US National Institutes of Health (NIH) and Pfizer [15]. Tofacitinib was initially described as a selective JAK3 inhibitor but later shown to target JAK1–3 and, to a lesser degree, also TYK2 [16]. The compound was approved by the FDA in 2012 for the treatment of rheumatoid arthritis (RA) and in May 2018 for the treatment of ulcerative colitis [17]. The EMA, however, only granted approval in 2017 [18] after re-evaluation of the application due to initial concerns regarding the compound's benefit-risk profile. In contrast, baricitinib (7), a JAK1/2 inhibitor with good selectivity against JAK3, was approved in Europe in early 2017 as a second-line therapy for the treatment of RA [19], while the FDA only granted approval in May 2018 [20]. Interestingly, ruxolitinib (8), a structural analog of baricitinib with a similar selectivity profile inside the JAK family, was already approved by the FDA in late 2011 (EMA: 2012) for the treatment of myelofibrosis [21] and later for polycythemia vera. Moreover, oclacitinib (9), a JAK inhibitor closely resembling tofacitinib in terms of structure and selectivity, has gained marketing authorization for veterinary purposes [22]. JAK inhibitors currently under late-stage clinical development (phase III according to <https://clinicaltrials.gov>) include the macrocyclic dual JAK2/FLT3 inhibitor pacritinib (10); the JAK1 inhibitors filgotinib (11), upadacitinib (12), PF-04965842 (13), and itacitinib (14); the dual JAK1/2 inhibitor momelotinib (15); and the JAK3/pan-JAK inhibitor decernotinib (16). However, it should be noted that these compounds generally possess only a moderate degree of selectivity for individual JAK family members. This can be attributed, at least in part, to the difficulties in designing truly isoform-selective JAK inhibitors as a result of the striking similarity of the ATP pockets within this family of protein kinases.

Non-covalent inhibitors with a certain degree of selectivity for JAK3 have also been described (e.g., NIBR3049 (17), WYE-151650 (18), decernotinib (16), and others (19–21); see Fig. 3 for selected examples) [23–28]. Among these compounds, NIBR3049 (17), a low nanomolar JAK3 inhibitor, has the most pronounced JAK3 selectivity (127-fold, 318-fold, and 1,000-fold against JAK1, JAK2, and TYK2, respectively) as determined in a biochemical Caliper assay format [29]. As

a) Approved covalent kinase inhibitors:



b) Approved JAK inhibitors:



c) Advanced investigational JAK inhibitors:

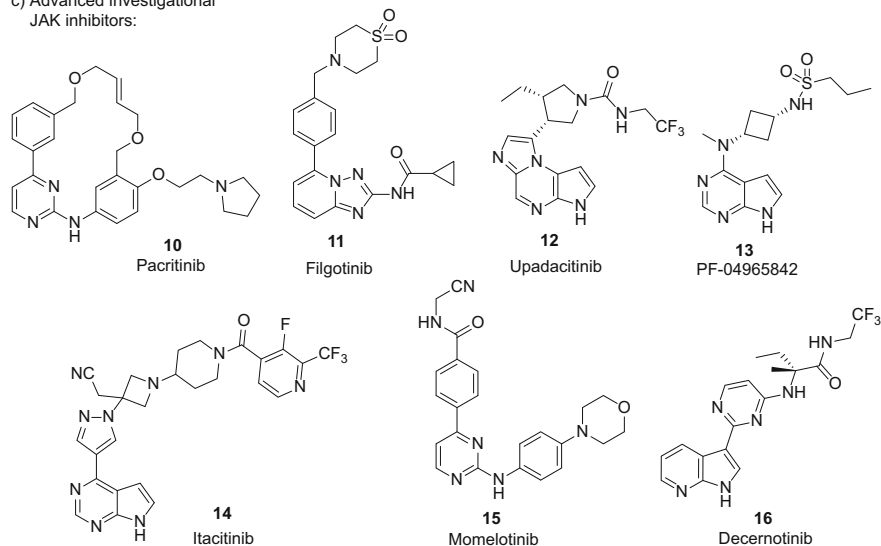


Fig. 2 (a) Currently approved covalent kinase inhibitors. (b) Currently approved JAK inhibitors. (c) Advanced investigational JAK inhibitors

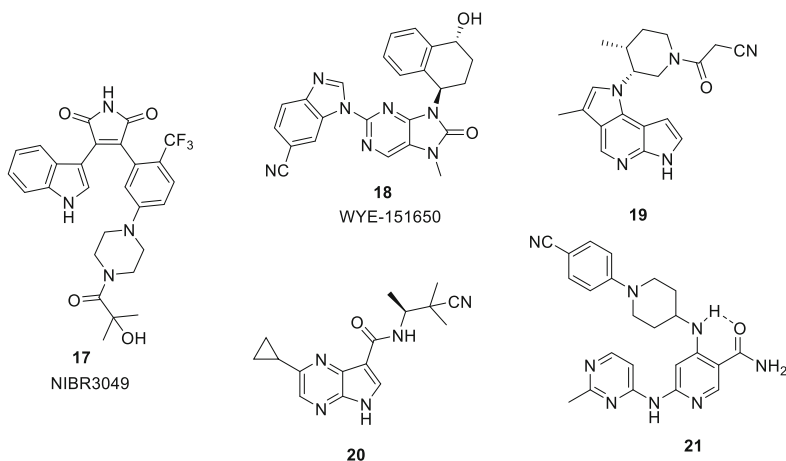


Fig. 3 NIBR3049 and other selected non-covalent JAK inhibitors with varying degrees of selectivity for JAK3

researchers from Novartis found this compound to be an unexpectedly weak suppressor of γ_c -cytokine-induced STAT phosphorylation, they conducted further experiments investigating IL-2 signaling in engineered cells reconstituted with “kinase-dead” and “analog-sensitive” JAK1 and JAK3 mutants. Their results challenged the notion that selective JAK3 inhibition would effectively block STAT phosphorylation to promote immunosuppression; they concluded that JAK1 was dominant over JAK3 in the γ_c -cytokine signaling [29]. According to their model, JAK3 is primarily responsible for the phosphorylation and (full) activation of JAK1. Consequently, they suggested that JAK1 inhibition would be indispensable for efficient suppression of immune response. Complementary results, however, were obtained from Thorarensen et al. at Pfizer [30]. They showed that JAK inhibitors undergo a potency shift eroding JAK3 selectivity, when moving from isolated biochemical to cellular systems. Biochemical assays usually apply ATP concentrations close to the enzyme’s K_m value, while cellular ATP concentrations are much higher, generally in the low millimolar range [31]. The observed shift in potency is caused by the higher ATP affinity of JAK3 relative to other JAKs, an effect that is especially pronounced when comparing JAK3 with JAK1. Consequently, NIBR3049 was found to be a much less potent JAK3 inhibitor at cellular ATP concentrations suggesting that the lack of efficacy observed in the aforementioned study resulted from NIBR3049’s insufficient inhibitory potency in cells rather than from its selectivity for JAK3. These conflicting results fueled a discussion on whether selective JAK3 inhibition would be sufficient to block STAT phosphorylation and thereby downstream signaling as is required for immunosuppression in vivo [16, 30, 32]. To finally end this debate, highly isoform-selective JAK3 inhibitors with sufficient cellular potency needed to be developed.

2 Covalent JAK3 Inhibitors

As mentioned before, the Janus kinases feature a highly conserved ATP pocket impeding the design of specific compounds. The very limited differences in this binding site are highlighted in the structure-derived sequence alignment depicted in Fig. 4. Accordingly, one of the few distinguishing features that could enable the rational design of selective JAK3 inhibitors is a cysteine at position 909 in the solvent exposed front region, which is amenable to covalent targeting. This residue is located in the α D-1 position (nomenclature according to ref. [33]) seven amino acids after the gatekeeper residue. Remarkably, there are ten other kinases (BLK, BMX, BTK, EGFR, HER2, HER4, ITK, MAP2K7, TEC, and TXK) known to feature an equivalently positioned cysteine [33]. The ligandability of this residue has long been proven for cysteine 797 in the EGFR kinase domain, for which the first covalent inhibitors had already been developed at the end of the last century [34]. Notably, cysteines in the α D-1 position are also targeted by all the currently approved covalent kinase inhibitors, i.e., the EGFR/HER-family inhibitors afatinib (**1**), neratinib (**2**), and osimertinib (**3**) and the BTK inhibitors ibrutinib (**4**) and acalabrutinib (**5**; see Fig. 2a). Addressing Cys909 in JAK3 has led to the phase II clinical candidate PF-06651600 [35], which is under investigation for the treatment of rheumatoid arthritis, Crohn's disease, ulcerative colitis, and alopecia areata (vide infra). Efforts which have enabled the development of this and other covalent JAK3 inhibitors are summarized in the following sections. For general consideration on the design and development of covalent kinase inhibitors, please consult the respective chapter in this book. It should also be noted at this point that IC_{50} values of covalent inhibitors are time-dependent and therefore difficult to compare. Thus, the kinetics of covalent inactivation described the second-order rate constant k_{inact}/K_I should be used to compare the overall efficiency of covalent inhibitors (see the aforementioned chapter on covalent kinase inhibitors for details). However, since no kinetic data was provided in most of the cited studies, the bulk of the discussion in this chapter is still based on IC_{50} data.

The first putatively covalent JAK3 inhibitors were described in the year 2000 by researchers from AstraZeneca [37]. They investigated naphthyl(β -aminoethyl) ketones and analogous Mannich bases (Fig. 5), which can form reactive vinylketones upon elimination of the β -amino substituent. The covalent modification of JAK3 was not scrutinized in this study. Nevertheless, a covalent mechanism of action is very likely since these relatively simple compounds, although being devoid of a classical hinge-binding motif, are potent JAK3 inhibitors (pIC_{50} values up to 7.1) while possessing only weak JAK1 inhibitory potency. In support of this assumption, the isolated vinyl 2-naphthyl ketone **25** possessed a similar inhibitory potency ($pIC_{50} = 7.1$) as the most potent compound **24**, while the stabilized derivatives **27** and **28**, which cannot undergo elimination (retro-aza-Michael addition), remained completely inactive.

A similar mode of action can be assumed for the macrocyclic JAK3 inhibitors NC1153 (**29**) and EP009 (**30**, Fig. 6), which were described in 2005 and 2014, respectively [38, 39]. However, neither was a medicinal chemistry optimization of these compounds disclosed nor was the covalent mode of action experimentally

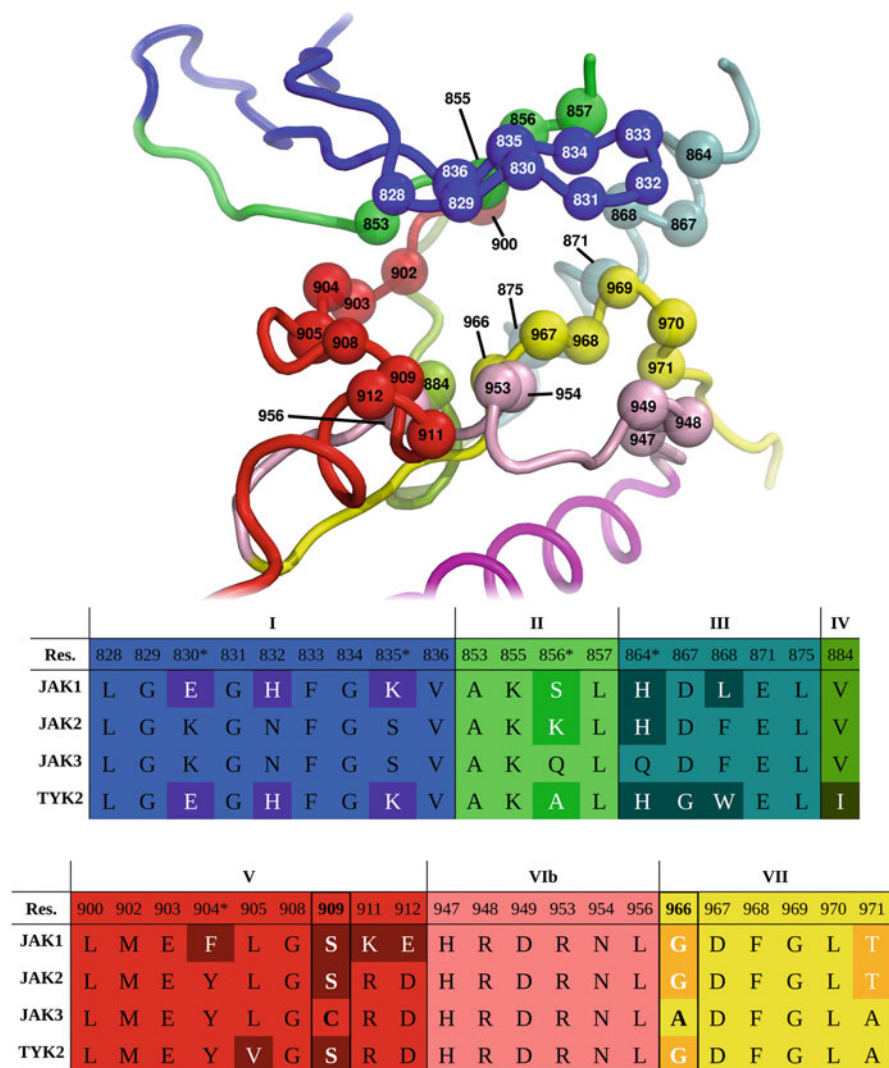


Fig. 4 Alignment of the amino acids contributing to the Janus kinases' ATP pockets and the adjacent regions (generated by superposition from the JAK3 X-ray crystal structure with the PDB-code 3LXX). Colors/roman numbers were assigned according to the kinases' subdomain structure proposed by Hanks and Hunter [36]. The sequence and numbering of JAK3 is used as basis for the alignment, and differing amino acids in other JAKs are highlighted in darker colors. Amino acids contributing to the binding pocket only via their backbone are further marked with an asterisk. Cys909 and Ala966 (highlighted with a black frame) are the key discriminators between JAK3 and other JAK family members

confirmed. Although a certain degree of specificity was claimed in the corresponding publications, it is likely that the highly reactive α,β -unsaturated ketones representing the active species covalently modify additional targets beyond JAK3.

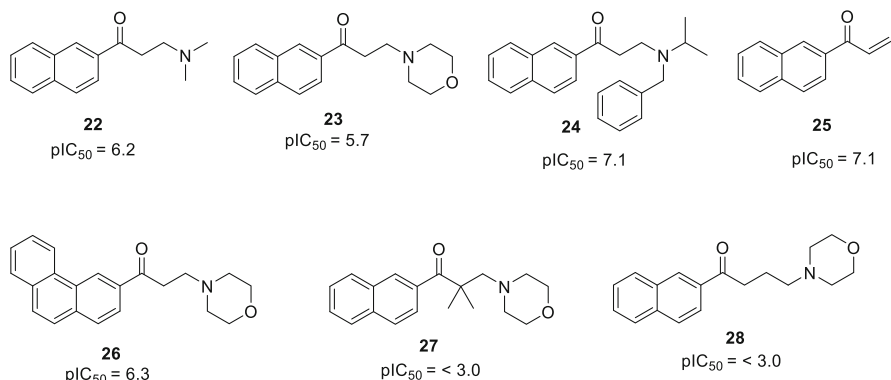


Fig. 5 Naphthyl(β -aminoethyl)ketones and analogous compounds

Fig. 6 Macrocyclic Mannich base NC-1153 and α,β -unsaturated analog EP009

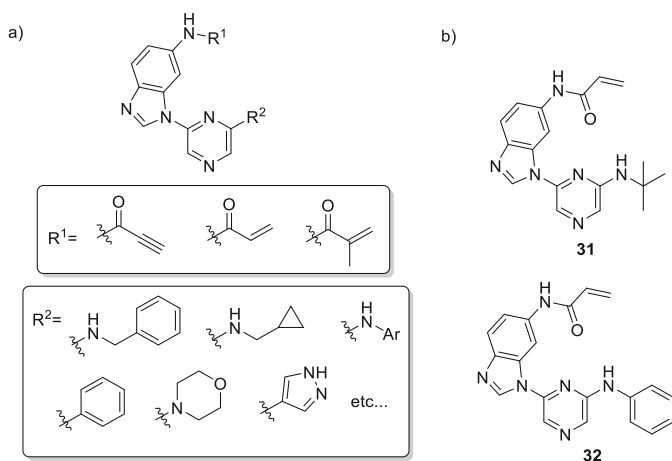
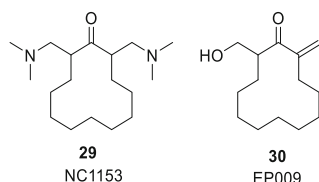


Fig. 7 Electrophilic JAK3 inhibitors from Cytopia Ltd. **(a)** General structure. **(b)** Selected example **31** and analog **32**, which was later crystallized in complex with JAK3 by Goedken et al. [41] (see Fig. 8)

Besides the above compounds, further early examples of (presumably) covalent JAK3 inhibitors have been reported in the patent literature. For example, a set of druglike acrylamide-derived JAK3 inhibitors were claimed as early as 2005 in a patent from Cytopia Ltd. (Fig. 7) [40]. These inhibitors possessed selectivity for

JAK3 vs. JAK2 at 20 μM , but inhibitory potencies were only assigned to a single structure (**31**). This compound showed a time-dependent IC_{50} value of 40 nM and 7 nM after 20 min and 90 min preincubation, respectively. Although the covalent binding mode was not unambiguously confirmed by experimental data in this patent, Goedken et al. later reported the X-ray crystal structure of close analog **32** covalently bound to JAK3 (Fig. 8) [41].

Two patents from Principia Biopharma published in 2012 and 2014 claimed JAK3 inhibitors based on a 5*H*-pyrrolo[2,3-*b*]pyrazine scaffold equipped with acrylamide or

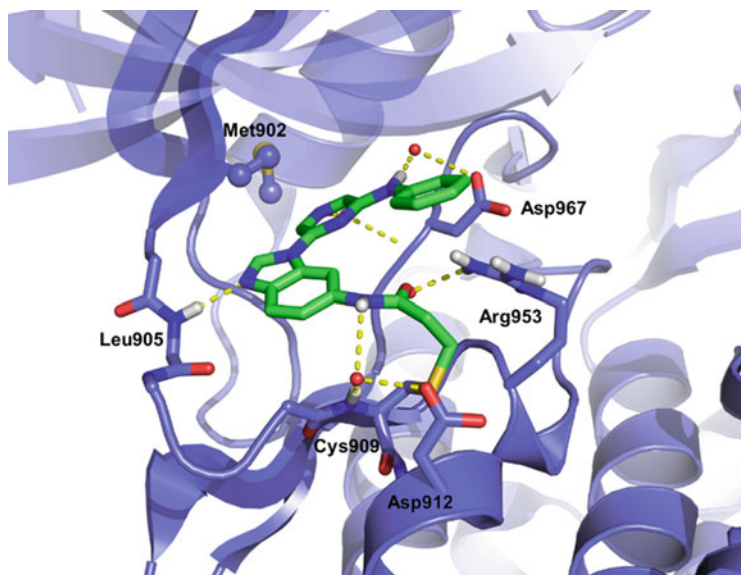


Fig. 8 JAK3 in covalent complex with inhibitor **32** (PDB-code: 4QPS). Hydrogen bonds are depicted as dashed yellow lines and water molecules as red spheres. The Met902 gatekeeper residue is highlighted in the ball and stick representation

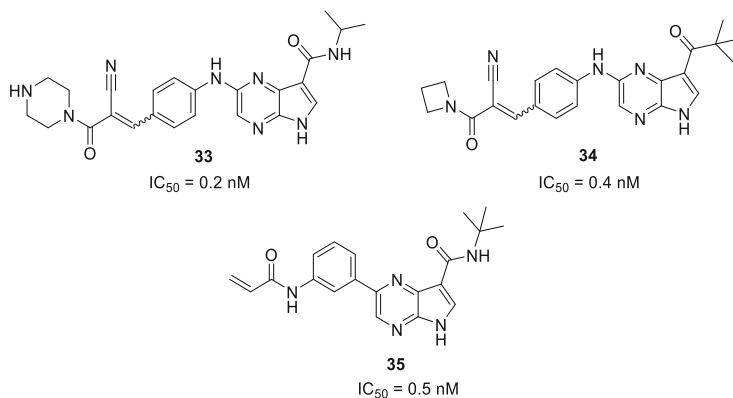


Fig. 9 Acrylamide- and α -cyanoacrylamide-derived JAK3 inhibitors from Principia Biopharma

α -cyanoacrylamide warheads (see Fig. 9 for selected examples **33–35**) [42, 43]. Very potent inhibitors with subnanomolar IC_{50} values were reported in both series, however, without providing further details on the binding modes.

Another patent from Merck Sharp & Dohme (MSD) published in 2013 included a large series of 4-aryl-7*H*-pyrrolo[2,3-*d*]pyrimidines with acrylamides attached to the *meta*-position of the 4-aryl-substituent. Many of these compounds featured IC_{50} values in the subnanomolar range and more than 10,000-fold selectivity over JAK2 [44]. Selected examples **36–39** are depicted in Fig. 10. Although no data except JAK2 and JAK3 inhibitory potencies were reported, compounds from the same structural class were later demonstrated to bind covalently to JAK3 by researchers from Pfizer (*vide infra*) [35]. Moreover, JAK3i (**39**), another compound of this structure type, was later used by the Taunton group to interrogate IL-2 triggered STAT5 signaling (*vide infra*) [45].

The first reports on the rational design of covalent JAK3 inhibitors occurred in the peer-reviewed literature only in 2014. Joint efforts of the groups of Shoichet and Taunton led to the identification of several covalent-reversible JAK3 inhibitors equipped with α -cyanoacrylamide warheads [46]. These ligands were identified from a targeted virtual library that was assembled and screened using a novel covalent docking approach termed DOCKoValent. Experimental evaluation of the most promising hits against JAK3 identified key compounds **40** and **41** (Fig. 11) with IC_{50} values of 93 nM and 49 nM, respectively. Notably, no substantial inhibition of other JAK isoforms was observed for either of the two inhibitors up to concentrations of 10 μ M. Compound **41** was further tested against nine other kinases featuring a cysteine at the same position and found to be a potent inhibitor of

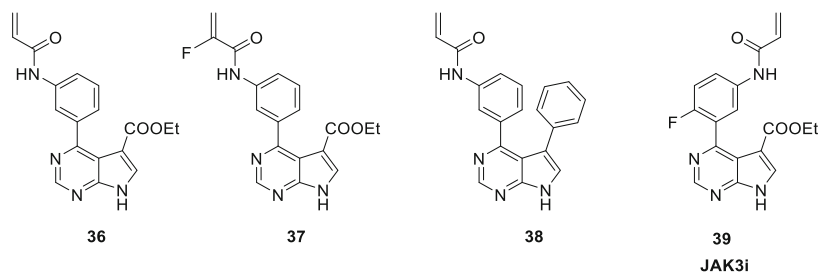
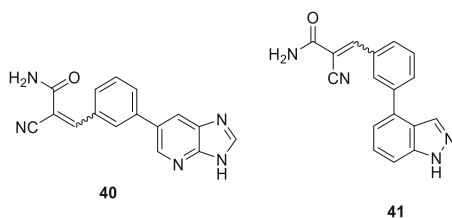


Fig. 10 Selected acrylamide-derived JAK3 inhibitors from Merck Sharp & Dohme

Fig. 11 Covalent-reversible JAK3 inhibitors identified by London et al. [46]



BLK, HER4, and ITK, with IC_{50} values of 22 nM, 44 nM, and 221 nM, respectively. Based on the computed binding mode and the provided selectivity data, covalent engagement of Cys909 can certainly be assumed although no X-ray or MS-data were provided.

Almost simultaneously, our own group reported on ruxolitinib-derived inhibitors designed to covalently address Cys909 [47]. To access ruxolitinib analogs in a convenient and highly flexible manner, we replaced the pyrazole ring attached to the 4-position of the 7*H*-pyrrolo[2,3-*d*]pyrimidine hinge-binding motif by an 1,4-disubstituted 1,2,3-triazole ring readily accessible by copper-catalyzed azide-alkyne cycloaddition (Fig. 12a). Classical (reversible) and covalent docking predicted that the attachment of a propylene oxide moiety to the triazole-*N*1-atom would place the epoxide warhead in an appropriate position to react with Cys909 (Fig. 12b). We prepared (racemic) key compound **43** and tested it against all JAK isoforms. In accordance with our design hypothesis, we found that this compound potently inhibits JAK3 (IC_{50} = 35 nM) while being 70-fold to 160-fold selective against the other JAK isoforms. Since we discontinued the development of this compound class in favor of tricyclic covalent-reversible JAK3-inhibitors (vide infra) [48], we did not confirm the binding mode by X-ray crystallography. However, the biological data being in line with data from modeling strongly supports covalent interaction with Cys909.

Only a few months later, researchers from AbbVie also reported on covalent JAK3 inhibitors with only moderate structural complexity [41]. These compounds were based on a 1-methyl-1,6-dihydroimidazo[4,5-*d*]pyrrolo[2,3-*b*]pyridin-2-amine scaffold which was linked to a chloroacetamide (**44**), acrylamide (**45**), or a (*E*)-4-(dimethylamino)-but-2-enamide (**46**) warhead (Fig. 13a). Inhibitory potency was measured at varying ATP concentrations and (pre)incubation times revealing a

a)

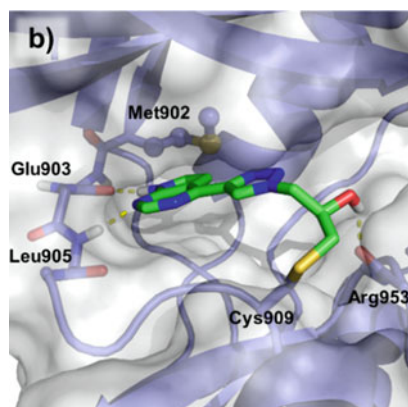
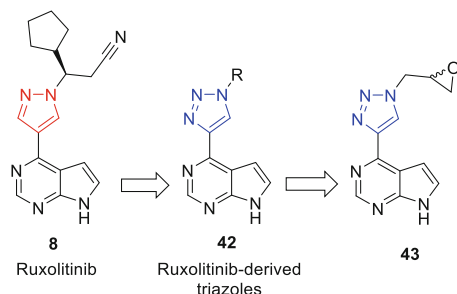


Fig. 12 Ruxolitinib-derived triazoles with a putative covalent binding mode. (a) Design strategy leading to compound **43**. (b) Compound **43** covalently docked in the JAK3 binding site (PDB-code: 3LXK) using the Schrodinger Small Molecule Drug Discovery Suite. Epoxide opening by the Cys909 side chain is predicted to occur at the terminal carbon atom. The generated hydroxy group forms a hydrogen bond to the Arg953 backbone carbonyl oxygen atom

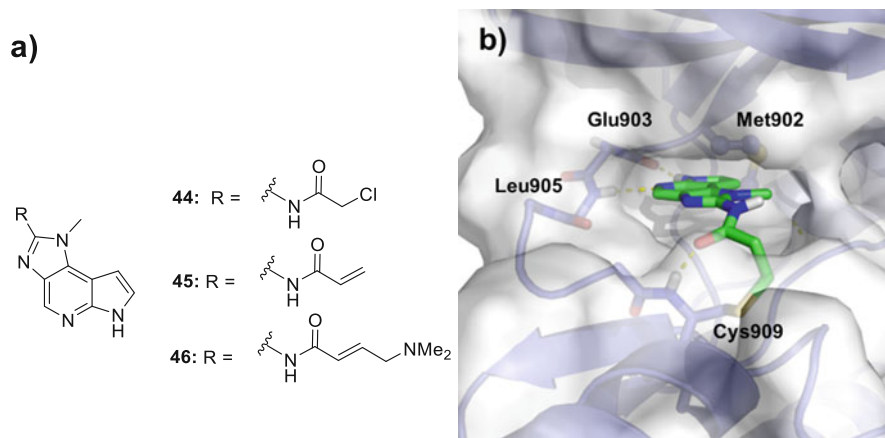


Fig. 13 (a) Covalent JAK3 inhibitors from Goedken et al. [41]. (b) Suggested binding mode of compound **45** remodeled by covalent docking into the X-ray crystal structure with the PDB-code 4QPS using the Schrodinger Small Molecule Drug Discovery Suite

time-dependent behavior indicative for covalent target engagement. Kinetic analysis in a trFRET displacement assay showed the overall efficiency of covalent inactivation (described by the second-order rate constant $k_{\text{inact}}/K_{\text{I}}$) of compound **44** ($k_{\text{inact}}/K_{\text{I}} = 3.5 \times 10^3 \text{ M}^{-1} \text{ s}^{-1}$) to be in the same range as for pyrazinyl benzimidazole **32** from Cytopia ($k_{\text{inact}}/K_{\text{I}} = 9.0 \times 10^3 \text{ M}^{-1} \text{ s}^{-1}$), while compound **45** ($k_{\text{inact}}/K_{\text{I}} = 1.7 \times 10^5 \text{ M}^{-1} \text{ s}^{-1}$) was even more efficient. Inhibitors **44** and **45** were selective for JAK3 when tested against all JAKs in vitro and in cells, and a time-dependent increase in inhibitory potency was observed exclusively for JAK3. Moreover, selectivity against the ten other kinases containing an equivalently positioned cysteine as well as in a panel of 78 protein kinases was demonstrated. However, it should be noted that compounds **44** and **32** suffered from insufficient (reversible) binding affinity as JAK3 inhibition was outcompeted by high ATP concentrations ($\text{IC}_{50} > 50 \text{ }\mu\text{M}$ at 1 mM ATP; **45** was not tested). Covalent modification of Cys909 was demonstrated by mass spectrometry for compound **45**. However, although an X-ray structure of the covalent complex between compound **32** from Cytopia (vide supra, Fig. 8) was provided in this study, no crystal structures of compounds **44–46** were included, and a docked model of the binding mode was deduced instead (see the model in Fig. 13b).

In the same year, the Gray group reported a comprehensive set of covalent JAK3 inhibitors derived from WZ4002 (**47**), a covalent ligand of the EGFR^{T790M} mutant [49, 50]. The key alteration with respect to WZ4002 was the extension of the spacer length by replacement of the *meta*-substituted phenoxy linker by a benzylamine residue (Fig. 14).

Further optimization of the other substituents and the heterocyclic hinge-binding motif furnished a set of over 70 compounds exhaustively showing the structure–activity relationships of this structural class. Most of the biological evaluation within

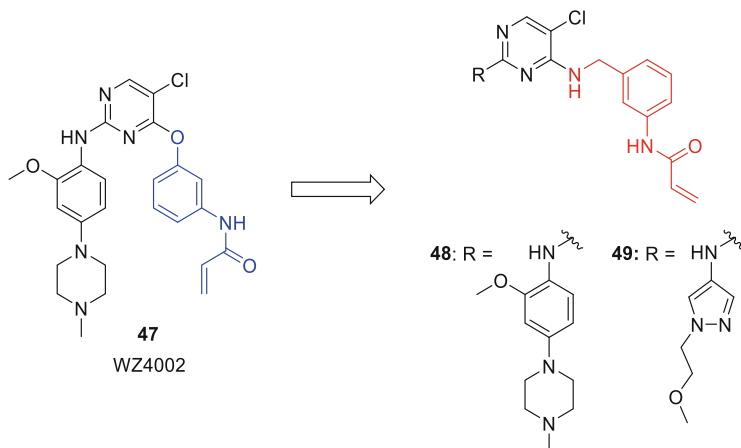
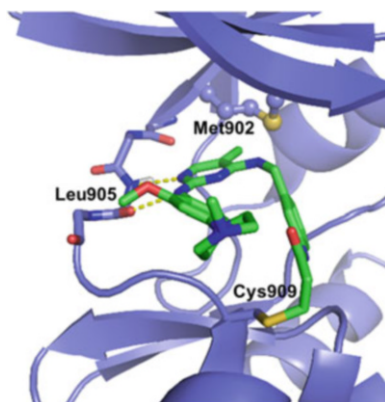


Fig. 14 Development of covalent JAK3 inhibitors derived from the irreversible EGFR inhibitor WZ4002 by Tan et al. [49]

this campaign was carried out by a cellular viability assay utilizing Ba/F3 cells, which were dependent on the constitutive activity of the respective Tel-JAK1–3 fusion proteins. The key compounds **48** and **49** showed an excellent JAK3 potency in an enzymatic assay with IC_{50} values of 4.8 nM and <0.5 nM, respectively, together with a favorable isoform selectivity of 190-fold, 220-fold, and >2,000-fold (**48**) and >70-fold, >100-fold, and >80-fold (**49**) over JAK1, JAK2, and TYK2 as measured at an ATP concentration near the K_m value. In the aforementioned Ba/F3 assay, **48** and **49** were able to inhibit JAK3 in presence of cellular ATP concentrations with IC_{50} values of 69 nM and 19 nM, respectively. The good isoform specificity was also maintained with an at least 33-fold (**48**) or 390-fold (**49**) selectivity window over the other three family members. The selectivity of the key compounds was further validated in several other cellular models. These inhibitors effectively blocked JAK3-dependent IL-2-mediated STAT5 phosphorylation in TALL-1 leukemia cells and the IL-4-induced phosphorylation of STAT6 in bone marrow-derived macrophages (BMDMs); JAK1/2 and TYK2-dependent pathways were influenced neither by **48** nor by **49**. A broad kinome selectivity screening was conducted with the DiscoverX KINOMEScan technology (456 kinases, competition-binding format) revealing 82 off-targets for **48** tested at 1 μ M. The IC_{50} values for major off-targets were subsequently determined with enzymatic assays confirming inhibition of Fms-related tyrosine kinase 3 (FLT3, IC_{50} = 13 nM), tyrosine protein kinase (TXK, IC_{50} = 36 nM), TTK protein kinase (TTK, IC_{50} = 49 nM), B lymphocyte kinase (BLK, IC_{50} = 157 nM), and EGFR^{WT} (IC_{50} = 409 nM). Compound **49** showed a higher selectivity in this panel where the most potently inhibited wild-type kinase was aurora kinase A with an IC_{50} value of 43 nM. Washout and pulldown experiments with a biotinylated inhibitor clearly demonstrated target engagement in cells, and the expected covalent binding mode was finally proven by mass spectrometry and X-ray crystallography (Fig. 15).

Fig. 15 Covalent complex of **48** and JAK3 (PDB-code: 4Z16). Hydrogen bonds are depicted as dashed yellow lines, and the Met902 gatekeeper residue is highlighted in the ball and stick representation

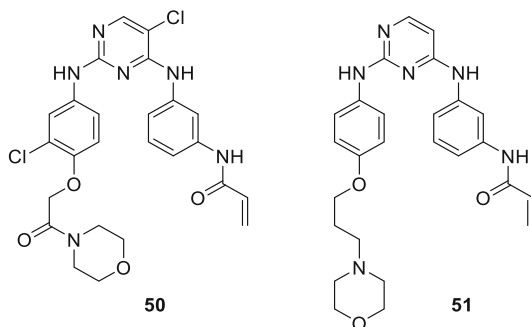


The inhibitor adopts a U-shaped conformation in which the 2-aminopyrimidine scaffold shows the typical hinge-binding pattern with two hydrogen bonds between the inhibitor and the backbone of Leu905. The benzylamine linker spans back through the catalytic cleft toward Cys909, where the covalent bond is formed between the acrylamide and the thiol of the cysteine side chain. The 2-methoxy-4-(4-methylpiperazin-1-yl) aniline moiety occupies the solvent-exposed front region.

Further evaluation of DMPK properties revealed that both, key compound **48** and **49**, were poorly stable in murine liver microsomes ($t_{1/2} < 5$ min). Nevertheless, compound **49** showed a moderate plasma half-life of 1.4 h after i.v. administration and a favorable oral bioavailability of 66%. Notably, due to the relatively rapid resynthesis rate of JAK3 ($t_{1/2}$ approx. 3.5 h in PBMCs [35]), it is likely that sustained exposure would be required for achieving prolonged in vivo effects despite irreversible binding.

Very recently, a report on “dual-specific” BTK/JAK3 inhibitors has been published by Ge et al. [51]. The authors presented a set of 2,6-diarylamino-pyrimidines bearing an *N*-arylacrylamide warhead, which were derived from the aforementioned EGFR inhibitor WZ4002. Interestingly, and in contrast to similar JAK3-selective inhibitors described by the Gray group (Fig. 14), these compounds do not possess a methylene group between the hinge-binding motif and the aryl linker. Both key compounds, **50** and **51** (Fig. 16), showed subnanomolar potencies on BTK. Furthermore, **51** was also found to be a picomolar JAK3 inhibitor, while **50** was about ten times less potent on this enzyme. However, no data on JAK isoform selectivity or specificity within the kinome were reported, and a confirmation of the proposed covalent interaction was not provided for either of the two target kinases. Further evaluation focused on the inhibition of proliferation of three B cell lymphoma cell lines (Ramos cells, Raji cells, and Namalwa cells). In these cells, both key compounds showed comparable profiles with IC_{50} values ranging from 2 to 9 μ M. Although no detailed DMPK data were provided in this report, the key compounds **50** and **51** were tested in a murine xenograft model using human Ramos cells. Tumor growth was inhibited dose-dependently by both compounds, with **50** being slightly more effective than **51** at same doses (30–60 mg/kg,

Fig. 16 Dual specific JAK3/BTK inhibitors from Ge et al.



p.o., QD). Due to the relatively poor characterization of these compounds, it remains unclear, however, to what extent the observed cellular and in vivo effects arise from specific inhibition of JAK3 and BTK.

In 2016, the Taunton group utilized JAK3i (**39**, Fig. 10), an acrylamide-based inhibitor from the aforementioned patent application by Merck Sharp & Dome, for the investigation of the time dependency of STAT5 phosphorylation in IL-2 stimulated CD4⁺ T cells [45]. In accordance with the data provided by MSD, the compound exhibited excellent JAK3 potency in an enzymatic assay ($IC_{50} = 0.43$ nM). Moreover, >3,000-fold selectivity over the other JAK family members at a fixed ATP concentration of 100 μ M was demonstrated. Kinome selectivity, however, was not determined in this study, but a promising selectivity against three kinases with an equivalently positioned cysteine was shown at 1 mM ATP (EGFR, ITK, and BTK with a 1,300-fold, 600-fold, and 50-fold selectivity, respectively). A final confirmation of the covalent engagement of Cys909 by **39** via X-ray crystallography was not part of this work, but other groups later reported such data for closely related molecules of the same structural class (vide infra) [35, 52]. Instead, Taunton and co-workers proved the involvement of Cys909 using murine CD4⁺ T cells, where overexpression of the JAK3^{C909S} mutant was protective against JAK3i-dependent effects. By using JAK3i as a chemical probe, they found that IL-2-induced STAT5 phosphorylation occurs in two independent waves, one after 15 min and a second one peaking approx. 2 h after stimulation. In contrast to the pan-JAK inhibitor tofacitinib, which blocked both waves, compound **39** preferentially affected the second wave of IL-2/pSTAT5 signaling. Blockage of the delayed STAT5 phosphorylation event was sufficient to prevent the cells from entering the S phase, and compound **39** (40 mg/kg, i.p., BID) inhibited proliferation of T cell blasts in mice.

Our own group published a small set of tricyclic covalent-reversible JAK3 inhibitors as chemical probes at the end of 2016 [48] and subsequently reported a detailed SAR study of the underlying compound class in 2018 [53]. Within this project, rational design started from tricyclic tofacitinib analogs [54] enabling the introduction of different aromatic linkers at the imidazole's C2-position, which were then decorated with a variety of Michael acceptor-derived warheads. Our optimization efforts culminated in the discovery of the key compounds **52** and **53** (Fig. 17).

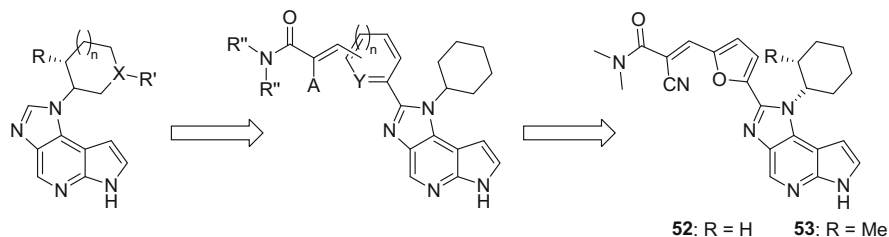


Fig. 17 Development of the covalent-reversible JAK3 inhibitors **52** and **53**

While *meta*- and *para*-substituted phenyl linkers combined with acrylamide warheads were not able to boost JAK3 inhibitory potency, the introduction of a 2,5-disubstituted furfuryl residue as the linker moiety and the use of an α -cyanoacrylamide as the electrophile were the key modifications to generate the highly active JAK3 inhibitors **52** and **53**. Both of these compounds exhibited subnanomolar JAK3 potencies and showed an extraordinarily good selectivity against the other JAKs (400-fold to 5,800-fold against JAK1, JAK2, and TYK2). The ATP dependency of the selectivity of **52** was further investigated at a fixed ATP concentration (200 μ M) confirming that a similar selectivity window was maintained [53]. In a broad kinome selectivity screen (ProKinase Kinase 410--Profiler), compound **52** showed 11 off-targets with less than 50% residual activity, while **53** was even more selective with only a single off-target (MAPKAPK2) at a tested concentration of 500 nM. When screened at 100 nM, both compounds showed a perfectly clean profile without any notable off-targets. The somewhat better selectivity of **53** can be attributed to the additional methyl group at the 2-position of the cyclohexyl side chain, which is known as the key driver of kinome selectivity from an analogous residue in tofacitinib [55]. The JAK3 selectivity determined by enzymatic assays was recapitulated in several cellular models. Selectivity against a set of other kinases with an equivalent cysteine placement (BLK, BTK, and TEC) was confirmed using a nanoBRET-based cellular assay [56]. In another model employing primary CD4⁺ T cells, both compounds only affected the signaling of JAK3-dependent pathways while leaving JAK1, JAK2, and TYK2 signaling unaffected even at the highest tested concentration (1 μ M).

The assumed covalent targeting of Cys909 was confirmed by X-ray crystallography for compound **53**. The ligand shows the expected tofacitinib-like binding mode with the typical bidentate hinge-binding pattern to the backbone of Glu903 and Leu905. The furan linker spans through the front region placing the electrophilic β -position of the warhead in proximity to the Cys909 thiol group (Fig. 18). Interestingly, the X-ray structure features two distinct binding modes, one with the ligand covalently attached to the protein (Fig. 18b) and the other one without the bond between the β C-atom of the α -cyanoacrylamide and the cysteine's thiol group (Fig. 18a). The simultaneous presence of the covalent and the non-covalent complex conforms to the concept of covalent-reversible targeting with α -cyanoacrylamides. Notably, we also recapitulated the reversible nature of thiol addition by experiments with model thiols (Forster & Laufer, unpublished).

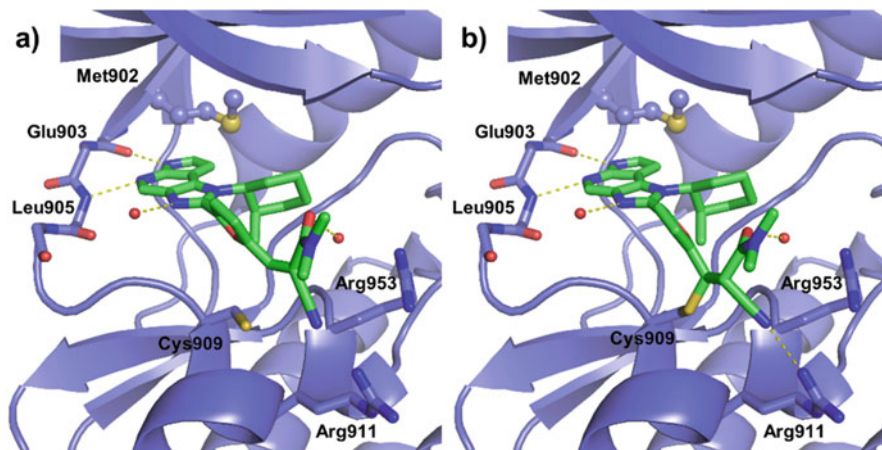


Fig. 18 Co-existing covalent and non-covalent complex of **53** and JAK3 (PDB-code: 5LWN). Hydrogen bonds are depicted as dashed yellow lines, and the Met902 gatekeeper residue is highlighted in the ball and stick representation. (a) Binding mode of **53** without covalent engagement of Cys909 and (b) ligand **53** covalently bound to Cys909

Another key feature of both, compound **52** and **53**, is the induction of a novel binding cleft through the reorientation of the side chains of Arg911, Asp912, and Arg953 by interactions with the inhibitor's nitrile group. We further investigated the SAR of the underlying compound class with a special emphasis on the induction of this "arginine pocket" to deduce its function in conferring activity and selectivity [53]. After iteratively modifying the linker moiety and the headgroup, we were able to show by X-ray crystallography that a relatively rigid α,β -unsaturated acrylonitrile moiety (exemplified by compound **54**, Fig. 19c) is necessary to induce this cavity, while the pocket is not formed by the corresponding propionitriles (e.g., compound **55**). As depicted in Fig. 19a, the formation of the arginine pocket was observed in the X-ray structure of acrylonitrile **54** in (non-covalent) complex with JAK3. Contrastingly, the complex with saturated analog **55** (Fig. 19b) showed the side chains of Arg911, Asp912, and Arg953 to adopt the typical conserved conformation known from other JAK crystal structures.

Accordingly, these inhibitors showed distinct biochemical profiles. Compound **55** exhibited only a moderate JAK3 potency ($IC_{50} = 129$ nM) and no evident isoform selectivity, while **54** was five times more potent on JAK3 ($IC_{50} = 27$ nM) and showed a 60-fold to 210-fold selectivity over the other isoforms. It is noteworthy that a covalent interaction with Cys909 was not detected in any of these structures, suggesting that a moderate JAK3 selectivity can be achieved solely by the induction of the arginine pocket without the need of establishing a covalent bond with Cys909.

Researchers from Pfizer have recently published two studies in which they modified the non-covalent pan-JAK inhibitor tofacitinib (**6**) with the aim of turning it into a covalent inhibitor [35, 57]. The key hypothesis of their effort was that the piperidinyl side chain of **6** could be modified to prefer an "anti-conformation" with respect to the heterocyclic hinge-binding motif enabling the covalent

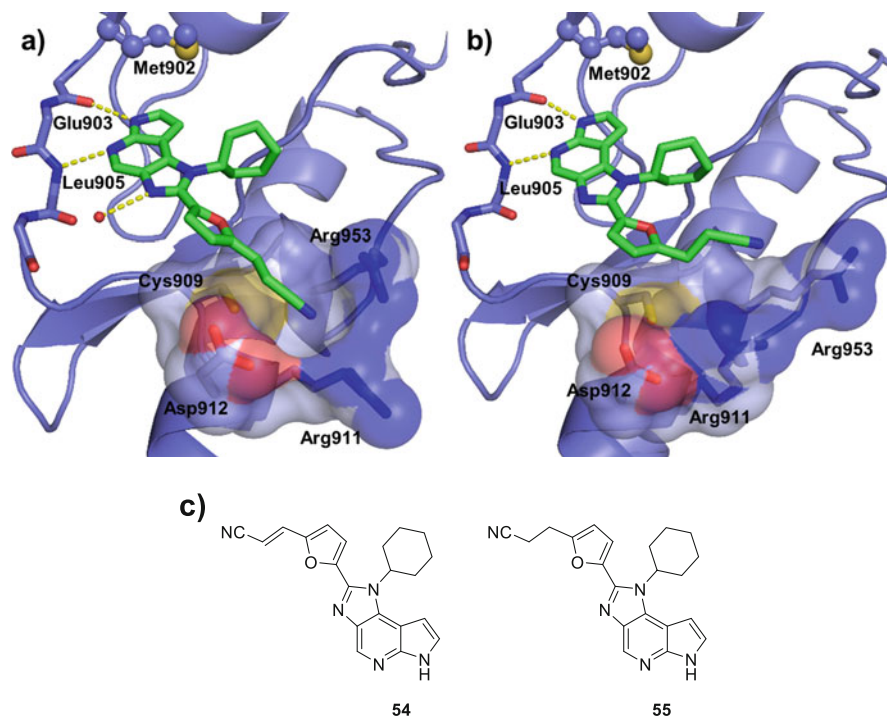


Fig. 19 X-ray structures of (a) **54** (PDB-code: 6GLA) and (b) **55** (PDB-code: 6GLB) in complex with JAK3. Hydrogen bonds are depicted as dashed yellow lines, and the Met902 gatekeeper residue is highlighted in the ball and stick representation. (c) Chemical structures of **54** and **55**

engagement of the Cys909 thiol with an acrylamide attached to the piperidine nitrogen atom (Fig. 20a).

One key modification to favor the *anti*-orientation was the removal of the *N*-methyl group to facilitate the rotation around the C–N bond, which is linking the aliphatic side chain to the heterocyclic hinge-binding motif. Simultaneously, the exocyclic 4-methyl group at the piperidine moiety was truncated as it was suspected to clash with the “roof” of the binding pocket in this inverted conformation. The optimization process aimed to increase the rate of inactivation (described by k_{inact}) by stabilizing the reactive conformation while decreasing the intrinsic chemical reactivity of the warhead to a necessary minimum. These efforts furnished two compound series represented by inhibitors **57** and **58** (Fig. 20b), the latter being related to the MSD compounds discussed above (see Fig. 10). Both inhibitors showed high JAK3 potency as well as excellent isoform selectivity, and their covalent binding mode was confirmed by X-ray crystallography (exemplified for compound **58** in Fig. 21a). However, the high intrinsic reactivity of the aniline-derived acrylamides such as **58** led to a poor correlation between data from enzymatic assays, cellular models, and human whole blood justifying the discontinuation of this series.

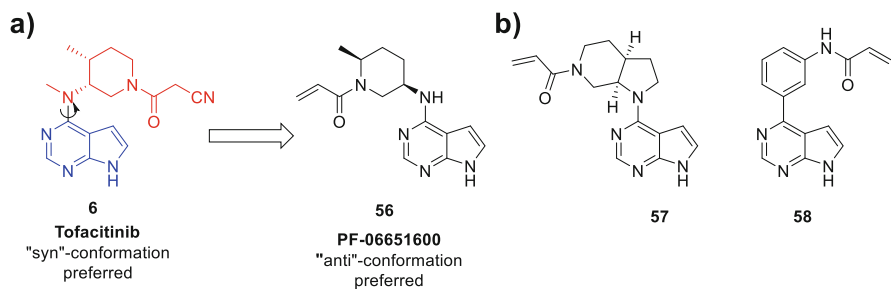


Fig. 20 (a) Development of **56** starting from reversible pan-JAK inhibitor tofacitinib. (b) Derivatives with a rigidized bicyclic side chain (**57**) or an aniline-derived acrylamide (**58**)

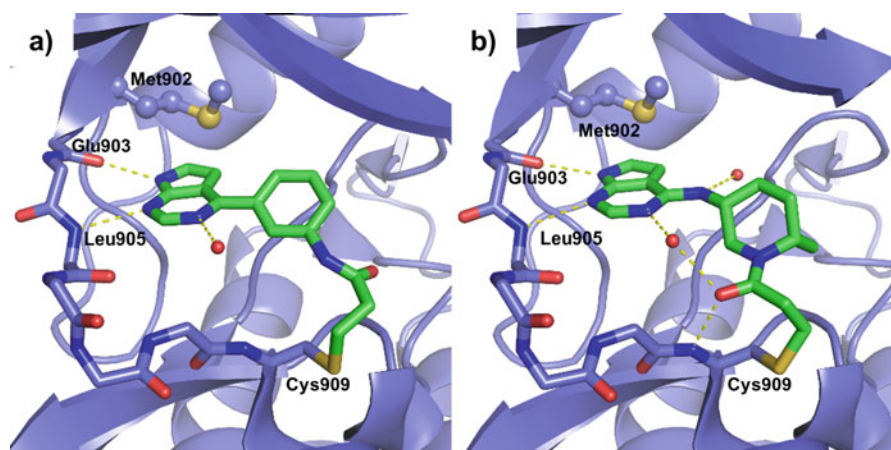


Fig. 21 X-ray structures of (a) **58** (PDB-code: 5TTV) and (b) **56** (PDB-code: 5TOZ) in complex with JAK3. Hydrogen bonds are depicted as dashed yellow lines, and the Met902 gatekeeper residue is highlighted in the ball and stick representation. Only water molecules interacting directly with the ligand are shown

Further optimization of the other series focused on metabolic stability with special emphasis on decreasing GST-mediated clearance. Ultimately, an (*S*)-methyl group in the 2-position of the piperidine ring was identified as the key feature to achieve favorable PK properties enabling the development of clinical candidate PF-06651600 (**56**, Fig. 20a).

Compound **56** is a highly potent JAK3 inhibitor with an IC_{50} value of 0.35 nM when measured at K_m ATP, which shifts to 33 nM when determined at a much higher ATP concentration of 1 mM. At the latter ATP concentration, an at least 300-fold selectivity was shown against the other JAK isoforms. In a panel of 304 kinases (Invitrogen, Z'-Lyte/LanthaScreen), **56** inhibited only 15 kinases more than 50% at a concentration of 1 μ M. Out of these, five kinases (BMX, HER4, TXK, EGFR^{T790M}, and EGFR^{T790M/L858R}) with cysteines equivalent to

Cys909 in JAK3 were strongly inhibited with less than 10% activity remaining. More detailed kinetic investigations were performed and demonstrated moderate selectivity for JAK3 ($k_{\text{inact}}/K_{\text{I}} = 3.7 \times 10^5 \text{ M}^{-1} \text{ s}^{-1}$) over TEC family kinases with an equivalently positioned cysteine (BMX, BLK, BTK, ITC, TEC, TXK; $k_{\text{inact}}/K_{\text{I}}$ ranging from 1.0×10^4 to $8.6 \times 10^2 \text{ M}^{-1} \text{ s}^{-1}$). Pronounced selectivity over the kinase TXK ($k_{\text{inact}}/K_{\text{I}} = 2.3 \times 10^3 \text{ M}^{-1} \text{ s}^{-1}$) was observed in kinetic analyses although the IC_{50} values were in the same range for both enzymes highlighting that IC_{50} data of covalent inhibitors should always be interpreted with caution. Remarkably, selectivity over TEC family kinases is caused by the more efficient covalent inactivation of JAK3 ($k_{\text{inact}} = 2.3 \text{ s}^{-1}$), while K_{I} values were significantly lower for the mentioned TEC kinases.

In a comprehensive set of cellular assays, compound **56** was able to suppress STAT phosphorylation only in the JAK3-dependent pathways triggered by IL-2, IL-4, IL-7, IL-15, and IL-21 with IC_{50} values in the range of 200–400 nM, while no inhibition of downstream STAT phosphorylation was observed after stimulation with IL-6, IL-10, IL-12, IL-23, IL-27, IFN- α , IFN- γ G-CSF, and EPO.

A comparison of **56**, pan-JAK inhibitor tofacitinib, and JAK1-selective inhibitor PF-02384554 in a human whole blood assay showed that tofacitinib was able to inhibit the STAT phosphorylation after stimulation with IL-15 and IL-21 slightly more efficient (fivefold to sevenfold) than **56**. The latter, however, was equipotent to JAK1-selective compound PF-02384554 in the same assay format. These results suggest once more that a dominant role of JAK1 over JAK3 should be considered unlikely.

The successful covalent targeting of Cys909 by **56** was also confirmed by X-ray crystallography, and the ligand adopted the predicted binding mode. The heterocyclic core is directed to the hinge region where it addresses the protein backbone via the two typical hydrogen bonds. Meanwhile, the piperidinyl side chain orients toward Cys909 in the proposed “*anti-conformation*” allowing the acrylamide to react with the sulfhydryl group. It is noteworthy that all hydrogen bond donors and acceptors of **56** are engaged in a hydrogen bonding network built up from the ligand, the protein backbone, and water bridging molecules (Fig. 21b).

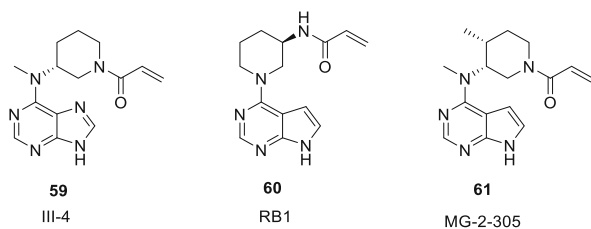
Unspecific protein binding of **56** was shown to be very low as demonstrated using human serum albumin (HSA) as a surrogate protein and in functional human hepatocytes. In the latter case, more than 98% of radiolabeled **56** remained unbound after incubation. Moreover, **56** was tested in several in vivo models and showed good pharmacokinetic properties although a certain interspecies variability was observed. In an adjuvant-induced arthritis (AIA) rat model, **56** was able to decrease paw swelling in a dose-dependent manner after oral administration (3–30 mg/kg, p. o., QD).

At the moment, **56** is being investigated in several phase II clinical trials for the treatment of rheumatoid arthritis (NCT02969044), ulcerative colitis (NCT02958865), and alopecia areata (NCT02974868).

A compound denominated III-4 (**59**, Fig. 22), representing a close structural analog of tofacitinib and PF-06651600, has very recently been characterized as a covalent JAK3 inhibitor by Chen and co-workers [58]. Analogous

compound RB1 (**60**, Fig. 22), which can be considered as a bioisostere of compound **58** (Fig. 20b), was published by the same group only a few months later [59]. Notably, our own group had already prepared a close analog of **60** termed MG-3-305 (**61**, Fig. 22, Gehringer & Laufer, unpublished) in early 2011. Interestingly, however, we found our compound, which is based on a 7*H*-pyrrolo [2,3-*d*]pyrimidine scaffold and features an additional methyl group at the *R*-configured 4-position of the piperidinyl side chain, to be only a moderate to weak suppressor of JAK3 activity ($IC_{50} = 494$ nM). In contrast, **59** and **60** from Chen and co-workers were potent JAK3 inhibitors with IC_{50} values of 40 nM and 57 nM, respectively. Both compounds exhibited very good selectivity against the other JAKs with IC_{50} 's above 5 μ M and 10 μ M, respectively. The compounds were also tested against all protein kinases with an equivalently positioned cysteine except MKK7 (MAP2K7) at 1 μ M. Weak off-target activity (20–40% inhibition of BLK, ITK, TEC, HER4, and TXK) could be observed for **59**, while none of these kinases was significantly hit by **60**. Only compound **60** was tested in a panel containing 75 kinases; weak inhibitory activity on Aurora kinase A and B, CLK2, PKG1 α , and MKK7 was found, the latter being among the kinases featuring an analogous cysteine. In a PBMC assay, the compounds suppressed JAK1/3-dependent IL-2-induced STAT5 phosphorylation with IC_{50} values of 105 nM and 40 nM for **60** and **59**, respectively, while tofacitinib showed an IC_{50} of 25–30 nM. However, while tofacitinib potently suppressed IL-6-triggered STAT3 phosphorylation (dependent on JAK1/JAK2/TYK2; $IC_{50} = 35$ nM) and to a lesser extent GM-CSF-promoted STAT5 phosphorylation (dependent on JAK2; $IC_{50} = 227$ nM), inhibition of these pathways was less pronounced for compound **59** ($IC_{50} = 592$ nM and 492 nM, respectively). Inhibitor **60** was even more selective and spared the last-mentioned pathways up to concentrations of 40 μ M (pSTAT3) and 10 μ M (pSTAT5). These results were supported by further cellular assays indicating a similar behavior. Covalent modification of Cys909 was demonstrated by tryptic digestion/LC-MS and jump dilution. Both compounds showed very little acute toxicity in rats, good oral bioavailability (57% and 73% for **59** and **60**, respectively), and plasma half-life (11.1 h and 14.6 h, respectively). The compounds were orally active in a mouse CIA model dosed at 30 mg/kg and possessed similar efficacy as tofacitinib applied at the same dose. For **60** and the control compound tofacitinib, it was further shown that serum levels of TNF α , IFN γ , and IL-6 as well as gene transcription levels of IL-1, IL-2, and IL-6 in articular tissue decreased in a dose-dependent manner, while IL-10 levels increased. Moreover, at 100 mg/kg, **60**

Fig. 22 Covalent JAK3 inhibitors III-4 (**59**) and RB1 (**60**) from the Chen group and the similar (unpublished) compound MG-2-305 (**61**) previously prepared in the Laufer group



showed some capacity to decrease Th1 and Th17 cell proliferation while increasing T_{reg} cell counts as shown by flow cytometry.

In another recent publication from Chen and co-workers, structure–activity relationships of analogs of compound **58** from Pfizer/MSD (vide supra) were reported [60]. In this study, the hinge-binding motif was varied, and a series of acrylamide- and 2-haloacetamide-derived warheads were installed (Fig. 23a). Within each series, the apparent potency roughly correlated with the intrinsic reactivity of the warhead [61–63], i.e., acrylamides were more potent than methacrylamides, *E*-crotylamides, or 3,3-dimethylacrylamides, while bromoacetamides were slightly more potent than chloroacetamides. As expected, sterically more hindered 2-chloropropionamides were poorly active. The activities of (unsubstituted) acrylamides and 2-haloacetamides were in the same range, and attachment of a methyl group at the *ortho*-position of the acrylamide moiety had a negligible effect on potency. Different purine-derived scaffolds (9*H*-purine, 7*H*-pyrrolo[2,3-*d*]pyrimidine, 1*H*-pyrrolo[2,3-*b*]pyridine, and the partially saturated 2,3-dihydro-1*H*-pyrrolo[2,3-*b*]pyridine) were probed as the hinge-binding motif. In accordance with a previous SAR study from our own laboratory evaluating a plethora of hinge-binding heterocycles for tofacitinib-derived reversible JAK3 inhibitors [64], 9*H*-purine-derived compounds were found to be less active than 7*H*-pyrrolo[2,3-*d*]pyrimidines, and saturation of the C2–C3 double bond also reduced activity. In contrast to our results, however, 1*H*-pyrrolo[2,3-*b*]pyridine-derived covalent JAK3 inhibitors were superior to the analogous 7*H*-pyrrolo[2,3-*d*]pyrimidines in the present study. Notably, many compounds showed a very pronounced selectivity against JAK1 and JAK2 ($IC_{50} > 0.5 \mu\text{M}$ or $5 \mu\text{M}$). The most potent derivative T29 (**63**), representing the 1*H*-pyrrolo[2,3-*b*]pyridine analog of **58** (see Fig. 20b), featured a JAK3 IC_{50} value of 0.14 nM and $>35,000$ selectivity against JAK1 and JAK2. Compounds T1 (**62**, Fig. 23b), T15 (equals compound **58** from Fig. 20b), and T29 were further characterized against nine kinases with an $\alpha\text{D-1}$ cysteine (all except MKK7). While **58** possessed significant activity on BMX ($IC_{50} = 24 \text{ nM}$), weaker BMX potency was observed for **62** and **63** ($IC_{50} = 105 \text{ nM}$ and 240 nM ,

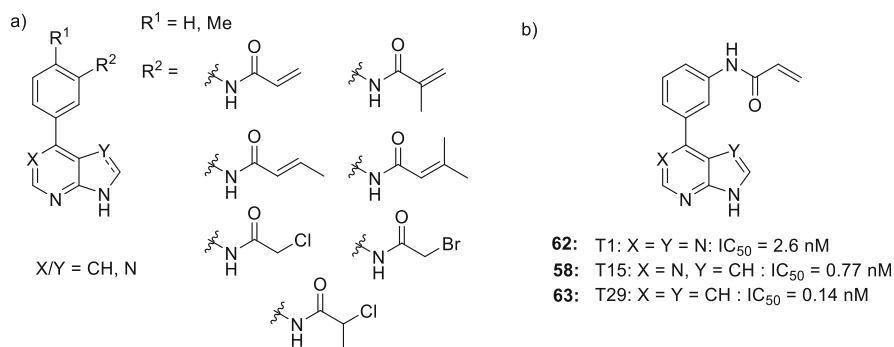


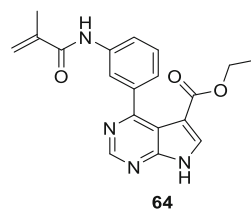
Fig. 23 (a) JAK3 inhibitors derived from **58** (see Fig. 20b) by He et al. [60]. (b) Key compounds T1 (**62**), T15 (equals **58**), and T29 (**63**)

respectively). The inhibitory activity of these compounds on other kinases in this set was less pronounced ($IC_{50} > 450$ nM). All three inhibitors orally dosed at 30 mg/kg inhibited carrageenan-induced paw edema in mice, compound **63** being more effective than the positive control compound tofacitinib (30 mg/kg). Irreversible binding was further supported by a jump dilution assay, and covalent docking recapitulated a similar binding mode as previously shown for compound **58** (see Fig. 21a) by researchers from Pfizer.

In early 2017, researchers from MSD published a comprehensive study of JAK3 biology where they focused on the aforementioned selectivity shift, which can be observed when comparing enzymatic assays at K_m ATP to cellular systems [52]. In good agreement with previously reported data from Thorarensen et al. [30], they showed that compared to JAK1, JAK3 possesses an about tenfold higher ATP affinity. The latter results in a more pronounced loss of JAK3 inhibitory activity relative to JAK1 when running assays at an invariable and high ATP concentration mimicking a cellular environment. A screening of a large collection of JAK inhibitors with various selectivity profiles in cellular assays and the comparison of the obtained data with results from enzymatic assays conducted at K_m ATP uncovered an average 44-fold loss in selectivity (JAK3 over JAK1). A decreased selectivity against JAK2 was observed as well but was less pronounced (approx. eightfold). In the light of these results, the researchers at MSD concluded that via elimination of the ATP competitiveness by using an irreversible inhibitor, much better JAK3 selectivity would be achievable in cells and in vivo. Therefore, they chose one of the irreversible inhibitors based on a 4-phenyl-7*H*-pyrrolo[2,3-*d*]pyrimidine scaffold (**64**, Fig. 24) from the aforementioned patent application (vide supra, see Fig. 10) and performed an extensive biological characterization.

The suggested covalent targeting of Cys909 by **64** was supported by jump dilution assays and reconfirmed by X-ray crystallography (no data deposited in the PDB). Like other compounds from this structural class, **64** was a very efficient JAK inhibitor ($IC_{50} = 0.15$ nM, $k_{inact}/K_I = 9.9 \times 10^5$ M⁻¹ s⁻¹) having an excellent selectivity over the other isoforms in enzymatic assays (4,300-fold over JAK1 and >10,000-fold over JAK2/TYK2). Additionally, a more than 100-fold selectivity was claimed against 24 other kinases, however, without providing detailed information about the underlying screening panel. In cellular models including several human and murine cell lines as well as PBMCs, the JAK3 selectivity of compound **64** was

Fig. 24 Irreversible JAK3 inhibitor **64** used by Elwood et al. from MSD for interrogating JAK3 biology [52]



corroborated. The inhibitor potently blocked JAK3-dependent STAT5 phosphorylation, e.g., after stimulation of murine CTLL-2 cells with IL-2 ($IC_{50} = 70$ nM) or IL-7 stimulation of human PBMCs ($IC_{50} = 280$ nM). At the same time, an at least 35-fold selectivity over the JAK3-independent pathways triggered by IL-6, GM-CSF, and EPO was observed. In agreement with the previously described results from Pfizer employing a structurally related aromatic acrylamide (**58**, Fig. 20b), a poor translation of the enzymatic and cellular assay data was observed when moving to human whole blood. Despite remaining an effective suppressor of JAK3-dependent pathways, the IC_{50} values of **64** were significantly higher in the latter case. This could be a result of the substantial intrinsic reactivity of *N*-aryl acrylamides and their susceptibility to inactivation by promiscuous thiol binding.

In animal models, **64** was combined with the CYP inhibitor 1-aminobenzotriazole (ABT) to prevent a rapid decrease in plasma concentration resulting from modest stability against hepatic metabolism. In a modified CIA model, **64** was able to reduce paw swelling in a dose-dependent manner. Nevertheless, even at the highest dose of 300 mg/kg (p.o., BID), compound **64** was still inferior to the positive control dexamethasone. However, JAK3 selectivity could be substantiated *in vivo*, since inhibition of T cell proliferation was observed, while hematopoiesis was not affected.

In further experiments investigating the connection between PD and PK, it was demonstrated that an extended effect of irreversible inhibition after clearance of **64** from plasma can only partially be achieved. This observation conforms to the previously described high resynthesis rate of JAK3.

Kempson et al. from Bristol-Myers Squibb recently disclosed their efforts on the development of nicotinamide-derived covalent JAK3 inhibitors [65]. In preliminary studies, they identified compound **65** (Fig. 25) as a potent non-covalent JAK3 inhibitor with a reasonable selectivity profile (JAK3 $IC_{50} = 4.5$ nM and ca. 40-fold to 180-fold selectivity against the other JAKs). This molecule served as the starting point for further investigations. Guided by molecular modeling, the *meta*-position of the benzylamine substituent was identified as promising attachment point for an acrylamide warhead. Indeed, this modification leading to compound **66** boosted JAK3 potency to reach subnanomolar IC_{50} values and concomitantly increased selectivity against the other isoforms (>1,100-fold, >1,300-fold, and >5,000-fold over JAK1, JAK2, and TYK2, respectively). A successful covalent capture of Cys909 can be assumed, since **66** demonstrated time-dependent inhibition of JAK3, while the analogous propanamide did not. However, a final confirmation by X-ray crystallography or mass spectrometry was not provided for this scaffold class.

Further characterization in cellular assays demonstrated **66** to potently inhibit IL-2 driven T cell proliferation ($IC_{50} = 22$ nM) and to decrease IFN γ production after IL-2 stimulation in human whole blood ($IC_{50} = 490$ nM). A favorable JAK3 selectivity was also confirmed in cellular models, since JAK2-dependent (EPO) and JAK1/TYK2-driven (IFN α) pathways were blocked less efficiently (IC_{50} values of 11 μ M and 5 μ M, respectively).

Good kinome-wide selectivity was proven for **66** in a panel of 350 kinases, where only 3 kinases (JAK3, FMS, and BMPR2) were strongly affected (<10% of the

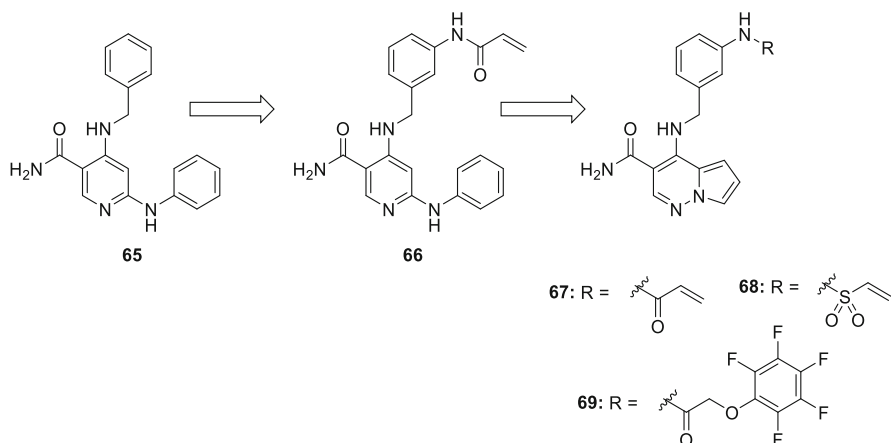
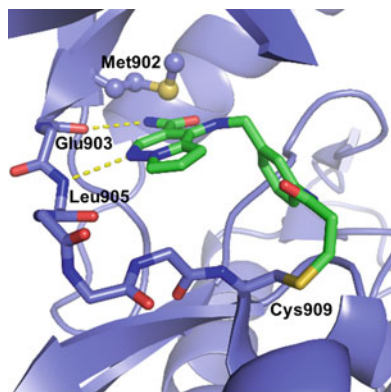


Fig. 25 Development of irreversible JAK3 inhibitors by Kempson et al. [65]. Lead compound **65** was substituted with an acrylamide at the *meta*-position of the benzylamine moiety to obtain covalent inhibitor **66**. Subsequent replacement of the hinge-binding motif lead to pyrrolo[1,2-*b*]pyridazine-derived compound **67** and derivatives thereof (exemplified by **68** and **69**)

Fig. 26 X-ray structure of **67** in complex with JAK3 (PDB-code: 5WFJ). Hydrogen bonds are depicted as dashed yellow lines, and the Met902 gatekeeper residue is highlighted in the ball and stick representation



control) at a concentration of 1 μM . A more detailed investigation of binding kinetics was provided for JAK3 vs. BTK, and it was shown that the k_{inact}/K_1 ratio was at least three orders of magnitude higher for JAK3 ($k_{\text{inact}}/K_1 = 3.0 \times 10^5 \text{ M}^{-1} \text{ s}^{-1}$) suggesting pronounced kinetic selectivity.

Nevertheless, compound **66** failed in murine PK models revealing low oral bioavailability and high clearance. Therefore, the same development strategy was transferred to a pyrrolo[1,2-*b*]pyridazine scaffold providing compound **67** (Fig. 25), which showed a similar biochemical profile as **66**. The X-ray crystal structure of **67** bound to JAK3 could be solved confirming the formation of a covalent link between Cys909 and the ligand (Fig. 26). The complex of **67** and JAK3 features a donor–acceptor hydrogen bonding pattern with hinge region, in which the hinge-binding heterocycle is inverted compared to most other JAK3 inhibitors.

One of these hydrogen bonds is formed between a heteroaryl nitrogen atom and Leu905, the other between the primary amide and the backbone carbonyl oxygen of Glu903. The benzyl linker adopts a similar conformation as in a previously mentioned compound from Gray et al. (**48**, see Fig. 15), which is further stabilized by an intramolecular hydrogen bond between the amide carbonyl oxygen and the NH of the secondary amino group.

Besides the classical acrylamide headgroup, a variety of other warheads were attached to this scaffold, including less common ones like the vinylsulfonamide (**68**) or a pentafluorophenoxy acetamide (**69**). However, these electrophiles, except the vinylsulfonamide in **68**, impaired JAK3 inhibitory activity to different extents, and all of them failed to achieve potent inhibition of IL-2-stimulated T cell proliferation (IC_{50} values of 5–25 μ M).

Additional characterization of such pyrrolo[1,2-*b*]pyridazine-derived compounds in comprehensive kinome panels or in vivo has not been provided yet, but follow-up reports including such data were announced by the authors.

3 Summary

Substantial efforts have been made to develop covalent kinase inhibitors for the treatment of inflammatory and autoimmune disorders. Here, JAK3 was among the most prominent targets, but specific and drug-like inhibitors for this enzyme with a covalent mode of action have only appeared in the literature during the last 5 years. However, a tremendous amount of work has been published in this field since 2014 providing a considerable set of covalent-reversible and irreversible JAK3 inhibitors with excellent selectivity within the JAK family and the kinome. Previous non-covalent inhibitors, which were supposed to be JAK3-selective typically suffered from limited cellular selectivity or lack of potency in cells due to the higher ATP affinity of JAK3 when compared to other JAKs. The latter is not taken into account by the typical IC_{50} determinations employing ATP concentrations at (or close to) the enzymes' K_m values. Experiments with such compounds have previously raised the question, whether selective JAK3 inhibition is enough to block STAT phosphorylation, sparking a discussion whether JAK1 had a dominant role over JAK3 in the signaling of γ_c cytokine receptors. The newly developed covalent JAK3 inhibitors, however, have resolved this issue and can now be used for the detailed investigation of JAK3-dependent JAK-STAT signaling. Based on the reports discussed in this chapter, we conclude that selective JAK3 inhibition is sufficient to suppress downstream signaling. If major issues such as limited in vivo stability, e.g., due to GSH/GST-mediated extrahepatic clearance, can be overcome, and long-term safety is proven, there is a considerable chance for specific covalent JAK3 inhibitors to become effective anti-inflammatory and immunosuppressive drugs with limited side effects outside the immune system. In this light, the results of further clinical studies with the currently most advanced compound, PF-06651600, and potential follow-up candidates are eagerly awaited.

Acknowledgments The authors thank Kristine Schmidt for proofreading. M.G. acknowledges financial support from the Institutional Strategy of the University of Tübingen (ZUK 63, German Research Foundation) and the Postdoctoral Fellowship Program of the Baden-Württemberg Stiftung.

Compliance and Ethical Standards

Conflict of Interest: The authors declare that they have no conflict of interest.

Funding: While preparing the manuscript, M.G. received funding from the Institutional Strategy of the University of Tübingen (ZUK 63, German Research Foundation) and the Postdoctoral Fellowship Program of the Baden-Württemberg Stiftung.

Ethical Approval: This chapter does not contain any studies with human participants or animals performed by any of the authors.

References

1. Ferguson FM, Gray NS (2018) Kinase inhibitors: the road ahead. *Nat Rev Drug Discov* 17:353–377. <https://doi.org/10.1038/nrd.2018.21>
2. Forster M, Gehringer M, Laufer SA (2017) Recent advances in JAK3 inhibition: isoform selectivity by covalent cysteine targeting. *Bioorg Med Chem Lett* 27:4229–4237. <https://doi.org/10.1016/j.bmcl.2017.07.079>
3. Pellegrini S, Dusanter-Fourt I (1997) The structure, regulation and function of the Janus kinases (JAKs) and the signal transducers and activators of transcription (STATs). *Eur J Biochem* 248:615–633. <https://doi.org/10.1111/j.1432-1033.1997.00615.x>
4. Clark JD, Flanagan ME, Telliez J-B (2014) Discovery and development of Janus kinase (JAK) inhibitors for inflammatory diseases. *J Med Chem* 57:5023–5038. <https://doi.org/10.1021/jm401490p>
5. Ghoreschi K, Laurence A, O’Shea JJ (2009) Janus kinases in immune cell signaling. *Immunol Rev* 228:273–287. <https://doi.org/10.1111/j.1600-065X.2008.00754.x>
6. Miyazaki T, Kawahara A, Fujii H, Nakagawa Y, Minami Y, Liu ZJ, Oishi I, Silvennoinen O, Witthuhn BA, Ihle JN, Et A (1994) Functional activation of Jak1 and Jak3 by selective association with IL-2 receptor subunits. *Science* 266:1045–1047. <https://doi.org/10.1126/science.7973659>
7. Rochman Y, Spolski R, Leonard WJ (2009) New insights into the regulation of T cells by γ c family cytokines. *Nat Rev Immunol* 9:480–490. <https://doi.org/10.1038/nri2580>
8. Gurniak CB, Berg LJ (1996) Murine JAK3 is preferentially expressed in hematopoietic tissues and lymphocyte precursor cells. *Blood* 87:3151–3160
9. Park SY, Saijo K, Takahashi T, Osawa M, Arase H, Hirayama N, Miyake K, Nakauchi H, Shirasawa T, Saito T (1995) Developmental defects of lymphoid cells in Jak3 kinase-deficient mice. *Immunity* 3:771–782
10. Roberts JL, Lengi A, Brown SM, Chen M, Zhou Y-J, O’Shea JJ, Buckley RH (2004) Janus kinase 3 (JAK3) deficiency: clinical, immunologic, and molecular analyses of 10 patients and outcomes of stem cell transplantation. *Blood* 103:2009–2018. <https://doi.org/10.1182/blood-2003-06-2104>

11. Sohn SJ, Forbush KA, Nguyen N, Witthuhn B, Nosaka T, Ihle JN, Perlmutter RM (1998) Requirement for Jak3 in mature T cells: its role in regulation of T cell homeostasis. *J Immunol* 160:2130–2138
12. Noguchi M, Yi H, Rosenblatt HM, Filipovich AH, Adelstein S, Modi WS, McBride OW, Leonard WJ (1993) Interleukin-2 receptor γ chain mutation results in X-linked severe combined immunodeficiency in humans. *Cell* 73:147–157. [https://doi.org/10.1016/0092-8674\(93\)90167-O](https://doi.org/10.1016/0092-8674(93)90167-O)
13. Pesu M, Laurence A, Kishore N, Zwillich SH, Chan G, O'Shea JJ (2008) Therapeutic targeting of Janus kinases. *Immunol Rev* 223:132–142. <https://doi.org/10.1111/j.1600-065X.2008.00644.x>
14. Changelian PS, Flanagan ME, Ball DJ, Kent CR, Magnuson KS, Martin WH, Rizzuti BJ, Sawyer PS, Perry BD, Brissette WH, McCurdy SP, Kudlacz EM, Conklyn MJ, Elliott EA, Koslov ER, Fisher MB, Strelevitz TJ, Yoon K, Whipple DA, Sun J, Munchhof MJ, Doty JL, Casavant JM, Blumenkopf TA, Hines M, Brown MF, Lillie BM, Subramanyam C, Shang-Poa C, Milici AJ, Beckius GE, Moyer JD, Su C, Woodworth TG, Gaweco AS, Beals CR, Littman BH, Fisher DA, Smith JF, Zagouras P, Magna HA, Saltarelli MJ, Johnson KS, Nelms LF, Etages SGD, Hayes LS, Kawabata TT, Finco-Kent D, Baker DL, Larson M, Si M-S, Paniagua R, Higgins J, Holm B, Reitz B, Zhou Y-J, Morris RE, O'Shea JJ, Borie DC (2003) Prevention of organ allograft rejection by a specific Janus kinase 3 inhibitor. *Science* 302:875–878. <https://doi.org/10.1126/science.1087061>
15. Garber K (2013) Pfizer's first-in-class JAK inhibitor pricey for rheumatoid arthritis market. *Nat Biotech* 31:3–4. <https://doi.org/10.1038/nbt0113-3>
16. Thoma G, Drückes P, Zerwes H-G (2014) Selective inhibitors of the Janus kinase Jak3 – are they effective? *Bioorg Med Chem Lett* 24:4617–4621. <https://doi.org/10.1016/j.bmcl.2014.08.046>
17. Press Announcements - FDA approves new treatment for moderately to severely active ulcerative colitis. <https://www.fda.gov/NewsEvents/Newsroom/PressAnnouncements/ucm609225.htm>. Accessed 18 Oct 2018
18. Xeljanz. European Medicines Agency. <https://www.ema.europa.eu/medicines/human/EPAR/xeljanz>. Accessed 18 Oct 2018
19. Markham A (2017) Baricitinib: first global approval. *Drugs* 77:697–704. <https://doi.org/10.1007/s40265-017-0723-3>
20. Mullard A (2018) FDA approves Eli Lilly's baricitinib. *Nat Rev Drug Discov* 17:460
21. Mesa RA, Yasothan U, Kirkpatrick P (2012) Ruxolitinib. *Nat Rev Drug Discov* 11:103–104. <https://doi.org/10.1038/nrd3652>
22. Gonzales AJ, Bowman JW, Fici GJ, Zhang M, Mann DW, Mitton-Fry M (2014) Oclacitinib (APOQUEL[®]) is a novel Janus kinase inhibitor with activity against cytokines involved in allergy. *J Vet Pharmacol Ther* 37:317–324. <https://doi.org/10.1111/jvp.12101>
23. Thoma G, Nuninger F, Falchetto R, Hermes E, Tavares GA, Vangrevelinghe E, Zerwes H-G (2010) Identification of a potent Janus kinase 3 inhibitor with high selectivity within the Janus kinase family. *J Med Chem* 54:284–288. <https://doi.org/10.1021/jm101157q>
24. Lin TH, Hegen M, Quadros E, Nickerson-Nutter CL, Appell KC, Cole AG, Shao Y, Tam S, Ohlmeyer M, Wang B, Goodwin DG, Kimble EF, Quintero J, Gao M, Symanowicz P, Wrocklage C, Lussier J, Schelling SH, Hewet AG, Xuan D, Krykbaev R, Togias J, Xu X, Harrison R, Mansour T, Collins M, Clark JD, Webb ML, Seidl KJ (2010) Selective functional inhibition of JAK-3 is sufficient for efficacy in collagen-induced arthritis in mice. *Arthritis Rheum* 62:2283–2293. <https://doi.org/10.1002/art.27536>
25. Farmer LJ, Ledebner MW, Hoock T, Armost MJ, Bethiel RS, Bennani YL, Black JJ, Brummel CL, Chakilam A, Dorsch WA, Fan B, Cochran JE, Halas S, Harrington EM, Hogan JK, Howe D, Huang H, Jacobs DH, Laitinen LM, Liao S, Mahajan S, Marone V, Martinez-Botella G, McCarthy P, Messersmith D, Namchuk M, Oh L, Penney MS, Pierce AC, Raybuck SA, Rugg A, Salituro FG, Saxena K, Shannon D, Shlyakter D, Swenson L, Tian S-K, Town C, Wang J, Wang T, Wannamaker MW, Winquist RJ, Zuccola HJ (2015) Discovery of VX-509

- (Decernotinib): a potent and selective Janus kinase 3 inhibitor for the treatment of autoimmune diseases. *J Med Chem* 58:7195–7216. <https://doi.org/10.1021/acs.jmedchem.5b00301>
26. Soth M, Hermann JC, Yee C, Alam M, Barnett JW, Berry P, Browner MF, Frank K, Frauchiger S, Harris S, He Y, Hekmat-Nejad M, Hendricks T, Henningsen R, Hilgenkamp R, Ho H, Hoffman A, Hsu P-Y, Hu D-Q, Itano A, Jaime-Figueroa S, Jahangir A, Jin S, Kuglstatter A, Kutach AK, Liao C, Lynch S, Menke J, Niu L, Patel V, Raikar A, Roy D, Shao A, Shaw D, Steiner S, Sun Y, Tan S-L, Wang S, Vu MD (2013) 3-Amido pyrrolopyrazine JAK kinase inhibitors: development of a JAK3 vs JAK1 selective inhibitor and evaluation in cellular and in vivo models. *J Med Chem* 56:345–356. <https://doi.org/10.1021/jm301646k>
 27. Gehringer M, Pfaffenrot E, Bauer S, Laufer SA (2014) Design and synthesis of tricyclic JAK3 inhibitors with picomolar affinities as novel molecular probes. *ChemMedChem* 9:277–281. <https://doi.org/10.1002/cmdc.201300520>
 28. Nakajima Y, Aoyama N, Takahashi F, Sasaki H, Hatanaka K, Moritomo A, Inami M, Ito M, Nakamura K, Nakamori F, Inoue T, Shirakami S (2016) Design, synthesis, and evaluation of 4,6-diaminonicotinamide derivatives as novel and potent immunomodulators targeting JAK3. *Bioorg Med Chem* 24:4711–4722. <https://doi.org/10.1016/j.bmc.2016.08.007>
 29. Haan C, Rolvering C, Raulf F, Kapp M, Drückes P, Thoma G, Behrmann I, Zerwes H-G (2011) Jak1 has a dominant role over Jak3 in signal transduction through γ c-containing cytokine receptors. *Chem Biol* 18:314–323. <https://doi.org/10.1016/j.chembiol.2011.01.012>
 30. Thorarensen A, Banker ME, Fensome A, Telliez J-B, Juba B, Vincent F, Czerwinski RM, Casimiro-Garcia A (2014) ATP-mediated Kinome selectivity: the missing link in understanding the contribution of individual JAK kinase isoforms to cellular signaling. *ACS Chem Biol* 9:1552. <https://doi.org/10.1021/cb5002125>
 31. Yoshida T, Kakizuka A, Imamura H (2016) BTeam, a novel BRET-based biosensor for the accurate quantification of ATP concentration within living cells. *Sci Rep* 6:39618. <https://doi.org/10.1038/srep39618>
 32. Leonard WJ, Mitra S, Lin J-X (2016) Immunology: JAK3 inhibition—is it sufficient? *Nat Chem Biol* 12:308–310. <https://doi.org/10.1038/nchembio.2066>
 33. Chaikuad A, Koch P, Laufer SA, Knapp S (2018) The cysteinome of protein kinases as a target in drug development. *Angew Chem Int Ed* 57:4372–4385. <https://doi.org/10.1002/anie.201707875>
 34. Fry DW, Bridges AJ, Denny WA, Doherty A, Greis KD, Hicks JL, Hook KE, Keller PR, Leopold WR, Loo JA, McNamara DJ, Nelson JM, Sherwood V, Smaill JB, Trumpp-Kallmeyer S, Dobrusin EM (1998) Specific, irreversible inactivation of the epidermal growth factor receptor and erbB2, by a new class of tyrosine kinase inhibitor. *PNAS* 95:12022–12027. <https://doi.org/10.1073/pnas.95.20.12022>
 35. Thorarensen A, Dowty ME, Banker ME, Juba B, Jussif J, Lin T, Vincent F, Czerwinski RM, Casimiro-Garcia A, Unwalla R, Trujillo JJ, Liang S, Balbo P, Che Y, Gilbert AM, Brown MF, Hayward M, Montgomery J, Leung L, Yang X, Soucy S, Hegen M, Coe J, Langille J, Vajdos F, Chrencik J, Telliez J-B (2017) Design of a Janus Kinase 3 (JAK3) specific inhibitor 1-((2S,5R)-5-((7H-Pyrrolo[2,3-d]pyrimidin-4-yl)amino)-2-methylpiperidin-1-yl)prop-2-en-1-one (PF-06651600) allowing for the interrogation of JAK3 signaling in humans. *J Med Chem* 60:1971–1993. <https://doi.org/10.1021/acs.jmedchem.6b01694>
 36. Hanks SK, Hunter T (1995) Protein kinases 6. The eukaryotic protein kinase superfamily: kinase (catalytic) domain structure and classification. *FASEB J* 9:576–596
 37. Brown GR, Bamford AM, Bowyer J, James DS, Rankine N, Tang E, Torr V, Culbert EJ (2000) Naphthyl ketones: a new class of Janus kinase 3 inhibitors. *Bioorg Med Chem Lett* 10:575–579. [https://doi.org/10.1016/S0960-894X\(00\)00051-2](https://doi.org/10.1016/S0960-894X(00)00051-2)
 38. Stepkowski SM, Kao J, Wang M-E, Tejpal N, Podder H, Furian L, Dimmock J, Jha A, Das U, Kahan BD, Kirken RA (2005) The Mannich base NC1153 promotes long-term allograft survival and spares the recipient from multiple toxicities. *J Immunol* 175:4236–4246. <https://doi.org/10.4049/jimmunol.175.7.4236>

39. Ross JA, Spadaro M, Rosado DC, Cavallo F, Kirken RA, Pericle F (2014) Inhibition of JAK3 with a novel, selective and orally active small molecule induces therapeutic response in T-cell malignancies. *Leukemia* 28:941–944. <https://doi.org/10.1038/leu.2013.309>
40. Styles M, Zeng J, Treutlein H, Wilks A, Kling M, Bu X, Burns C (2005) Selective kinase inhibitors
41. Goedken ER, Argiriadi MA, Banach DL, Fiamengo BA, Foley SE, Frank KE, George JS, Harris CM, Hobson AD, Ihle DC, Marcotte D, Merta PJ, Michalak ME, Murdock SE, Tomlinson MJ, Voss JW (2015) Tricyclic covalent inhibitors selectively target Jak3 through an active site thiol. *J Biol Chem* 290:4573–4589. <https://doi.org/10.1074/jbc.M114.595181>
42. Goldstein DM, Brameld KA, Verner E (2012) Azaindole derivatives as tyrosine kinase inhibitors
43. Goldstein D, Brameld K, Owens T (2014) Azaindole derivatives as JAK3 inhibitors
44. Ahearn S, Christopher M, Jung J, Pu Q, Rivkin A, Scott M, Witter D, Woo HC, Cash B, Dinsmore C, Guerin D (2013) Pyrrolopyrimidines as Janus kinase inhibitors
45. Smith GA, Uchida K, Weiss A, Taunton J (2016) Essential biphasic role for JAK3 catalytic activity in IL-2 receptor signaling. *Nat Chem Biol* 12:373–379. <https://doi.org/10.1038/nchembio.2056>
46. London N, Miller RM, Krishnan S, Uchida K, Irwin JJ, Eidam O, Gibold L, Cimermančič P, Bonnet R, Shoichet BK, Taunton J (2014) Covalent docking of large libraries for the discovery of chemical probes. *Nat Chem Biol* 10:1066–1072. <https://doi.org/10.1038/nchembio.1666>
47. Gehringer M, Forster M, Laufer SA (2015) Solution-phase parallel synthesis of Ruxolitinib-derived Janus kinase inhibitors via copper-catalyzed Azide–Alkyne cycloaddition. *ACS Comb Sci* 17:5–10. <https://doi.org/10.1021/co500122h>
48. Forster M, Chaikuad A, Bauer SM, Holstein J, Robers MB, Corona CR, Gehringer M, Pfaffenrot E, Ghoreschi K, Knapp S, Laufer SA (2016) Selective JAK3 inhibitors with a covalent reversible binding mode targeting a new induced fit binding pocket. *Cell Chem Biol* 23:1335–1340. <https://doi.org/10.1016/j.chembiol.2016.10.008>
49. Tan L, Akahane K, McNally R, Reyskens KMSE, Ficarro SB, Liu S, Herter-Sprue GS, Koyama S, Pattison MJ, Labella K, Johannessen L, Akbay EA, Wong K-K, Frank DA, Marto JA, Look TA, Arthur JSC, Eck MJ, Gray NS (2015) Development of selective covalent Janus kinase 3 inhibitors. *J Med Chem* 58:6589–6606. <https://doi.org/10.1021/acs.jmedchem.5b00710>
50. Zhou W, Ercan D, Chen L, Yun C-H, Li D, Capelletti M, Cortot AB, Chirieac L, Iacob RE, Padera R, Engen JR, Wong K-K, Eck MJ, Gray NS, Jänne PA (2009) Novel mutant-selective EGFR kinase inhibitors against EGFR T790M. *Nature* 462:1070–1074. <https://doi.org/10.1038/nature08622>
51. Ge Y, Wang C, Song S, Huang J, Liu Z, Li Y, Meng Q, Zhang J, Yao J, Liu K, Ma X, Sun X (2018) Identification of highly potent BTK and JAK3 dual inhibitors with improved activity for the treatment of B-cell lymphoma. *Eur J Med Chem* 143:1847–1857. <https://doi.org/10.1016/j.ejmech.2017.10.080>
52. Elwood F, Witter DJ, Piesvaux J, Kraybill B, Bays N, Alpert C, Goldenblatt P, Qu Y, Ivanovska I, Lee H-H, Chiu C-S, Tang H, Scott ME, Deshmukh SV, Zielstorff M, Byford A, Chakravarthy K, Dorosh L, Rivkin A, Klappenbach J, Pan B-S, Kariv I, Dinsmore C, Slipetz D, Dandliker PJ (2017) Evaluation of JAK3 biology in autoimmune disease using a highly selective, irreversible JAK3 inhibitor. *J Pharmacol Exp Ther* 361:229–244. <https://doi.org/10.1124/jpet.116.239723>
53. Forster M, Chaikuad A, Dimitrov T, Döring E, Holstein J, Berger B-T, Gehringer M, Ghoreschi K, Müller S, Knapp S, Laufer SA (2018) Development, optimization, and structure–activity relationships of covalent-reversible JAK3 inhibitors based on a tricyclic Imidazo[5,4-d]pyrrolo[2,3-b]pyridine scaffold. *J Med Chem* 61:5350–5366. <https://doi.org/10.1021/acs.jmedchem.8b00571>
54. Kulagowski JJ, Blair W, Bull RJ, Chang C, Deshmukh G, Dyke HJ, Eigenbrot C, Ghilardi N, Gibbons P, Harrison TK, Hewitt PR, Liimatta M, Hurley CA, Johnson A, Johnson T, Kenny JR,

- Bir Kohli P, Maxey RJ, Mendonca R, Mortara K, Murray J, Narukulla R, Shia S, Steffek M, Ubhayakar S, Ulsch M, van Abbema A, Ward SI, Waszkowycz B, Zak M (2012) Identification of imidazo-pyrrolopyridines as novel and potent JAK1 inhibitors. *J Med Chem* 55:5901–5921. <https://doi.org/10.1021/jm300438j>
55. Chrencik JE, Patny A, Leung IK, Korniski B, Emmons TL, Hall T, Weinberg RA, Gormley JA, Williams JM, Day JE, Hirsch JL, Kiefer JR, Leone JW, Fischer HD, Sommers CD, Huang H-C, Jacobsen EJ, Tenbrink RE, Tomasselli AG, Benson TE (2010) Structural and thermodynamic characterization of the TYK2 and JAK3 kinase domains in complex with CP-690550 and CMP-6. *J Mol Biol* 400:413–433. <https://doi.org/10.1016/j.jmb.2010.05.020>
56. Robers MB, Dart ML, Woodroffe CC, Zimprich CA, Kirkland TA, Machleidt T, Kupcho KR, Levin S, Hartnett JR, Zimmerman K, Niles AL, Ohana RF, Daniels DL, Slater M, Wood MG, Cong M, Cheng Y-Q, Wood KV (2015) Target engagement and drug residence time can be observed in living cells with BRET. *Nat Commun* 6:1–10. <https://doi.org/10.1038/ncomms10091>
57. Telliez J-B, Dowty ME, Wang L, Jussif J, Lin T, Li L, Moy E, Balbo P, Li W, Zhao Y, Crouse K, Dickinson C, Symanowicz P, Hegen M, Banker ME, Vincent F, Unwalla R, Liang S, Gilbert AM, Brown MF, Hayward M, Montgomery J, Yang X, Bauman J, Trujillo JI, Casimiro-Garcia A, Vajdos FF, Leung L, Geoghegan KF, Quazi A, Xuan D, Jones L, Hett E, Wright K, Clark JD, Thorarensen A (2016) Discovery of a JAK3-selective inhibitor: functional differentiation of JAK3-selective inhibition over pan-JAK or JAK1-selective inhibition. *ACS Chem Biol* 11:3442–3451. <https://doi.org/10.1021/acscchembio.6b00677>
58. He L, Pei H, Lan T, Tang M, Zhang C, Chen L (2017) Design and synthesis of a highly selective JAK3 inhibitor for the treatment of rheumatoid arthritis. *Arch der Pharm* 350:1700194. <https://doi.org/10.1002/ardp.201700194>
59. Pei H, He L, Shao M, Yang Z, Ran Y, Li D, Zhou Y, Tang M, Wang T, Gong Y, Chen X, Yang S, Xiang M, Chen L (2018) Discovery of a highly selective JAK3 inhibitor for the treatment of rheumatoid arthritis. *Sci Rep* 8:5273. <https://doi.org/10.1038/s41598-018-23569-y>
60. He L, Shao M, Wang T, Lan T, Zhang C, Chen L (2018) Design, synthesis, and SAR study of highly potent, selective, irreversible covalent JAK3 inhibitors. *Mol Divers* 22:1–16. <https://doi.org/10.1007/s11030-017-9803-2>
61. Jackson PA, Widen JC, Harki DA, Brummond KM (2017) Covalent modifiers: a chemical perspective on the reactivity of α,β -unsaturated carbonyls with thiols via hetero-Michael addition reactions. *J Med Chem* 60:839–885. <https://doi.org/10.1021/acs.jmedchem.6b00788>
62. Flanagan ME, Abramite JA, Anderson DP, Aulabaugh A, Dahal UP, Gilbert AM, Li C, Montgomery J, Oppenheimer SR, Ryder T, Schuff BP, Uccello DP, Walker GS, Wu Y, Brown MF, Chen JM, Hayward MM, Noe MC, Obach RS, Philippe L, Shanmugasundaram V, Shapiro MJ, Starr J, Stroh J, Che Y (2014) Chemical and computational methods for the characterization of covalent reactive groups for the prospective design of irreversible inhibitors. *J Med Chem* 57:10072–10079. <https://doi.org/10.1021/jm501412a>
63. Allimuthu D, Adams DJ (2017) 2-Chloropropionamide as a low-reactivity electrophile for irreversible small-molecule probe identification. *ACS Chem Biol* 12:2124–2131. <https://doi.org/10.1021/acscchembio.7b00424>
64. Gehringer M, Forster M, Pfaffenrot E, Bauer SM, Laufer SA (2014) Novel hinge-binding motifs for Janus kinase 3 inhibitors: a comprehensive structure–activity relationship study on Tofacitinib Bioisosteres. *ChemMedChem* 9:2516–2527. <https://doi.org/10.1002/cmdc.201402252>
65. Kempson J, Ovalle D, Guo J, Wroblewski ST, Lin S, Spergel SH, Duan JJ-W, Jiang B, Lu Z, Das J, Yang BV, Hynes J, Wu H, Tokarski J, Sack JS, Khan J, Schieven G, Blatt Y, Chaudhry C, Salter-Cid LM, Fura A, Barrish JC, Carter PH, Pitts WJ (2017) Discovery of highly potent, selective, covalent inhibitors of JAK3. *Bioorg Med Chem Lett* 27:4622–4625. <https://doi.org/10.1016/j.bmcl.2017.09.023>